UNIVERSIDADE ESTADUAL PAULISTA
"JÚLIO DE MESQUITA FILHO"

Faculdade de Odontologia de Araçatuba - UNESP
Departamento de Odontologia Preventiva e Restauradora
Programa de Pós-Graduação em Ciências - Área: Endodontia

HENRIQUE AUGUSTO BANCI

Influência da terapia fotodinâmica e do hidróxido de cálcio nas propriedades da dentina intrarradicular e do cimento resinoso, resistência de união dos pinos de fibra de vidro, caracterização e morfologia da interface adesiva

Araçatuba
2023

HENRIQUE AUGUSTO BANCI

Influência da terapia fotodinâmica e do hidróxido de cálcio nas propriedades da dentina intrarradicular e do cimento resinoso, resistência de união dos pinos de fibra de vidro, caracterização e morfologia da interface adesiva

Tese apresentada à Faculdade de Odontologia de Araçatuba da Universidade Estadual Paulista "Júlio de Mesquita Filho" – UNESP, como parte dos requisitos para a obtenção do título de Doutor em Endodontia.

Orientador: Prof. Assoc. Gustavo Sivieri de Araújo

Araçatuba
2023

Catalogação na Publicação (CIP)

Diretoria Técnica de Biblioteca e Documentação – FOA / UNESP

Banci, Henrique Augusto.
B213i Influência da terapia fotodinâmica e do hidróxido de cálcio nas propriedades da dentina intrarradicular e do cimento resinoso, resistência de união dos pinos de fibra de vidro, caracterização e morfologia da interface adesiva / Henrique Augusto Banci. - Araçatuba, 2023
159 f. : il. ; tab., graf.

Tese (Doutorado) – Universidade Estadual Paulista, Faculdade de Odontologia de Araçatuba
Orientador: Prof. Gustavo Sivieri de Araújo

1. Hidróxido de cálcio 2. Fotoquimioterapia 3. Resistência ao cisalhamento 4. Análise espectral Raman 5. Microscopia confocal 6. Microtomografia por raio-x I. T.

Black D24
CDD 617.67

Claudio Hideo Matsumoto – CRB-8/5550

Dedicatória

A Deus

Neste momento agradeço esta conquista à Deus, que me deu força e persistência para ultrapassar todos os obstáculos encontrados, iluminando meu caminho em todos os momentos e colocando pessoas ao meu lado, não permitindo que eu desistisse desta longa caminhada.

Cada dia é um recomeço, é um renascimento. Cada dia de vida merece ser celebrado e vivido com alegria, com motivação. Pois todos os dias temos a chance de ser felizes, e ser feliz é uma escolha.

"As pessoas felizes lembram o passado com gratidão, alegram-se com o presente e encaram o futuro sem medo."

Epicuro

Dedicatória

Aos Meus Pais e Meus Familiares

Este trabalho é dedicado as pessoas que estiveram ao meu lado ao longo de toda vida:

À minha mãe Maria Cleonice*, meu pai* Adalberto João*, minha irmã* Aline*, por toda ajuda, suporte para a vida, contribuindo para minha a formação pessoal e profissional.*

Aos meus avós, Maria Marcato *e* Antônio Banci *(in memoriam), que apesar de não ter conhecido carrego um grande respeito. Os Senhores fazem muita falta.*

Aos meus tios e padrinhos, Rosa *e* Vadilson*, agradeço por todas orações, conversas e conselhos encorajadores e suporte que me deram. Se não fosse vocês, não conseguiria realizar mais um sonho.*

Agradeço todo carinho e força que me deram em todo momento que estive fora, se não fossem vocês, seria tudo mais difícil.

Obrigado por caminharem ao meu lado!

Agradecimentos Especiais

Ao meu orientador Prof. Assoc. Gustavo Sivieri de Araújo*, serei sempre grato pela oportunidade que me proporcionou em ser seu orientado. Tudo começou com a entrevista para o processo seletivo, e hoje estamos alcançando algo maior. Obrigado por sua dedicação, atenção, paciência e disposição no decorrer deste tempo. Obrigado por me acalmar nos momentos de angústia e por me fazer acreditar que ia dar certo. Me sinto orgulhoso em ser seu orientado e muito privilegiado em acompanhar seus ensinamentos tanto em sala de aula quanto nas clínicas. Obrigado por seus conselhos nos momentos difíceis, por me ajudar a se tornar um profissional melhor e por participar comigo das minhas conquistas. O Sr. é uma pessoa ímpar.*

Ao meu co-orientador Prof. Assoc. Paulo Henrique dos Santos *agradeço por me auxiliar durante esta caminhada. O senhor foi meu primeiro exemplo de professor a ser "copiado" quando entrei na pós-graduação, sua paixão pelo que faz é de se admirar. Obrigado por sua disposição, carinho e atenção em nossos trabalhos sempre extremamente solícito e ágil com todas as necessidades, pelas poucas conversas que tivemos, mas que foram suficientes para me ajudar a tomar algumas decisões na vida. Agradeço a oportunidade e por ter contribuído para minha formação e para este momento se tornar realidade!*

Ao Prof. Assoc. Luciano Tavares Ângelo Cintra*, que privilégio ter o senhor conosco durante esse tempo, obrigado por todo apoio, ensinamentos, conversas. Admiro demais sua dedicação para com a pesquisa e o crescimento daqueles que estão ao seu redor. É uma honra poder aprender com uma pessoa que nos inspira sempre.*

Ao Prof. Tit. Marco Antônio Hungaro Duarte*, meu agradecimento especial pela contribuição no trabalho e por nos responder tão solicitamente. Foi uma honra poder conhecer a Faculdade de Odontologia de Bauru e executar parte da pesquisa lá. Meus sinceros agradecimentos!*

Aos professores Prof. Tit. João Eduardo Gomes Filho, Prof. Assoc. Eloi Dezan Junior e Prof. Assoc. Rogério de Castilho Jacinto, *é um enorme privilégio poder aprender todos os dias no departamento com vocês. Obrigado pelos conselhos, ensinamentos e dicas, muitas delas me ajudaram a tomar importantes decisões e a não desistir. Vocês refletem bem o que a Endodontia da FOA é reconhecida: a excelência com a uma humildade sem igual.*

Ao PósDoutorando Henrico Badaui Strazzi Sayhon *que se tornou um grande amigo! Obrigado por cada momento de ensinamento, pesquisa e de risadas! Você tem um coração admirável, dono de uma humildade sem igual. Obrigado!*

Aas meus amigos da Pós-Graduação: Flavio, Ana Paula, Ana Maria, Caroline, Pedro, Daniela, Cristiane, Isabela, Marina, Nathália, Carol e Gladiston, *obrigado por todos os momentos partilhados! Vocês me fizeram sentir em casa! Serei pra sempre grato.*

"O discípulo não está acima do seu mestre; todo aquele, porém, que for bem instruído será como o seu mestre." **(Lucas 6:40)**

Agradecimentos

À Faculdade de Odontologia de Araçatuba - UNESP, nas pessoas do Diretor **Prof. Tit. Glauco Issamu Miyhara**, e do senhor Vice-Diretor **Prof. Tit. Alberto Carlos Botazzo Delbem** por proporcionar a realização desta pesquisa e pelo período da pós-graduação e crescimento profissional.

A coordenação do Curso de Pós-Graduação em Ciência Odontológica, na pessoa do **Prof. Assoc Juliano Pelim Pessan**. A Chefe de Departamento **Profª Assoc. Ticiane Cestari Fagundes Tozzi**. Aos funcionários do Departamento **Jorge Luis Trevelim** e **Carlos Suetake** pela convivência e por sempre estarem preparados a me ajudar.

A todos os funcionários e estimados amigos da Biblioteca da Faculdade de Odontologia de Araçatuba - UNESP**, Cláudio Hideo Matsumoto, Ana Claudia Grieger Manzatti, Luzia Anderlini, Denise Haruyo Nakamura Maeda, Luís Cláudio Sedlacek, Ana Paula Rímoli de Oliveira** e **Maria Cláudia de Castro Benez,** pela atenção e eficiência com que sempre me atenderam.

Aos funcionários da seção de Pós-Graduação da Faculdade de Odontologia de Araçatuba - UNESP, **Valéria de Queiroz M. Zagatto, Cristiane Regina Lui Matos, Lilian Sayuri Mada** pelo excelente trabalho, atenção dispensada, grande disposição em atender e ótimo relacionamento.

Aos **professores da Pós-Graduação do Programa de Ciência Odontológica da Faculdade de Odontologia do Campus de Araçatuba – UNESP**, pelos ensinamentos durante todo o decorrer do curso.

A **Faculdade de Odontologia de Bauru, FOB-USP** e ao **Centro Integrado de Pesquisa I** que juntamente da **Dra. Márcia Sirlene Zardin Graeff** nos ajudou prontamente a executar parte crucial deste trabalho. Meu muito obrigado!

A **Faculdade de Física da UNESP de Bauru**, ao **Prof. Tit. Carlos Roberto Grandini** e ao **Laboratório de Microscopia Eletrônica de Varredura** por nos auxiliar em parte da execução e imagens desse projeto. Meus sinceros agradecimentos.

O presente trabalho foi realizado com apoio da **Coordenação de Aperfeiçoamento de Pessoal de Nível Superior – Brasil (CAPES)** – Código de Financiamento 001.

Finalmente, agradeço à Deus, ser superior, por ter me concedido essa oportunidade e ter colocado todas essas pessoas maravilhosas em meu caminho.

OBRIGADO!

Epígrafe

"Only the gentle are ever really strong".

(James Byron Dean)

SUMÁRIO

1	**Resumo Geral**	**07**
2	**Abstract**	**09**
3	**Introdução Geral**	**11**
4	**Objetivos** **2.1 Objetivo Geral** **2.2 Objetivos Específicos**	**15**
5	***CHAPTER* 1 - In vitro study on how photodynamic therapy and calcium hydroxide medication influence adhesive interface properties of glass-fiber posts to intraradicular dentin**	**17**
6	***CHAPTER* 2 - Effect of methylene blue-mediated antimicrobial photodynamic therapy and calcium hydroxide medication on physico-chemical and mechanical characteristics of intraradicular dentin and bonding interface of glass fiber posts**	**50**
7	**Discussão Geral**	**83**
8	**Conclusão Geral**	**90**
9	**Apêndice - Metodologia Expandida**	**91**
10	**Referências: Introdução Geral, Metodologia Expandida e Discussão Geral**	**107**
11	**Anexo 1 - Comitê de Ética no Uso de Animais**	**117**
12	**Anexo 2 - Journal of the Mechanical Behavior of Biomedical Materials - Guidelines**	**118**
13	**Anexo 3 – Photodiagnosis and Photodynamic Therapy - Guidelines**	**135**
14	**Anexo 4 – Publicação do Artigo - In vitro study on how photodynamic therapy and calcium hydroxide medication influence adhesive interface properties of glass-fiber posts to intraradicular dentin**	**148**

Listas de Figuras

Chapter 1

Figure 1 - Preparation of the specimens. A, Removal of anatomical crowns of the bovine incisors. B, Length and diameter standardization of root canals. C, Sealing of the apical region of the root canals. D, Photodynamic therapy session with methylene blue photosensitizer with red Laser (λ = 660 nm). E, Insertion of calcium hydroxide medication into root canals. F, Obturation process of the specimens. G, Obtainment of 1.3-mm thick intraradicular slices for push-out bond strength test. H, Specimen preparation for the confocal microscopy analysis with fluorescein and rhodamine B dyes. I, Obtainment of 1.3-mm thick intraradicular slices for the confocal microscopy analysis. J, Adhesive interface integrity analysis (volume and quantification of voids) using microtomography equipment.

Figure 2 - Fracture pattern incidence (samples thirds numbers) according to type of specimen failure.

Figure 3 - Scanning electron micrographs of representative failure types of the experimental groups under original magnification of × 30 and × 300. AB – mixed-type failure of root canals non-treated with methylene blue photosensitizer, photodynamic therapy, and calcium hydroxide medication (negative control group); CD – mixed-type failure of root canals filled with calcium hydroxide medication and non-treated with methylene blue photosensitizer and photodynamic therapy (positive control group); EF – mixed-type failure of root canals filled with calcium hydroxide medication and 50 mg/L of methylene blue photosensitizer and non- treated with photodynamic therapy (MB_{50WA} + $Ca(OH)_2$ group); GH – mixed-type failure of root canals filled with calcium hydroxide medication and 100 mg/L of methylene blue photosensitizer and non-treated with photodynamic therapy (MB_{100WA} + $Ca(OH)_2$ group); IJ – mixed-type failure of root canals filled with calcium hydroxide medication and 50 mg/L of methylene blue photosensitizer and treated with photodynamic therapy (MB_{50A} + $Ca(OH)_2$ group); KL – mixed-type failure of root canals filled with calcium hydroxide medication and 100 mg/L of methylene blue photosensitizer and treated with photodynamic therapy (MB_{100A} + $Ca(OH)_2$ group).

Figure 4 - Confocal laser scanning micrographs of adhesive interface sealing according to the experimental groups and intraradicular thirds under original magnification of ×5. 1C, 1M, 1A - Cervical, middle, and apical slices of intraradicular dentin irrigated with deionized water solution (negative control group). 2C, 2M, 2A - Cervical, middle, and apical slices of intraradicular dentin after irrigated with deionized water and filled with calcium hydroxide intracanal medication (positive control group). 3C, 3M, 3A - Cervical, middle, and apical slices of intraradicular dentin after treatment with calcium hydroxide intracanal medication + 50 mg/L of methylene blue without activation (MB_{50WA} + $Ca[OH]_2$). 4C, 4M, 4A - Cervical, middle, and apical slices of intraradicular dentin after treatment with calcium hydroxide intracanal medication + 100 mg/L of methylene blue without activation (MB_{100WA} + $Ca[OH]_2$). 5C, 5M, 5A - Cervical, middle, and apical slices of intraradicular dentin after treatment with calcium hydroxide intracanal medication + 50 mg/L of methylene blue activated by red laser (λ 660 nm) (MB_{50A} + $Ca[OH]_2$). 6C, 6M, 6A - Cervical, middle, and apical slices of intraradicular dentin after treatment with calcium hydroxide intracanal medication + 100 mg/L of methylene blue activated by red laser (λ 660 nm) (MB_{100A} + $Ca[OH]_2$).

Figure 5 - Microcomputed tomography images of adhesive interface integrity according to the experimental groups and intraradicular thirds. G1, 1C, 1M, 1A – Transaxial, cervical, middle, and apical slices of intraradicular dentin irrigated with deionized water solution (negative control group). G2, 2C, 2M, 2A – Transaxial, cervical, middle, and apical slices of intraradicular dentin

after irrigated with deionized water and filled with calcium hydroxide intracanal medication (positive control group). G3, 3C, 3M, 3A – Transaxial, cervical, middle, and apical slices of intraradicular dentin after treatment with calcium hydroxide intracanal medication + 50 mg/L of methylene blue without activation (MB_{50WA} + $Ca[OH]_2$). G4, 4C, 4M, 4A – Transaxial, cervical, middle and apical slices of intraradicular dentin after treatment with calcium hydroxide intracanal medication + 100 mg/L of methylene blue without activation (MB_{100WA} + $Ca[OH]_2$). G5, 5C, 5M, 5A - Transaxial, cervical, middle, and apical slices of intraradicular dentin after treatment with calcium hydroxide intracanal medication + 50 mg/L of methylene blue activated by red laser (λ 660 nm) (MB_{50A} + $Ca[OH]_2$). G6, 6C, 6M, 6A – Transaxial, cervical, middle, and apical slices of intraradicular dentin after treatment with calcium hydroxide intracanal medication + 100 mg/L of methylene blue activated by red laser (λ 660 nm) (MB_{100A} + $Ca[OH]_2$). White arrows indicate the presence of voids on the luting interface.

Chapter 2

Figure 1. Specimen preparation. A, Bovine incisors and removal of anatomic crowns. B, Standardization of root canal diameter and length. C, Apical portion sealing. D, Antimicrobial photodynamic therapy session. E, Insertion of calcium hydroxide medication into root canals. F, Specimen obturation. G, Obtainment of 1.3-mm thick intraradicular slices for the mechanical properties analyses. H, Specimen preparation for the Raman microscopy analysis. I, Specimen preparation for the Micro-CT analysis. J, SEM and EDS analyses.

Figure 2. Scanning electron microscopy images of each experimental group under original magnification (×300). A - intraradicular dentin irrigated with deionized water solution (negative control group). B - intraradicular dentin irrigated with deionized water and filled with calcium hydroxide intracanal medication ($Ca[OH]_2$) (positive control group). C - intraradicular dentin after treatment $Ca[OH]_2$ + methylene blue 50 mg/L without activation (MB_{50WA} + $Ca[OH]_2$). D - intraradicular dentin after treatment with $Ca[OH]_2$ + methylene blue 100 mg/L without activation (MB_{100WA} + $Ca[OH]_2$). E - intraradicular dentin after treatment with $Ca[OH]_2$ + methylene blue 50 mg/L activated by red laser(MB_{50A} + $Ca[OH]_2$). F - intraradicular dentin after treatment with $Ca[OH]_2$ + methylene blue 100 mg/L activated by red laser (MB_{100A} + $Ca[OH]_2$).

Figure 3. Energy dispersive x-ray spectra of intraradicular dentin surface according to each experimental group. A - intraradicular dentin irrigated with deionized water solution (negative control group). B - intraradicular dentin irrigated with deionized water and filled with calcium hydroxide intracanal medication ($Ca[OH]_2$) (positive control group). C - intraradicular dentin after treatment $Ca[OH]_2$ + methylene blue 50 mg/L without activation (MB_{50WA} + $Ca[OH]_2$). D - intraradicular dentin after treatment with $Ca[OH]_2$ + methylene blue 100 mg/L without activation (MB_{100WA} + $Ca[OH]_2$). E - intraradicular dentin after treatment with $Ca[OH]_2$ + methylene blue 50 mg/L activated by red laser(MB_{50A} + $Ca[OH]_2$). F - intraradicular dentin after treatment with $Ca[OH]_2$ + methylene blue 100 mg/L activated by red laser (MB_{100A} + $Ca[OH]_2$).

Figure 4. Images from MicroCT of each experimental group and intraradicular dentin thirds (DataViwer Software). 1C, 1M, 1A - Cervical, middle, and apical slices of intraradicular dentin irrigated with deionized water solution (negative control group). 2C, 2M, 2A - Cervical, middle, and apical slices of intraradicular dentin after irrigated with deionized water and filled with calcium hydroxide intracanal medication ($Ca[OH]_2$) (positive control group). 3C, 3M, 3A - Cervical, middle, and apical slices of intraradicular dentin after treatment $Ca[OH]_2$ + methylene blue 50 mg/L without activation (MB_{50WA} + $Ca[OH]_2$). 4C, 4M, 4A - Cervical, middle and apical slices of intraradicular dentin after treatment with $Ca[OH]_2$ + methylene blue 100 mg/L without

activation (MB_{100WA} + $Ca[OH]_2$). 5C, 5M, 5A - Cervical, middle, and apical slices of intraradicular dentin after treatment with $Ca[OH]_2$ + methylene blue 50 mg/L activated by red laser(MB_{50A} + $Ca[OH]_2$). 6C, 6M, 6A - Cervical, middle, and apical slices of intraradicular dentin after treatment with $Ca[OH]_2$ + methylene blue 100 mg/L activated by red laser (MB_{100A} + $Ca[OH]_2$).

Listas de Tabelas

Chapter 1

Table 1. Materials, classification, composition, and batch numbers of the materials used

Table 2. Distribution of the experimental groups.

Table 3. Mean ± standard deviation values of bond strength (push-out) (MPa) of the intraradicular dentin as a function of the experimental groups and intraradicular

Table 4. Scores of the adhesive interface morphology as a function of the experimental groups and intraradicular thirds.

Table 5. Mean ± standard deviation values of volume (mm^3) and quantification of voids formation on resin cement as a function of the experimental groups and intraradicular thirds.

Chapter 2

Table 1. Materials, classification, composition, and batch numbers of the materials used

Table 2. Distribution of the experimental groups.

Table 3. Mean ± standard deviation values of Martens hardness (GPa) and elastic modulus (GPa) of dentin substrate as a function of the experimental groups and intraradicular thirds.

Table 4. Mean ± standard deviation values of Martens hardness (GPa) and elastic modulus (GPa) of resin cement as a function of the experimental groups and intraradicular thirds.

Table 5. Mean ± standard deviation values of degree of conversion (%) of the resin cement as function of the experimental groups and intraradicular thirds.

Table 6. Mean ± standard deviation values of volume (mm^3) and quantification of gaps formation on resin cement as a function of the experimental groups and intraradicular thirds.

LISTA DE ABREVIATURAS, SÍMBOLOS E SIGLAS

α Alpha

> Maior que

< Menor que

≥ Maior ou igual

≤ Menor ou igual

oC Grau Celsius

± Mais ou menos

≅ Aproximadamente igual

% Percentagem

µm Micrometro

µg Micro grama

TFD Terapia Fotodinamica

FS Fotossensibilizador

RU Resistencia de União

PFV Pino de Fibra de Vidro

PBM Preparo Biomecânico

AM Azul de Metileno

CR Canais Radiculares

$Ca(OH)_2$ Hidróxido de Cálcio

MEV Microscopia Eletrônica de Varredura

EDS Espectroscopia de Energia Dispersiva

micro-CT Microtomografia Computadorizada

G1, G2, G3, G4, G5 e **G6** Grupos 1 a 6

PDT Photodynamic Therapy

GFP Glass fiber Post

PS Photossensitizer

BP Biomechanical Preparation

MB Methylene Blue

SEM Scanning Electron Microscopy

CFM Confocal Fluorescense Microscopy

DC Degree of Conversion

Banci HA. Influência da terapia fotodinâmica e do hidróxido de cálcio nas propriedades da dentina intrarradicular e do cimento resinoso, resistência de união dos pinos de fibra de vidro, caracterização e morfologia da interface adesiva [tese]. Araçatuba: Universidade Estadual Paulista "Júlio de Mesquita Filho" (UNESP), Faculdade de Odontologia; 2023.

1) RESUMO GERAL

O objetivo do presente estudo consistiu em avaliar o efeito da terapia fotodinâmica (TFD) e da medicação intracanal de hidróxido de cálcio, nas propriedades mecânicas (dureza Martens e módulo de elasticidade) e grau de conversão. Além disso, avaliou a resistência de união (RU) de pinos de fibra de vidro (PFV), analisou a morfologia e caracterização da interface adesiva. Foram utilizados dentes incisivos bovinos onde foram realizados o preparo biomecânico (PBM) em todos os canais radiculares (CR). Foi empregado o fotossensibilizador azul de metileno (AM) ativado com Laser vermelho. Grupos experimentais: G1-PBM + Água Deionizada (Controle Negativo); G2-PBM + Água Deionizada + $Ca(OH)_2$ (Controle Positivo); G3-PBM + AM 50 mg/L + $Ca(OH)_2$; G4-PBM + AM 100 mg/L + $Ca(OH)_2$; G5-PBM + AM 50 mg/L + Laser Vermelho (TFD) + $Ca(OH)_2$; G6-PBM + AM 100 mg/L + Laser Vermelho (TFD) + $Ca(OH)_2$. Após o período de 14 dias de medicação intracanal a mesma foi removida e os CR foram obturados e preparados para a cimentação dos PFV. **Estudo 1:** A resistência de união dos PFV foi mensurada por *push-out* dos *slices* obtidos (cervical, médio e apical). O padrão de fratura das amostras foi qualificado pela Microscopia Eletrônica de Varredura (MEV). A morfologia da interface entre o cimento resinoso e o tecido dentinário intrarradicular foi caracterizada pela Microscopia Confocal de Fluorescência (MCF). **Estudo 2:** Após a obtenção dos *slices* dos terços cervical, médio e apical, as propriedades dureza Martens e módulo de elasticidade foram avaliadas no substrato dentinário e no cimento resinoso com ultramicrodurômetro. A identificação da composição química do substrato dentinário foi analisada pela Espectroscopia de Energia Dispersiva (EDS). O grau de conversão do material resinoso foi analisado pela Espectroscopia de Raman. O volume e a presença de bolhas foram analisados pela Microtomografia computadorizada (micro-CT). Para a resistência de união os grupos Controle Positivo ($p=0,0058$) e G4 ($p=0,0080$), no terço apical apresentou menores valores de resistência de união em relação ao terço cervical e ao terço médio. Para os grupos G3 e G5, o terço apical apresentou menores valores de resistência de união em relação ao terço cervical ($p>0,05$). Para o terço apical, os grupos G4 apresentaram menores valores de resistência de união em relação aos grupos Controle Negativo e G6 ($p=0,0020$). O tipo de falha mista verificada por MEV, foi o mais encontrado em todos os grupos. Não houve diferença estatisticamente significante na interface adesiva ($p>0,05$). Os menores valores de dureza da dentina foram observados para o grupo G4 onde o terço apical apresentou valores menores em relação ao terço médio ($P < 0,05$). Para o módulo de elasticidade o grupo G4 apresentou valores mais baixos para

o terço apical quando comparado ao terço médio (P < 0,05). Já para o cimento resinoso a dureza quando comparando grupos para o terço médio o G6 e o Controle Positivo demonstraram menores valores que os demais grupos (P<0,05). Os dados do modulo de elasticidade mostraram que comparando o terço cervical entre os grupos G4 teve menores valores quando comparado ao Controle Negativo, G3 e G5 (P<0,05). A composição química observada por EDS, se manteve constante em todas as amostras analisadas com o Ca+ sendo o elemento mais abundante e o P^- com mais variações. Para o grau de conversão o terço cervical do grupo G6 apresentou valores inferiores quando comparado ao grupo Controle Positivo (P<0,05). Para o volume de bolhas os dados do grupo G6 para o terço cervical mostraram um maior volume de bolhas quando comparados aos terços médio e apical (P<0,05). Além disso, o terço apical do mesmo grupo apresentou maior volume de bolhas quando comparado ao terço médio (P<0,05). A TFD com FS azul de metileno 50 mg/L, associado à medicação intracanal de hidróxido de cálcio não afetou negativamente a resistência de união dos pinos de fibra à dentina intrarradicular em qualquer profundidade do canal radicular e não alterou a morfologia da interface adesiva. Além disso, não afetou negativamente as propriedades mecânicas do canal radicular e não alterou a composição química da interface adesiva e o volume das bolhas.

Palavras-chave: Hidróxido de cálcio, terapia fotodinâmica, resistência ao cisalhamento, espectroscopia de energia dispersiva, análise espectral Raman, microscopia confocal, microtomografia por raio-x.

Banci HA.
Influence of photodynamic therapy and calcium hydroxide on the properties of intraradical dentin and resin cement, bond strength of fiberglass posts, characterization and morphology of the adhesive interface [thesis]. Araçatuba: UNESP – São Paulo State University; 2023.

2) ABSTRACT

The objective of the present study was to evaluate the effect of photodynamic therapy (PDT) and the intracanal medication of calcium hydroxide, on the mechanical properties and the degree of conversion. Furthermore, it is intended to evaluate the bond strength of glass-fiber posts (GFP), to analyze the morphology and characterization of the adhesive interface. It will be used bovine incisor teeth, which the biomechanical preparation (BP) in all root canals (RC) will be performed. To realize the PDT methylene blue (MB) PS will be used, activated with Red Laser. Experimental groups: G1-BP + Deionized Water (Negative Control); G2-BP + Deionized Water + $Ca(OH)_2$ (Positive Control); G3-BP + MB 50 mg/L + $Ca(OH)_2$; G4-BP + MB 100 mg/L + $Ca(OH)_2$; G5-BP + MB 50 mg/L + Red Laser (PDT) + $Ca(OH)_2$; G6-BP + MB 100 mg/L + Red Laser (PDT) + $Ca(OH)_2$. After the period of 14 days of intracanal medication, it will be removed, and the RC will be filled and prepared for the cementation of the GFPs. **Study 1:** The bond strength of the GFP was measured by push-out of the slices obtained (cervical, middle and apical). The fracture pattern of the samples was qualified by Scanning Electron Microscopy (SEM). The morphology of the interface between the resin cement and the intraradical dentin tissue was characterized by Confocal Fluorescence Microscopy (CFM). **Study 2:** After obtaining the cervical, middle and apical third slices, the Martens hardness and elastic modulus properties were evaluated in the dentin substrate and in the resin cement with an ultramicrodurometer. The identification of the chemical composition of the dentin substrate was analyzed by Energy Dispersive Spectroscopy (EDS). The degree of conversion of the resinous material was analyzed by Raman Spectroscopy. The volume and presence of bubbles were analyzed by Computed microtomography (micro-CT). For the bond strength of the positive control ($p=0.0058$) and G4 ($p=0.0080$) groups, the apical third presented lower values of bond strength in relation to the cervical third and the middle third. For groups G3 and G5, the apical third presented lower values of bond strength in relation to the cervical third ($p>0.05$). For the apical third, the G4 groups presented lower values of bond strength in relation to the negative control and G6 groups ($p=0.0020$). The mixed failure type was the most found in all groups. There was no statistically significant difference in the adhesive interface ($p>0.05$). There was no statistically significant difference in the adhesive interface ($p>0.05$). The lowest hardness values were observed for the G4 group where the apical third presented lower values in

relation to the middle third (P < 0.05). For the modulus of elasticity, the G4 group presented lower values for the apical third when compared to the middle third (P < 0.05). As for the resin cement, the hardness when comparing groups for the middle third, the G6 and the positive control showed lower values than the other groups (P<0.05). Data on the modulus of elasticity showed that comparing the cervical third between the G4 groups had lower values when compared to the negative control, G3 and G5 (P<0.05). The chemical composition remained constant in all samples analyzed with Ca being the most abundant element and P with the most variations. For the degree of conversion, the cervical third of the G6 group showed lower values when compared to the positive control group (P < 0.05). Finally, for the bubble volume. Data from the G6 group for the cervical third showed a greater volume of bubbles when compared to the middle and apical thirds (P < 0.05). In addition, the apical third of the same group had a greater volume of bubbles when compared to the middle third (P < 0.05). The use of a PDT application with 50 mg/L methylene blue PS associated with intracanal calcium hydroxide medication did not negatively affect the bond strength of fiber posts to intraradicular dentin at any depth of the root canal and did not change the morphology of the interface. adhesive. Furthermore, it did not adversely affect the mechanical properties at any root canal depth and did not change the chemical composition of the adhesive interface and bubble volume.

Keywords: Calcium hydroxide, photodynamic therapy, bond strength, spectrum analysis Raman, confocal microscopy, X-Ray Microtomography.

3) INTRODUÇÃO GERAL

O tratamento endodôntico tem como principal objetivo a descontaminação eficaz do sistema de canais radiculares (SCR) em dentes com necrose pulpar (1). Para este objetivo ser alcançado lançamos mão de diferentes estratégias terapêuticas como: preparo biomecânico do canal radicular (PBM) (2), uso de soluções irrigadoras de hipoclorito de sódio (2,3) e emprego de medicação intracanal de hidróxido de cálcio (4-7), diminuindo assim, a carga de micro-organismos (MO) e seus produtos tóxicos (2). Entretanto, estudos apontam que somente o PBM combinado às soluções irrigadoras e a medicação intracanal, não permitem que o SCR fique totalmente isento dos MO, devido à complexidade anatômica principalmente em casos de infecções persistentes (8). Portanto, novas estratégias terapêuticas são constantemente investigadas a fim de erradicar as infecções endodônticas.

Com o avanço dos aparelhos de Laser e Led, inovações ocorreram para diversos tratamentos na Área da Saúde (9,10), como por exemplo, a terapia fotodinâmica (TFD), que consiste na ação de um fotossensibilizador exógeno (FS) que quando ativado por uma luz de comprimento de onda específico (Laser ou Led) tem a finalidade de promover uma destruição seletiva em um sítio específico (célula-alvo) (11-13).

O mecanismo de ação básico se dá quando o FS absorve os fótons da luz irradiada e seus elétrons passam do estado normal para o mais estimulado. Na presença de oxigênio, o FS transfere sua energia ao substrato. Ao retornar ao seu estado normal, forma espécies altamente reativas e de vida curta (oxigênio singleto), oxidação de lipídios, aminoácidos e proteínas, que levam nos locais específicos a desencadear injúrias como: necrose, apoptose, autofagia e inativação dos MO, ou seja, destruição da célula-alvo (14-19).

A TFD é utilizada na Endodontia após a realização do PBM e antes do emprego da medicação intracanal de hidróxido de cálcio, para potencializar a descontaminação do SCR (20-25). Estudos comprovam que a TFD aumenta a desinfecção do canal radicular, pois ao contrário dos antibióticos, que possuem uma ação específica, o oxigênio singleto derivado de uma reação fotodinâmica tem um mecanismo de ação inespecífico, evitando o desenvolvimento de resistência microbiana (20-25).

Dentre os FS encontrados comercialmente, destacamos o azul de metileno (cloreto de metiltionínio), que é um composto químico, desinfetante e antisséptico, empregado como corante ou indicador nas reações de oxirredução (26). O azul de metileno possui características fotossensibilizadoras, sendo utilizado na TFD, por possuir uma banda de absorção na faixa de 500nm a 700nm, portanto este é ativado pela luz vermelha (27,28). O azul de metileno quando ativado reage resultando no oxigênio singleto, o que poderia influenciar no processo de polimerização e nas propriedades mecânicas do material resinoso e da dentina radicular,

comprometendo diretamente a longevidade e o sucesso da reabilitação oral com pinos de fibra de vidro (PFV) (29,30).

Além disso, o FS azul de metileno é um composto hidrofílico que causa a sorção de água, que pode potencializar a deterioração da resistência de união o que vai de encontro com os achados de Wainright et al. 1997 (36), onde foi descrito que a sorção está diretamente relacionada com a concentração do FS utilizado (32,36).

O FS azul de metileno sendo uma substância catiônica que se liga a moléculas aniônicas, como o fosfato presente na hidroxiapatita e na dentina, influencia a relação cálcio/fosfato (32,37). A reação entre o FS azul de metileno e fosfato resulta em precipitados que agem como uma barreira física formando uma película entre a interface do cimento resinoso e da dentina intrarradicular podendo ou não influenciar a sua resistência de união (32). Desta forma, as propriedades mecânicas da dentina intrarradicular e do cimento resinoso devem ser avaliadas.

A dureza Martens que é a capacidade da superfície do material em resistir à penetração por uma ponta, sob uma carga específica. Este teste é adequado para testes de dureza da maioria dos materiais sólidos (41). A razão é que o valor da dureza vem da profundidade de indentação sob carga de trabalho e, portanto, é menos afetado pelas propriedades visco-elásticas e ópticas do material. Inclui os efeitos da deformação elástica e plástica e efeitos visco-elásticos durante o carregamento. Além disso, a geometria do penetrador, idêntica ao penetrador de diamante piramidal de Vicker, torna o resultado teoricamente independente da força de teste escolhida (41).

O módulo de elasticidade, é definido como um objeto ou resistência da substância a ser deformado elasticamente (isto é, não permanentemente) quando uma força é aplicada a este. O módulo de elasticidade é calculado como a inclinação da curva tensão-deformação na região de deformação elástica. Além disso, um módulo de recuo pode ser avaliado a partir de técnicas de profundidade de indentação, como a inclinação da linha tangente adaptada ao início (na força máxima) da curva de profundidade de recuo não linear (42). Suzuki et al. 2015 (43), que avaliaram as propriedades mecânicas dureza Martens e módulo de elasticidade da dentina na interface adesiva entre cimentos resinosos em diferentes terços da dentina intrarradicular. Entretanto, estas propriedades mecânicas em relação ao emprego da TFD para a Endodontia, apresentavam-se escassas na literatura pertinente nesta época.

Na busca destas respostas, concluímos um Projeto de Pesquisa sobre a influência da TFD com FS azul de metileno na dentina intrarradicular investigando as propriedades mecânicas (dureza Martens e o módulo de elasticidade) (44). Os resultados demonstraram favoráveis ao emprego da TFD, pois não houve influência negativa nas propriedades mecânicas da dentina intrarradicular. Porém, estas propriedades foram estudadas com apenas uma aplicação de TFD e sem a associação com a medicação intracanal de hidróxido de cálcio.

A espectroscopia de Raman permite avaliar a qualidade de polimerização do cimento resinoso (grau de conversão) utilizado na cimentação de dispositivos intrarradiculares, uma vez que este estará sujeito a terapia fotodinâmica e seus produtos de reação, como também, a medicação intracanal na dentina intrarradicular (45).

A resistência de união de pinos intrarradiculares, que geralmente são indicados para restaurar dentes com grande perda estrutural, é uma importante característica a ser estudada. A escolha por este tipo de material é baseada na estética e no aumento de retenção da reabilitação final (46,47). Para analisar a retenção de pinos de fibra de vidro em diferentes regiões do canal radicular, podemos dispor dos testes mecânicos de microtração e cisalhamento por extrusão (*push-out*), uma vez que o preparo das amostras é simples, com número mínimo de falhas prematuras (48,49). A microscopia eletrônica de varredura (MEV) (32,49), por sua vez, permite analisar a amostra após o teste de *push-out* e permite visualizar o tipo de falha da amostra, podendo ser: falha adesiva, falha coesiva ou falha mista. Na microscopia eletrônica de varredura a imagem é formada a partir dos elétrons secundários e os retroespalhados. À medida que o feixe de elétrons primários vai varrendo a amostra estes sinais vão sofrendo modificações de acordo com as variações da superfície. Os elétrons secundários fornecem imagem de topografia da superfície da amostra e são os responsáveis pela obtenção das imagens de alta resolução, já os retroespalhados fornecem imagem característica de variação de composição (49).

A espectroscopia de energia dispersiva (EDS) por sua vez pode ser usada para determinar a caracterização dos elementos químicos presentes na amostra e pode ser usada para estimar sua abundância relativa. Dessa maneira, é possível também fornecer informações complementares sobre a dureza associando os achados das duas metodologias (50).

Para melhor analisar a morfologia da interface adesiva utilizamos microscopia confocal de fluorescência (MCF). Este método tem como objetivo avaliar a micropermeabilidade e a capacidade de selamento dos *tags* resinosos, por meio da utilização de corantes fluorescentes sobre o substrato dentário intrarradicular e o cimento resinoso (51). Estes corantes, os quais são utilizados em baixas concentrações, não interferem nas propriedades dos materiais resinosos, permitindo, assim, avaliar a subsuperfície do espécime (52). Trata-se de um método não-destrutivo, que oferece mais detalhes com relação a identificação das diferentes estruturas que constituem a interface adesiva, com menos artefatos e menor formação de halos na imagem para essa finalidade, em comparação à microscopia eletrônica de varredura (MEV) (53,54).

A Microtomografia Computadorizada (micro-CT) permite avaliar além do volume de cimento resinoso a presença de bolhas, gerando uma imagem tridimensional. A imagem obtida por micro-CT é considerada um método não invasivo e reprodutível que permite a aquisição de

dados quantitativos sem comprometer as amostras. (55,56,57). Essa tecnologia é considerada ideal para quantificar o volume de material de preenchimento (58,59).

Porém, poucos estudos da resistência de união relacionando à TFD na Endodontia foram encontrados na literatura pertinente. Portanto, esta escassez de resultados nos estimulou a buscar respostas, e desenvolver um Projeto de Pesquisa, que avaliou a influência da TFD realizada antes da obturação dos canais radiculares com diferentes FSs (32,42,48,49), na resistência de união de pinos de fibra de vidro. Os resultados com os FSs azul de metileno ou curcumina (ambos sem medicação intracanal de hidróxido de cálcio), demonstraram que a TFD não influenciou negativamente na resistência de união de pinos de fibra de vidro à dentina intrarradicular. Vale a pena destacar que parte destes estudos receberam o apoio da FAPESP, Processo Nº: 2015/06056-3 e Processo Nº: 2016/24718-6 (32,49).

Entretanto, existem poucos estudos sobre o emprego da influência da TFD na resistência de união de pinos de fibra de vidro, em dentes que previamente receberam a medicação intracanal de hidróxido de cálcio (Processo FAPESP Nº: 2019/16171-5). Sendo assim, a aplicação de TFD foi após o PBM e antes da medicação intracanal de hidróxido de cálcio. Assim, podemos responder nosso atual questionamento, sobre o efeito da TFD e da medicação intracanal de hidróxido de cálcio, na dentina intrarradicular e na polimerização do cimento resinoso, que pode influenciar ou não a resistência de união dos pinos de fibra de vidro dentina radicular.

No presente momento há questionamentos que necessitam ser bem elucidados e carecem de evidências científicas para o emprego da TFD na Endodontia empregando o FS azul de metileno, o que encorajou a realização do presente Projeto de Pesquisa.

Desta forma, o estudo das propriedades mecânicas da dentina intrarradicular e do cimento resinoso, resistência de união de pinos de fibra de vidro, interface adesiva e composição química e morfologia dos substratos submetidos a TFD com o FS azul de metileno seguido de medicação intracanal de hidróxido de cálcio, além do volume de formação de bolhas torna este trabalho oportuno e de grande relevância científica, a fim de constituir melhores embasamentos científicos do assunto pertinente.

A importância circunstancial da necessidade do desenvolvimento deste trabalho consistiu em determinar protocolos mais precisos para o emprego TFD na Endodontia com o FS azul de metileno, analisando se existe alguma influência ou não desta terapia realizada na presença da medicação de hidróxido de cálcio e na interface adesiva entre o cimento resinoso nos diferentes terços da dentina intrarradicular.

4) OBJETIVOS

4.1) Objetivo Geral

Neste projeto de pesquisa foram avaliados o emprego da terapia fotodinâmica e a medicação intracanal de hidróxido de cálcio: nas propriedades mecânicas da dentina intrarradicular e do cimento resinoso. Além disso, foram avaliadas a resistência de união de pinos de fibra de vidro, a morfologia da interface adesiva e caracterização da composição química entre o cimento resinoso e a dentina intrarradicular e o volume de bolhas na interface adesiva.

4.2) Objetivos Específicos

O objetivo do presente estudo avaliou os efeitos da terapia fotodinâmica com o fotossensibilizador azul de metileno e da medicação intracanal de hidróxido de cálcio:

1) Avaliou a resistência de união dos pinos de fibra de vidro na dentina intrarradicular pelo teste de *push-out*, analisou o padrão de fratura das amostras representativas por meio da microscopia eletrônica de varredura (MEV), analisou a morfologia da interface entre o cimento resinoso e o tecido dentinário intrarradicular pela Microscopia Confocal de Fluorescência (MCF);

2) Nas propriedades na dentina intrarradicular por meio da dureza Martens e módulo de elasticidade pelo Ultramicrodurômetro Digital, identificou e caracterizou a composição química do substrato da dentina intrarradicular pela Espectroscopia de Energia Dispersiva (EDS), o Grau de conversão do cimento resinoso pela Espectroscopia de Raman e o volume e presença de bolhas pela Microtomografia computadorizada (micro-CT).

As hipóteses nulas testadas foram: a) A terapia fotodinâmica com a medicação intracanal de hidróxido de cálcio não alteraria as propriedades mecânicas da dentina intrarradicular, cimento resinoso e resistência de união de pinos de fibra de vidro à dentina radicular além da a morfologia da interface entre o cimento resinoso e o tecido dentinário intrarradicular e a composição quimica do substrato, grau de conversão do cimento resinoso e volume de bolhas da interface adesiva; b) A terapia fotodinâmica com a medicação intracanal de hidróxido de cálcio não modificaria essas mesmas caracteristicas porém nos dos terços radiculares.

Chapter 1

5) *CHAPTER* 1

IN VITRO STUDY ON HOW PHOTODYNAMIC THERAPY AND CALCIUM HYDROXIDE MEDICATION INFLUENCE ADHESIVE INTERFACE PROPERTIES OF GLASS-FIBER POSTS TO INTRARADICULAR DENTIN

5.1 Abstract

Purpose: This in vitro study evaluated the influence of antimicrobial photodynamic therapy (aPDT), using methylene blue (MB) as photosensitizer (PS) and calcium hydroxide (CH) as intracanal medication on adhesive bond strength, sealing, and integrity of the luting interface of glass-fiber posts to different thirds of endodontically treated root canal dentin.

Material and Methods: 102 incisors were sorted into 6 groups: a negative control irrigated with deionized water; a positive control irrigated with deionized water and filled with CH; CH + MB 50 mg/L without laser radiation; CH + MB 100 mg/L without laser radiation; CH + MB 50 mg/L radiated by red laser; and CH + MB 100 mg/L radiated by red laser. Push-out bond strength (n = 8), adhesive interface sealing (n = 3), and volume and quantification of voids (n = 6) were assessed using a universal testing machine, confocal laser scanning mi- croscope, and computerized microtomography, respectively. Scanning electron micrographs were obtained from representative samples to qualify the fracture patterns. Push-out bond strength and adhesive interface integrity data were subjected to 2-way ANOVA for repeated measures followed by Tukey's test ($\alpha = 0.05$). Adhesive interface sealing was evaluated by the inter-examiner Kappa test and submitted to Kruskal-Wallis and Dunns tests ($\alpha = 0.05$).

Results: Assessing the apical region, the positive control and MB_{100WA}+$Ca(OH)_2$ groups showed lower adhesive bond strength compared to the MB_{100A}+$Ca(OH)_2$ group ($P < 0.05$). The cervical third showed higher bond strength than the apical third for the positive control, MB_{50WA}+$Ca(OH)_2$, MB_{100WA}+$Ca(OH)_2$, and MB_{50A}+$Ca(OH)_2$ groups ($P < 0.05$). A prevalence of mixed failure was observed in all experimental groups. There were no statistically significant differences in adhesive interface sealing for any of the parameters assessed ($P > 0.05$). MB_{100WA}+$Ca(OH)_2$ and MB_{100A}+$Ca(OH)_2$ groups promoted a higher volume and quantification of voids compared to the negative control group evaluating the cervical third ($P < 0.05$). In general, there were no differences in the quantification of voids comparing the intraradicular thirds ($P > 0.05$), differently to the volume of voids in which, in general, the cervical third promoted higher values compared to the middle and apical thirds ($P < 0.05$).

Conclusion: aPDT with methylene blue PS at 50 mg/L associated with calcium hydroxide as intracanal medication demonstrated satisfactory bond strength, sealing, and integrity of the adhesive interface at any intraradicular depth.

Keywords: Bond strength; Dentin; Calcium hydroxide; Methylene blue; Photodynamic therapy; Resin cements.

5.2. INTRODUCTION

The success and longevity of endodontic treatment and the reconstruction of teeth with excessive coronal structure loss using glass-fiber posts or endocrowns are directly related to factors such as the mechanical properties of intraradicular dentin, adhesion effectiveness, and satisfactory bacterial microbiota eradication.[1] Several clinicians still use post retained restoration and a crown, as this technique increases the assembly restoration into the root canal.[2,3] According to Lin et al., endocrown and post retained restorations present similar performance under normal occlusion, showing similarity of failure probability.[2] Studies demonstrate unsatisfactory results of conventional methods on the reduction in microorganisms and inflammatory processes, such as biomechanical instrumentation and irrigating agents.[4,5] Due to the anatomical complexity of root canal systems, endodontic instruments and chemical solutions are unable to completely reach deeper intraradicular regions, such as apical thirds, favoring the occurrence of persistent infections.[6]

Enterococcus faecalis is one of the main causes of persistent infections in endodontic treatment.[7,8] Calcium hydroxide ($Ca[OH]_2$) is a strongly alkaline compound, with a pH ≅ 12.5, presenting antimicrobial and biological effects, such as the dissolution of tissues and biofilms, inhibition of tooth resorption, and induction of hard tissue repair, being the gold standard of intracanal medication for persistent infections.[9,10] However, Enterococcus faecalis presents a proton pump that promotes the acidulation of its cytoplasm, and due to its ability to penetrate deep into complex anatomical regions, such as apical deltas, lateral canals, and dentinal tubule constrictions, this pathogen hinders the efficacy of calcium hydroxide medication.[6,11] Several adjunctive therapy modalities have been introduced in oral health to improve the disinfection effectiveness of root canal systems, such as antimicrobial photodynamic therapy (aPDT).[12,13]

Previous studies claim that aPDT alone is unable to completely eradicate the presence of biofilm.[14,15] Biofilm is composed of a community of microorganisms, and its maturation can be 10-1000 times more resistant to treatment using antimicrobial medication, contributing to the development of tolerance in microorganisms.[16,17] This scenario suggests that aPDT application associated with calcium hydroxide intracanal medication potentializes the microbial load reduction.[18,19] Thus, the literature establishes that aPDT is not intended to substitute conventional endodontic therapies, but operates concomitantly with them, aiming at the eradication of persistent infections.[15] Several studies have assessed the influence of different photosensitizers (PSs) at distinct concentrations, irradiated or not by laser, on the mechanical properties and bond strength of glass-fiber posts luted to intraradicular dentin.[1,20-22] However, studies investigating the influence of methylene blue and other PSs at distinct concentrations, activated or not by red laser,

concomitantly with calcium hydroxide action as intracanal medication along the intraradicular dentin are scarce in the literature.[23]

Methylene blue is a hydrophilic compound, presenting a low molecular weight and positive charge, which allow it to easily pass through the membrane of gram-positive and negative bacteria, being a satisfactory choice to be used as PS in PDT.[21] Strazzi-Sahyon et al. assessed the influence of calcium hydroxide intracanal medication and two sessions of methylene blue PS application, radiated or not by red laser, on intraradicular dentin mechanical properties.23 However, because of the lack of in-depth information regarding the influence of aPDT and calcium hydroxide as intracanal medication on the adhesion process, there is no consensus on how the association of these therapies could affect the sealing and integrity of the luting interface of glass-fiber posts to intraradicular dentin. Thus, the purpose of this in vitro study was to determine the influence of methylene blue PS, radiated or not by red laser, with aPDT and calcium hydroxide administered as intracanal medication on the adhesion effectiveness of glass-fiber posts. The push-out bond strength, sealing, and integrity of the luting interface were evaluated of intraradicular restorations to different thirds of endodontically treated root canal dentin. Two null hypotheses were tested, as follows: 1) The performance of methylene blue, activated or not, and calcium hydroxide intracanal medication would not result in differences on push-out bond strength, sealing, and integrity of the luting interface of glass-fiber posts to intraradicular dentin; and 2) different depths of intraradicular dentin treated with methylene blue PS, activated or not, and calcium hydroxide intracanal medication would not promote differences on glass-fiber post adhesion effectiveness.

5.3. MATERIAL AND METHODS

5.3.1 Experimental design

The information regarding the materials used in the present study is listed in Table 1. This in vitro study was analyzed and approved by the local ECUA (Ethics Committee on the Use of Animals; Protocol: #18–01003).

A total of one hundred and two bovine incisors, from cattle aged from 28 to 34 months, were used.[24-26] Teeth were discarded and substituted if they exhibited any curved roots, fractures, or cracks. Using a low-speed diamond disc under water cooling, the anatomical crowns were divided from the root portion 1.0 mm above the cementum-enamel junction (Fig. 1–A). The canal length and diameter were standardized at 20 mm and 4 mm, respectively (Fig. 1-B). Prior to mechanical instrumentation, the measurement of 1.0 mm less than the original tooth length was established for the working length of the root canals (Fig. 1–B). The root canal instrumentation was performed using endodontic files until reaching the #80 K-file (Maillefer Instruments, Tulsa, OK, USA) (Fig. 1–B), and for each file change the root canals were irrigated with 10 ml of 1%

sodium hypochlorite for 15 s. The canals were then filled with 10 ml of 17% ethylenediaminetetraacetic acid (EDTA) (Biodinâmica Química e Farmacêutica LTDA, Ibiporã, PR, Brazil) for smear layer removal, which remained in contact with the root dentin substrate for 3 min, before being removed using irrigation with 10 ml of distilled water for 15 s and dried with sterile absorbent paper tips (Dentsply Sirona, York, PA, USA) and air jets. To avoid any PS escape, the apical foramens were restored and sealed with dental adhesive (Adper Single Bond 2; 3 M ESPE) and resin composite (Filtek Z350 XT; 3 M ESPE) according to the manufacturer's recommendations (Fig. 1– C).[1,20-22,27]

5.3.2 Experimental groups and aPDT

The endodontically-treated root specimens were randomly sorted into six experimental groups (n = 17), as described in Table 2. In the experimental groups, the methylene blue PS was submitted to a 3 min pre-irradiation period,[27] and agitated for 1 min using ultrasonic equipment (Nac Plus, Adiel LTDA, São Paulo, SP, Brazil) coupled to an ultrasonic tip (Irrisonic E1; Helse Dental Technology, Santa Rosa de Viterbo, SP, Brazil).[1,20-22,27] During the PS agitation, the ultrasonic tip was carefully handled to avoid contact with the root canal walls.[1,20- 23]

The methylene blue PS from the MB50A and MB100A groups was radiated with the red laser (Laser Duo - 660 nm wavelength; MMO, São Carlos, SP, Brazil) for 1 min using a 300-µm flexible optical fiber, resulting in a final energy of 72 J/cm2 (Fig. 1–Da).[1,21,22,27,28] The radiation was performed by applying helicoidal movements of the optical fiber in the cervical- apical direction (10 times/minute) at a depth of 2 mm less than the root canal working length.[27] In the MB_{50WA} and MB_{100WA} groups, the methylene blue PS was not radiated (without activation) (Fig. 1–Db). After the treatment, the methylene blue dye was removed from the root canals by irrigation with 10 mL of deionized water, then the canals were dried with air jets and sterile paper.[23]

5.3.3 Calcium hydroxide medication

All the experimental groups, except the negative control group, were filled with calcium hydroxide (Biodinâmica Química e Farmacêutica) mixed with propylene glycol (Farma Formula) and iodoform (Biodinâmica Química e Farmacêutica) using a #4 Lentulo instrument (Maillefer Instruments) for a period of 14 days (Fig. 1–E).[23] Interim cement (Cimpat Branco; Septodont Ltda, Barueri, SP, Brazil) was used to seal the coronal region of the root canal samples. To certify the complete filling of the root canal extension with intracanal medication, radiographic analysis as performed on the tooth specimens (Digital X-Ray – 1.0.9.1; Micro Image, Indaiatuba, SP, Brazil). All sealed root canal specimens were stored at 100% relative humidity at 37ºC. After 14 days,

coronal sealing and calcium hydroxide intracanal medication were removed, and the root canals were cleaned under irrigation with 10 ml of 1% sodium hypochlorite solution and a K #80 file.[23]

5.3.4 Push-out bond strength Analysis

Forty-eight teeth were used for the push-out bond strength analysis (n = 8). MTA Fillapex endodontic cement (Angelus, Londrina, PR, Brazil) and #80 gutta-percha cones and fine (F) and medium-fine (MF) auxiliary cones (Tanari, Manacapuru, AM, Brazil) were inserted into the root canals. The obturation method used was Tagger's technique, with a McSpadden compactor #70 (Maillefer Instruments) (Fig. 1-F).[27] Provisional cement (Cimpat Branco; Septodont Ltda) was used to seal the coronal portion of the specimens, then the samples were kept at 37◦C in 100% humidity for 7 days.[23]

Nine millimeters of gutta-percha was removed using #1 and #2 White Post DCE system drills (White Post DCE #2; FGM, Joinville, SC, Brazil). The #2 double-tapered glass-fiber post (18 mm length, 2.2 mm top diameter, and 1.05 mm bottom diameter) was inserted into the post space to verify the adaptation. The post space was then irrigated with 10 ml of physiological saline solution (0.9%) to remove any debris or residual gutta-percha. The root canals were dried with sterile paper and an air jet.[1,20-22]

The surface of the glass-fiber posts was conditioned with 35% phosphoric acid (3M ESPE) during 60 sec, washed, and dried with an air jet. The conditioned surfaces were then silanized (RelyX Ceramic Primer; 3 M ESPE) for 60 sec, and intraradicular posts that would not be further manipulated were gently dried with an air jet, preventing surface contamination. Dual-cured self-adhesive resin cement (RelyX U200; 3M ESPE) coupled to a mixing root canal tip was used. The tip was introduced into the root canal and the cement was injected into the post space and on the post surface, before the glass-fiber post was settled into the intraradicular canal. The assembly was polymerized for 40 sec from the top root canal surface using a single wave LED light curing unit (Radii-Cal; SDI, Bayswater, Australia) at 1200 mW/cm2. After being stored in 100% relative humidity at 37ºC for seven days, the specimens were cut into 1.3-thick slices for each intraradicular third (cervical, middle, and apical), obtaining one slice per specimen for each intraradicular region (Fig. 1– G). The intraradicular slice thicknesses were confirmed using a digital caliper (Mitutoyo, Aurora, IL, USA).[1,20-22]

Three distinct diameters of active tips were used according to the intraradicular thirds to perform the extrusion testing (push-out bond strength). The tips were coupled to a universal testing machine (DL3000, EMIC, Sao José dos Pinhais, PR, Brazil). The active tip diameter used for the cervical third was 1.90 mm, for the middle third was 1.40 mm, and for the apical third was 1.20 mm (Fig. 1– G). A compressive load was applied onto the center of the glass- fiber post to each

root third in a top (coronal) to bottom (apical) direction, not touching the intraradicular dentin substrate, using the tips at a crosshead speed of 0.5 mm/min.[1,20-22] The push-out bond strength of the glass-fiber posts to the intraradicular dentin was determined according to the following formula:[1,20-22,27]

$$POBS = F/A,$$

where *POBS* is the push-out bond strength, expressed in MPa; *F* is the maximum force, expressed in N; and *A* is the adhesive interface area, expressed in mm^2, calculated using the following equation:[1,20-22,27]

$$A = \pi (R_C + R_A) \sqrt{(R_C - R_A)^2 + h^2},$$

where π is 3.14; R_C and R_A are the largest (coronal) and smallest (apical) post radii, respectively; and h is the height of the third slice, measured with a digital caliper (Mitutoyo).[1,20- 22,27]

5.3.5 Scanning electron microscopy (SEM)

After the bond strength test, root canal dentin samples were cleaved into two pieces to expose the bonding interface and analyzed by a stereomicroscope (Stemi SV11, Zeiss, NY, USA) at ×6 and ×66 magnification to analyze the fracture pattern.[23] The fracture patterns were divided and classified into 1) cohesive failure in dentin; 2) adhesive failure on dentin substrate; and 3) mixed failure. The most representative specimens of each group were sputter-coated with gold using a vacuum metalizing machine (Balzers SCD-050 Sputter Coater, Germany), and submitted to scanning electron microscopy (JSM5600LV, JEOL, Tokyo, Japan) to illustrate the fracture patterns. The micrographs were obtained and recorded under ×30 and ×300 magnification.

5.3.6 Adhesive interface sealing analysis

Eighteen root canals were arranged into six experimental groups (n = 3) as described above and filled with distilled water and fluorescein dye (0.1 %) (FDA, Sigma Chemical Co, St. Louis, MO, USA) for 4 h for the dye to infiltrate into the dentinal tubules (Fig. 1-H).[29] Then, to remove the fluorescein, 10 mL of deionized water was inserted into the intraradicular canals, and the root canals were dried with an air jet and sterile paper points. For adhesive interface sealing analysis, Rhodamine B (FDA, Sigma Chemical Co, St. Louis, MO, USA) was incorporated into the resin cement (16 μg/g) (Fig. 1-H),[29] and the luting procedure was performed as described above for push-out bond strength analysis. Specimens were stored at 100 % relative humidity and at 37°C for 7 days and then sectioned using a diamond saw under water-cooling to obtain different thirds

of the intraradicular dentin, as described above (Fig. 1- I). Slices were assessed from coronal to apex surfaces with a confocal laser scanning microscope (Leica TCS SP2; Leica Microsystems, Heidelberg, Germany), excited with an argon laser at 488 nm and an He-Ne laser at 453 nm (Figure 1-I). Confocal micrographs were obtained and recorded in the fluorescent mode with oil-immersion objective lenses (×40, numerical aperture 1.25).[29] The confocal micrographs were evaluated using two previously calibrated examiners. The evaluation was performed using the double-blind method. In cases where there was disagreement between the two evaluators, the confocal micrographs were re- evaluated until a final consensus was reached.

The following criteria were evaluated:

a) Quality of the dentin/cement adhesive interface:[30]

Score 0 - no cracks, clear, continuous adhesive interface;

Score 1 - partial presence of cracks, partially continuous adhesive interface, present in less than 50% of the interface;

Score 2 - presence of cracks with discontinuous interface, present in more than approximately 50% of the interface.

b) Formation of tags in intraradicular dentin:[30]

Score 0 - not detectable;

Score 1- few tags visible;

Score 2- uniform formation of tags with few lateral branches; Score 3- formation of long tags with many side branches.

c) Tag penetration depth:[30]

Score 0 - no tags;

Score 1 - tags ≤ 3μm on average;

Score 2 - tags = 3 to 8.9 μm on average;

Score 3 - tags ≥ 9 μm on average.

5.3.7 Adhesive interface integrity analysis

Adhesive interface integrity was evaluated in relation to the volume and quantification of voids on the adhesive interface. Six specimens from each experimental group (n = 6) were analyzed in high resolution microtomography (SkyScan 1272; Bruker, Kontich, Belgium).[31,32] The microtomography was calibrated using the standard "phantom" function and operated under power conditions of 80 kilovolts and 125 milli-amps. The images were generated at medium resolution

(13 µm/slice) and at 180o, the specimens were rotated at 0.4o angular steps, with an exposure time of 3000 milliseconds; a 16.5 mm tube and a 1 mm thick aluminum filter were also used.[31,32]

The specimens were scanned following the restorative procedures. The data obtained in the scan were converted into DICOM files and later rendered into 3D models (SolidWorks Corp., MA, USA). Initially, the images were reconstructed in 3D in NRecon software (SkyScan, Kontich, Belgium) from the coronal to the apical portion of the roots. Then, using DataViewer software (SkyScan, Kontich, Belgium), the images were visualized and linearly analyzed in the coronal, sagittal, and transaxial axes, as well as the determination of a standard position for the measurement of volume and quantification of voids.[31,32]

Quantification of voids in the cement layer was performed using CTAnalyser software (SkyScan, Kontich, Belgium) in the transaxial position of the images.[31] Initially, the area to be analyzed was established by selecting an average of 1013 to 1200 slices, followed by image segmentation to separate the desired object from other objects present in the image. Then, a freehand template (area of interest) was designed, delimiting only the cement layer. Subsequently, the images were binarized, and the quantification and volume of voids present in the root canal were calculated.[31] Finally, CTVOX software (SkyScan, Kontich, Belgium) was used to reconstruct these images into three-dimensional models to assess the integrity of the interface by observing areas of the cement that were in discontinuity with the walls of the root canal.[31]

5.3.8 Statistical Analysis

Push-out bond strength, sealing, and integrity of adhesive interface data were submitted to normality (Shapiro-Wilk; Bioestat 2.0 Program) and homogeneity tests (Bartlett; Bioestat 2.0 Program). Push-out bond strength and adhesive interface integrity data were analyzed using two-way repeated measures Analysis of Variance (ANOVA; 5.0 Statview Program; Version 5.0.1). The Tukey protected least significant difference test (α=.05) was also performed. Adhesive interface sealing was evaluated by the inter-examiner Kappa test and submitted to Kruskal-Wallis and Dunn´s tests (α=.05) (SigmaPlot; Version 12.0).

5.4. RESULTS

5.4.1 Push-out Bond Strength

The push-out bond strength values are listed in Table 3. There were no significant differences among the experimental groups for cervical and middle thirds ($P > 0.05$), however, for the apical third, the positive control and MB_{100WA} + $Ca(OH)_2$ groups presented lower values compared to the MB_{100A} + $Ca(OH)_2$ group ($P < 0.05$) (Table 3).

There were no significant differences among distinct intraradicular thirds for the negative control and MB_{100A} + $Ca(OH)_2$ groups ($P > 0.05$) (Table 3). However, for the positive control and MB_{100WA} + $Ca(OH)_2$ groups, the cervical and middle thirds promoted higher bond strength values compared to the apical third ($P < 0.05$). For the MB_{50WA} + $Ca(OH)_2$ and MB_{50A} + $Ca(OH)_2$ groups, only the cervical region promoted higher bond strength values compared to the apical region ($P < 0.05$)(Table3).

When analyzing the intraradicular thirds for each group, a higher incidence of mixed-type failure was observed in all experimental groups (Fig. 2). Figure 3 (A–L) presents the representative scanning electron micrographs of this fracture pattern, showing the presence of resin cement particles bonded to the intraradicular dentin surface.

5.4.2 Adhesive Interface Sealing

The adhesive interface sealing scores and representative confocal scanning laser micrographs are illustrated in Table 4 and Figure 4, respectively. A kappa inter-examiner test was carried out and values of 0.77, 0.81, and 0.78 were obtained for adhesive interface quality, tag formation in dentin, and tag penetration depth parameters, respectively. Regarding the adhesive interface quality, there were no significant differences among the groups ($P > 0.05$) (Table 4), with the score 0 being prevalent, as integrity and a well-organized adhesive interface were noted (Figure 4). In relation to the tag formation in dentin parameter, there were no significant differences between the groups ($P > 0.05$), with a score of 1 prevailing for the negative control, MB_{50WA} + $Ca(OH)_2$, and MB_{100WA} + $Ca(OH)_2$ groups, and a score of 2 prevailing for the positive control, MB_{50A} + $Ca(OH)_2$, and MB_{100A} + $Ca(OH)_2$ experimental groups (Table 4). Regarding the tag penetration depth parameter, there were no significant differences among the experimental groups ($P > 0.05$) (Table 4), with a score of 1 prevailing for the negative control, positive control, MB_{50A} + $Ca(OH)_2$, and MB_{100A} + $Ca(OH)_2$ groups, and a score of 2 prevailing for the MB_{50WA} + $Ca(OH)_2$ and MB_{100WA} + $Ca(OH)_2$ groups (Table 4).

5.4.3 Adhesive interface integrity

5.5. DISCUSSION

The administration of aPDT with methylene blue PS at different concentrations, activated or not by red laser, and associated with calcium hydroxide intracanal medication influenced the push-out bond strength and adhesive interface integrity analyses, thus rejecting the first null hypothesis of the study (Tables 3 and 5). Additionally, significant differences were observed among distinct depths of intraradicular dentin treated with aPDT associated with calcium hydroxide intracanal medication on adhesive resistance and volume of voids of the bonding interface, leading to rejection of the second null hypothesis (Tables 3 and 5).

According to Strazzi-Sahyon et at., aPDT is characterized by photon absorption by a specific PS from a precise wavelength irradiation, promoting electron stimulation. This energy is transmitted to the dental substrate, and in the presence of oxygen promotes free radical generation and highly reactive oxygen species, denominated singlet oxygen.[33] This photophysical-chemical reaction is characterized by an irreversible oxidation process, damaging the target cells and microorganism, and thus promoting microbial load reduction.[34] However, there is a lack of in-depth information regarding the possible effects of this reactive oxygen on the adhesive interface properties, such as bonding resistance, and adhesive interface sealing and integrity, when assessing different concentrations of methylene blue PS, irradiated or not by red laser, associated with calcium hydroxide as intracanal medication along the intraradicular dentin.

Debonding of the resin cement/intraradicular dentin interface is one of the most common factors of intracanal restoration failure, due to the inefficient root canal substrate hybridization.[23] From this perspective, the push-out test is a satisfactory method to investigate the bond strength performance of materials determinate to the intraradicular dentin substrate by applying a specific force compatible with a clinical situation, promoting the restorative assembly displacement.[23] In the present study, despite the non-statistical difference, the administration of methylene blue PS at the higher concentration tended to present glass-fiber posts with lower bond strength values compared to the PS at the lower concentration, regardless of the irradiation by red laser or not (Table 2). Methylene blue PS is characterized as a hydrophilic compound, allowing water sorption, and thus jeopardizing the bond strength of the resin cement to the dentin substrate.[21] According to a study by Wainwright et al., the water sorption intensity is directly proportional to the PS concentration,[35] corroborating the push-out bond strength results and the failure patterns assessed, which demonstrated a higher incidence of mixed failures in the groups submitted to the lowest PS concentration, activated or not by red laser (Figs. 2 and 3).

The adhesive interface was also assessed by micromechanical interactions between the resin cement and intraradicular dentin substrate using confocal laser scanning microscopy. This

methodology consists of the micropermeability evaluation and sealing capacity of the resin monomer infiltration into dentin substrate, qualitatively representing the adhesive interface, containing less artifact interference compared to scanning electron microscopy.[29] As shown by the scores of the confocal analysis and confocal micrographs, there were no differences in the adhesive interface parameters evaluated (Table 4) (Fig. 4). A study carried out by de Oliveira et al. compared different techniques of removing calcium hydroxide intracanal medication from the dentin walls of radicular canals, such as conventional irrigation, passive ultrasonic irrigation, and Easy Clean tools, and observed that none of these alternatives were able to satisfactorily remove all calcium hydroxide medication.[36] Thus, it can be speculated that the presence of remaining calcium hydroxide on intraradicular dentin walls may have influenced the adhesive interface parameters, hampering satisfactory resinous monomer infiltration in the dentinal tubules, and this could explain the lack of differences found in these parameters in the current study (Table 4). Furthermore, the adhesive interface data obtained may be influenced by the penetration depth measurement method adopted in the present investigation, as Eğemen and Belli claim that tubule penetration depth measurement techniques may present varying performances for the intraradicular thirds.[37] Therefore, tubule penetration depth data measured by distinct methods must be interpreted carefully.

However, despite the non-statistical difference, the experimental group of methylene blue PS at the higher concentration, activated by red laser promoted a higher incidence of cracks present on the dentin/cement adhesive interface (Table 4) (Fig. 4). The singlet oxygen formation resulting from an irreversible oxidation process may have interfered in the sealing capacity and quality of the dentin/cement adhesive interface (Table 4) (Fig. 4). This performance corroborates the tendency of the PS to present lower bond strength values at a higher concentration (Table 3).

Common methodologies applied to evaluate void formation at the glass-fiber post/resin cement/dental interface are characterized by destructive and 2D tests, which are vulnerable to false-positive data, without a volumetric scale precision.[31] 3D scanning of luted root canals with intraradicular retainers by microcomputed tomography technology promotes a non-destructive analysis of the external and internal structures of the specimens, allowing their visualization and reconstruction in 3D to detect and measure the presence of gaps and voids in the bonding interface.[31] Furthermore, evaluation of the adhesive interface integrity can be related to push- out analysis,[31] which increases understanding about the influence of aPDT on the adhesion process along the intraradicular dentin.

It can be noted by the microcomputed tomography images that the adhesive interface integrity showed a higher volume and quantification of voids for the experimental groups submitted to methylene blue PS at the higher concentration, activated or not by red laser (Table 5) (Fig. 5). The quantity of singlet oxygen formation is directly equivalent to the PS concentration used,[23] and its presence may affect the adhesive interface of resin-based materials due to the competition of free radicals necessary for the methacrylate polymerization process.[38] Furthermore, it can be speculated that the released oxygen trapped inside the dentinal tubules from the aPDT process may act as a mechanical barrier, hampering the more intimate contact between the resin cement and the intraradicular dentine wall.[38] This fact could corroborate the incidence of a higher adhesive-type failure for the experimental group of methylene blue PS at the higher concentration activated by red laser (Fig. 2), in addition to the greater volume and quantification of voids at the luting interface (Table 5) (Fig. 5).

Comparing distinct regions of intraradicular dentin, there was a tendency for the apical third to exhibit lower bond strength, and volume and quantification of voids than the cervical region (Tables 3 and 5) (Fig. 5). These results can be explained by some factors, such as the anatomical configurations of the root canals, presence of apical sclerosis, difficulty accessing and cleaning the apical third, and reduction in light diffusion capacity at this depth, promoting a lower degree of conversion of the resin cement.[20-23] All these conditions can result in inhomogeneous distribution of the luting agent on the apical third, resulting in lower bond strength values (Table 3).

Furthermore, methylene blue is characterized as a cationic compost that allows binding to anionic compounds, such as the phosphate ions incorporated into hydroxyapatite crystals, thereby reacting with, and influencing the phosphate/calcium ratio.[1,21-23] This reaction forms precipitates, accumulating in higher concentrations in the apical third due to gravity, acting as a physical barrier and satisfactorily avoiding the resin cement/dentin surface interaction.[21] This photosensitizer/phosphate interaction could also justify the lower bond strength values in the apical region (Table 3).

The cervical third exhibits the biggest diameter when compared with the middle and apical intraradicular regions, presenting a higher volume of resin cement, which makes it more susceptible to void formation, proven by the adhesive interface integrity analysis and microcomputed tomography images in the present study (Table 5) (Fig. 5). The highest volume and quantification of voids in the cervical region can be justified by the amount of resin cement and the shrinkage stress performed by the photoactivation process.[39] According to D'Arcangelo et

al., polymerization stress is a crucial factor for the longevity of restorations, and a thicker cement layer would generate higher microporosity and polymerization shrinkage.[39] Another reason that can be mentioned is that the cervical region was subjected to a higher volume of methylene blue compound, increasing its susceptibility to the PS effects and action. All these factors may result in higher void formation, affecting the adhesive interface integrity, as proven by the microcomputed tomography images (Table 5) (Fig. 5).

Strazzi-Sahyon et al., in previous studies, investigated the influence of one and two sessions of aPDT combined with 50 mg/L and 100 mg/L of methylene blue PS, associated or not with laser radiation, on the push-out bond strength of the glass-fiber post to the intraradicular dentin, demonstrating substantially lower bond strength values than those found in the present study (Table 3).[1,21,22] Despite methodological similarities, this difference may be related by the fact that these previous investigations did not evaluate the association of calcium hydroxide as an intracanal medication.[1,21,22] According to Singh et al., calcium hydroxide-based medication leads to an increase in pH in the environment that may favor the photoreaction process, since highly reactive oxygen formation is intensified in an alkaline medium, which could justify the bond strength values of the present study.[14]

As mentioned previously, investigations regarding the influence of methylene blue PS at distinct concentrations, activated or not by red laser, concomitantly with the action of calcium hydroxide as intracanal medication along the intraradicular dentin are scarce in the literature, which makes it difficult to correlate the present results with previously published data. Only one study conducted by Strazzi-Sahyon et al. presented similarities in the methodology and factors evaluated, enabling this correlation.[23] It can be noted that the mentioned study showed slightly higher push-out bond strength values than the present study (Table 3).[23] A possible explanation for this slight difference is that the aforementioned study evaluated two sessions of aPDT, after biomechanical preparation and before the glass-fiber post luting procedure, while the present study assessed only one session.[23] A second therapy session could have potentialized the PS action on the Ca-P ratio, influencing the mineral content of dentin substrate, inducing higher microporosity generation, and promoting higher interaction between the root canal substrate and resin cement, thus favoring the micromechanical retentions.[22]

On the other hand, distinct concentrations of methylene blue PS, associated or not with aPDT, may not always promote satisfactory results in all analyses. In general, the use of laser-irradiated 50 mg/L methylene blue PS associated with calcium hydroxide as intracanal medication resulted in closer values to the negative control group regarding the adhesive interface properties

than laser-irradiated PS at 100 mg/L (Tables 3 – 5) (Figs. 2 – 5).This enables us to assume that using aPDT with methylene blue sensitizer at 50 mg/L associated with calcium hydroxide as intracanal medication is a viable choice as it does not alter the adhesive interface properties of glass-fiber posts to intraradicular dentin.

The use of bovine root canals in this in vitro study is an appropriate and acceptable substitute to human teeth for push-out bond strength analysis.[40] Silva et al. state that bovine teeth exert no influence on the bond strength of intracanal restorations.[24] The authors claim that in this experimental model, the load is applied only to the intracanal retainer and resin cement that completely filled the root canals, providing better control over the type of failure.[24] Furthermore, the choice of employing this experimental model is based on a study previously evaluated by Camargo et al. that investigated the diffusion rate of $Ca(OH)_2$ medication in both human and bovine substrate and found no significant differences between them.[26]

The present in vitro study presents some limitations that should be pointed out, such as the non-homogeneity of dental substrate in relation to the quantity and size of dentinal tubules, non-standardization of the mineral concentrations, difficulty in performing procedures in regions of limited access and visibility, and the use of only one type of $Ca(OH)_2$ paste. The applicability of laboratory results to clinical circumstances must be correlated carefully, as this in vitro research precludes accurately simulating oral cavity conditions, such as the interference of saliva, enzymes, temperature, and microorganisms. Thus, further in-depth longitudinal and clinical investigations should be performed to enrich discussions regarding the influence of aPDT on collagen fibers, permeability, and other physical-mechanical properties under aging conditions, aimed at increasing the use of this therapy in Dentistry.

5.6. CONCLUSION

Based on the methodology and findings of this in vitro study, it is possible to conclude that:

1. Antimicrobial photodynamic therapy with methylene blue photosensitizer, associated with calcium hydroxide as intracanal medication influenced the bond strength and adhesive interface integrity of glass-fiber posts to intraradicular dentin.

2. Intraradicular depth also had an influence on push-out bond strength and adhesive interface integrity.

3. Methylene blue at 50 mg/L associated with calcium hydroxide as intracanal medication is a suitable photosensitizer and concentration to be applied for intracanal disinfection subsequent to the biomechanical procedure, as, in general, it yields satisfactory bond strength, sealing, and integrity of the adhesive interface at any intraradicular depth.

5.7 REFERENCES

1. Strazzi Sahyon HB, Pereira da Silva P, Silva de Oliveira M, Angelo Cintra LT, Gomes-Filho JE, Henrique dos Santos P & Sivieri-Araujo G (2018) Effect of photodynamic therapy on the mechanical properties and bond strength of glass-fiber posts to endodontically treated intraradicular dentin *The Journal of Prosthetic Dentistry* **120(2)** 317.

2. Govare N & Contrepois M (2020) Endocrowns: A systematic review The Journal of Prosthetic Dentistry 123(3) 411-418.

3. Lin CL, Chang YH, Chang CY, Pai CA & Huang SF (2010) Finite element and Weibull analyses to estimate failure risks in the ceramic endocrown and classical crown for endodontically treated maxillary premolar European Journal of Oral Science 118(1) 87-93.

4. Josic U, Mazzitelli C, Maravic T, Fidler A, Breschi L & Mazzoni A (2022) Biofilm in endodontics: in vitro cultivation possibilities, sonic-, ultrasonic- and laser-assisted removal techniques and evaluation of the cleaning efficacy. Polymers (Basel) 14(7) 1334.

5. Martinho FC, Corazza BJM, Khoury RD, Orozco EIF, Toia CC, Machado FP & Valera MC (2023) Impact of N-acetylcysteine (NAC) and calcium hydroxide intracanal medications in primary endodontic infection: a randomized clinical trial Clinical Oral Investigations 27(2) 817-826.

6. Chalub LO, Nunes GP, Ferrisse TM, Strazzi-Sahyon HB, Dos Santos PH, Gomes-Filho JE, Cintra LTA & Sivieri-Araujo G (2022) Postoperative pain in root canal treatment with ultrasonic versus conventional irrigation: A systematic review and meta-analysis of randomized controlled trials Clinical Oral Investigations 26(4) 3343–3356.

7. Rodrigues CT, de Andrade FB, de Vasconcelos LR, Midena RZ, Pereira TC, Kuga MC, Duarte MAH & Bernardineli N (2018) Antibacterial properties of silver nanoparticles as a root canal irrigant against enterococcus faecalis biofilm and infected dentinal tubules International Endodontic Journal 51(8) 901–911.

8. Balto H, Bukhary S, Al-Omran O, BaHammam A & Al-Mutairi B (2020) Combined effect of a mixture of silver nanoparticles and calcium hydroxide against enterococcus faecalis biofilm Journal of Endodontics 46(11) 1689–1694.

9. Corazza BJ, Martinho FC, Khoury RD, Toia CC, Orozco EI, Prado RF, Machado FP & Valera MC (2020) Clinical influence of calcium hydroxide and n- acetylcysteine on the levels of resolvins E1 and D2 in apical periodontitis International Endodontic Journal 54(1) 61–73.

10. Best S, Ammons CL, Karunanayake GA, Saemundsson SR & Tawil PZ (2021) Outcome assessment of teeth with necrotic pulps and apical periodontitis treated with long-term calcium hydroxide Journal of Endodontics 47(1) 11–18.

11. Evans M, Davies JK, Sundqvist G & Figdor D (2002) Mechanisms involved in the resistance of enterococcus faecalis to calcium hydroxide International Endodontic Journal 35(3) 221–228.

12. Keskin G & Çiloğlu M (2021) Efficacy of antimicrobial photodynamic therapy and ER,CR:YSGG laser-activated irrigation on dentinal tubule penetration of MTA-based root canal sealer: A confocal microscopy study Photodiagnosis and Photodynamic Therapy 36 102584.

13. Nunes LP, Nunes GP, Ferrisse TM, Strazzi-Sahyon HB, Cintra LTÂ, dos Santos PH, & Sivieri- Araujo G (2022) Antimicrobial photodynamic therapy in endodontic reintervention: A systematic review and meta-analysis Photodiagnosis and Photodynamic Therapy 39 103014.

14. Singh S, Nagpal R, Manuja N & Tyagi SP (2014) Photodynamic therapy: An adjunct to conventional root canal disinfection strategies Australian Endodontic Journal 41(2) 54–71.

15. Garcez AS, Ribeiro MS, Tegos GP, Núñez SC, Jorge AOC & Hamblin MR (2007) Antimicrobial photodynamic therapy combined with conventional endodontic treatment to eliminate root canal biofilm infection Lasers in Surgery and Medicine 39(1) 59–66.

16. Ferrisse TM, Dias LM, de Oliveira AB, Jordão CC, Mima EG de O & Pavarina AC (2022) Efficacy of curcumin-mediated antibacterial photodynamic therapy for oral antisepsis: A systematic review and network meta-analysis of randomized clinical trials Photodiagnosis and Photodynamic Therapy 39 102876.

17. Davies D (2003) Understanding biofilm resistance to antibacterial agents Nature Reviews Drug Discovery 2(2) 114–122.

18. Meire MA, Coenye T, Nelis HJ & De Moor RJG (2012) Evaluation of Nd:YAG and Er:YAG irradiation, antibacterial photodynamic therapy and sodium hypochlorite treatment on Enterococcus faecalis biofilms International Endodontic Journal 45(5) 482–491.

19. Hidalgo LR, da Silva LAB, Nelson-Filho P, da Silva RAB, de Carvalho FK, Lucisano MP & Novaes AB Jr (2016) Comparison between one-session root canal treatment with aPDT and two-session treatment with calcium hydroxide-based antibacterial dressing, in dog's teeth with apical periodontitis Lasers in Medical Science 31(7) 1481–1491.

20. Strazzi Sahyon HB, Silva PP, Oliveira MS de, Cintra LTA, Dezan-Júnior E, Gomes-Filho JE, Jacinto RC, Dos Santos PH & Sivieri-Araujo G (2019) Influence of curcumin photosensitizer

in photodynamic therapy on the mechanical properties and push-out bond strength of glass-fiber posts to intraradicular dentin Photodiagnosis and Photodynamic Therapy 25 376–381.

21. Strazzi-Sahyon HB, de Oliveira MS, da Silva PP, Banci HA, de Melo FS, Martinez CMT, Cintra LTA, Gomes-Filho JE, Dezan-Júnior E, Dos Santos PH & Sivieri-Araujo G (2020) Does photodynamic therapy with methylene blue affect the mechanical properties and bond strength of glass-fiber posts in different thirds of intraradicular dentin? Photodiagnosis and Photodynamic Therapy 30 101673.

22. Strazzi-Sahyon HB, da Silva PP, Nakao JM, da Silva PZ, Nunes LP, Seron MA, Cintra LTA, Dos Santos PH & Sivieri-Araujo G (2021) Influence of two photodynamic therapy sessions and different photosensitizers on the bond strength of glass-fiber posts in different regions of intraradicular dentin Photodiagnosis and Photodynamic Therapy 33 102193.

23. Strazzi-Sahyon HB, Oliveira AKL, Carvalho AP, Figueiredo RB, Cintra LTA, Gomes-Filho JE, Dos Santos PH & Sivieri-Araujo G (2021) Influence of photodynamic therapy and intracanal medication on Martens hardness, elastic modulus and bond strength of glass-fiber posts to endodontically treated root dentin Photodiagnosis and Photodynamic Therapy 36 102571.

24. Silva EJNL, Carvalho NK, Prado MC, Senna PM, Souza EM & De- Deus G (2019) Bovine teeth can reliably substitute human dentine in an intra- tooth push- out bond strength model? International Endodontic Journal 52(7) 1063–1069.

25. Schilke R, Lisson JA, Bauß O & Geurtsen W (2000) Comparison of the number and diameter of dentinal tubules in human and bovine dentine by scanning electron microscopic investigation Archives of Oral Biology 45(5) 355–361.

26. Camargo CHR, Bernardineli N, Valera MC, de Carvalho CAT, de Oliveira LD, Menezes MM, Afonso SE & Mancini MN (2006) Vehicle influence on calcium hydroxide pastes diffusion in human and bovine teeth Dental Traumatology 22(6) 302–306.

27. Banci HA, Strazzi-Sahyon HB, Duarte M, Cintra L, Gomes-Filho JE, Chalub LO, Berton SA, de Oliveira V, Dos Santos PH & Sivieri-Araujo G (2020) Influence of photodynamic therapy on bond strength and adhesive interface morphology of MTA based root canal sealer to different thirds of intraradicular dentin Photodiagnosis and Photodynamic Therapy 32 102031.

28. Jurič IB, Plečko V, Pandurić DG & Anić I (2014) The antimicrobial effectiveness of photodynamic therapy used as an addition to the conventional endodontic re-treatment: A clinical study Photodiagnosis and Photodynamic Therapy 11(4) 549–555.

29. Strazzi-Sahyon HB, da Silva LMAV, Briso ALF & dos Santos PH (2022) In vitro study on how antioxidant solutions affect enamel surface characteristics and bonding interface of ceramic laminate veneers luting after dental bleaching Journal of the Mechanical Behavior of Biomedical Materials 133 105322.

30. Moda MD, Fagundes TC, Briso ALF & dos Santos PH (2018) Analysis of the bond interface between self-adhesive resin cement to eroded dentin in vitro PLOS ONE 13(11) 0208024.

31. Hoshino IAE, dos Santos PH, Briso ALF, Sundfeld RH, Yamaguchi S, Rocha EP & Anchieta RB (2022) Biomechanical performance of three fiberglass post cementation techniques: Imaging, in vitro, and in silico analysis Journal of Prosthodontic Research.

32. Rivera-Peña ME, Duarte MAH, Alcalde MP, DE Andrade FB & Vivan RR (2018) A novel ultrasonic tip for removal of filling material in flattened/oval-shaped root canals: a microCT study Brazilian Oral Research 13(32) 88.

33. Strazzi-Sahyon HB, Cintra LTA, Nakao JM, Takamiya AS, Queiroz IOA, Dos Santos PH, Oliveira SHP & Sivieri-Araujo G (2022) Cytotoxicity of root canal irrigating solutions and photodynamic therapy using curcumin photosensitizer Photodiagnosis and Photodynamic Therapy 38 102795.

34. Banci HA, Strazzi-Sahyon HB, Bento VAA, Sayeg JMC, Bachega MO, Pellizzer EP & Sivieri- Araujo G (2022) Influence of antimicrobial photodynamic therapy on the bond strength of endodontic sealers to intraradicular dentin: A systematic review and meta-analysis Photodiagnosis and Photodynamic Therapy 31 103270.

35. Wainwright M, Phoenix DA, Rice L, Burrow SM & Waring J (1997) Increased cytotoxicity and phototoxicity in the methylene blue series via chromophore methylation Journal of Photochemistry and Photobiology B: Biology 40(3) 233–239.

36. de Oliveira RL, Guerisoli DMZ, Duque JA, Alcalde MP, Onoda HK, Domingues FHF, Vivan RR & Duarte MAH (2019) Computed microtomography evaluation of calcium hydroxide-based root canal dressing removal from oval root canals by different methods of irrigation Microscopy Research and Technique 82(3) 232–237.

37. Eğemen A & Belli S (2022) The effect of primary root canal treatment on dentinal tubule penetration of calcium silicate-based sealers during endodontic retreatment Journal of Endodontics 48(9)1169-1177.

38. Ramos ATPR, Belizário LG, Jordão-Basso KCF, Shinohara AL & Kuga MC (2018) Effects of photodynamic therapy on the adhesive interface using two fiber posts cementation systems Photodiagnosis and Photodynamic Therapy 24 136–141.

39. D'Arcangelo C, Cinelli M, De Angelis F & D'Amario M (2007) The effect of resin cement film thickness on the pullout strength of a fiber-reinforced post system The Journal of Prosthetic Dentistry98(3)193–198.

40. Soares FZM, Follak A, da Rosa LS, Montagner AF, Lenzi TL & Rocha RO (2016) Bovine

tooth is a substitute for human tooth on bond strength studies: A systematic review and meta-analysis of in vitro studies Dental Materials 32(11) 1385–1393.

Table 1. Materials, classification, composition, and batch numbers of the materials used.

Material	Classification	Composition *	Batch
Adper Single Bond 2 (3M ESPE)	Adhesive System	BisGMA, HEMA, glycerol 1,3-dimethacrylate, diurethane dimethacrylate, water, ethanol, photoinitiators, 5 nm silanized silica, polyacrylic and itaconic acid copolymer.	N820206
Filtek Z350XT (3M ESPE)	Resin Composite	Bis-EMA, Bis-GMA, TEGDMA, UDMA, silica and zirconia nanofillers, and agglomerated zirconia silica nanoclusters.	HB004209993
Calcium Hydroxide (Biodinamica)	Intracanal Medication	38% of calcium hydroxide and 62% of barium oxide.	36870
Iodoform (Biodinamica)	Intracanal Medication	Iodoform (99 - 100%)	005-22
Propylene Glycol (Farma Formula)	Intracanal Medication	100% propylene glycol	530080
MTA Fillapex (Angelus)	Endodontic Sealer	Salicylate resin, natural resin, diluting resin, bismuth oxide, nanoparticulated silica, MTA (mineral trioxide aggregate) and pigments.	102564
RelyX Ceramic Primer (3M ESPE)	Ceramic Primer	Ethyl alcohol, water, and 3-MPS.	2106800707
RelyX U200 (3M ESPE)	Resin Cement	Base: methacrylate phosphoric acid esters, glass fiber, triethylene glycol dimethacrylate, sodium persulfate, silane-treated silica. Catalyst: substitute dimethacrylate,glass fiber, sodiump-toluenesulfonate, silane-treated silica, calcium.	2115100124

Abbreviations: Bis-EMA, ethoxylated bisphenol A glycol dimethacrylate; HEMA, hydroxyethyl methacrylate; UDMA, urethane dimethacrylate; Bis-GMA, bisphenol-A diglycidyl ether dimethacry- late; TEGDMA, triethylene glycol dimethacrylate; MTA, mineral trioxide aggregate; 3-MPS, 3-methacryloxypropyl-trimethoxy silane.

* According to manufacturer's information.

Table 2 - Distribution of the experimental groups.

Group Abbreviation	Group Treatment Detail
Negative Control	Root canals non-treated with photosensitizer and photodynamic therapy. Root canals were irrigated with deionized water.
Positive Control	Root canals non-treated with photosensitizer and photodynamic therapy. Root canals were irrigated with deionized water and filled with intracanal calcium hydroxide medication.
$MB_{50WA} + Ca(OH)_2$	Root canals were filled with 50 mg/L of methylene blue photosensitizer without red laser activation and filled with intracanal calcium hydroxide medication.
$MB_{100WA} + Ca(OH)_2$	Root canals were filled with 100 mg/L of methylene blue photosensitizer without red laser activation and filled with intracanal calcium hydroxide medication.
$MB_{50A} + Ca(OH)_2$	Root canals were filled with 50 mg/L of methylene blue photosensitizer activated by red laser (λ 660 nm) and filled with intracanal calcium hydroxide medication.
$MB_{100A} + Ca(OH)_2$	Root canals were filled with 100 mg/L of methylene blue photosensitizer activated by red laser (λ 660 nm) and filled with intracanal calcium hydroxide medication.

Table 3 – Mean ± standard deviation values of bond strength (push-out) (MPa) of the intraradicular dentin as a function of the experimental groups and intraradicular thirds.

Groups / Thirds	Negative Control	Positive Control	MB_{50WA} + $Ca(OH)_2$	MB_{100WA} + $Ca(OH)_2$	MB_{50A} + $Ca(OH)_2$	MB_{100A} + $Ca(OH)_2$
Cervical	7.12 ± 2.85 Aa	5.21 ± 1.10 Aa	8.13 ± 3.04 Aa	5.33 ± 2.74 Aa	7.50 ± 3.21 Aa	6.74 ± 3.11 Aa
Middle	5.55 ± 2.54 Aa	4.52 ± 0.80 Aa	6.37 ± 3.07 ABa	5.04 ± 1.76 Aa	4.95 ± 2.14 ABa	5.92 ± 2.78 Aa
Apical	4.74 ± 2.36 Aab	2.81 ± 1.51 Bbc	4.40 ± 1.94 Babc	2.21 ± 0.88 Bc	3.65 ± 0.60 Babc	5.62 ± 2.00 Aa

Different letters, uppercase in column and lowercase in row, indicate statistically significant differences (P<.05).

Table 4 – Scores of the adhesive interface morphology as a function of the experimental groups and intraradicular thirds.

Adhesive Interface Quality

Groups	Control					Positive Control					MB_{50WA} + $Ca(OH)_2$					MB_{100WA} + $Ca(OH)_2$					MB_{50A} + $Ca(OH)_2$					MB_{100A} + $Ca(OH)_2$				
Scores	**0**	**1**	**2**	**3**		**0**	**1**	**2**	**3**		**0**	**1**	**2**	**3**		**0**	**1**	**2**	**3**		**0**	**1**	**2**	**3**		**0**	**1**	**2**	**3**	
Thirds																														
Cervical	2	1	-	-	Aa	2	1	-	-	Aa	3	-	-	-	Aa	3	-	-	-	Aa	3	-	-	-	Aa	-	2	1	-	Aa
Middle	2	1	-	-	Aa	1	2	-	-	Aa	3	-	-	-	Aa	3	-	-	-	Aa	3	-	-	-	Aa	-	2	1	-	Aa
Apical	3	-	-	-	Aa	2	1	-	-	Aa	1	2	-	-	Aa	2	1	-	-	Aa	3	-	-	-	Aa	2	1	-	-	Aa

Tags Formation in Dentin

Groups	Control					Positive Control					MB_{50WA} + $Ca(OH)_2$					MB_{100WA} + $Ca(OH)_2$					MB_{50A} + $Ca(OH)_2$					MB_{100A} + $Ca(OH)_2$				
Scores	**0**	**1**	**2**	**3**		**0**	**1**	**2**	**3**		**0**	**1**	**2**	**3**		**0**	**1**	**2**	**3**		**0**	**1**	**2**	**3**		**0**	**1**	**2**	**3**	
Thirds																														
Cervical	-	1	2	-	Aa	-	2	1	-	Aa	-	1	2	-	Aa	-	1	2	-	Aa	-	1	2	-	Aa	-	1	2	-	Aa
Middle	-	2	1	-	Aa	-	-	3	-	Aa	-	1	2	-	Aa	-	2	1	-	Aa	-	1	2	-	Aa	-	1	2	-	Aa
Apical	-	3	-	-	Aa	-	1	2	-	Aa	-	3	-	-	Aa	-	2	1	-	Aa	-	2	1	-	Aa	-	1	2	-	Aa

Tags Penetration Depth

Groups	Control					Positive Control					MB_{50WA} + $Ca(OH)_2$					MB_{100WA} + $Ca(OH)_2$					MB_{50A} + $Ca(OH)_2$					MB_{100A} + $Ca(OH)_2$				
Scores	**0**	**1**	**2**	**3**		**0**	**1**	**2**	**3**		**0**	**1**	**2**	**3**		**0**	**1**	**2**	**3**		**0**	**1**	**2**	**3**		**0**	**1**	**2**	**3**	
Thirds																														
Cervical	-	2	-	1	Aa	-	1	2	-	Aa	-	2	1	-	Aa	-	1	2	-	Aa	-	3	-	-	Aa	-	3	-	-	Aa
Middle	-	1	2	-	Aa	-	3	-	-	Aa	-	1	2	-	Aa	-	1	2	-	Aa	-	3	-	-	Aa	-	3	-	-	Aa
Apical	-	2	1	-	Aa	-	1	1	1	Aa	-	1	2	-	Aa	-	1	2	-	Aa	-	3	-	-	Aa	-	3	-	-	Aa

Different letters, uppercase in column and lowercase in row, indicate statistically significant differences for each adhesive interface parameter (P<.05).

Table 5 – Mean ± standard deviation values of volume (mm^3) and quantification of voids formation on resin cement as a function of the experimental groups and intraradicular thirds.

Groups / Thirds	Negative Control	Positive Control	MB_{50WA} + $Ca(OH)_2$	MB_{100WA} + $Ca(OH)_2$	MB_{50A} + $Ca(OH)_2$	MB_{100A} + $Ca(OH)_2$
Volume						
Cervical	2.04 ± 0.95 Ab	4.01 ± 2.40 Aab	4.01 ± 1.26 Aab	4.80 ± 0.86 Aa	4.86 ± 0.93 Aa	6.08 ± 1.02 Aa
Middle	1.50 ± 0.35 Aa	1.50 ± 0.90 Ba	1.38 ± 0.37 Ba	1.68 ± 0.37 Ba	2.26 ± 0.98 Ba	2.02 ± 0.34 Ca
Apical	2.04 ± 0.95 Aa	1.94 ± 1.24 Ba	1.91 ± 1.43 Ba	2.12 ± 0.44 Ba	2.43 ± 0.47 Ba	3.04 ± 0.51 Ba
Quantification						
Cervical	9.56 ± 0.76 Ac	9.85 ± 0.72 Ac	12.55 ± 1.24 Abc	15.99 ± 2.76 Aa	12.50 ± 0.79 Abc	15.28 ± 2.99 Aab
Middle	9.40 ± 0.36 Ac	9.74 ± 0.50 Ac	12.21 ± 0.36 Abc	15.21 ± 2.96 Aa	12.68 ± 1.27 Aab	15.26 ± 2.29 Aa
Apical	7.67 ± 0.39 Bc	10.04 ± 0.68 Abc	12.44 ± 0.52 Aab	15.50 ± 3.36 Aa	12.40 ± 1.20 Aab	14.40 ± 2.59 Aa

Different letters, uppercase in column and lowercase in row, indicate statistically significant differences for each parameter evaluated (P<.05).

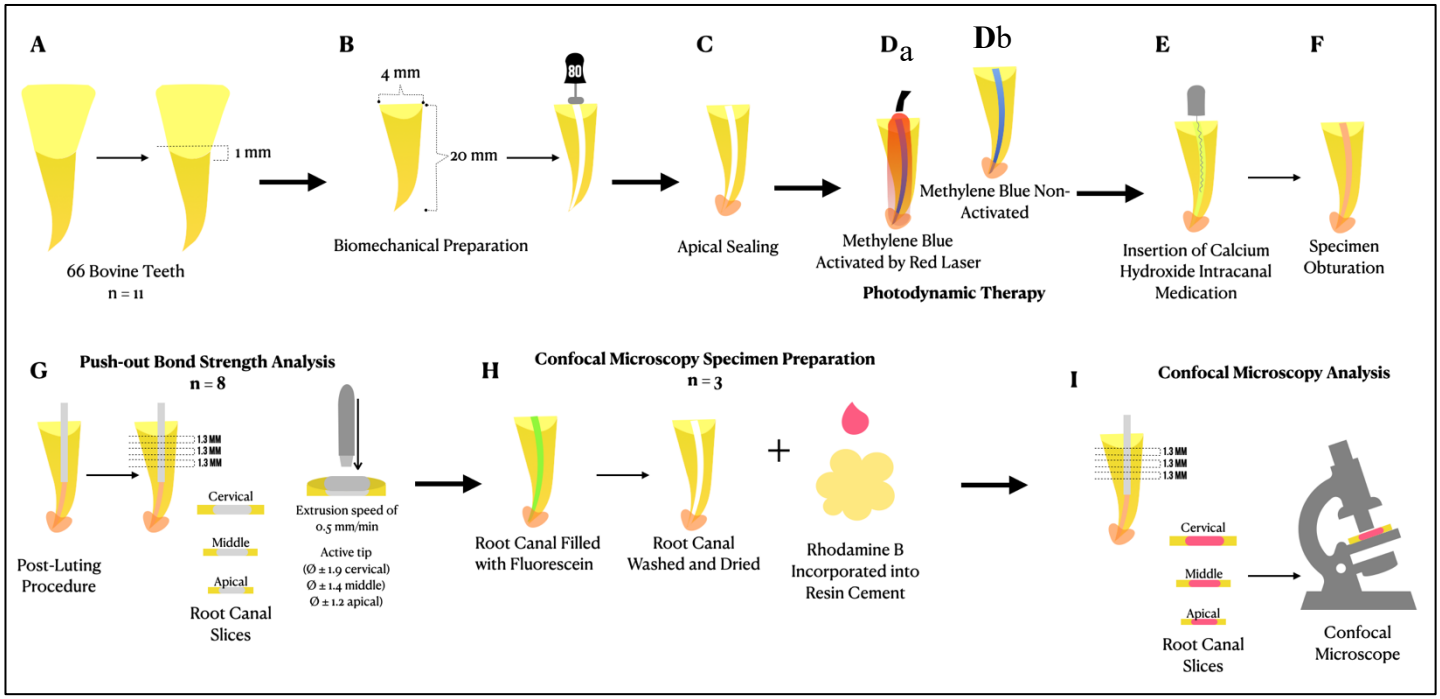
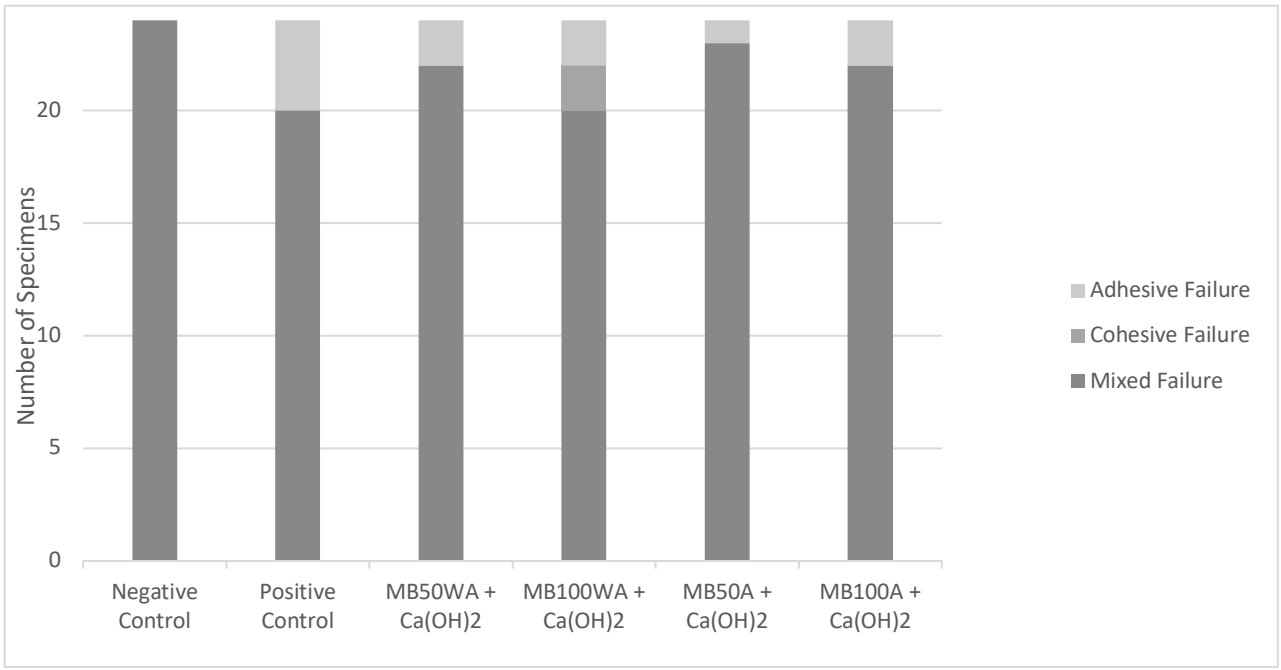


Figure 1. Specimen preparation. A, Bovine incisors and removal of anatomic crowns. B, Standardization of root canal diameter and length. C, Apical portion sealing. D, Photodynamic therapy session. E, Insertion of calcium hydroxide medication into root canals. F, Specimen obturation. G, Obtainment of 1.3-mm thick intraradicular slices for push-out bond strength test. H, Specimen preparation for the confocal microscopy analysis. I, Obtainment of 1.3-mm thick intraradicular slices for the confocal microscopy analysis.

Figure 2. Fracture patterns incidence (samples thirds numbers) according to type of failure.



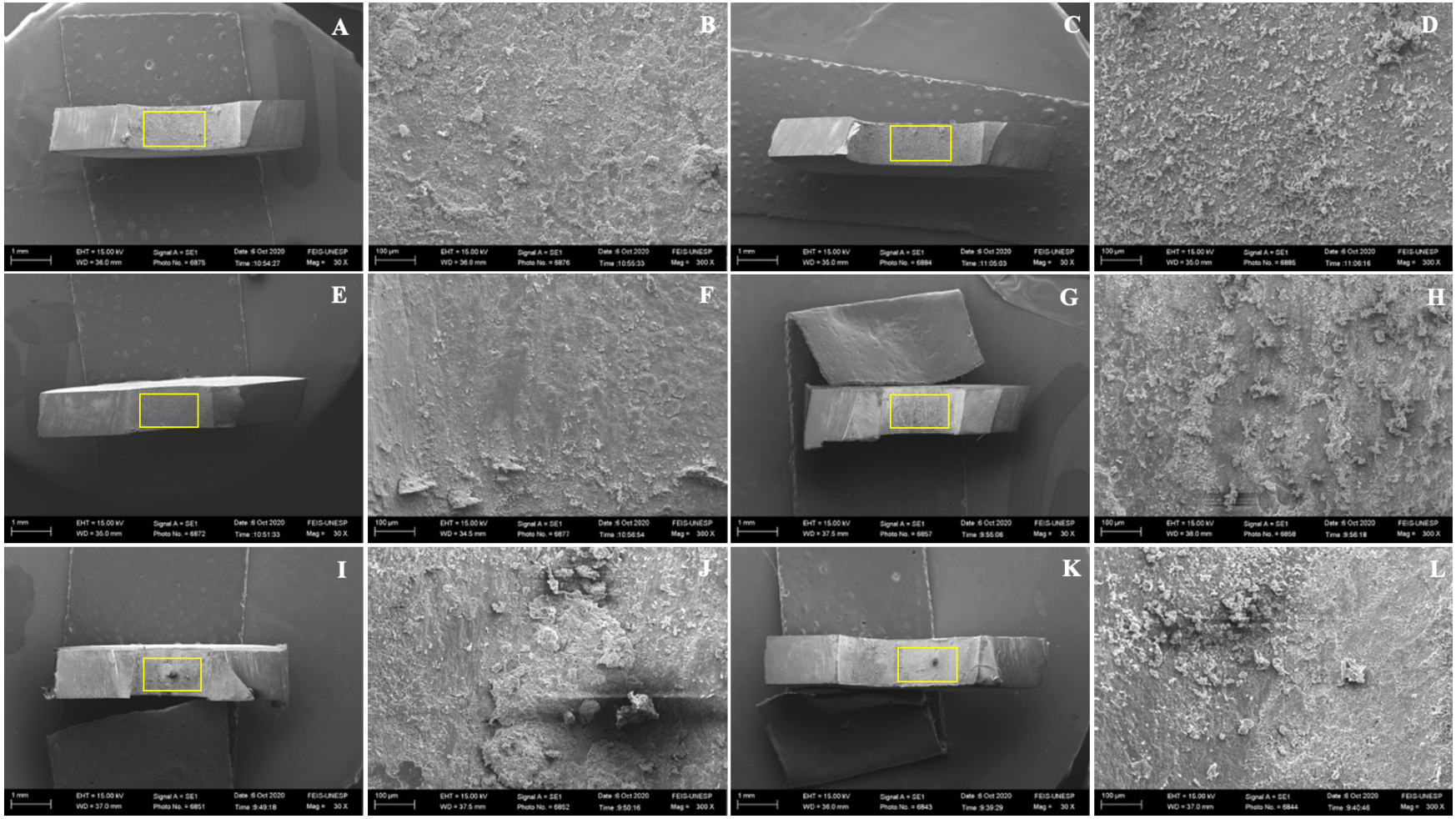


Figure 3. Scanning electron microscopy images of each experimental group under original magnification (× 30 and × 300). AB – mixed-type failure (negative control group); CD – mixed-type failure (positive control group); EF – mixed-type failure (MB_{50WA} + $Ca(OH)_2$ group); GH – mixed-type failure (MB_{100WA} + $Ca(OH)_2$ group); IJ – mixed-type failure (MB_{50A} + $Ca(OH)_2$ group); KL – mixed-type failure (MB_{100A} + $Ca(OH)_2$ group).

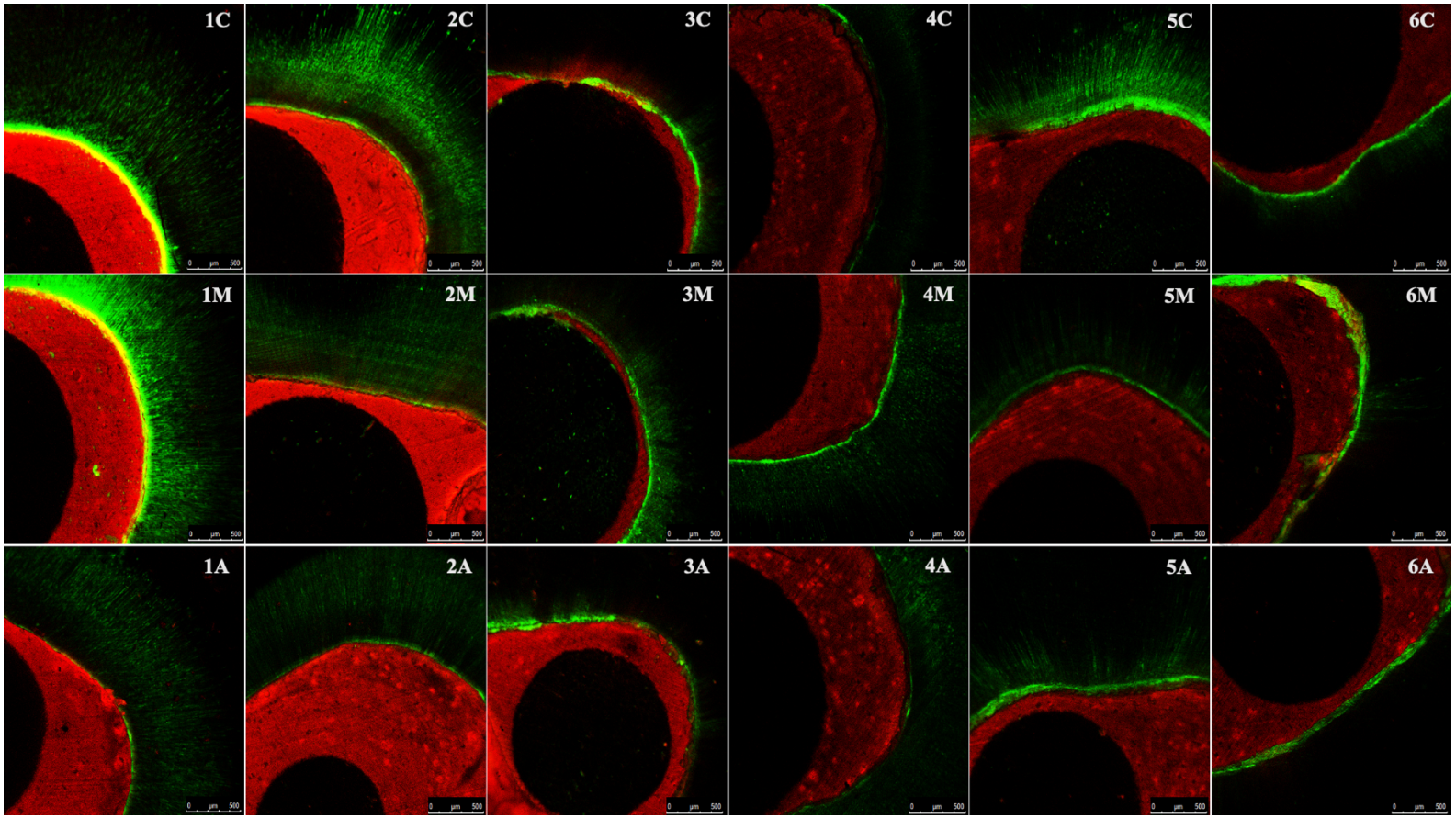


Figure 4. Images from confocal laser scanning microscopy of each experimental group and intraradicular dentin thirds, with original magnification ×5. 1C, 1M, 1A - Cervical, middle, and apical slices of intraradicular dentin irrigated with deionized water solution (negative control group). 2C, 2M, 2A - Cervical, middle, and apical slices of intraradicular dentin after irrigated with deionized water and filled with calcium hydroxide intracanal medication ($Ca[OH]_2$)

(positive control group). 3C, 3M, 3A - Cervical, middle, and apical slices of intraradicular dentin after treatment $Ca[OH]_2$ + methylene blue 50 mg/L without activation (MB_{50WA} + $Ca[OH]_2$). 4C, 4M, 4A - Cervical, middle and apical slices of intraradicular dentin after treatment with $Ca[OH]_2$ + methylene blue 100 mg/L without activation (MB_{100WA} + $Ca[OH]_2$). 5C, 5M, 5A - Cervical, middle, and apical slices of intraradicular dentin after treatment with $Ca[OH]_2$ + methylene blue 50 mg/L activated by red laser(MB_{50A} + $Ca[OH]_2$). 6C, 6M, 6A - Cervical, middle, and apical slices of intraradicular dentin after treatment with $Ca[OH]_2$ + methylene blue 100 mg/L activated by red laser (MB_{100A} + $Ca[OH]_2$).

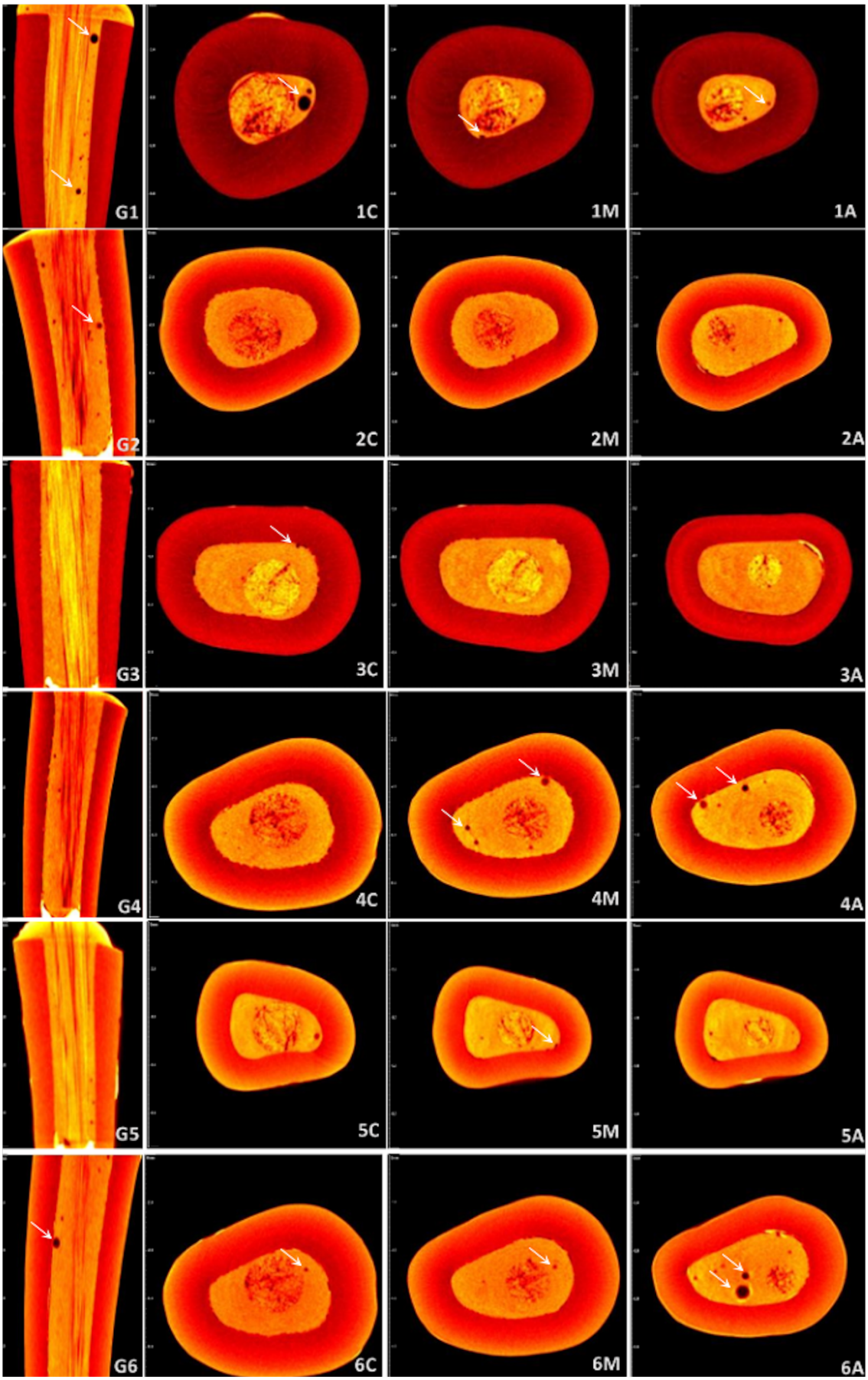

G1
1C
1M
1A
G2
2C
2M
2A
G3
3C
3M
3A
G4
4C
4M
4A
G5
5C
5M
5A
G6
6C
6M
6A

Figure 5 - Microcomputed tomography images of adhesive interface integrity according to the experimental groups and intraradicular thirds. G1, 1C, 1M, 1A – Transaxial, cervical, middle, and apical slices of intraradicular dentin irrigated with deionized water solution (negative control group). G2, 2C, 2M, 2A – Transaxial, cervical, middle, and apical slices of intraradicular dentin after irrigated with deionized water and filled with calcium hydroxide intracanal medication (positive control group). G3, 3C, 3M, 3A – Transaxial, cervical, middle, and apical slices of intraradicular dentin after treatment with calcium hydroxide intracanal medication + 50 mg/L of methylene blue without activation (MB_{50WA} + $Ca[OH]_2$). G4, 4C, 4M, 4A – Transaxial, cervical, middle and apical slices of intraradicular dentin after treatment with calcium hydroxide intracanal medication + 100 mg/L of methylene blue without activation (MB_{100WA} + $Ca[OH]_2$). G5, 5C, 5M, 5A - Transaxial, cervical, middle, and apical slices of intraradicular dentin after treatment with calcium hydroxide intracanal medication + 50 mg/L of methylene blue activated by red laser (λ 660 nm) (MB_{50A} + $Ca[OH]_2$). G6, 6C, 6M, 6A – Transaxial, cervical, middle, and apical slices of intraradicular dentin after treatment with calcium hydroxide intracanal medication + 100 mg/L of methylene blue activated by red laser (λ 660 nm) (MB_{100A} + $Ca[OH]_2$). White arrows indicate the presence of voids on the luting interface.

Chapter 2

6) *CHAPTER* 2

Effect of methylene blue-mediated antimicrobial photodynamic therapy and calcium hydroxide medication on physico-chemical and mechanical characteristics of intraradicular dentin and bonding interface of glass fiber posts

6.1 Abstract

BACKGROUND: The longevity and success of oral restorations using glass fiber posts for tooth reconstruction with excessive crown loss are directly related to the mechanical properties of root dentin. Studies have shown that antimicrobial photodynamic therapy (aPDT) may influence the mechanical properties of the intrarradicular dentin. Nevertheless, studies evaluating the influence of aPDT and calcium hydroxide ($Ca[OH]_2$) as intracanal medication on physico-chemical and mechanical characteristics of intraradicular dentin and bonding interface of glass fiber posts are scarce. Thus, this *in vitro* study evaluated the influence of methylene blue (MB)-mediated aPDT and $Ca[OH]_2$ medication on the mechanical properties, degree of conversion (DC), volume and quantification of gaps on the adhesive interface of glass fiber posts. Furthermore, the microhardness (MH), elastic modulus (Eit), morphology, and chemical composition of the intraradicular dentin were also assessed.

METHODS: 102 bovine incisors were biomechanically instrumented, and sorted into 6 experimental groups: a negative control irrigated with deionized water; a positive control irrigated with deionized water and filled with $Ca[OH]_2$; $Ca[OH]_2$ + MB at 50 mg/L without irradiation; Ca[OH]2 + MB at 100 mg/L without irradiation; $Ca[OH]_2$ + MB at 50 mg/L irradiated by red laser (λ = 660 nm); and $Ca[OH]_2$ + MB at 100 mg/L irradiated by red laser (λ = 660 nm) (n = 17). MH, Eit, and DC of resin cement and dentin substrates were assessed using an ultramicrodurometer and a microRaman spectrometer, respectively (n = 8). The volume and quantification of gaps on

bonding interface were investigated by computerized microtomography (n = 6), while dentin morphology and chemical composition were assessed by scanning electron microscope (n = 3). MH, Eit, DC, volume and quantification of gaps data were subjected to 2-way ANOVA for repeated measures followed by Tukey's test (α=.05).

RESULTS: Distinct intraradicular thirds and treatment with methylene blue-mediated aPDT, activated or not, associated with $Ca[OH]_2$ significantly influenced on the values of the mechanical properties of the root dentin, as well as the MH, Eit, DC, volume and quantification of voids in the luting interface ($P < .05$). In general, higher concentration of methylene blue, activated or not by red laser, promoted lower values of mechanical properties of the root dentin, as well as on the MH, Eit, and DC of the adhesive interface ($P < .05$). Furthermore, MB_{100WA} + $Ca(OH)_2$ and MB_{100A} + $Ca(OH)_2$ groups promoted higher values of volume and quantification of gaps on the luting interface ($P < .05$). Scanning electron micrographs and energy dispersive X-ray spectra showed qualitative similarity for all experimental groups, excepted to negative control group.

CONCLUSIONS: The use of one application of aPDT with methylene blue PS at 50 mg/L associated with calcium hydroxide intracanal medication did not affect negatively the mechanical properties at any root canal depth and it did not alter the chemical composition of the adhesive interface and volume of gaps.

KEYWORDS: Calcium Hydroxide; Degree of Conversion; Dentin; Mechanical Properties; Methylene Blue; Photodynamic Therapy.

6.2 INTRODUCTION

The success of oral restorations using glass fiber posts for tooth reconstruction with considerable crown loss are directly related to the mechanical properties of root dentin, effective adhesion between the glass fiber posts/luting agents/dentin substrates, and the success of endodontic treatment [1]. The correct and satisfactory pathogens load elimination is critical to the success of endodontic treatment and immediate restorative care [2,3]. Therefore, diverse protocols can be applied to reduce the presence of microorganisms and inflammatory processes, such as: root canal biomechanical instrumentation [4] and the use of irrigation fluids like sodium hypochlorite and chlorhexidine under distinct concentrations [5,6]. However, *in vivo* and *in vitro* works claim that the conventional instrumentation associated to irrigation solutions do not promote complete eradication of bacteria and their residual toxic derivatives (apical biofilms and endotoxins) in persistent infections. In addition to their negative effects in periapical tissues [7,8], these solutions could interfere on the adhesion of luting agents, such as dental adhesives and resin cements to dentin substrate [9-11].

Because of its antimicrobial and natural impacts, the calcium hydroxide-based compound ($Ca[OH]_2$) is the most utilized intracanal drug to upgrade bacterial disinfection after biomechanical instrumentation [12,13]. $Ca(OH)_2$ is a basic substance, with a pH of roughly 12.5, which empowers its separation into calcium and hydroxyl particles in a watery medium [12,13]. This compound has a few organic properties, such as antimicrobial action, capacity to disintegrate tissues and biofilms, restraint of tooth resorption, and enlistment of hard tissue formation [14,15], pursuing it the essential decision of intracanal medication for different clinical circumstances. Nonetheless, in some cases, calcium hydroxide has a restricted antimicrobial action to persistent contamination [16], such as *Enterococcus faecalis* infection, inspiring searches on new alternative approaches for eliminating endodontic infections, for example, antimicrobial photodynamic therapy (aPDT) [17].

Furthermore, several studies claim that aPDT in itself does not allow completely the eradication of biofilms [18,19], once it is formed by an association of diversified microorganisms,

and its ripeness can be 10-1000 times more resistant to the use of conventional endodontics therapies [15,16]. Authors suggest that the use of aPDT concomitantly to $Ca(OH)_2$ intracanal medication potentializes the bacterial eradication [15]. Thus, the applicability of aPDT is not designated to displace the conventional endodontic approaches, but to operate concurrently with them to extinguish persistent infections [19-22].

Considerable works have assessed the influence of different photosensitizers (PS) at distinct concentrations, irradiated or not by LED and laser sources, on the mechanical properties, such as microhardness and elastic modulus of root dentin, and on the adhesive strength of luting agents used to lute glass fiber post to root dentin [17,23-26]. However, works on the influence of methylene blue-mediated aPDT at distinct concentrations, light-activated or not by red laser, concomitantly to $Ca(OH)_2$ as intracanal medication along the root dentin are scarce in the literature. Strazzi-Sahyon et al. [35] investigated the effect of $Ca(OH)_2$ intracanal medication and two session of methylene blue-mediated aPDT, light activated or not by red laser, on mechanical properties of intraradicular dentin [34]. However, there is no consensus on how the association of aPDT with $Ca(OH)_2$ medication could influence the mechanical properties, degree of conversion, and integrity of the bonding interface of glass fiber posts to intraradicular dentin.

Thus, this *in vitro* study aimed to investigate the influence of $Ca(OH)_2$ as intracanal medication and methylene blue PS-mediated aPDT, irradiated or not by red laser, on the mechanical properties such as Martens hardness (MH) and elastic modulus (Eit), as well as on morphology and chemical composition of intraradicular dentin in different depths. Additionally, effects on MH, Eit, degree of conversion, and integrity of the luting interface of glass fiber post to different thirds of endodontically treated intraradicular dentin were also assessed. The null hypotheses tested were: 1) The performance of methylene blue-mediated aPDT, irradiated or not, and $Ca(OH)_2$ intracanal medication would not result in differences on mechanical properties of intraradicular dentin, as well as on the mechanical properties, degree of conversion, and integrity of the adhesive interface; and 2) different depths of root dentin treated with methylene blue-

mediated aPDT and $Ca(OH)_2$ medication would not promote differences on MH and Eit of root dentin, as well as on MH, Eit, degree of conversion, and integrity of the luting interface of glass fiber posts.

6.3 MATERIAL AND METHODS

6.3.1 Experimental design

Table 1 presents information on the materials used in the study. This work was approved by the local Ethics Committee on the Use of Animals (#18–01003).

A total of 102 bovine incisors obtained from cattle aged from 2 to 3 years old were selected. Teeth exhibiting cracks, fractures, or curved roots were discarded and substituted. Clinical crowns were separated from the roots 1.0 mm above the cementoenamel junction using a cutter machine (Isomet 1000; Buehler, Lake Bluff, IL, USA) with a low speed diamond saw under constant water cooling (Fig. 1–A), standardizing root length at 20 mm and canal diameter at 4 mm. The working length of the roots was established 1.0 mm short of the original teeth length, and specimens were endodontically treated by mechanical instrumentation (Fig. 1–B). Canals were irrigated using a syringe containing 10 ml of 1% sodium hypochlorite solution for 15 s for each file change, until reaching the #80 K-files (Maillefer Instruments, Tulsa, OK, USA). For smear layer removal, 10 ml of 17% ethylenediaminetetraacetic acid (EDTA) (Biodinâmica Química e Farmacêutica LTDA, Ibiporã, PR, Brazil) was inserted into root canals for 3 min and removed upon irrigation using 10 ml of 1% sodium hypochlorite for 15 s. Then, root canals were aspirated and dried with sterile absorbent paper tips (Dentsply Sirona, York, PA, USA) and air jets. To avoid PS escape, apical foramens were sealed using 35% phosphoric acid (3 M ESPE, St Paul, MN, USA), dental adhesive (Adper Single Bond 2; 3 M ESPE), and resin composite (Filtek Z350 XT; 3 M ESPE) (Fig. 1– C) [17,23-25].

6.3.2 Experimental groups and aPDT

Root specimens were randomly distributed into six experimental groups (n = 17), as exemplified in Table 2. In the negative control group, root canals were irrigated with deionized water. In the positive control group, root canals were irrigated with deionized water and filled with $Ca[OH]_2$ medication. Neither control groups were submitted to PS or aPDT. Two experimental groups received methylene blue PS at 50 mg/L (MB_{50WA} and MB_{50A}), whereas the other two received the dye at 100 mg/L (MB_{100WA} and MB_{100A}). In these experimental groups, the methylene blue dye underwent a 3-minute pre-irradiation period [27], and was agitated for 60 s after the PS using an ultrasonic equipment (Nac Plus, Adiel LTDA, São Paulo, SP, Brazil) equipped with an ultrasonic tip (Irrisonic E1; Helse Dental Technology, Santa Rosa de Viterbo, SP, Brazil) [17,22-25]. Every effort was made to minimize the contact of the tip with the root canal walls and promote the PS agitation [23].

In the MB_{50A} and MB_{100A} groups, the methylene blue PS was activated by red laser radiation (Laser Duo; MMO, São Carlos, SP, Brazil) for 60 s under a 660 nm wavelength using a 300-µm flexible optical fiber coupled to the laser source, resulting in a final energy of 72 J/cm2 [17, 22,23,25]. The laser was applied with helicoidal movements in the cervical-apical direction 10 times per minute at 2 mm short the root canal working length [28–30]. The methylene blue dye was not irradiated in the MB_{50WA} and MB_{100WA} groups (without activation) (Fig. 1–D). Immediately after the treatment, the methylene blue PS was removed by inserting 10 mL of deionized water into the root canals, which were then dried with a jet of air and sterile paper [23,25].

6.3.3 Calcium hydroxide medication

Except the negative control group, the root canal spaces of all experimental groups were filled with calcium hydroxide paste (Biodinâmica Química e Farmacêutica) associated with iodoform (Biodinâmica Química e Farmacêutica) and propylene glycol using the #4 Lentulo spiral

(Maillefer Instruments) for a 14-day period [31] (Fig. 1–E). Then, root canals were sealed in the coronal portion with interim cement (Cimpat Branco; Septodont Ltda, Barueri, SP, Brazil). To confirm complete filling of the root canal extension with calcium hydroxide, the teeth underwent radiographic analysis using Digital X-Ray – 1.0.9.1 Dental Master Dicom Software and Micro Image EVO digital sensor (Micro Image, Indaiatuba, SP, Brazil). All root specimens were kept for 7 days at 100% relative humidity and 37ºC. After 14 days, coronal sealing and intracanal medication were pull out upon irrigation with 1% sodium hypochlorite solution (10 mL) and K #80 file [32].

6.3.4 Analysis of mechanical properties (MH and Eit)

The root canals of all experimental groups (n = 8) were filled with endodontic cement (MTA Fillapex; Angelus, Londrina, PR, Brazil) and #80 gutta-percha cones and fine (F) and medium-fine (MF) auxiliary cones (Tanari, Manacapuru, AM, Brazil), using the Tagger's obturation technique with McSpadden compactor #70 (Maillefer Instruments) [35] (Fig. 1–F). The coronal access was sealed with provisional cement (Cimpat Branco; Septodont Ltda) [34], and teeth were kept in 100% humidity at 37ºC for 7 days [29,30,34,35]. The intraradicular retainer system used was White Post DCE #2 glass-fiber posts (FGM, Joinville, SC, Brazil). Post space was prepared by removing 9 mm of gutta-percha using a #1 low-speed wide drill (Maillefer Instruments), followed by the corresponding #2 drill to glass- fiber system for standardizing the post space [29,30,34,35]. Then, intraradicular space was irrigated with 10 mL of physiological saline solution (0.9%) to remove any debris or residual gutta percha, and canals were dried with sterile paper and air jets [29,30,34,35].

The intraradicular retainer surface was etched with 35% phosphoric acid (3M ESPE) for 1 min, washed, and dried with air jet. Etched surfaces were silanized (RelyX Ceramic Primer; 3 M ESPE) for 1 min, and glass fiber posts that would not be further manipulated were gently dried with air jet, preventing surface contamination. Post surfaces received dual-cure self-adhesive resin cement (RelyX U200; 3M ESPE) and were inserted into the root canals, allowing the glass fiber

posts to adapt within the post spaces. Intracanal restoration was light-activated for 40 s from the occlusal region using a polywave light curing unit (Radii; SDI, South Jordan, UT, USA) at 1200mW/cm^2.

For measuring the mechanical properties (Martens hardness [MH] and elastic modulus [Eit] of intraradicular dentin and resin cement substrates, eight specimens per group (n = 8) were cut perpendicular to the long axis under constant water refrigeration using a diamond saw connected to a precision cutter machine (Isomet 1000; Buehler Lake), obtaining slices of approximately 1.3 mm from each third analyzed (cervical, middle, and apical thirds; Fig. 1- G), confirmed by a digital caliper (Mitutoyo, Aurora, IL, USA) [23-25,32,33].

Each intraradicualr third was fixed in acrylic resin (Classic, Sao Paulo, SP, Brazil) and manually abraded and flattened using #320, #600, #800, and # 1200 grit silicon carbide papers (Extec Corp, Enfield, CT, USA) and polished using diamond pastes (6, 3, and 1 μm) for 4 min. Between each finishing and polishing step and at the end of the procedure, specimens were cleaned in an ultrasonic unit (model 2210, Branson Ultrasonic Corp., Danbury CT, USA) with deionized water for 2 min [23–25].

MH and Eit were assessed using the DUH-211 digital ultramicrodurometer (Shimadzu, Kyoto, Japan) under a load action of 3mN at 0.2926 mN/s, maintaining the same load for 5 s in each analyzed dentin and resin cement region (Fig. 1– G). Ten readings were performed in each third (five indentations in the root dentin substrate and five indentations in the resin cement layer) using a Bercovich diamond indentation tip. The MH and Eit values were automatically calculated according to the load-displacement curve, and an arithmetic mean was calculated for each property. MH was obtained dividing the maximum load (Lmax) by the contact surface area (A) [23-25,33,34], as follows equation:

$$MH = \frac{Lmax}{A}$$

The Eit value was calculated according to the following formula:

$$Er = \frac{\sqrt{\pi}}{2\sqrt{A}}S,$$

$$\frac{1}{Er} = \frac{(1-v^2)}{Eit} + \frac{(1-vi^2)}{Ei},$$

where A is the area for contact indentation; S is the stiffness of the material collected from the slope of the unloading curve; and π is 3.14, obtaining the reduced modulus (Er); v and vi is related to the Poisson's coefficient of the specimens and the diamond indenter tip, respectively, and Ei to the elastic modulus of the indenter [23–25].

6.3.5 Degree of conversion

The resin cement degree of conversion (DC) was conducted using the same samples prepared for the MH and Eit mechanical property analysis (n = 8). The DC analysis was carried out using a confocal Raman microscope (In Via; Renishaw, New Mills, Gloucestershire, UK) under a diffraction grating of 1800 grooves/mm, associated to an optical microscope (Leica TCS SPE@, Leica, Mannheim, Germany) (Fig. 1– H). A spatial resolution of 1.0 μm was selectively recorded the Raman spectrum of the interest region (from 1550 to 1700 cm^{-1}) of the specimens under the He–Ne laser action (λ = 633 nm) [37].

Raman measures were carried out using a ×50 objective, and each spectrum was recorded with an integration time of 10 s (Figure 1-H). Five spectra of the resin cement layer were carried out for each intraradicular third. During the analysis, the light in the room was attenuated to minimized any interference with the Raman reading. The room temperature was maintained at 23 ± 1°C, with a controlled relative humidity of ± 34% [37].

The height ratio of the peaks at 1607 cm−1 (aromatic) and 1637 cm−1 (aliphatic) of the polymerized and nonpolymerized resin cement were assessed to calculate the DC. The nonpolymerized resin cement was placed onto glass microscope slides, and the material was read

using the microRaman equipment. The DC values of the resin cement were obtained through specific software installed in the Raman machine, and measured as follows [37]:

$$DC\ (\%) = 100 \times [1 - (R\ polymerized / R\ nonpolymerized)],$$

where R represents the ratio between the peaks of the polymerized and nonpolymerized luting material.

6.3.6 Adhesive interface integrity analysis

To evaluate the adhesive integrity, such as volume and quantification of gaps on the luting interface, six specimens from each experimental group (n = 6) were evaluated using a high resolution microtomography (SkyScan 1272, Bruker, Kontich, Belgium) (Fig. 1– I) [39]. The microtomograph was obtained using the standard "phanton" function and operated under power of 80 kilovolts and 125 milli-amps. The microtomographs were obtained at medium resolution (13µm/slice) and at 180º. The specimens were rotated at 0.4º angular steps with an exposure time of 3000 milliseconds; a 16.5 mm tube and a 1 mm thick aluminum filter were also used [39].

The scanning process of the specimens was carried out subsequently the luting process of the glass fiber posts. The data collected in the scan were converted into DICOM files and thus rendered into three-dimensional models (SolidWorks Corp., MA, USA). First, the microtomographs were reconstructed in three-dimensional in the NRecon software (SkyScan, Kontich, Belgium) from the coronal to the apical region of the root canals, with the parameters "Smoothing" (6), "Misalignment compensation" (-3.5), " Ring artifacts reduction" (6), "Beam-hardening correction (34%)" and "change dynamic image range" (0.003169-0.230010) the same for all specimens. Then, applying the DataViewer software (SkyScan, Kontich, Belgium), the microtomographs were linearly analyzed in the coronal, sagittal and transaxial axes, as well as the determination of a standard position for the volumetric and quantification of gaps.

Quantitative analyzis of gaps in the resin cement layer was accomplished by the CTAnalyser software (SkyScan, Kontich, Belgium) in the transaxial position of the microtomographs [39].

Firstly, the extension to be evaluated was determined by selecting an average of 1013 to 1200 slices, followed by image segmentation to divide the desired artefact from other artefacts present in the microtomograph. Later, a freehand template (interest area) was designed and defined only the resin cement layer. The microtomographs were binarized, and the volume and quantification of gaps present between the root canal and resin cement were determined [39]. Finally, using the CTVOX software (SkyScan, Kontich, Belgium), these microtomographs were rendered into 3D models to investigate the integrity of the luting interface by observing areas of the resin cement in discontinuity with the walls of the intraradicular dentin [36].

6.3.7 Scanning electron microscopy (SEM) and energy dispersive X-ray spectroscopy (EDS)

For the SEM and EDS analyses, three specimens per experimental groups were qualitatively evaluated (n = 3). The specimens were sputter-coated with gold (Baltec SCD 050, Balzers, Liechtenstein, Austria) to evaluate the morphology and chemical composition of the intraradicular dentin. Root dentin micrographs were illustrated using scanning electron microscope (SEM - JSM5600LV, LEOL, Tokyo, Japan) under ×300 magnification, and the root substrate was evaluated by energy-dispersive X-ray spectroscopy coupled to the SEM equipment (Fig. 1– J) [38]. Data on oxygen (O), carbon (C), calcium (Ca), phosphorus (P), sodium (Na), magnesium (Mg), silicon (Si), zirconium (Zr), tellurium (Te), tungsten (W), and molybdenum (Mo) were collected from the SEM – EDS analysis under ×300 magnification.

6.3.8 Statistical analysis

Mechanical properties data of the intraradicular dentin, as well as the MH, Eit, DC, and integrity data of the luting interface were submitted to normality (Shapiro-Wilk; Bioestat 2.0 Program) and homogeneity tests (Bartlett; Bioestat 2.0 Program). Data were analyzed using two-way repeated measures Analysis of Variance (ANOVA; 5.0 Statview Program; Version 5.0.1). The Tukey protected least significant difference test ($\alpha = .05$) was also performed.

6.4 RESULTS

6.4.1 Mechanical properties (MH and Eit)

6.4.1.1 Intraradicular dentin

The MH and Eit values of the intraradicular dentin are listed in Table 3. There were no significant differences in the MH values of the root dentin comparing the intraradicular depths and the experimental groups ($P > .05$), excepted for the $MB_{100WA} + Ca(OH)_2$ group in which the middle third showed higher MH values compared to the apical region ($P < .05$) (Table 3). The same trend can be noted to the Eit mechanical property once the apical region promoted lower values than middle third ($P < .05$). Comparing the experimental groups, there were no significant differences in the Eit values regardless the intraradicular depth evaluated ($P > .05$), excepted for the cervical third, as the positive control group presented lower Eit values compared to the $MB_{100WA} + Ca(OH)_2$ and $MB_{100A} + Ca(OH)_2$ groups ($P < .05$) (Table 3).

6.4.1.2 Resin cement

The MH and Eit values of the resin cement are presented in Table 4. Comparing the experimental groups, there were no significant differences in the MH values regardless the intraradiculer depth investigated ($P > .05$), excepted for the middle third where the positive control and $MB_{100A} + Ca(OH)_2$ groups showed lower MH valued compared to the negative control and $MB_{50WA} + Ca(OH)_2$ groups ($P < .05$) (Table 4). Comparing the intraradicular thirds, there were no significant differences to positive, $MB_{100WA} + Ca(OH)_2$, and $MB_{100A} + Ca(OH)_2$ ($P > .05$), however, for the negative control and $MB_{50WA} + Ca(OH)_2$ groups, the middle third showed lower MH values compared to the cervical and apical regions ($P < .05$). For the $MB_{50A} + Ca(OH)_2$ experimental group, there were significance differences only between the cervical and apical thirds, in which the last presented lower HM values ($P < .05$) (Table 4).

Analyzing the mechanical property of Eit, it can be noted that in general there were no significant differences comparing the intrarradicular thirds regardless the experimental groups investigated (P > .05), excepted for the MB_{50WA} + $Ca(OH)_2$ group, in which the cervical third promoted higher Eit values compared to the middle and apical regions (P < .05) (Table 4). Evaluating the middle intraradicular region, there were no significant differences on Eit values among the experimental groups (P > .05), however, for the apical region, MB_{100WA} + $Ca(OH)_2$ group promoted lower Eit values compared to the negative control, MB_{50A} + $Ca(OH)_2$, and MB_{100A} + $Ca(OH)_2$ groups (P < .05). Furthermore, for the cervical third, it can be noted that the MB_{50A} + $Ca(OH)_2$ showed higher Eit values in relation to the positive control and MB_{100WA} + $Ca(OH)_2$ groups (P < .05) (Table 4).

6.4.2 Degree of conversion

The DC values of the resin cement are listed in Table 5. Assessing the cervical root depth, the positive control group promoted higher DC values compared to the MB_{50WA} + $Ca(OH)_2$, MB_{100WA} + $Ca(OH)_2$, MB_{50A} + $Ca(OH)_2$, and MB_{100A} + $Ca(OH)_2$ experimental groups (P < .05) (Table 5). Evaluating the middle third, the negative control groups showed higher DC values compared to the MB_{50WA} + $Ca(OH)_2$, MB_{100WA} + $Ca(OH)_2$, MB_{50A} + $Ca(OH)_2$, and MB_{100A} + $Ca(OH)_2$ experimental groups (P < .05). For the apical intraradicular depth, the MB_{50A} + $Ca(OH)_2$ and MB_{100A} + $Ca(OH)_2$ groups presented lower DC values in relation to the negative and positive control groups (P < .05) (Table 5). Comparing the intraradicular thirds, it can be noted that, in general, there were no significant differences on DC values for all experimental groups (P > .05), excepted for MB_{100WA} + $Ca(OH)_2$ group, in which the middle third showed lower DC values in relation to the cervical and apical regions (P < .05) (Table 5).

6.4.3 Adhesive interface integrity

The volume and quantification of gaps on the adhesive interface and representative microtomographs are illustrated in Table 6 and Figure 4, respectively. Comparing the groups for the cervical intraradicular third, the negative and positive control, and MB_{50A} + $Ca(OH)_2$ groups showed a lower volume of gaps values compared to the MB_{100WA} + $Ca(OH)_2$, and MB_{100A} + $Ca(OH)_2$ groups ($P < .05$) (Table 6). Assessing the middle third, the negative and positive control groups showed lower volume of gaps values in relation to the other experimental groups ($P < .05$). For the apical root third, it can be noted that the negative control, positive control, MB_{50WA} + $Ca(OH)_2$, and MB_{50A} + $Ca(OH)_2$ exhibited lower volume of gaps values compared to the MB_{100A} + $Ca(OH)_2$ group ($P < .05$). Comparing the intraradicular thirds, there were no significant differences in volume of void values for the positive control, MB_{50WA} + $Ca(OH)_2$, MB_{50A} + $Ca(OH)_2$, and MB_{100A} + $Ca(OH)_2$ groups ($P > .05$) (Table 6). However, for negative control group, the cervical third promoted higher volume of gaps compared to the middle and apical intraradicular regions ($P < .05$). In addition, for the MB_{100WA} + $Ca(OH)_2$ group, there were significant differences among the intraradicular thirds, as the middle region promoted lower volume of gaps values compared to the cervical third ($P < .05$) (Table 6).

Comparing the experimental groups, the negative control, positive control, MB_{50WA} + $Ca(OH)_2$, and MB_{50A} + $Ca(OH)_2$ groups promoted lower gap quantification values compared to the MB_{100WA} + $Ca(OH)_2$ and MB_{100A} + $Ca(OH)_2$ groups for all intraradicular thirds investigated ($P < .05$) (Table 6). There were no statistical differences in gap quantification values among distinct intraradicular thirds for all experimental groups evaluated ($P > .05$) (Table 6).

6.4.4 Scanning electron microscope (SEM) and energy dispersive spectroscopy (EDS)

Scanning electron micrographs showed qualitative similarity in the intraradicular dentin substrate to positive control, MB_{50WA} + $Ca(OH)_2$, MB_{100WA} + $Ca(OH)_2$, MB_{50A} + $Ca(OH)_2$ and MB_{100A} + $Ca(OH)_2$ groups, in which can be observed the presence of residual particles of the

calcium hydroxide medication (Fig. 2 B - F). However, for the negative control group, it can be noted a regular and homogeneous surface (Fig. 2 A). Energy dispersive X-ray spectra showed qualitatively higher oxygen percentage in the MB_{50WA} + $Ca(OH)_2$, MB_{100WA} + $Ca(OH)_2$, MB_{50A} + $Ca(OH)_2$ and MB_{100A} + $Ca(OH)_2$ groups in relation to the negative and positive control groups (Fig. 3). The presence of zirconium (Zr), tellurium (Te), tungsten (W), and molybdenum (Mo) chemical elements were observed in the experimental groups submitted to $Ca(OH)_2$ medication action (Fig. 3).

6.5 DISCUSSION

Methylene blue-mediated aPDT at different concentrations, activated or not by red laser, and associated with calcium hydroxide intracanal medication influenced the mechanical properties of MH and Eit of the dentin substrate, as well as the MH, Eit, DC, and the adhesive interface integrity of the luting layer, thus rejecting the first null hypothesis of the study (Tables 3 - 6). Additionally, significant differences were observed among distinct depths of intraradicular dentin treated with methylene blue-mediated aPDT associated with calcium hydroxide intracanal medication on the MH and Eit properties of root dentin and resin cement, as well as on DC, volume and quantification of voids in the luting interface, leading to rejection of the second null hypothesis (Tables 3 - 6).

The results demonstrate that the action of the PS in a higher concentration activated or not by red laser followed by intracanal medication of calcium hydroxide promoted lower values for the Eit the cervical third. A possible explanation is that the cervical and middle thirds are more susceptible to PS action, as the substance cationicity caused phosphate precipitates to accumulate in the middle third, reducing the interaction between the resin cement and root dentin surface [30,32]. Besides, the distribution and location of dentinal tubules and concentration decreases in the middle and apical direction [34].

Comparing the results of the degree of conversion both groups of methylene blue at 50 mg/L and the group of PDT at 100 mg/L had lower values than the positive control group when comparing the cervical third (Table 5). This result may be explained by the action of the PS with the dentin substrate, that may have influenced the degree of conversion of the resin cement. Also, among all the groups for the middle third, the values were lower when compared to the negative control group (except for the positive control group). The comparison data of the apical third among groups established that MB_{50A} + $Ca(OH)_2$ and MB_{100A} + $Ca(OH)_2$ groups had lower values when compared to both control groups ($P < .05$). A possible explanation is the anatomy of the root canal where when more coronal the polymerization of the resin cement is more due to the light action and in the middle and apical thirds the curing is more due to its chemical process [34].

The EDS analyses demonstrated that the levels of phosphate were different among groups. The positive control group had the highest percentage and the PDT group of MB at 50 mg/L as well as both groups of methylene blue at 100mg/L had the lowest values of phosphate. This may be due to changes in the phosphate $Ca_{10}(PO_4)_6(OH)_2$ ratio resulting from PS cationicity and its laser activation associated with the effects of intracanal medication leading to a lower concentration of this element on these groups [34,35].

The volume of gaps can be assessed by Micro-CT technology, which had the option to nondestructively measure the volume of it on the resin cement interface. Micro-CT uses X-beam sources delivering 3D reproduced pictures. Since the imaging system is nondestructive, the interior highlights of a similar example might be inspected. Regarding the volume of gaps in general the cervical third had more gaps than the middle and apical third this finding may be explained by the gravity which the air flow naturally to the cervical direction. Also the group with the higher volume of gaps in the apical third was the MB_{100A} + $Ca(OH)_2$ group, that associated a higher concentration of methylene blue [40].

6.6 CONCLUSION

Based on the methodology applied and the results obtained in this study, it is possible to conclude that the use of one application of PDT with methylene blue PS at 50 mg/L associated with calcium hydroxide intracanal medication did not affect negatively the mechanical properties at any root canal depth and it did not alter the chemical composition of the adhesive interface and volume of gaps.

6.7 REFERENCES

1. M.S. Bin-Shuwaish, Impact of photodynamic therapy on the push-out bond strength of fiber posts to root dentin: a systematic review and meta-analysis, Photodiagnosis Photodyn. Ther. 32 (2020), 102010.

2. H. Zandi, A.K. Kristoffersen, D. Ørstavik, I.N. Roças, F.J.R Siqueira, M Enersen, Microbial analysis of endodontic infections in root-filled teeth with apical periodontitis before and after irrigation using pyrosequencing, J. Endod. 44 (2018) 372–378.

3. C. Estrela, R. Holland, C.R. Estrela, A.H. Alencar, M.D. Sousa-Neto, J.D. P´ecora, Characterization of successful root canal treatment, Braz. Dent. J. 25 (2014) 3–11.

4. M.K. Wu, P.M. Dummer, P.R. Wesselink, Consequences of and strategies to deal with residual post-treatment root canal infection, Int. Endod. J. 39 (2006) 343–356.

5. R. Viapiana, M.D. Sousa-Neto, A.E. Souza-Gabriel, E. Alfredo, Y.T Silva-Sousa, Microhardness of radicular dentin treated with 980-nm diode laser and different irrigant solutions, Photomed. Laser Surg. 30 (2012) 102–106.

6. L.S. Gonçalvez,R.C.Rodrigues,C.V.AndradeJunior,R.G.Soares,M.VVettore,The effect of sodium hypochlorite and chlorhexidine as irrigant solutions for root canal disinfection: a systematic review of clinical trials, J. Endod. 42 (2016) 527–532.

7. M.E.Vianna,B.P.Gomes,V.B.Berber,A.A.Zaia,C.C.Ferraz,F.J.deSouza-Filho,In vitro evaluation of the antimicrobial activity of chlorhexidine and sodium hypochlorite, Oral Surg. Oral Med. Oral Pathol. Oral Radiol. Endod. 97 (2004) 79–84.

8. E. Ercan, T. Ozekinci, F. Atakul, K. Gül, Antibacterial activity of 2% chlorhexidine gluconate and 5.25% sodium hypochlorite in infected root canal: in vivo study, J. Endod. 30 (2004) 84–87.

9. T.Y.U. Suzuki, M.A. Pereira, J.E. Gomes-Filho, L. Wang, W.G. Assunç˜ao, P.H. D Santos, Do irrigation solutions influence the bond interface between glass fiber posts and dentin? Braz. Dent. J. 30 (2019) 106–116.

10. F.M. Pascon, K.R. Kantovitz, L.E. Soares, A.M. Santo, A.A. Martin, R.M. Puppin-Rontani, Morphological and chemical changes in dentin after using endodontic agents: fourier transform Raman spectroscopy, energy-dispersive x-ray fluorescence spectrometry, and scanning electron microscopy study, J. Biomed. Optcis 17 (2012) 0750081–0750086.

11. A.T.P.R. Ramos, L. Garcia Beliza´rio, A.C. Venç˜ao, K.C. Fagundes Jordão-Basso, A. N. de Souza Rastelli, M.F. de Andrade, M.C Kuga, Effects of photodynamic therapy on the adhesive interface of fiber posts cementation protocols, J. Endod. 44 (2018) 173–178.

12. B.J.M.Corazza,F.C.Martinho,R.D.Khoury,C.C.Toia,E.I.F.Orozco,R.F.Prado,F. P. Machado, M.C. Valera, Clinical influence of calcium hydroxide and N- acetylcysteine on the levels of resolvins E1 and D2 in apical periodontitis, Int. Endod. J. 54 (2021) 61–73.

13. S.Best,C.L.Ammons,G.A.Karunanayake,S.R.Saemundsson,P.Z.Tawil,Outcome Assessment of Teeth with Necrotic Pulps and Apical Periodontitis Treated with Long-term Calcium Hydroxide, J. Endod. 47 (2021) 11–18.

14. Z.Mohammadi,P.M.Dummer,Propertiesandapplicationsofcalciumhydroxidein endodontics and dental traumatology, Int. Endod. J. 44 (2011) 697–730.

15. G.H. Yassen, J.A. Platt, The effect of nonsetting calcium hydroxide on root fracture and mechanical properties of radicular dentine: a systematic review, Int. Endod. J. 46 (2013) 112–118.

16. Faria CM, Inada NM, Kurachi C, Bagnato VS. Determination of the threshold dose distribution in photodynamic action from in vitro experiments. J Photochem Photobiol B 2016;162:168-75.

17. Allison RR, Sibata CH. Photodynamic therapy: mechanism of action and role in the treatment of skin disease. G Ital Dermatol Venereol 2010;145:491-507.

18. Allison RR, Moghissi K. Oncologic photodynamic therapy: clinical strategies that modulate mechanisms of action. Photodiagnosis Photodyn Ther 2013;10:331-41.

19. Sivieri-Araujo G, Queiroz IOA, Fabbro RD, Esteves F, Cintra LTA, Duarte PCT, Bagnato VS, Oliveira SHP, Gomes-Filho JE. Rat tissue reaction and cytokine production induced by antimicrobial photodynamic therapy. Photodiagnosis Photodyn Ther 2017;18:315-318.

20. Souza MA, Dias CT, Zandoná J, Hoffmann IP, Menchik VHS, Palhano HS, Bertol DC, Rossato-Grando LG, Cecchin D, Figueiredo JAP. Antimicrobial activity of hypochlorite solutions and reciprocating T instrumentation associated with photodynamic therapy on root canals infected with Enterococcus faecalis. Photodiagnosis Photodyn Ther 2018;23;347-352.

21. Okamoto CB, Motta LJ, Prates RA, Mota ACC, Gonçalves MLL, Horliana ACRT, Ferrari RAM, Fernandes KPS, Bussadori SK. Antimicrobial Photodynamic Therapy as a Co-adjuvant in Endodontic Treatment of Deciduous Teeth: Case Series. J Photochem Photobiol 2018;94;760-4.

22. Shrestha A, Cordova M, Kishen A. Photoactivated polycationic bioactive chitosan nanoparticles inactivate bacterial endotoxins. J Endod 2015;41:686-91.

23. Bulit F, Grad I, Manoil D, Simon S, Wataha JC, Filieri A, Feki A, Schrenzel J, Lange N, Bouillaguet S. Antimicrobial activity and cytotoxicity of 3 photosensitizers activated with blue light. J Endod. 2014;40:427-31.

24. Neelakantan P, Cheng CQ, Ravichandran V, Mao T, Sriraman P, Sridharan S, Subbarao C, Sharma S, Kishen A. Photoactivation of curcumin and sodium hypochlorite to enhance antibiofilm efficacy in root canal dentin. Photodiagnosis Photodyn Ther. 2015;12:108-14.

25. Silva LAB, Novaes AB Jr, Oliveira RR, Nelson-Filho P, Santamaria M Jr, Silva RA. Antimicrobial photodynamic therapy for the treatment of teeth with apical periodontitis: a histopathological evaluation. J Endod 2012;38:360-6.

26. ANVISA Agência Nacional de Vigilância Sanitária. Consolidado de Normas COFID, versão IV, p. 178, Brasília, abril 2013. Disponível em: http://portal.anvisa.gov.br/wps/wcm/connect/6805ba804f5ea576920df79a71dcc661/ConsolidadoVersaoIVpublicar.pdf?MOD=AJPERES. Acess in may 25th 2022.

27. Tardivo JP, Del Giglio A, de Oliveira CS, Gabrielli DS, Junqueira HC, Tada DB, Severino D, de Fátima Turchiello R, Baptista MS. Methylene blue in photodynamic therapy: From basic mechanisms to clinical applications. Photodiagnosis Photodyn Ther 2005;2:175-91.

28. Sivieri-Araujo G, Santos LMS, Queiroz IOA, Wayama MT, Yamanari GH, Martins CM, Dezan-Júnior E, Cintra LTA, Gomes-Filho JE. Photodynamic therapy in Endodontics: Use of a supporting strategy to deal with endodontic infection. Dental Press Endod. 2013;3:52-8.

29. Strazzi Sahyon HBS, Silva PP, Oliveira MS, Cintra LTA, Gomes-Filho JE, Santos PH, Sivieri-Araujo G. Effect of photodynamic therapy on the mechanical properties and bond strength of glass-fiber posts to endodontically treated intraradicular dentin. J Prosthet Dent 2018;120:317

30. Strazzi-Sahyon HB, Oliveira AKL, Carvalho AP, Figueiredo RB, Cintra LTA, Gomes-Filho JE, et al. Influence of photodynamic therapy and intracanal medication on Martens hardness, elastic modulus and bond strength of glass-fiber posts to endodontically treated root dentin. Vol. 36, Photodiagnosis and Photodyn Ther 2021;102571. Available from: http://dx.doi.org/10.1016/j.pdpdt.2021.102571

31. Liu Y, Tjäderhane L, Breschi L, Mazzoni A, Li N, Mao J, Pashley DH, Tay FR. Limitations in bonding to dentin and experimental strategies to prevent bond degradation. Journal of Dental Research. 2011;90;953-68.

32. Souza MA, Lana DD, Gabrielli E, Ribeiro MR, Miyagaki DC, Cecchin D. Effectiveness of final decontamination protocols against Enterococcus faecalis and its influence on bond strength of filling material to root canal dentin. Photodiagnosis Photodyn Ther 2017;17;92-7.

33. Ramos ATPR, Belizário LG, Venção AC, Jordão-Basso KCF, Rastelli ANS, Andrade MF, Kuga MC. Effects of Photodynamic Therapy on the Adhesive Interface of Fiber Posts Cementation Protocols. J Endod 2018;44:173-8.

34. Banci HA, Strazzi-Sayhon HB, Duarte MAH, Cintra LTA, Gomes-Filho JE, Chalub LO, Berton SA, de Oliveira VHD, dos Santos PH, Sivieri-Araujo G. Influence of photodynamic therapy on bond strength and adhesive interface morphology of MTA based root canal sealer to different thirds of intraradicular dentin. Photodiagnosis Photodyn Ther 2020;32:102031.

35. Strazzi-Sahyon HB, de Oliveira MS, da Silva PP, Banci HA, de Melo FS, Martinez CMT, Cintra LTA, Gomes-Filho JE, Dezan-Júnior E, dos Santos PH, Sivieri-Araujo G. Does photodynamic therapy with methylene blue affect the mechanical properties and bond strength of glass-fiber posts in different thirds of intraradicular dentin?. Vol. 30, Photodiagnosis and Photodyn Ther 2020;101673. Available from: http://dx.doi.org/10.1016/j.pdpdt.2020.101673

36. Fagundes TC, Somensi DS, Dos Santos PH, Navarro MF. Confocal laser scanning microscopy investigation of Bond interfaces involved in fiber glass post cementation. Braz Dent Sci 2014;17(2).

37. Komori PC, de Paula AB, Martin AA, Tango RN, Sinhoreti MA, Correr-Sobrinho L. Effect of light energy density on conversion degree and hardness of dual-cured resin cement. Oper Dent 2010; 35: 120-4.

38. Rubira RJG, Aoki PHB, Constantino CJL, Alessio P. Supramolecular architectures of iron phthalocyanine Langmuir-Blodgett films: The role played by the solution solvents. Appl Surf Sci 2017; 416: 482-91.

39. Crozeta BM, Silva-Sousa YT, Leoni GB, Mazzi-Chaves JF, Fantinato T, Baratto-FilhoF et al. Micro computed tomography study of filling material removal from oval-shaped canals by using rotary, reciprocating and adaptive motion systems. J Endod. 2016 May;42(5):793-7.

Table 1. Materials, classification, composition, and batch numbers of materials.

Material	Classification	Composition	Batch
Filtek Z350XT (3M ESPE)	Resin Composite	Bis-EMA, Bis-GMA, TEGDMA, UDMA, silica and zirconia nanofillers, and agglomerated zirconia-silica nanoclusters	HB004209993
Calcium Hydroxide (Biodinamica)	Intracanal Medication	38% of calcium hydroxide, 62% of barium oxide, and propilenoglicol	36870
MTA Fillapex (Angelus)	Endodontic Sealer	Salicylate resin, natural resin, diluting resin, bismuth oxide nanoparticulated silica, MTA (mineral trioxide aggregate) and pigments	102564
RelyX Ceramic Primer (3M ESPE)	Ceramic Primer	Ethyl alcohol, water, and 3-MPS.	2106800707
RelyX U200 (3M ESPE)	Resin Cement	Base: methacrylate phosphoric acid esters, glass fiber, triethyl glycol dimethacrylate, sodium persulfate, silane-treated silic Catalyst: substitute dimethacrylate,glass fiber, sodium p-toluenesulfonate, silane-treated silica, calcium.	2115100124

Abbreviations: Bis-EMA, ethoxylated bisphenol A glycol dimethacrylate; UDMA, urethane dimethacrylate; Bis-GMA, bisphenol-A diglycidyl ether dimethacry- late; TEGDMA, triethylene glycol dimethacrylate; MTA, mineral trioxide aggregate; 3-MPS, 3-methacryloxypropyl-trimethoxy silane.

Table 2 - Distribution of the experimental groups.

Group Abbreviation	Group Treatment Detail
Negative Control	Root canals non-treated with photosensitizer and photodynamic therapy. Root canals were irrigated with deionized water.
Positive Control	Root canals non-treated with photosensitizer and photodynamic therapy. Root canals were irrigated with deionized water and filled with intracanal calcium hydroxide medication.
$MB_{50WA} + Ca(OH)_2$	Root canals were filled with 50 mg/L of methylene blue photosensitizer without red laser activation and filled with intracanal calcium hydroxide medication.
$MB_{100WA} + Ca(OH)_2$	Root canals were filled with 100 mg/L of methylene blue photosensitizer without red laser activation and filled with intracanal calcium hydroxide medication.
$MB_{50A} + Ca(OH)_2$	Root canals were filled with 50 mg/L of methylene blue photosensitizer activated by red laser (λ 660 nm) and filled with intracanal calcium hydroxide medication.
$MB_{100A} + Ca(OH)_2$	Root canals were filled with 100 mg/L of methylene blue photosensitizer activated by red laser (λ 660 nm) and filled with intracanal calcium hydroxide medication.

Table 3 – Mean ± standard deviation values of Martens hardness (GPa) and elastic modulus (GPa) of dentin substrate as a function of the experimental groups and intraradicular thirds.

Groups / Thirds	Negative Control	Positive Control	MB_{50WA} + $Ca(OH)_2$	MB_{100WA} + $Ca(OH)_2$	MB_{50A} + $Ca(OH)_2$	MB_{100A} + $Ca(OH)_2$
Martens Hardness						
Cervical	0.95 ± 0.06 Aa	1.11 ± 0.16 Aa	1.09 ± 0.09 Aa	0.97 ± 0.09 ABa	1.01 ± 0.20 Aa	1.02 ± 0.17 Aa
Middle	1.05 ± 0.23 Aa	1.09 ± 0.16 Aa	1.07 ± 0.12 Aa	1.04 ± 0.22 Aa	1.07 ± 0.14 Aa	1.00 ± 0.09 Aa
Apical	1.13 ± 0.34 Aa	1.10 ± 0.33 Aa	1.08 ± 0.26 Aa	0.82 ± 0.15 Ba	1.02 ± 0.23 Aa	0.87 ± 0.13 Aa
Elastic Modulus						
Cervical	23.33 ± 6.08 Aab	14.57 ± 10.72 Ab	22.68 ± 4.93 Aab	26.40 ± 3.04 ABa	24.76 ± 5.02 Aab	27.99 ± 8.73 Aa
Middle	23.49 ± 4.90 Aa	22.86 ± 5.40 Aa	24.76 ± 5.95 Aa	27.99 ± 2.40 Aa	26.48 ± 4.11 Aa	30.70 ± 14.22 Aa
Apical	25.85 ± 3.56 Aa	25.54 ± 7.46 Aa	23.23 ± 7.42 Aa	24.80 ± 2.57 Ba	27.74 ± 8.63 Aa	26.40 ± 7.95 Aa

Different letters, uppercase in column and lowercase in row, indicate statistically significant differences for each mechanical property ($P<.05$).

Table 4 – Mean ± standard deviation values of Martens hardness (GPa) and elastic modulus (GPa) of resin cement as a function of the experimental groups and intraradicular thirds.

Groups / Thirds	Negative Control	Positive Control	MB_{50WA} + $Ca(OH)_2$	MB_{100WA} + $Ca(OH)_2$	MB_{50A} + $Ca(OH)_2$	MB_{100A} + $Ca(OH)_2$
Martens Hardness						
Cervical	0.98 ± 0.21 Ba	0.95 ± 0.14 Aa	0.86 ± 0.24 Ba	0.97 ± 0.26 Aa	1.12 ± 0.07 Aa	0.87 ± 0.24 Aa
Middle	1.17 ± 0.17 Aa	0.93 ± 0.14 Ab	1.25 ± 0.16 Aa	1.05 ± 0.07 Aab	1.02 ± 0.17 ABab	0.85 ± 0.22 Ab
Apical	0.98 ± 0.11 Ba	0.98 ± 0.21 Aa	0.94 ± 0.21 Ba	1.00 ± 0.13 Aa	0.98 ± 0.13 Ba	0.89 ± 0.23 Aa
Elastic Modulus						
Cervical	19.04 ± 2.78 Aab	17.54 ± 3.98 Abc	19.40 ± 4.76 Aab	13.41 ± 0.96 Ac	23.15 ± 4.15 Aa	17.70 ± 3.85 Abc
Middle	20.01 ± 4.27 Aa	20.79 ± 5.25 Aa	14.14 ± 2.03 Ba	14.33 ± 4.37 Aa	20.61 ± 2.92 Aa	19.78 ± 8.23 Aa
Apical	21.25 ± 4.99 Aa	19.78 ± 5.18 Aab	14.58 ± 4.21 Bab	13.29 ± 3.05 Ab	20.60 ± 2.93 Aa	20.63 ± 6.87 Aa

Different letters, uppercase in column and lowercase in row, indicate statistically significant differences for each mechanical property ($P<.05$).

Table 5 – Mean ± standard deviation values of degree of conversion (%) of the resin cement as function of the experimental groups and intraradicular thirds.

Groups / Thirds	Negative Control	Positive Control	MB_{50WA} + $Ca(OH)_2$	MB_{100WA} + $Ca(OH)_2$	MB_{50A} + $Ca(OH)_2$	MB_{100A} + $Ca(OH)_2$
Cervical	82.19 ± 6.38 Aab	87.79 ± 4.03 Aa	77.58 ± 3.48 Abc	81.19 ± 2.93 Abc	75.48 ± 4.06 Ac	74.91 ± 5.84 Abc
Middle	87.82 ± 2.74 Aa	84.09 ± 6.64 Aab	77.67 ± 2.56 Abc	75.74 ± 3.57 Bc	73.38 ± 4.40 Ac	76.52 ± 5.83 Ac
Apical	84.28 ± 4.53 Aa	83.22 ± 5.92 Aa	80.41 ± 1.63 Aab	79.93 ± 2.08 Aab	75.23 ± 2.77 Abc	72.61 ± 5.21 Ac

Different letters, uppercase in column and lowercase in row, indicate statistically significant differences (P<.05).

Table 6 – Mean ± standard deviation values of volume (mm^3) and quantification of gaps formation on resin cement as a function of the experimental groups and intraradicular thirds.

Groups / Thirds	Negative Control	Positive Control	MB_{50WA} + $Ca(OH)_2$	MB_{100WA} + $Ca(OH)_2$	MB_{50A} + $Ca(OH)_2$	MB_{100A} + $Ca(OH)_2$
Volume						
Cervical	3.29 ± 0.25 Acd	2.90 ± 0.27 Ad	4.16 ± 0.44 Aab	4.53 ± 0.29 Aa	3.81 ± 0.68 Abc	4.68 ± 0.30 Aa
Middle	2.77 ± 0.30 Bb	2.94 ± 0.23 Ab	3.82 ± 0.57 Aa	4.17 ± 0.24 Ba	3.99 ± 0.63 Aa	4.67 ± 0.61 Aa
Apical	2.82 ± 0.28 Bc	2.77 ± 0.45 Ac	3.76 ± 0.55 Ab	4.45 ± 0.51 ABab	3.68 ± 0.48 Ab	4.57 ± 0.13 Aa
Quantification						
Cervical	2.30 ± 0.23 Ac	3.05 ± 0.50 Abc	2.82 ± 0.25 Abc	4.23 ± 0.35 Aa	3.23 ± 0.54 Ab	4.19 ± 0.36 Aa
Middle	2.34 ± 0.24 Ac	3.09 ± 0.37 Ab	2.87 ± 0.32 Abc	3.81 ± 0.32 Aa	3.30 ± 0.17 Ab	4.29 ± 0.36 Aa
Apical	2.23 ± 0.29 Ac	2.79 ± 0.53 Abc	3.05 ± 0.60 Abc	4.10 ± 0.21 Aa	3.22 ± 0.16 Ab	4.47 ± 0.29 Aa

Different letters, uppercase in column and lowercase in row, indicate statistically significant differences for each parameter evaluated (P<.05).

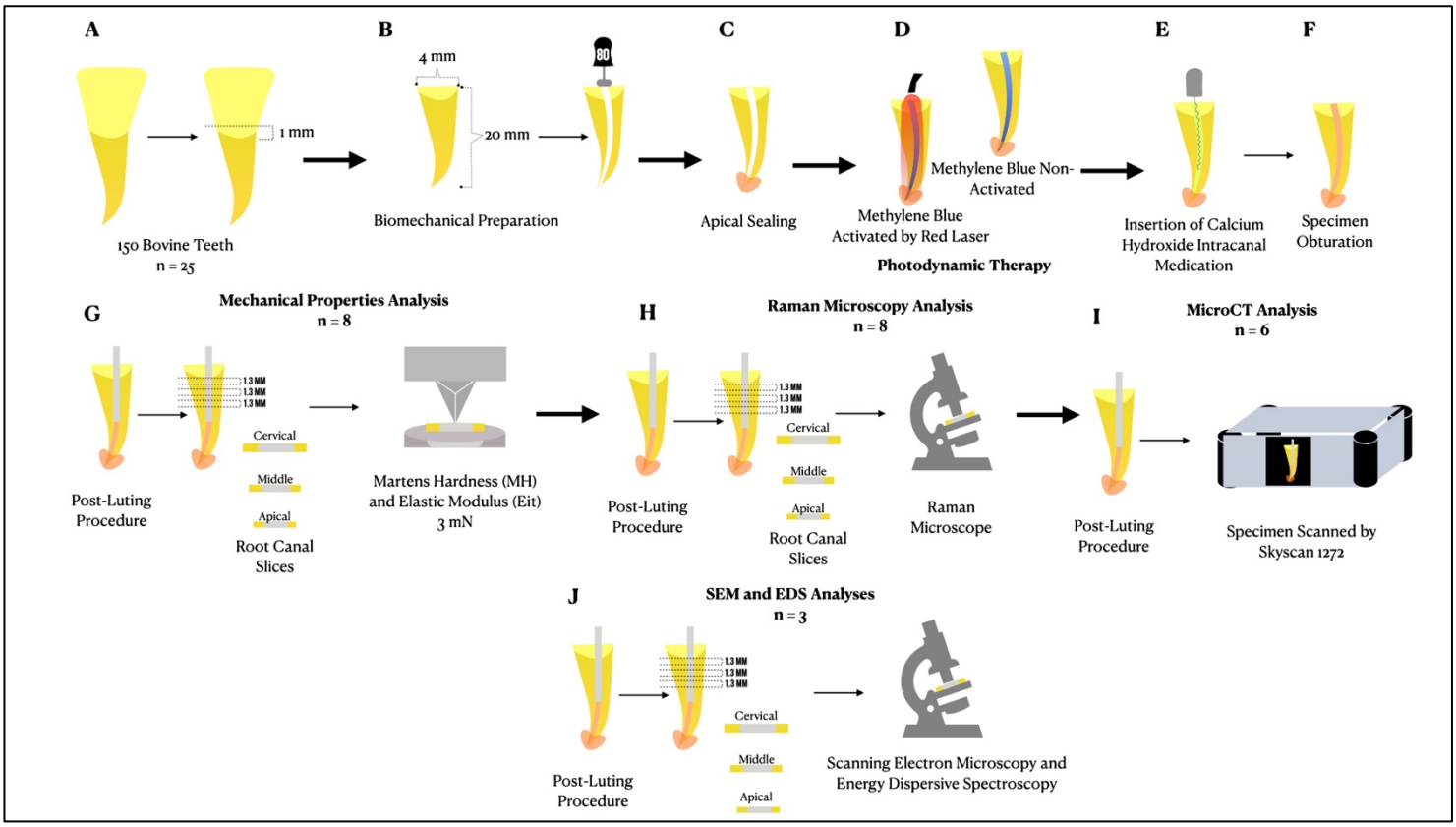


Figure 1. Specimen preparation. A, Bovine incisors and removal of anatomic crowns. B, Standardization of root canal diameter and length. C, Apical portion sealing. D, Antimicrobial photodynamic therapy session. E, Insertion of calcium hydroxide medication into root canals. F, Specimen obturation. G, Obtainment of 1.3-mm thick intraradicular slices for the mechanical properties analyses. H, Specimen preparation for the Raman microscopy analysis. I, Specimen preparation for the Micro-CT analysis. J, SEM and EDS analyses.

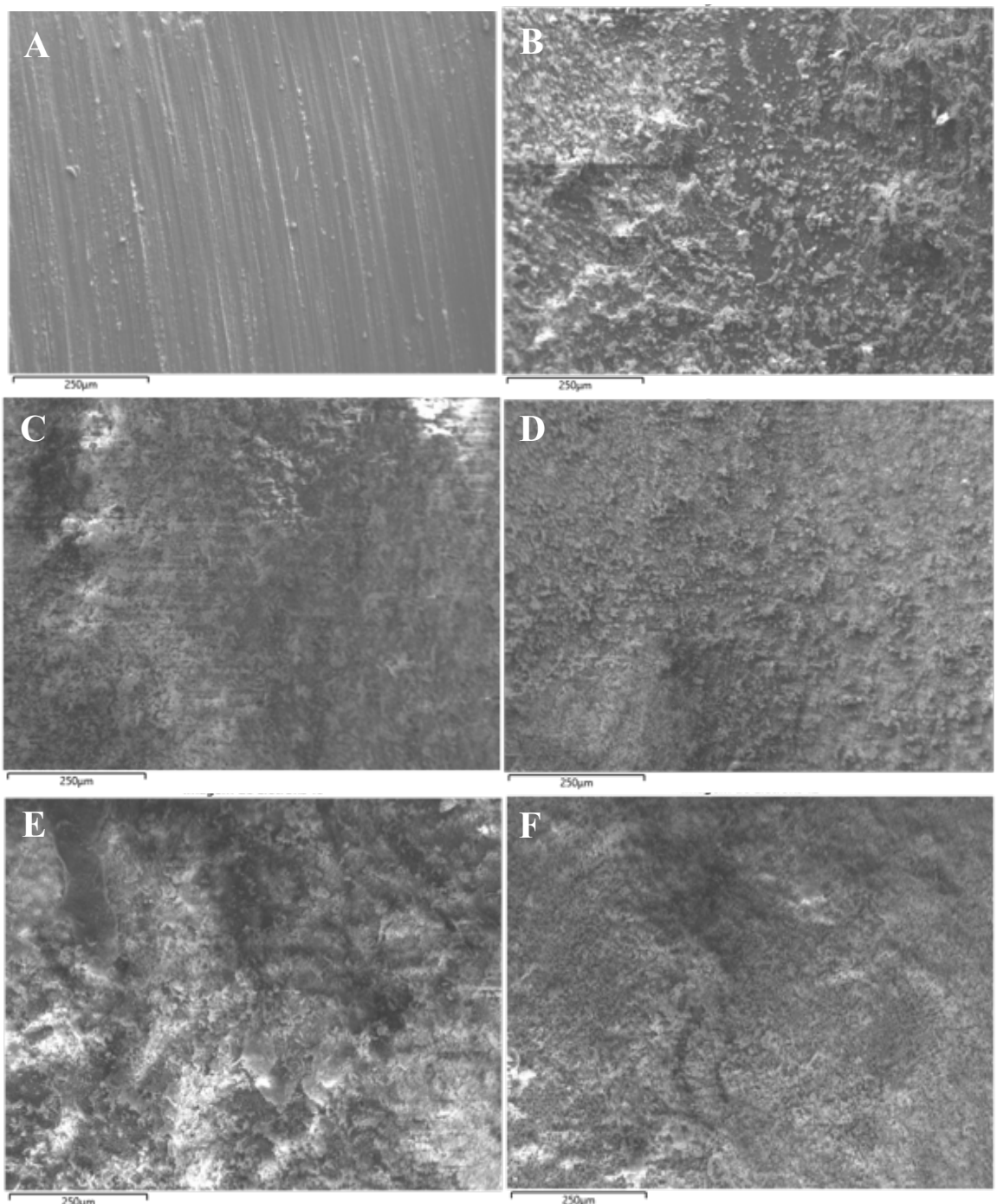


Figure 2. Scanning electron microscopy images of each experimental group under original magnification (×300). A - intraradicular dentin irrigated with deionized water solution (negative control group). B - intraradicular dentin irrigated with deionized water and filled with calcium hydroxide intracanal medication ($Ca[OH]_2$) (positive control group). C - intraradicular dentin after treatment $Ca[OH]_2$ + methylene blue 50 mg/L without activation (MB_{50WA} + $Ca[OH]_2$). D - intraradicular dentin after treatment with $Ca[OH]_2$ + methylene blue 100 mg/L without activation (MB_{100WA} + $Ca[OH]_2$). E - intraradicular dentin after treatment with $Ca[OH]_2$ + methylene blue 50 mg/L activated by red laser(MB_{50A} + $Ca[OH]_2$). F - intraradicular dentin after treatment with $Ca[OH]_2$ + methylene blue 100 mg/L activated by red laser (MB_{100A} + $Ca[OH]_2$).

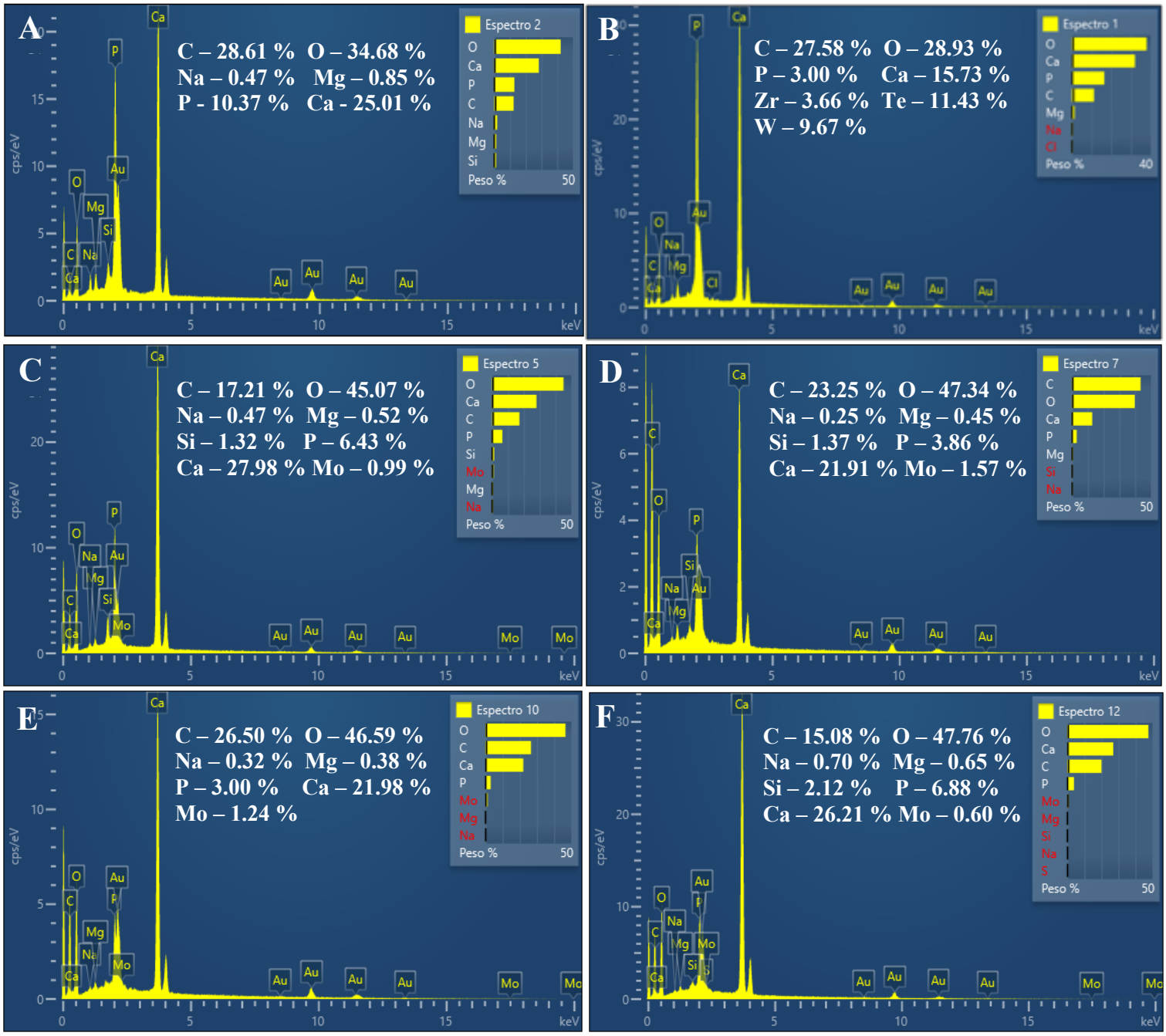


Figure 3. Energy dispersive x-ray spectra of intraradicular dentin surface according to each experimental group. A - intraradicular dentin irrigated with deionized water solution (negative control group). B - intraradicular dentin irrigated with deionized water and filled with calcium hydroxide intracanal medication ($Ca[OH]_2$) (positive control group). C - intraradicular dentin after treatment $Ca[OH]_2$ + methylene blue 50 mg/L without activation (MB_{50WA} + $Ca[OH]_2$). D - intraradicular dentin after treatment with $Ca[OH]_2$ + methylene blue 100 mg/L without activation (MB_{100WA} + $Ca[OH]_2$). E - intraradicular dentin after treatment with $Ca[OH]_2$ + methylene blue 50 mg/L activated by red laser(MB_{50A} + $Ca[OH]_2$). F - intraradicular dentin after treatment with $Ca[OH]_2$ + methylene blue 100 mg/L activated by red laser (MB_{100A} + $Ca[OH]_2$).

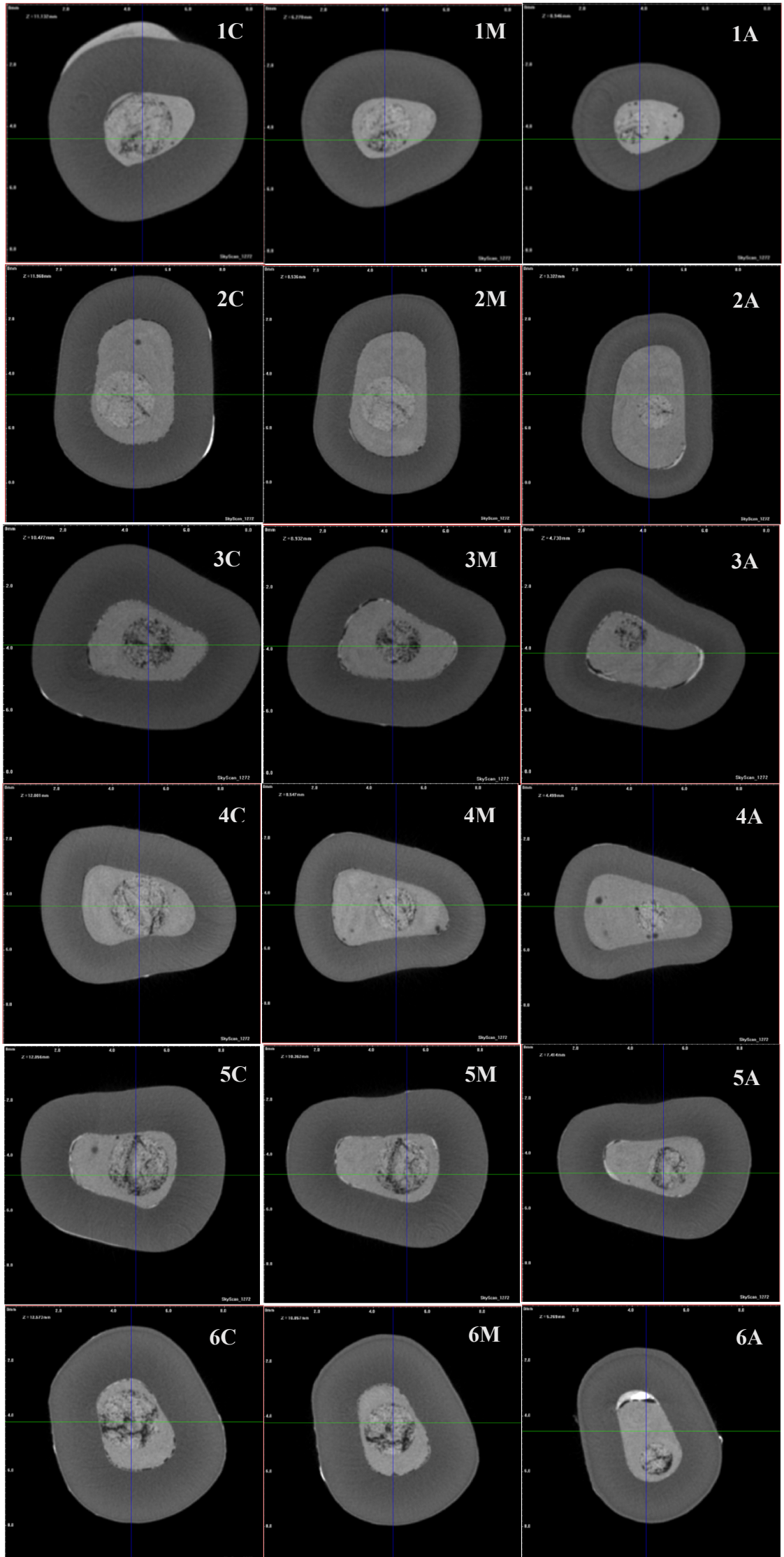

1C
1M
1A
2C
2M
2A
3C
3M
3A
4C
4M
4A
5C
5M
5A
6C
6M
6A

Figure 4. Images from MicroCT of each experimental group and intraradicular dentin thirds (DataViwer Software). 1C, 1M, 1A - Cervical, middle, and apical slices of intraradicular dentin irrigated with deionized water solution (negative control group). 2C, 2M, 2A - Cervical, middle, and apical slices of intraradicular dentin after irrigated with deionized water and filled with calcium hydroxide intracanal medication ($Ca[OH]_2$) (positive control group). 3C, 3M, 3A - Cervical, middle, and apical slices of intraradicular dentin after treatment $Ca[OH]_2$ + methylene blue 50 mg/L without activation (MB_{50WA} + $Ca[OH]_2$). 4C, 4M, 4A - Cervical, middle and apical slices of intraradicular dentin after treatment with $Ca[OH]_2$ + methylene blue 100 mg/L without activation (MB_{100WA} + $Ca[OH]_2$). 5C, 5M, 5A - Cervical, middle, and apical slices of intraradicular dentin after treatment with $Ca[OH]_2$ + methylene blue 50 mg/L activated by red laser(MB_{50A} + $Ca[OH]_2$). 6C, 6M, 6A - Cervical, middle, and apical slices of intraradicular dentin after treatment with $Ca[OH]_2$ + methylene blue 100 mg/L activated by red laser (MB_{100A} + $Ca[OH]_2$).

7) DISCUSSÃO GERAL

Na comparação entre os grupos, pode-se observar que para o terço apical, G4 apresentou menores valores de resistência de união em relação aos grupos controle negativo e G6, levando à rejeição da primeira hipótese nula. Comparando os terços, os resultados mostraram que nos grupos controle positivo, G3, G4 e G5, o terço apical apresentou menores valores de resistência de união quando comparado ao terço cervical, levando também à rejeição da segunda hipótese nula.

Os resultados demonstram que a ação do FS em maior concentração não ativado pelo laser vermelho seguido de medicação intracanal de hidróxido de cálcio promoveu menores valores na resistência de união do terço apical. Uma possível explicação seria a interação tanto da ativação do FS pelo Laser, que por si só já pode causar alterações significativas no substrato dentinário, pois quando ativado o azul de metileno cria espécies reativas de oxigênio (oxigênio singleto), que poderiam influenciar componentes do substrato de dentina, como fosfato (30,34,35).

Comparando terços os resultados mostraram que os grupos controle positivo e G4 apresentam diferença estatisticamente significante, onde o terço apical apresentou menores valores de resistência de união quando comparado aos terços cervical e médio. Já para os grupos G3 e G5, o terço apical apresentou menores valores de resistência de união quando comparado ao terço cervical. O uso de fotopolimerizador para iniciar o processo de polimerização do cimento resinoso, mesmo sendo caracterizado como dupla polimerização, foi utilizado apenas no terço cervical radicular, o que pode ter promovido maior polimerização e cura do cimento neste terço. Nos outros terços, devido à atenuação da passagem da luz com a progressão do canal radicular, a cura do material foi essencialmente química. Isso poderia explicar nossos resultados ao observar o terço cervical dos grupos G3 e G5 em comparação com o terço apical e médio dos mesmos grupos. A configuração anatômica dos terços no canal radicular poderia contribuir para os resultados encontrados. (28,33,56).

Quanto à comparação do terço cervical entre os grupos a Eit* do grupo controle positivo apresentou valores inferiores quando comparados aos grupos G4 e G6. Também para o Eit*, o grupo G4 apresentou valores mais baixos para o terço apical quando comparado ao terço médio ($P < 0,05$), levando à rejeição da primeira hipótese nula. Comparando os terços, os menores valores de HM foram observados para o grupo G4 onde o terço apical apresentou valores menores em relação ao terço médio ($P<0,05$), levando também à rejeição da segunda hipótese nula.

Os resultados demonstram que a ação do FS em maior concentração ativado ou não por laser vermelho seguido de medicação intracanal de hidróxido de cálcio promoveu menores valores para o Eit* no terço cervical. Uma possível explicação é que os terços cervical e médio são mais suscetíveis à ação do FS, pois a cationicidade da substância fez com que os precipitados de fosfato se acumulassem no terço médio, reduzindo a interação entre o cimento resinoso e a superfície

dentinária radicular (36). Além disso, a distribuição e localização dos túbulos dentinários e a concentração diminuem na direção média e apical (45).

Comparando os resultados do grau de conversão ambos os grupos de azul de metileno a 50 mg/L e o grupo de TFD a 100 mg/L apresentaram valores inferiores ao grupo controle positivo quando comparado o terço cervical. Este resultado pode ser explicado pela ação do FS com o substrato dentinário, que pode ter influenciado no grau de conversão do cimento resinoso. Além disso, entre todos os grupos do terço médio, os valores foram menores quando comparados ao grupo controle negativo (exceto o grupo controle positivo). Os dados de comparação do terço apical entre os grupos estabeleceram que os grupos G5 e G6 apresentaram valores menores quando comparados aos dois grupos controle ($P < 0,05$). Uma possível explicação é a anatomia do canal radicular onde quanto mais coronal a polimerização do cimento resinoso se dá mais pela ação da luz e nos terços médio e apical a polimerização é mais devido ao seu processo químico.

As análises de EDS demonstraram que os níveis de fosfato foram diferentes entre os grupos. O grupo controle positivo e o grupo de TFD de AM a 50 mg/L apresentaram o maior percentual assim como ambos os grupos de azul de metileno a 100mg/L apresentaram os menores valores de fosfato. Isso pode ser devido a alterações na proporção do fosfato $Ca_{10}(PO_4)_6(OH)_2$ decorrentes da cationicidade do FS e sua ativação do laser associada aos efeitos da medicação intracanal levando a uma menor concentração desse elemento nesses grupos.

O volume de bolhas pode ser avaliado pela tecnologia Micro-CT, que teve a opção de medir de forma não destrutiva o volume de bolhas da interface do cimento resinoso. O Micro-CT usa fontes de raios X fornecendo imagens reproduzidas em 3D. Como o sistema de imagem não é destrutivo, os destaques internos de um exemplo semelhante podem ser inspecionados. Em relação ao volume de bolhas em geral o terço cervical apresentou mais bolhas que o terço médio e apical este achado pode ser explicado pela gravidade com que o ar flui naturalmente para a direção cervical. Também o grupo com maior volume de bolhas no terço apical foi o grupo G6, que utilizou a maior concentração de azul de metileno.

O PBM associado a irrigação dos canais radiculares e a medicação intracanal de hidróxido de cálcio tem como principais objetivos a modelagem e limpeza do SCR, com a finalidade diminuir a contaminação da cavidade pulpar e torná-la propícia para receber a obturação dos canais radiculares (18). Contudo, algumas regiões podem ficar inacessíveis a essas estratégias aplicadas devido a alta complexidade da anatomia do SCR. O emprego de uma medicação intracanal de hidróxido de cálcio, por ser empregada por 14 dias após o PBM, tem como principal função potencializar a redução dos MO e seus produtos tóxicos no SCR (1). Todavia, ainda com o avanço de diversas tecnologias empregadas no tratamento endodôntico, MO podem resistir a estas estratégias terapêuticas, sendo assim, responsáveis pela resistência da infecção endodôntica e

grande parte dos casos de insucesso (3). Portanto, a constante investigação científica desta estratégia terapêutica justifica-se para o combate e erradicação das infecções endodônticas.

Com o avanço das tecnologias relacionadas a biofotônica como o Laser e Led, inúmeras inovações ocorreram para os tratamentos da Área da Saúde (11,12), como por exemplo, a terapia fotodinâmica (TFD). Esta modalidade terapêutica associada aos FS ativados por uma fonte de luz de comprimento de onda específico provocam uma destruição seletiva de um tecido em um local específico (célula-alvo) (17). No tratamento endodôntico, a TFD é utilizada como uma terapia coadjuvante, ou seja, após o PBM e antes da medicação intracanal de hidróxido de cálcio, a fim de potencializar a descontaminação do SCR, principalmente em relação aos MO resistentes as terapias convencionais utilizadas (18).

Neste estudo foi realizada a TFD com o FS azul de metileno, pois estudos comprovam que estes potencializaram a desinfecção do canal radicular (5). O azul de metileno (cloreto de metiltionínio) é um composto químico, desinfetante e antisséptico, empregado como corante ou indicador nas reações de oxirredução (11). Este também é utilizado como FS para a realização da TFD e por possuir uma banda de absorção na faixa de 500 a 700nm é ativado por Laser vermelho. Concluímos recentemente outro estudo, que avaliou a influência da TFD realizada antes da obturação dos canais radiculares com FS azul de metileno, sem a medicação intracanal de hidróxido de cálcio (9), na resistência de união de pinos de fibra de vidro; obtivemos resultados que demonstraram que a TFD não influenciou na resistência de união de pinos e fibra de vidro à dentina radicular.

No presente estudo, realizamos a microscopia eletrônica de varredura (MEV) de amostras representativas após a classificação do tipo de fratura dos pinos intrarradiculares de fibra de vidro, pois estes são geralmente empregados para realizar reconstruções coronárias quando há uma perda de extensa estrutura dentária. A metodologia empregada neste estudo é conhecida e consagrada, e está de acordo com outros estudos (28,33,56). Entretanto, na literatura são inexistentes a análise em MEV em dentes que foram realizados TFD e medicação intracanal de hidróxido de cálcio nos canais radiculares. Portanto, a ideia em busca desta resposta é oportuna no presente momento.

Neste estudo, foram empregados dentes bovinos devido sua facilidade de aquisição e por estes terem sido utilizados em pesquisas de testes de infiltração marginal, adesão de materiais, avaliação antimicrobiana de medicação intracanal e cimentos obturadores, conforme relatado por Silva et al. em 2019 (46). Os dentes bovinos são semelhantes aos dentes humanos quanto a morfologia, menor variabilidade de permeabilidade do tecido e anatomia interna (19). A dentina de incisivos bovinos pode ser empregue como substrato para substituição da dentina humana em trabalhos in vitro (46).

A remoção das coroas dentárias à 1 mm acima da junção amelocementária com auxílio de cortadeira Isomet 1000, está de acordo com outros estudos (28,33,46,56) e permitiu que as amostras fossem separadas em cortes mais precisos. O comprimento real do dente (CRD) foi estabelecido e posteriormente padronizou-se o comprimento real de trabalho (CRT), com um instrumento tipo K #15 a 1 mm aquém do CRD, estando de acordo com o preconizado pela Disciplina de Endodontia da Faculdade de Odontologia de Araçatuba, FOA-UNESP (28,33,46,56). O preparo biomecânico dos canais radiculares, o emprego da solução irrigadora de hipoclorito de sódio a 1% e a obturação dos canais radiculares foi realizado conforme preconizado por Strazzi-Sayhon et al. 2020 (33) e Banci et al. 2020 (56).

Para realizarmos a TFD propriamente dita, foi utilizado o período de 3 minutos de pré irradiação do FS azul de metileno e posteriormente 60 segundos da ativação de Laser vermelho, λ 660 nm e o diâmetro da fibra óptica do Laser foi de 300 μm, realizando movimentos helicoidais no sentido ápico-cervical (28,33,46,56). A realização da agitação com ultrassom (irrigação passiva) do FS realizada em nosso estudo, concorda com o preconizado por Strazzi-Sayhon et al. 2020 (33), para que ocorra melhor espalhamento do FS no sistema de canais radiculares, empregando a escala de potência 2 para Endodontia, sempre 2 mm aquém do CRT.

Em concordância com os resultados de Strazzi-Sayhon et al. 2020 (33), empregamos a broca de largo n.º1 para desobturar e remover a guta-percha dos canais radiculares, o que facilitou logo depois, o preparo intrarradicular com a broca correspondente ao pino de fibra de vidro White Post DCE nº2. Posteriormente foi realizada a inserção do pino de fibra de vidro White Post DCE nº2, que foi cimentado com o cimento RelyX U200 Dual, de acordo com as instruções do fabricante, como também, em concordância com Strazzi-Sayhon et al. 2018 (32) e 2020 (33).

A escolha do cimento RelyX U200, pode ser explicada pelo fato que Suzuki TY et al. 2015 (55), obtiveram com este cimento os maiores valores de resistência de união, quando comparados aos adesivos convencionais Single Bond 2 em todos os terços estudados e comparado ao adesivo Dual Excite DSC no terço cervical.

O cimento resinoso autoadesivo RelyX U200 apresenta hidrofobicidade acentuada, sendo esta uma característica essencial para promover uma união eficaz e estável (55). Por sua vez, a substância azul de metileno é um corante que possui uma estrutura básica de caráter hidrofílico. Esta característica indica que os componentes hidrofílicos poderiam deteriorar a resistência de união, otimizando a maior sorção de água em função da presença de agentes agregadores como polieletrólitos, ou em função de solventes que favorecem a formação de agregados, como por exemplo, a água. Segundo Wainright et al. (37) a intensidade de sorção hídrica estaria diretamente relacionada à concentração do azul de metileno utilizada, assim sendo, a utilização em grandes

concentrações da solução poderia não trazer benefícios à resistência de união de pinos de fibra de vidro.

Por outro lado, as propriedades do azul de metileno como FS mostraram que não houve influência negativa na resistência de união do material obturador (cimento AH Plus e cones de guta-percha), a dentina radicular quando comparado aos grupos de TFD com ou sem fibra óptica no SCR (31), corroborando com resultados de Strazzi-Sayhon et al. 2018 (32), onde a TFD com o azul de metileno não produziu alterações nas propriedades mecânicas da dentina.

No entanto, Ramos et al. 2018 (33), demonstraram que a TFD com azul de metileno afetou negativamente a resistência de união do cimento RelyX ARC no terço cervical da dentina quando comparado ao cimento RelyX U200 e o adesivo Adper Scotchbond Multiuso. Em contrapartida, Yavari et al. 2017 (34), obtiveram resultados maiores de resistência de união entre o cimento resinoso AH plus e a dentina radicular após a TFD. Contudo, Ok et al. 2013 (35), relataram que não ocorreu um efeito negativo na resistência de união do cimento obturador após a realização da TFD.

Os resultados obtidos neste estudo, mostraram que todos os grupos não apresentaram diferença entre seus terços avaliados em relação ao tipo de fratura encontrada (Gráfico 1).

Acredita-se também que a inserção do cimento resinoso no terço cervical possa reduzir possíveis falhas e formação de bolhas, resultando em uma união mais estável e duradoura (40).

Um estudo prévio realizado por Strazzi-Sayhon et al. 2018 (32) demonstrou que a utilização da TFD com azul de metileno nas concentrações de 50 mg/L e 100 mg/L sem a utilização da medicação intracanal de hidróxido de cálcio não influenciou as propriedades mecânicas, módulo de elasticidade e dureza martens quando comparadas ao grupo controle onde foi utilizado apenas a irrigação com água deionizada. Este estudo também avaliou a resistência de união por meio do teste de *push-out* e obteve diferença estatística no grupo onde foi empregado a TFD com azul de metileno a 100 mg/L. Os resultados da resistência de união foram menores quando comparados ao grupo controle. Considerando que o azul de metileno é uma substância catiônica que tem capacidade de se ligar as moléculas aniônicas, como o fosfato presente na hidroxiapatita. O fosfato está presente no complexo carbonato de cálcio da dentina dessa maneira, o FS azul de metileno poderia induzir alterações na relação cálcio-fosfato, o que poderia justificar tais valores (28,33,46,56).

Em contrapartida um avanço natural dos questionamentos foi levantado sob a influência da TFD com o FS azul de metileno nas propriedades mecânicas da dentina intrarradicular e resistência de união de pinos de fibra de vidro, porém avaliando diferentes terços radiculares, dessa forma outro estudo foi desenvolvido por Strazzi-Sayhon et al. 2020 (33). O estudo confirmou os achados anteriores em relação as propriedades mecânicas pois avaliando os diferentes terços

(cervical, médio e apical) não houve diferença estatística significativa para todos os grupos quando comparados ao grupo controle. Já quando considerados os valores oriundos do teste de resistência de união por *push-out* os resultados demonstraram que o grupo onde foi realizada a TFD com azul de metileno a 100 mg/L o terço médio apresentou menores valores quando comparado ao grupo controle. Os resultados obtidos neste estudo, mostraram que houve uma homogeneidade entre os elementos mais encontrados nas amostras em todos os grupos. A análise EDS mostrou homogeneidade entre os elementos mais encontrados nas amostras em todos os grupos. O cálcio (Ca) foi o elemento mais abundante, com variação entre e 10,46 e 82,18% nas amostras analisadas. Em seguida, oxigênio (O) e carbono (C) foram os elementos observados entre 16,82 e 25% respectivamente. O fosfato (P) foi encontrado em maior quantidade (58,30%) no grupo controle positivo, enquanto nos demais grupos, principalmente os grupos controle negativo, G3, G4, G5 e G6, foi encontrado em quantidades significativamente menores entre 2,51 e 23,23%. Outros estudos realizados utilizando a TFD com o FS azul de metileno mostraram demonstraram que esse FS é uma substância catiônica que tem capacidade de se ligar as moléculas aniônicas, como o fosfato presente na hidroxiapatita (9,16,17). O fosfato está presente no complexo carbonato de cálcio da dentina dessa maneira, o FS azul de metileno poderia induzir alterações na relação cálcio-fosfato, o que poderia justificar os menores valores de fosfato nos grupos 5 e 6.

Em contrapartida a interação tanto da ativação do FS pelo Laser por si só já pode causar mudanças significativas no substrato dentinário, pois quando ativado o azul de metileno cria espécies reativas de oxigênio (oxigênio-singleto) estas reagem com o substrato dentinário, o que poderia influenciar componentes do substrato dentinário, como por exemplo o fosfato (9,17).

A literatura endodôntica clássica comprova a importância fundamental do emprego da medicação de hidróxido de cálcio nos casos de necrose pulpar para complementar a desinfecção do sistema de canais radiculares (1,3). Ao isolar esta variável (hidróxido de cálcio), pudemos investigar se este influencia a composição química do substrato dentinário após sua aplicação e no comportamento do cimento resinoso e o pino de fibra de vidro. A literatura descreve que a medicação intracanal, em especial a de hidróxido de cálcio, quando empregada por longos períodos pode gerar o enfraquecimento da dentina, tornando o dente mais vulnerável à fratura (18,19).

O azul de metileno é uma substância catiônica que tem capacidade de se ligar as moléculas aniônicas, como o fosfato presente na hidroxiapatita (11,32,33,56). Considerando o fato de que o fosfato está presente no complexo carbonato de cálcio da dentina, o FS azul de metileno poderia induzir alterações na relação Ca-P, porém a utilização da medicação de hidróxido de cálcio posteriormente demonstrou que os tipos de falhas encontradas em todos os grupos foram consistentes. A reação entre o fosfato da dentina e o FS azul de metileno, resultaria em precipitados

que seriam responsáveis pela diminuição na resistência de união, uma vez que esses precipitados poderiam criar uma barreira física, reduzindo assim a interação entre cimento resinoso e a superfície da dentina intrarradicular (32,33,56). Neste estudo foi empregado a TFD com azul de metileno seguido da medicação intracanal de hidróxido de cálcio, fato que acreditamos que pode ter ocorrido uma interação da medicação na relação de cálcio no complexo do substrato dentinário.

Assim, observamos que a TFD realizada com o FS azul de metileno seguida da medicação intracanal de hidróxido de cálcio não influenciou de maneira significativa os padrões de fratura das amostras na interface adesiva entre pinos de fibra de vidro em diferentes terços da dentina intrarradicular. Estudos futuros são necessários a fim de se complementar as discussões em torno da TFD e certificar que esta, independente do FS e do laser empregado, não interfira na capacidade de retenção dos pinos de fibra de vidro ao dente, e assim, a TFD possa contribuir na preservação das estruturas dentárias remanescentes.

8) CONCLUSÃO GERAL

Com base na metodologia aplicada e nos resultados obtidos neste estudo, é possível concluir que o uso da aplicação de terapia fotodinâmica com o fotossensibilizador azul de metileno a 50 mg/L associado à medicação intracanal de hidróxido de cálcio não afetou negativamente a resistência de união dos pinos de fibra de vidro à dentina intrarradicular em qualquer um dos terços e não alterou a morfologia da interface adesiva. Além disso, não afetou negativamente as propriedades mecânicas em nenhum dos terços do canal radicular e não alterou a composição química e o volume das bolhas da interface adesiva.

9) APENDICÊ - METODOLOGIA EXPANDIDA

9.1 MATERIAL E MÉTODOS

Este projeto de pesquisa foi submetido e aprovado pela Comissão de Ética no Uso de Animais - CEUA da Faculdade de Odontologia de Araçatuba-UNESP (Processo FOA nº 01003-2018, ANEXO 1).

Foram utilizados 216 dentes incisivos bovinos, recém-extraídos, doados para fins de pesquisa (Frigorífico JBS S.A., Andradina, SP, Brasil), (Figura 1A). Os dentes foram avaliados com lupa de 0,75 de diâmetro e 3,5X de aumento (Bio-Art Equipamentos Odontológicos Ltda, São Carlos, SP, Brasil), sob iluminação adequada, de forma a se observar a ausência de micro-trincas e/ou fraturas induzidas pela extração. Os dentes que apresentaram algum tipo de curvatura apical, micro-trincas e/ou fratura foram imediatamente descartados, sendo os demais armazenados em congelador sob temperatura de -20ºC, até o início do estudo (32).

Os dentes foram radiografados com Raio-X Digital - Software Dental Master Dicom versão 1.0.9.1 e sensor digital Micro Imagem EVO (Micro Imagem, Indaiatuba, SP, Brasil) para auxiliar na confirmação da integridade da estrutura dentária (49), (Figura 1B).

9.2 Preparo do Canal Radicular

A coroa anatômica de todos os dentes foi removida, por meio de uma secção transversal, com disco de diamante em cortadeira de precisão Isomet 1000 (Buheler, Lake Bluff, USA) sob refrigeração, em baixa velocidade, para padronizar as raízes em 20 mm (32,49,60-62), (Figura 1C). O comprimento real do dente (CRD) foi estabelecido por meio de um instrumento tipo K #20 (Dentsply-Maillefer, Ballaigues, Suiça) posicionado no canal radicular até a abertura foraminal. O comprimento real de trabalho (CRT) foi determinado 1 mm aquém do CRD. O PBM foi realizado com instrumento inicial, lima tipo K #50 no CRT e o batente apical foi confeccionado com lima tipo K #80 no CRT. Foi realizada irrigação com 2ml de solução de hipoclorito de sódio a 1% (Apothicário - Farmácia de Manipulação, Araçatuba, SP, Brasil), a cada troca de lima, até a lima K #80 em todos os dentes. Após o término do PBM, foi inserido nos canais radiculares, EDTA 17% (Biodinâmica Química e Farmacêutica LTDA, Ibiporã - PR - Brasil), por 3 minutos para remover a camada de *smear layer*. Posteriormente, o EDTA foi removido com solução de hipoclorito de sódio a 1%, e os canais radiculares foram aspirados e secos com pontas de papel absorvente #80 (Dentsply, Maillefer, Petrópolis, RJ, Brasil) (32,49).

9.3 Distribuição dos Grupos

Os dentes foram distribuídos aleatoriamente em 6 grupos experimentais (n=36), de acordo com a Quadro 1. Posteriormente foram distribuídos aleatoriamente em 2 estudos: sendo o primeiro estudo (n=17), e o segundo estudo (n=8).

Quadro 1: Distribuição dos grupos e procedimentos realizados.

Grupos Experimentais	Procedimentos realizados
G1	PBM + Água Deionizada (Controle Negativo)
G2	PBM + Água Deionizada + $Ca(OH)_2$ (Controle Positivo)
G3	PBM + AM 0,005% + $Ca(OH)_2$
G4	PBM + AM 0,01% + $Ca(OH)_2$
G5	PBM + AM 0,005% + Laser Vermelho λ 660nm (TFD) + $Ca(OH)_2$
G6	PBM + AM 0,01% + Laser Vermelho λ 660nm (TFD) + $Ca(OH)_2$

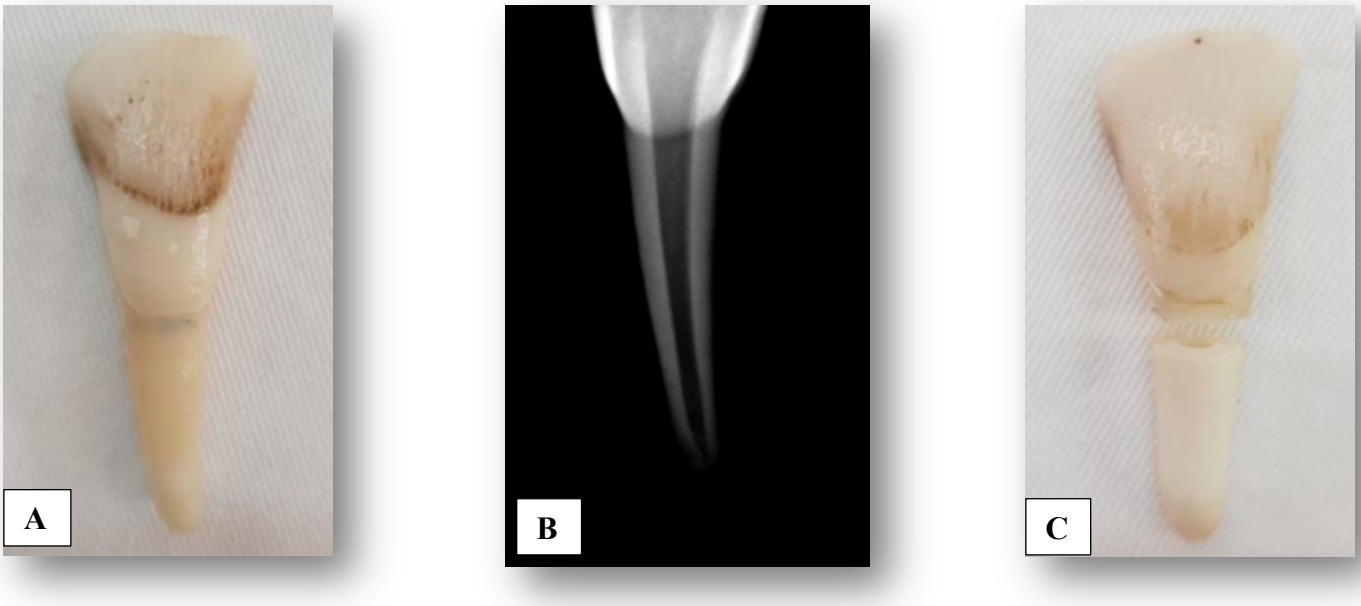


Figura 1. A. Dente Bovino recém extraído. **B.** Dente Bovino radiografado. **C.** Coroa removida 1mm acima da junção amelo-cementária

9.4 Selamento Apical e Terapia Fotodinâmica

Previamente ao emprego da TFD, foi realizado o selamento dos forames apicais para evitar o extravasamento do FS azul de metileno, pois estes podem ser amplos, além de facilitar a obturação dos canais radiculares. O selamento dos forames apicais, foi realizado nos últimos 2mm apicais (32,49), com o auxilio do ácido fosfórico 37% (FGM, Joinville, SC, Brasil), (Figura 2A), sistema adesivo Adper Single Bond 2 (3M ESPE, St Paul, MN, USA) e resina composta Fotopolimerizável Filtek Z250 XT (3M ESPE, St Paul, MN, USA), (Figura 2B).

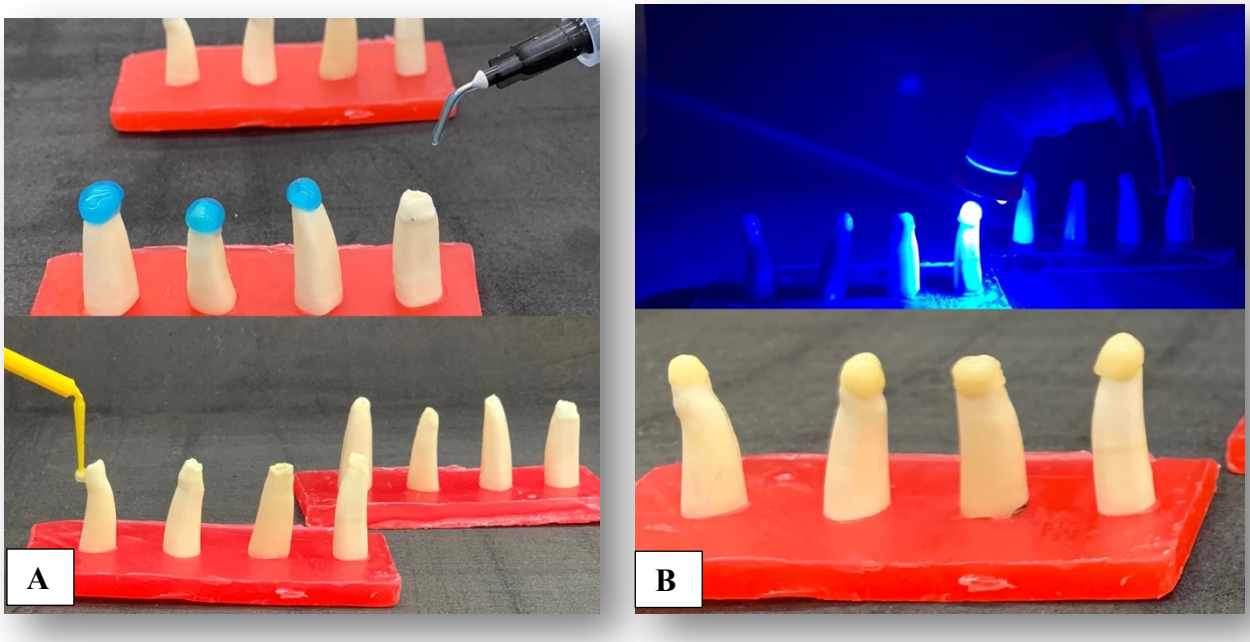


Figura 2. A. Ataque ácido. **B.** Fotopolimerização e amostra selada.

pasta de hidróxido de cálcio, foram preenchidos com água deionizada e não receberam FS, como também não foram realizadas as TFD.

Os grupos G3 e G5 (Figura 3), foram preenchidos com o FS azul de metileno ChimioLux 0,005% (DCM Importação e Exportação de Equipamentos LTDA, São Carlos-SP). Os grupos G4 e G6, foram preenchidos com o FS azul de metileno ChimioLux 0,01% (DCM Importação e Exportação de Equipamentos LTDA, São Carlos-SP). O FS azul de metileno, ficou no interior dos canais radiculares por um período de 180 segundos (período de pré-irradiação) (32,62,63). Sendo os FS agitados por 60 segundos com ultrassom (Ultrassom Satelec Newtron Booster, Acteon, São Paulo, SP, Brasil), na escala de potência 2 para Endodontia, com auxílio de um inserto ultrassônico Irrisonic E1 (Helse Dental Technology, Santa Rosa de Virtebo, SP, Brasil), sem refrigeração, a 2mm aquém do CRT (41,42,46,47). Todo esforço foi feito para minimizar o contato da ponta de ultrassom com as paredes dos canais radiculares e promover a agitação do FS (32,44,49,60,61), (Figura 4).

Após o período de pré-irradiação, foi realizada a irrigação final nos grupos (G3 e G4) com 10mL de água deionizada para remoção do FS e secagem com cânulas de aspiração e pontas de papel absorvente #80.

Nos grupos experimentais G5 e G6 foi realizada a TFD com azul de metileno nas diferentes concentrações (32,47). O FS azul de metileno foi ativado por Laser vermelho 660nm, Laser Therapy XT (DMC, São Carlos, SP, Brasil), por 60 segundos, com auxílio de uma fibra óptica flexível descartável de diâmetro de 300 µm (DMC, São Carlos, SP, Brasil) (32). Utilizamos movimentos helicoidais no sentido ápico-cervical, com a fibra óptica para difusão uniforme da luz por toda a extensão dos canais radiculares (32,44,49,60-62), criando melhores possibilidades de entrega da luz no SCR. Após a realização da TFD, foi realizada a irrigação final com 10mL de água deionizada para remoção do FS e secagem com cânulas de aspiração e pontas de papel absorvente #80.

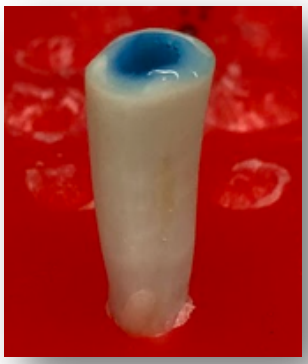


Figura 3. Canal radicular -Azul de Metileno

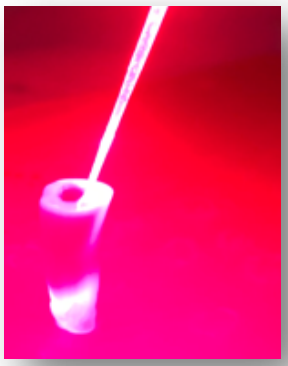


Figura 4. Ativação do fotossensibilizador

Durante o período de pré-irradiação do FS e também durante a ativação do Laser para realizar a TFD, a iluminação do ambiente no laboratório foi reduzida, para que não ocorra algum tipo de degradação do FS azul de metileno e eliminar possíveis interferências nos resultados (32,44,49,60-62).

9.5 Medicação de Hidróxido de Cálcio e Selamento Coronário

Após o PBM (G2 controle positivo), emprego do FS (G3 e G4) e TFD (G5 e G6), foi empregada por um período de 14 dias a medicação intracanal de hidróxido de cálcio (Biodinâmica Química e Farmacêutica, Ibiporã-PR, Brasil), acrescida de iodofórmio (Biodinâmica Química e Farmacêutica, Ibiporã-PR, Brasil) e propilenoglicol usado como veículo viscoso (1,4), exceto no G1 (controle negativo). A medicação intracanal foi levada por meio da espiral de Lentulo #4 (Maillefer-Dentsply, Petrópolis, RJ, Brasil), (Figura 5).

A seguir, os dentes foram radiografados para comprovação do preenchimento do hidróxido de cálcio, em toda extensão dos canais radiculares, de acordo com Holland et al. 2003 (1).

Posteriormente, os dentes foram selados com selamento duplo de cimento Cimpat Branco (Septodont do Brasil Importadora Ltda, Barueri, SP, Brasil) e cimento de ionômero de vidro Maxxion R (FGM, Joinville, SC, Brasil) e armazenados em 100% de umidade, a 37°C, (Figura 6).

Após o período de 14 dias, foram removidos o selamento coronário e a medicação intracanal de hidróxido de cálcio com irrigação copiosa da solução de hipoclorito de sódio à 1% e auxílio de uma lima K #80 no CRT.

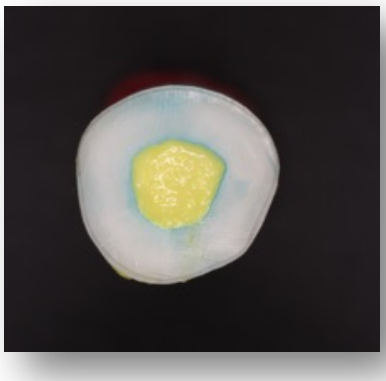


Figura 5. Canal radicular preenchido com Hidróxido de cálcio e Iodofórmio



Figura 6. Dente selado

9.6 Obturação dos canais radiculares

Os canais radiculares de todos os grupos, foram obturados com cones de guta-percha principal #80 e cones de guta-percha auxiliares F e MF (Tanariman Indústria Ltda., Manacapuru, AM, Brasil) e cimento obturador MTA Fillapex (Angelus Indústria de Produtos Odontológicos S/A, Londrina, PR, Brasil), adaptados no CRT, utilizando a técnica de obturação híbrida de *Tagger* com compactador de *McSpadden* #90 (Dentsply, Petrópolis, RJ, Brasil), (Figura 7). O acesso coronário foi selado com selamento duplo de cimento Cimpat Branco (Septodont do Brasil Importadora Ltda, Barueri, SP, Brasil) e cimento de ionômero de vidro Maxxion R (FGM, Joinville, SC, Brasil) (63,64). Os dentes foram armazenados em 100% de umidade, a 37°C, por um período de 7 dias (32,64-68).



Figura 7. Radiografia Digital de canal radicular obturado

9.7 Preparo para os pinos de fibra de vidro

O preparo intrarradicular foi confeccionado em todos os espécimes. O retentor intrarradicular utilizado foi o pino de fibra de vidro White Post DCE nº 2 (FGM, Joinville, SC, Brasil). Primeiramente, utilizando uma broca de largo n.º1 (Dentsply-Maillefer, Tulsa, OK, USA) em baixa velocidade, foi removida a guta-percha e confeccionado o espaço para posterior cimentação dos pinos (cavidade pulpar), que foi calibrado em profundidade de aproximadamente 9 mm, tendo como referência a medida do comprimento de trabalho do dente. Para a padronização do canal radicular foi usada a broca correspondente ao pino nº 2 (FGM, Joinville, SC, Brasil), garantindo a adaptação do pino ao canal radicular (47,60-62).

9.8 Cimentação dos pinos de fibra de vidro

Os pinos foram limpos com acido fosfórico a 37% durante 60 segundos, lavados com água corrente e secos com jatos de ar. Na sequência, foi aplicado o Silano RelyX Ceramic Primer (3M ESPE, St Paul, MN, USA) com um *microbrush* e aplicados jatos de ar para volatizar o solvente do Silano. A cimentação dos pinos foi realizada com o cimento RelyX^{TM} U200 (3M ESPE, St Paul, MN, USA). Antes, os canais radiculares foram irrigados com soro fisiológico 0,9% e posteriormente foi feita aspiração com cânulas endodônticas e secagem com pontas de papel absorvente #80 (Dentsply-Maillefer, Ballaigues, Suiça). A técnica de cimentação dos pinos de fibra de vidro foi por ativação dual, de acordo com as instruções do fabricante, como também, em concordância com outros estudos (32,49,61,62,65), (Figura 8).



Figura 8. Cimentação dos pinos de fibra de vidro no canal radicular com cimento RelyX U200.

9.9 ESTUDO 1 - ANÁLISE DA RESISTÊNCIA DE UNIÃO DOS PINOS DE FIBRA DE VIDRO À DENTINA INTRARRADICULAR

Os 66 espécimes (n=11) selecionados para o Estudo 1, foram armazenados em 100% de umidade, a 37°C, após a cimentação dos pinos de fibra de vidro até a realização do teste de

cisalhamento por extrusão (*push-out*) (período de 7 dias), para máxima polimerização do cimento resinoso (65).

9.9.1 Análise da resistência de união

Os espécimes foram separados para o teste de resistência de união (n=8), foram cortados perpendicularmente ao longo eixo (Isomet 1000), (Figura 9A), obtendo-se *slices* de 1,3mm, (Figura 9B e 9C), que foram analisados (terços cervical, médio e apical) (32,49,65,71). No teste *push-out*, os dispositivos foram adaptados à máquina universal EMIC DL3000 (Emic, São José dos Pinhais, PR, Brasil). Na porção superior, foi fixada uma haste metálica ponta de 0,8mm de diâmetro, e na porção inferior foi fixada a amostra em apoio de aço inoxidável (32,49,65,71).

A haste metálica da porção superior da máquina foi posicionada bem próxima ao corpo de prova, sem tocá-lo, de modo que sua ponta ativa coincida com o centro do pino, (Figura 10A), para evitar tensões nas paredes radiculares ao redor. Uma carga compressiva foi aplicada com velocidade de 0,5mm/min, (Figura 10B).

Os valores de resistência de união ao teste de *push-out* foram calculados pela seguinte divisão: **Ru = N/A**.

Sendo, Ru (Resistência de União) a divisão da carga necessária para ruptura (N) pela área de interface de união (mm^2). Para determinar a área da interface de união, a seguinte formula foi utilizada: $\mathbf{A = \pi\ (R1 + R2)\ \sqrt{(R1 - R2)^2 + h^2}}$.

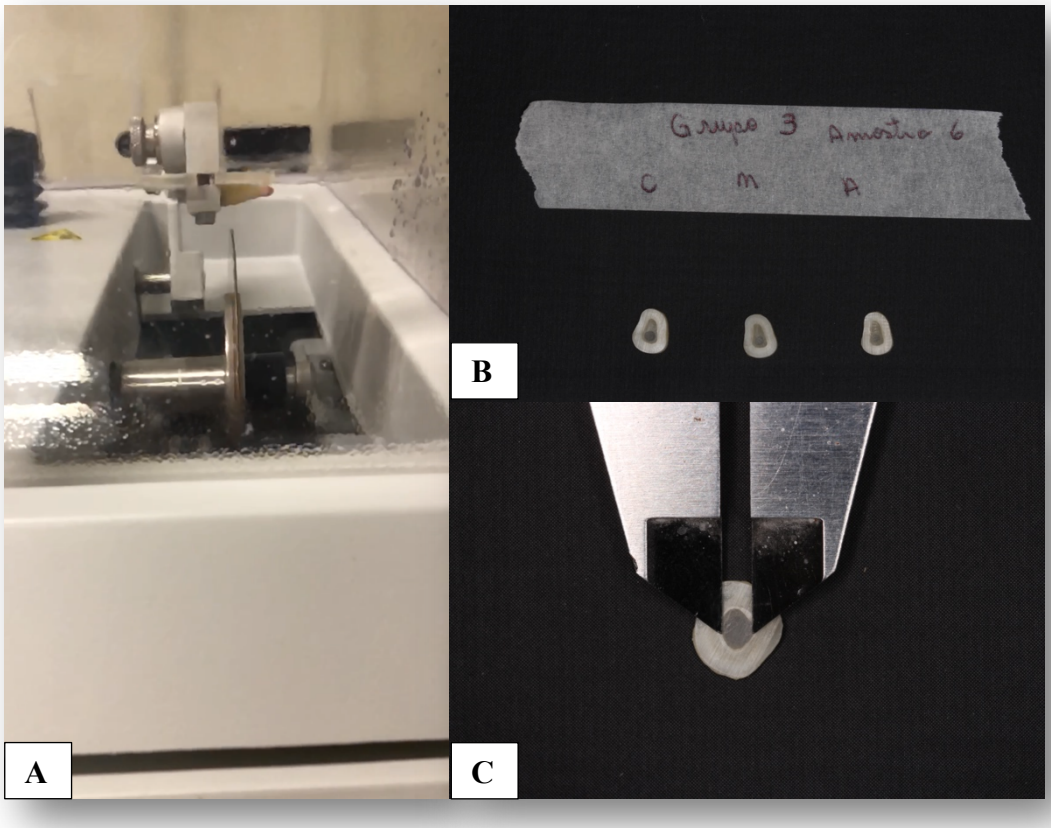


Figura 9. A. Amostra posicionada na cortadeira de precisão. **B.** *Slices* obtidos. **C.** Mensuração do diâmetro central dos *slices.*

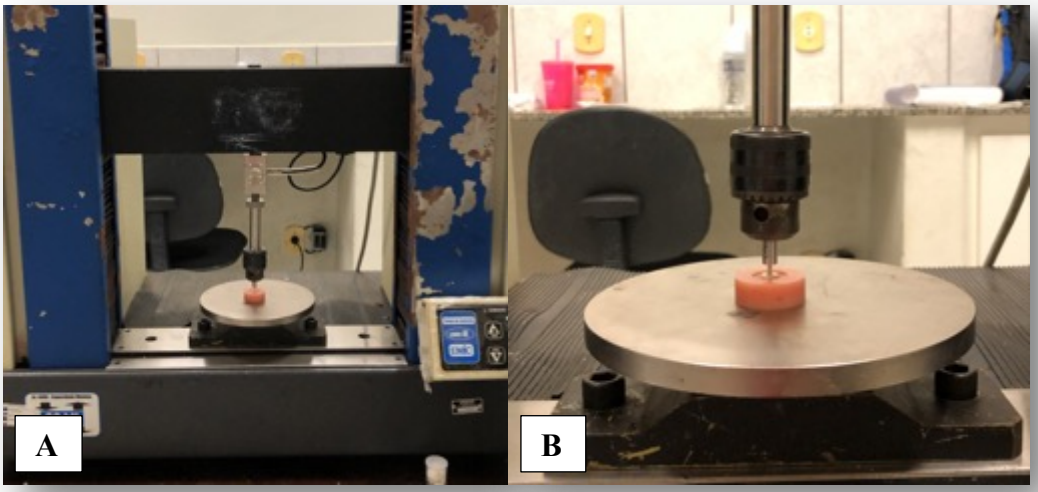


Figura 10. A. Máquina universal EMIC DL3000. **B.** Dispositivos adaptados à máquina EMIC.

Sendo, π = 3,14, R1 = maior diâmetro, R2 = menor diâmetro, h = altura de corte. R1 e R2 foram obtidos pela mensuração dos diâmetros internos da base (maior e menor), os quais correspondem ao diâmetro interno entre as paredes do canal radicular, (Figura 11).

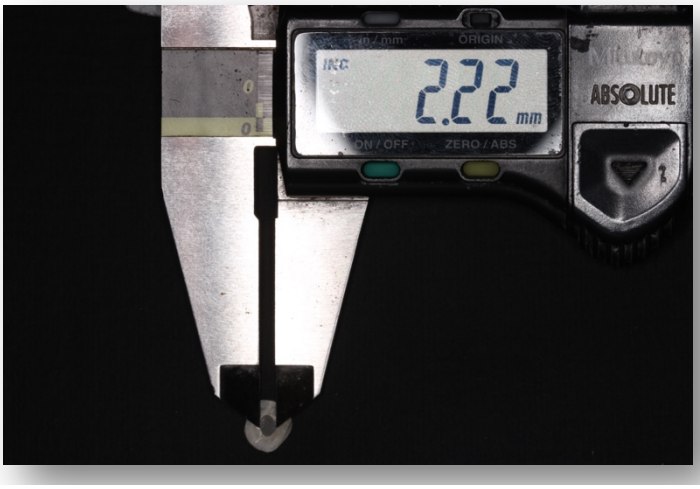


Figura 11. Paquímetro digital mensurando o diâmetro central do *slice*

9.9.2 Análise em Microscopia Eletrônica de Varredura (MEV)

Após o teste de resistência de união, as amostras da dentina radicular foram seccionadas ao meio para exposição da interface adesiva. As amostras fraturadas foram analisadas em lupa

estereoscópica (Stemi SV11, Zeiss, NY, USA) nos aumentos de 6 e 66 vezes, (Figuras 12A e 12 B), para análise do modo de fratura segundo os escores adotados por Suzuki et al. 2015 (43), Sayhon et al. 2018 (32), Sayhon et al. 2019 (49) e Banci et al. 2020 (79). As fraturas foram classificadas em: 1) falha adesiva, 2) falha coesiva na dentina e 3) falha mista. Amostras representativas de cada grupo foram fixadas em *stub* metálico, (Figura 13), sendo metalizados com ouro em metalizador (Balzers SCD-050 Sputter Coater, Alemanha), e levados em microscopia eletrônica de varredura (MEV) (JEOL, JSM 5600LV, Tóquio, Japão) para a ilustração dos padrões de fratura, (Figura 14).

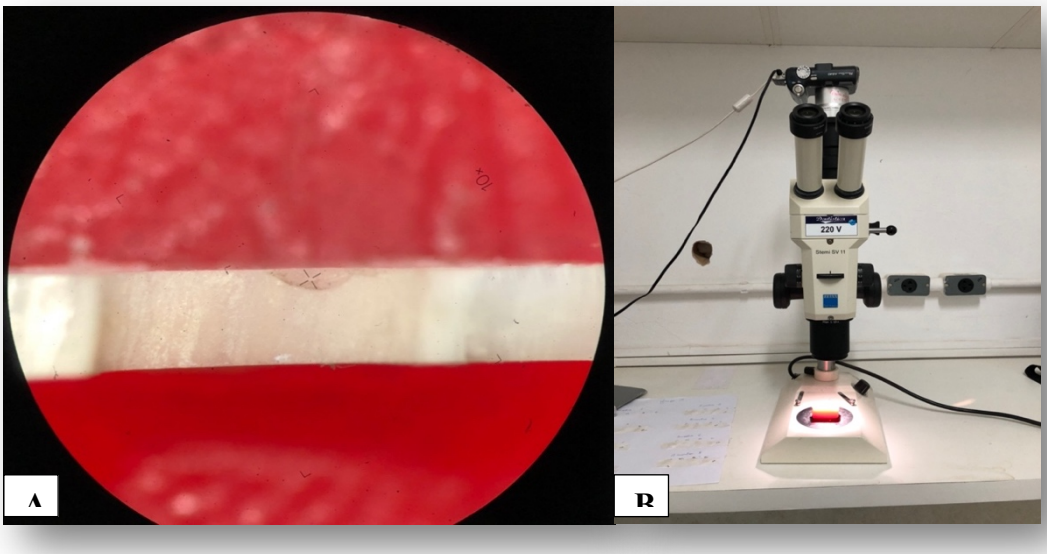


Figura 12. A. *Slice* de amostra em aumento por lupa estereoscópica *slice*. **B.** Lupa estereoscópica

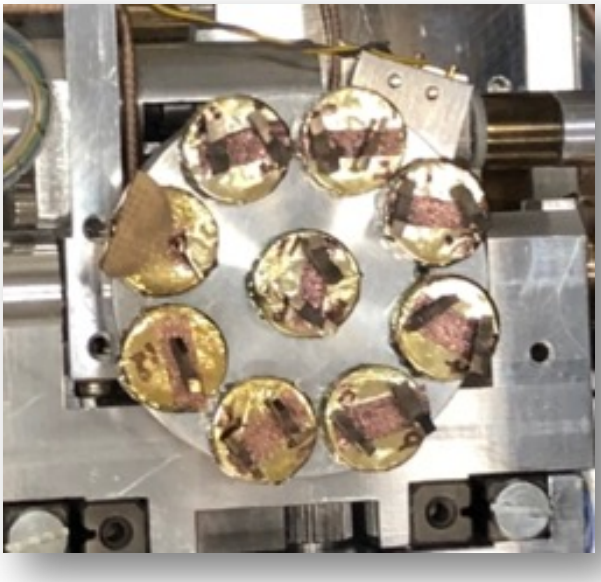


Figura 13. Amostras representativas metalizadas com ouro em metalizador.



Figura 14. Microscópio para microscopia eletrônica de varredura.

9.9.3 Análise em Microscopia Confocal de Fluorescência (MCF)

Foram selecionados 18 incisivos bovinos que foram distribuídos em seis grupos (n=3). Para que as estruturas fossem visualizadas em Microscopia Confocal foi necessária a adição de corante fluorescente Rodamina 0,1% no cimento resinoso. Este corante na cor fúcsia foi adicionado ao cimento na proporção de 0,16 mg/g previamente ao processo de união (54,74,75), (Figura 15A). Um outro corante, a Fluoresceína, foi inserida no canal radicular 4h antes do processo de união dos PFV. Os dentes foram mantidos em reservatório com água destilada por no mínimo 4h, para que a solução contendo o corante Fluoresceína atinja a interface adesiva (54,74,75). Após esse período, os dentes foram secos com papel absorvente e seccionados ao meio no sentido transversal, com disco diamantado em cortadeira de precisão (Isomet 1000, Buheler, Ltd, Lake Bluff, Ill, EUA), sendo obtidas três fatias de cada espécime.

As secções foram colocadas em cuba ultrassônica contendo água para remoção dos debris do procedimento de corte durante 10 minutos. Em seguida, foram examinadas em Microscópio Confocal de Fluorescência (Leica TCS SP2, Leica, Mannheim, Alemanha), (Figura 15B). Um laser de gás misto foi usado como fonte de luz. A excitação da luz foi utilizada com um comprimento de onda máximo de 543nm, (Figura 15C). As imagens foram registradas no modo fluorescente.

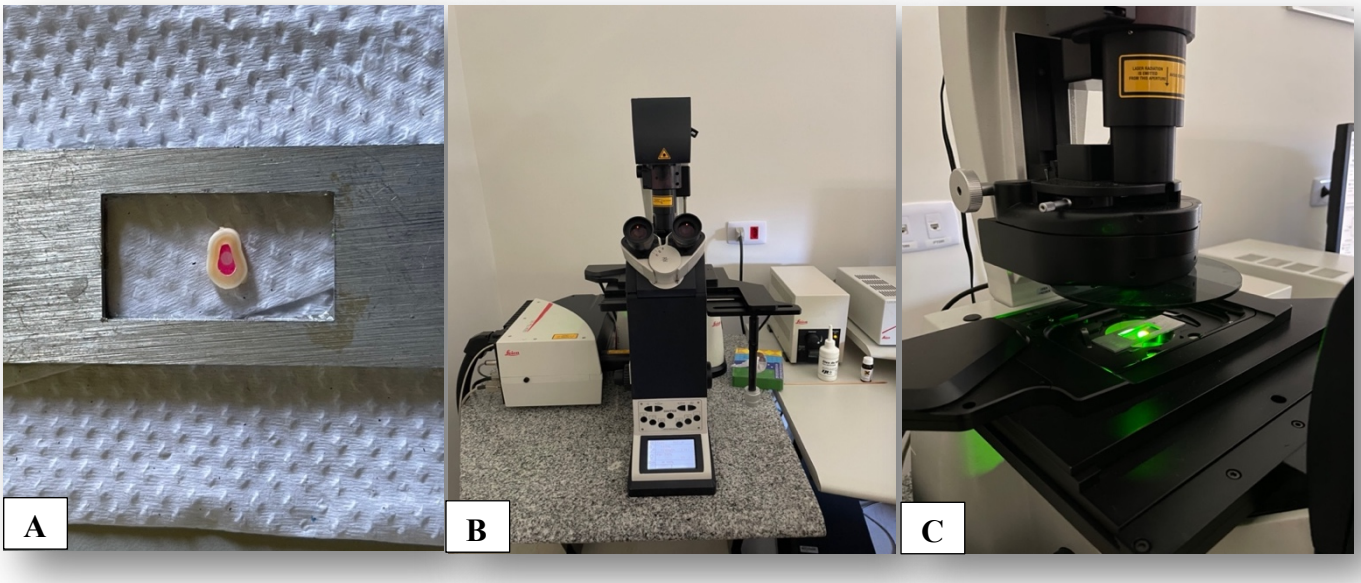


Figura 15. A. *Slice* preparado com cimento + corante rodamina b. **B.** Microscópio Confocal de Fluorescência. **C.** *Slice* da asmostra sob o laser de gás misto.

Uma objetiva imersa em óleo foi utilizada (40x, abertura de 1,25). Uma área representativa de cada fatia foi escaneada em 11 secções de 2µm cada. A imagem obtida da média das 11 secções foi analisada por dois avaliadores previamente calibrados. A avaliação foi realizada pelo método duplo-cego. Nos casos em que houve divergência entre os dois examinadores, ambos avaliaram a imagem novamente até a obtenção de um consenso final. Os seguintes critérios foram avaliados:

a) Qualidade da interface adesiva dentina/cimento (76):

Escore 0 - ausência de fendas, interface adesiva nítida, contínua;

Escore 1 - presença parcial de fendas, interface adesiva parcialmente contínua, presente em menos do que 50% da interface;

Escore 2 - presença de fendas com interface descontínua, presente em aproximadamente mais do que 50% da interface.

b) Formação de *tags* na dentina intraradicular (76):

Escore 0 - não detectável;

Escore 1- poucos tags visíveis;

Escore 2- formação uniforme de *tags* com poucas ramificações laterais;

Escore 3- formação de longos *tags* com muitas ramificações laterais.

c) Profundidade de penetração dos *tags* (77):

Escore 0 - sem tags;

Escore 1 - *tags* ≤ 3µm em média;

Escore 2 - *tags* = 3 a 8,9 µm em média;

Escore 3 - *tags* = 9 a 15 µm em média;

Escore 4 - *tags* ≥ 15 µm em média.

9.10 ESTUDO 2 - ANÁLISE DAS PROPRIEDADES MECÂNICAS (DUREZA MARTENS, MÓDULO DE ELASTICIDADE, ESPECTROSCOPIA DE ENERGIA DISPERSIVA, VOLUME DE BOLHAS E GRAU DE CONVERSÃO)

9.10.1 Propriedades Mecânicas - Dureza Martens e Módulo de Elasticidade

Foram selecionados, 48 espécimes (n=8), que foram cortados perpendicularmente ao longo eixo, com disco diamantado montado em cortadeira de precisão Isomet 1000, obtendo-se uma fatia (*slice*) de aproximadamente 1,3mm de cada terço a serem analisados (terços cervical, médio e apical) (32,40,43,49).

Os *slices* foram embutidos em resina acrílica (Clássico, São Paulo, SP, Brasil), e posteriormente desgastadas manualmente com lixas abrasivas de granulação 320, 600, 800 e 1200 (Extec Corp, Enfield, CT, USA). Posteriormente foram polidas com pastas diamantadas (6, 3 e 1µm) por um período de 4 minutos cada etapa. As amostras foram limpas em cuba ultrassônica (modelo 2210, Branson Ultrasonic Corp., Danbury CT, USA) com água deionizada durante 2 minutos entre as lixas e pastas e ao final do processo (32,40,43,49).

A superfície dental preparada foi conduzida ao Ultramicrodurômetro Digital DUH- 211 (Shimadzu, Kyoto, Japão) (Figura 16A), para verificar a dureza Martens (HM) e módulo de elasticidade (Eit*), sob ação de carga de 3mN a uma velocidade de 0,2926mN/s, com tempo de manutenção de carga de 5 segundos, em cada região de dentina analisada: terço cervical, médio e apical. A ponta indentadora que foi utilizada é a Bercovich. Foram realizadas cinco leituras em cada região (dentina e cimento) (32,40,43,49), (Figura 16B).

Essas grandezas foram obtidas a partir de um ciclo completo de carregamento e descarregamento de cargas. A dureza Martens foi obtida por meio da carga máxima (P max) dividida pela área de superfície indentada (A):

$$\boldsymbol{HM = \frac{Pmax}{A}}$$

O módulo de elasticidade (Eit*) é calculado segundo a equação:

$$\boldsymbol{\frac{1}{Er} = \frac{(1 - v^2)}{Eit} + \frac{(1 - vi^2)}{Ei}},$$

Onde v e vi são respectivamente, os coeficientes de Poisson da amostra e do indentador, sendo o Ei é o módulo de elasticidade do indentador. O módulo de elasticidade reduzido (Er) é calculado pela seguinte equação:

$$\boldsymbol{Er = \frac{\sqrt{\pi}}{2\sqrt{A}} S}$$

Onde (A) é a área projetada pela impressão de contato, (s) é a rigidez do material obtido a partir da inclinação da porção inicial da curva de descarga e π é 3,14.

Os valores do módulo de elasticidade (Eit*) e dureza Martens (HM) foram calculados automaticamente por meio do programa de software do Ultramicrodurômetro Digital DUH- 211 da própria Shimadzu.

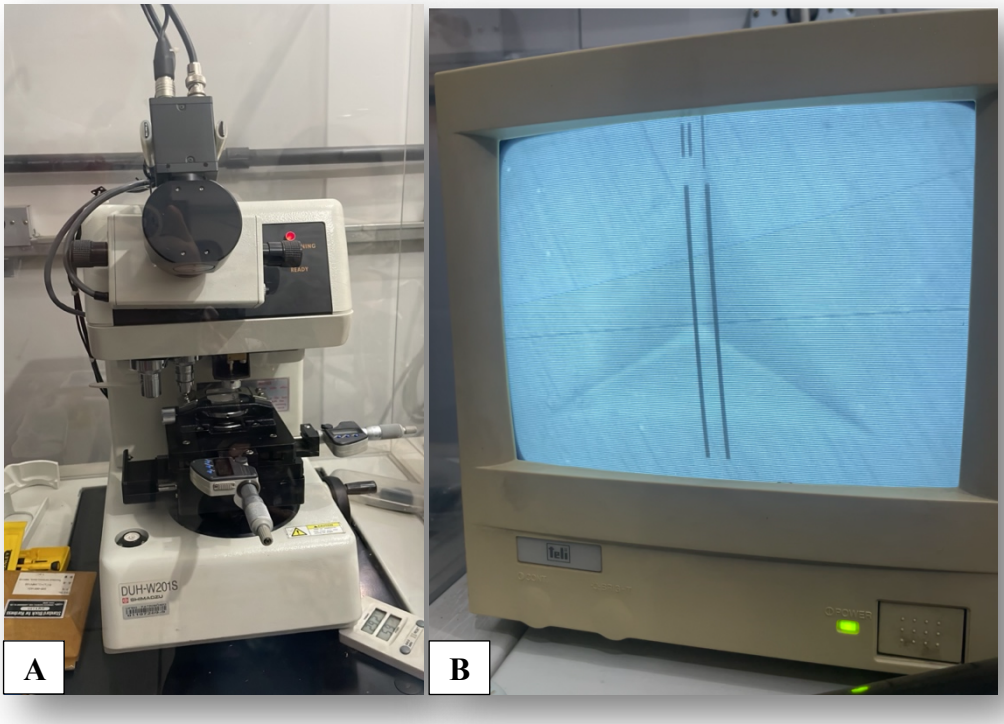


Figura 16. A. Ultramicrodurômetro Digital DUH- 211. **B.** Indentação com a ponta Bercovich sob o tecido dentinário.

9.10.2 Caracterização das amostras por Espectroscopia de Energia Dispersiva (EDS)

O microscópio Stemi SV11 possui ainda um sistema de EDS (Espectroscopia De Energia Dispersiva), (Figura 17), utilizado para identificar a composição química do substrato da dentina intrarradicular, além de permitir o mapeamento dos mesmos, em toda a área selecionada (72). As análises por EDS permitem a caracterização dos elementos químicos presentes em cada superfície dentária (73). Foi realizada a qualificação do substrato da dentina intrarradicular com um detector de estado sólido de Si (Li) a 15 kV após revestimento a plasma por 5 minutos usando um pulverizador de íons em cinco posições diferentes pré-estipuladas de cada espécime.

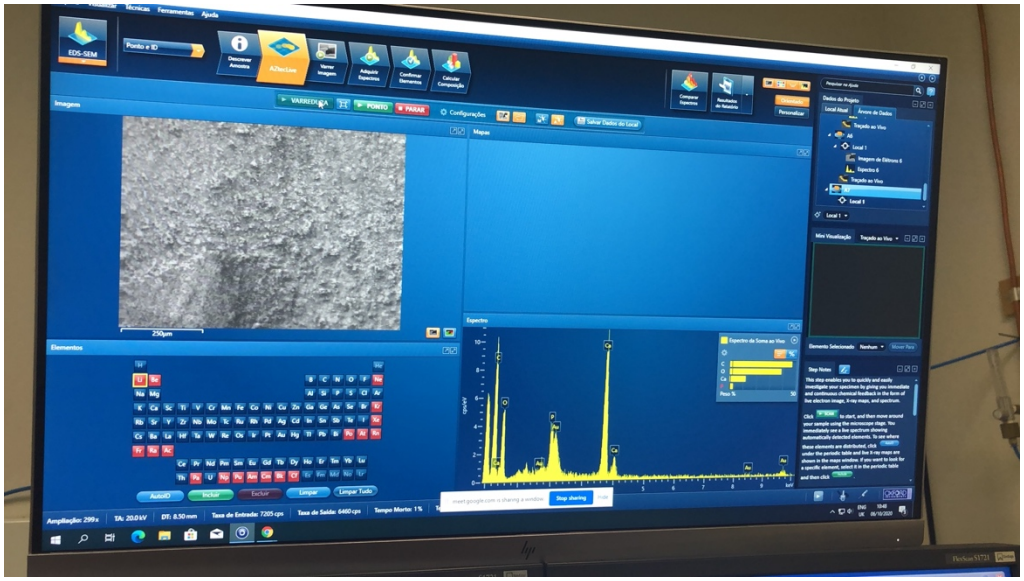


Figura 17. Software de Espectroscopia de Energia Dispersiva

9.10.3 Análise em Microtomografia Computadorizada (Micro-CT)

Para avaliação da integridade, do volume e da presença de bolhas na interface de cimentação, seis espécimes de cada grupo (n=6) foram analisados em um Microtomógrafo de Alta Resolução (SkyScan 1272, Bruker, Kontich, Bélgica) (59,78), (Figura 18A e 18B).

O microtomógrafo foi calibrado usando a função padrão "*phanton*" e operado em condições de energia de 80 kilovolt e 125 mili-amperes. As imagens foram geradas na resolução média (13µm/fatia) e em 180º, os espécimes foram rotacionados a passos angulares de 0,4º com tempo de exposição de 3000 milissegundos; também foram empregados um tubo de 16,5 mm e filtro de alumínio de 1 mm de espessura.

Foi realizado o escaneamento dos espécimes logo após os procedimentos restauradores. Os dados obtidos no escaneamento foram transformados em arquivos DICOM e posteriormente renderizados em modelos tridimensionais (SolidWorks Corp., MA, USA).

Primeiramente, as imagens foram reconstruídas em 3D no software NRecon (SkyScan, Kontich, Bélgica) da parte coronária até a parte apical da raiz, com os parâmetros "*Smoothing*" (6), "*Misalignment compensation*" (-3,5), "*Ring artifacts reduction*" (6), "*Beam-hardening correction* (34%)" e "*change dynamic image range*" (0.003169- 0.230010) iguais para todos os espécimes.

Em seguida, por meio do software DataViewer (SkyScan, Kontich, Bélgica), ocorreu a visualização e análise linear das imagens nos eixos coronal, sagital e trans-axial, bem como a determinação de uma posição padrão para as análises volumétricas.

As análises quantitativas de bolhas na camada de cimento foram determinadas pelo software CTAnalyser (SkyScan, Kontich, Bélgica) na posição transaxial das imagens.

Inicialmente foi estabelecida a área a ser analisada com a seleção em média de 1013 a 1200 fatias, seguida da segmentação da imagem para separar o objeto desejado de outros objetos presentes na imagem. Para tal, foi desenhado um *template* (área de interesse) a mão livre, delimitando apenas a camada de cimento. Na sequência, as imagens foram binarizadas, o volume de bolhas presentes no canal radicular foi calculado (59,78).

Após, com o software CTVOX (SkyScan, Kontich, Bélgica) foi feita a renderização destas imagens em modelos tridimensionais para avaliação da integridade da interface pela observação de áreas do cimento que estavão em descontinuidade com as paredes do canal radicular.

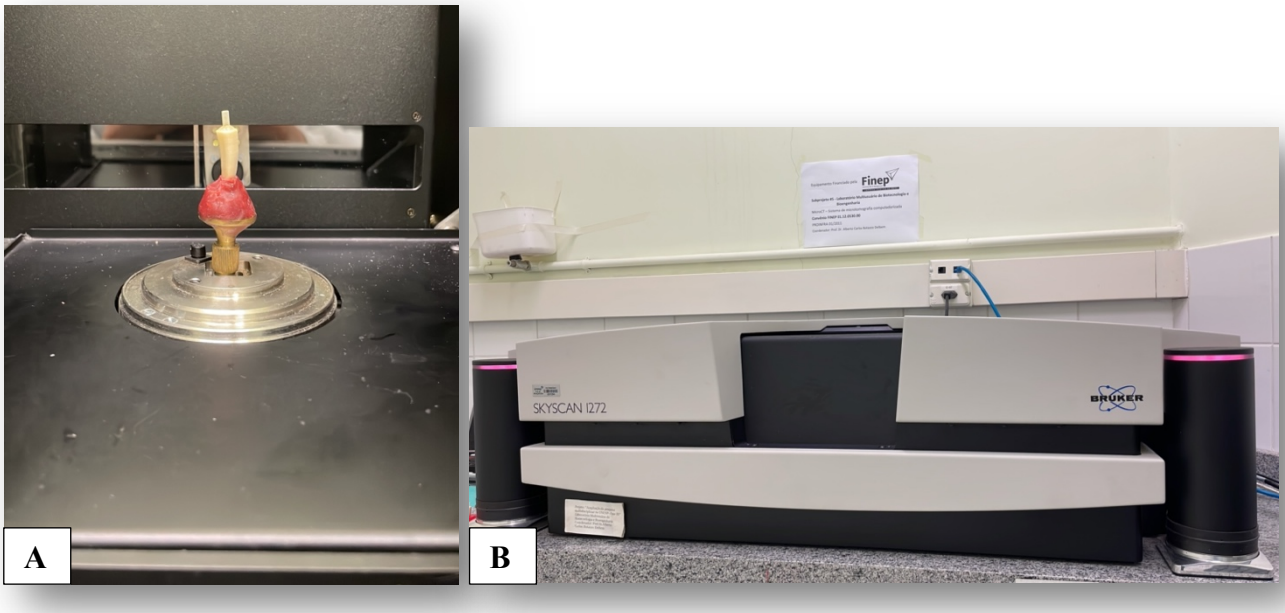


Figura 18. A. Espécime dentro do Microtomógrafo SkyScan 1272. **B.** Microtomógrafo SkyScan 1272.

9.10.4 Propriedades Mecânicas - Grau de Conversão (Espectroscopia de Raman)

As amostras confeccionadas para a avaliação das propriedades mecânicas de dureza Martens e módulo de elasticidade foram utilizadas para avaliar o grau de conversão do material resinoso utilizado na cimentação dos pinos de fibra de vidro na dentina radicular utilizando o equipamento Renishaw Micro-Raman (In-Via, New Mills, Gloucestershire, Reino Unido) (Figura 19) (66). A análise foi realizada com rede de difração de 1800 grooves/mm, acoplado a um microscópio óptico (Leica TCS SPE@, Leica, Mannheim, Alemanha), com resolução espacial de 1,0 µm que permite selecionar a região de interesse da amostra para a obtenção do espectro Raman utilizando o laser de He-Ne (λ=633nm) (66).

Antes do início das leituras, a calibração do aparelho foi realizada com o auxílio de uma placa de Silício (Si) com pico principal de 521 cm^{-1}. Esse material é utilizado constantemente por possuir um pico Raman bem definido (padrão adotado em todos os equipamentos Raman). Após

a calibração ser devidamente realizada, o aparelho foi alinhado e a amostra posicionada. As leituras pelo espectrofotômetro de Raman foram realizadas utilizando-se a objetiva de 50X e aquisição de quatro espectros com um tempo de integração de 10s para cada espectro. Durante a realização do experimento, a luz da sala foi desligada a fim de não influenciar de alguma forma na leitura do espectrofotômetro de Raman. A temperatura ambiente foi mantida constante a 23ºC ± 1ºC, com umidade relativa controlada em ± 34% (67,68).

Nesse tipo de técnica, também conhecida como técnica fotônica ou física quântica, cada gráfico a ser gerado representa a intensidade da radiação espalhada a partir da excitação de um feixe de raio laser, conhecida como "Espectro Raman". Os espécimes foram posicionados na plataforma do microscópio óptico acoplado ao espectrofotômetro de Raman (67,68).

Para calcular o grau de conversão, é necessária a determinação das intensidades relativas do cimento não polimerizado. Para isso, o cimento resinoso não polimerizado foi inserido em uma matriz pré-fabricada em aço inox com 4 mm de diâmetro e 1 mm de espessura, realizando a leitura do material resinoso no aparelho Micro-Raman.

Os valores do grau de conversão do cimento resinoso foram fornecidos por meio de um software específico do aparelho Raman por meio da seguinte equação matemática (69,70):

$$GC\ (\%) = 100\ .\ [\ 1 - (R\ polimerizado\ /\ R\ não\text{-}polimerizado)]$$

Onde R representa a razão entre os picos do cimento polimerizado e não polimerizado respectivamente. A fim de comprovar a viabilidade da análise e do equipamento mencionado, foi realizado um teste piloto da análise dos espectros de Micro-Raman.



Figura 19. Aparelho de Microscopia Renishaw Micro-Raman

10) REFERÊNCIAS DA INTRODUÇÃO GERAL, METODOLOGIA EXPANDIDA E DISCUSSÃO GERAL

1. Holland R, Otoboni Filho JA, de Souza V, Nery MJ, Bernabé PF, Dezan-Jr E. A comparison of one versus two appointment endodontic therapy in dogs' teeth with apical periodontitis. J Endod 2003;29:121-4.
2. Alves FR, Andrade-Junior CV, Marceliano-Alves MF, Pérez AR, Rôças IN, Versiani MA, Sousa-Neto MD, Provenzano JC, Siqueira-Jr JF. Adjunctive Steps for Disinfection of the Mandibular Molar Root Canal System: A Correlative Bacteriologic, Micro-Computed Tomography, and Cryopulverization Approach. J Endod 2016;42:1667-72.
3. Lin LM, Ricucci D, Lin J, Rosenberg PA. Nonsurgical root canal therapy of large cyst-like inflammatory periapical lesions and inflammatory apical cysts. J Endod 2009;35:607-15.
4. Antimicrobial Activity and Physicochemical Properties of Calcium Hydroxide Pastes Used as Intracanal Medication. J Endod 2016;42:1822-28.
5. Ferreira NS, Martinho FC, Cardoso FG, Nascimento GG, Carvalho CA, Valera MC. Microbiological Profile Resistant to Different Intracanal Medications in Primary Endodontic Infections. J Endod 2015;41:824-30.
6. Silva LAB, Nelson-Filho P, Leonardo MR, Rossi MA, Pansani CA. Effect of calcium hydroxide on bacterial endotoxin in vivo. J Endod 2002;28:94-8.
7. Vera J, Siqueira JF Jr, Ricucci D, Loghin S, Fernández N, Flores B, Cruz AG. One- versus two-visit endodontic treatment of teeth with apical periodontitis: a histobacteriologic study. J Endod 2012;38:1040-52.
8. Siqueira JF Jr, Rôças IN, Ricucci D, Hülsmann M. Causes and management of post-treatment apical periodontitis. Br Dent J 2014;216:305-12.
9. Berbert FLCV, Sivieri-Araujo G, Ramalho LT, Pereira SA, Rodrigues DB, Araújo MS. Quantification of fibrosis and mast cells in the tissue response of endodontic sealer irradiated by low-level laser therapy. Lasers Med Sci 2011;26:741-7.

10. Sivieri-Araujo G, Berbert FLCV, Ramalho LTO, Rastelli ANS, Crisci FS, Bonetti-Filho I, Tanomaru-Filho M. Effect of red and infrared low-level laser therapy in endodontic sealer on subcutaneous tissue. Laser Phys 2011;21:1-7.
11. Allison RR, Moghissi K. Photodynamic Therapy (PDT): PDT Mechanisms. Clin Endosc 2013;46:24-9.
12. Bilkis I, Silman I, Weiner L. Generation of Reactive Oxygen Species by Photosensitizers and their Modes of Action on Proteins. Curr Med Chem. 2018 Jan 4. [Epub ahead of print].
13. Gomes-Filho JE, Sivieri-Araujo G, Sipert CR, Santos LMS, Queiroz IOA, Men CM, Maia NKC, Cintra LTA, Dezan-Junior E, Bagnato VS, Chaves-Neto AH, Oliveira SHP. Evaluation of photodynamic therapy on fibroblast viability and cytokine production. Photodiagnosis Photodyn Ther. 2016;13:97-100.
14. Cushnie TP, O'Driscoll NH, Lamb AJ. Morphological and ultrastructural changes in bacterial cells as an indicator of antibacterial mechanism of action. Cell Mol Life Sci 2016;73:4471-92.
15. Rego-Filho FG, de Araujo MT, Bagnato VS. Validation of Photodynamic Action via Photobleaching of a New Curcumin-Based Composite with Enhanced Water Solubility. J Fluoresc 2014;24:1407-13.
16. Faria CM, Inada NM, Kurachi C, Bagnato VS. Determination of the threshold dose distribution in photodynamic action from in vitro experiments. J Photochem Photobiol B 2016;162:168-75.
17. Allison RR, Sibata CH. Photodynamic therapy: mechanism of action and role in the treatment of skin disease. G Ital Dermatol Venereol 2010;145:491-507.
18. Allison RR, Moghissi K. Oncologic photodynamic therapy: clinical strategies that modulate mechanisms of action. Photodiagnosis Photodyn Ther 2013;10:331-41.
19. Sivieri-Araujo G, Queiroz IOA, Fabbro RD, Esteves F, Cintra LTA, Duarte PCT, Bagnato VS, Oliveira SHP, Gomes-Filho JE. Rat tissue reaction and cytokine production induced by antimicrobial photodynamic therapy. Photodiagnosis Photodyn Ther 2017;18:315-318.

20. Souza MA, Dias CT, Zandoná J, Hoffmann IP, Menchik VHS, Palhano HS, Bertol DC, Rossato-Grando LG, Cecchin D, Figueiredo JAP. Antimicrobial activity of hypochlorite solutions and reciprocating T instrumentation associated with photodynamic therapy on root canals infected with Enterococcus faecalis. Photodiagnosis Photodyn Ther 2018;23;347-352.
21. Okamoto CB, Motta LJ, Prates RA, Mota ACC, Gonçalves MLL, Horliana ACRT, Ferrari RAM, Fernandes KPS, Bussadori SK. Antimicrobial Photodynamic Therapy as a Co-adjuvant in Endodontic Treatment of Deciduous Teeth: Case Series. J Photochem Photobiol 2018;94;760-4.
22. Shrestha A, Cordova M, Kishen A. Photoactivated polycationic bioactive chitosan nanoparticles inactivate bacterial endotoxins. J Endod 2015;41:686-91.
23. Bulit F, Grad I, Manoil D, Simon S, Wataha JC, Filieri A, Feki A, Schrenzel J, Lange N, Bouillaguet S. Antimicrobial activity and cytotoxicity of 3 photosensitizers activated with blue light. J Endod. 2014;40:427-31.
24. Neelakantan P, Cheng CQ, Ravichandran V, Mao T, Sriraman P, Sridharan S, Subbarao C, Sharma S, Kishen A. Photoactivation of curcumin and sodium hypochlorite to enhance antibiofilm efficacy in root canal dentin. Photodiagnosis Photodyn Ther. 2015;12:108-14.
25. Silva LAB, Novaes AB Jr, Oliveira RR, Nelson-Filho P, Santamaria M Jr, Silva RA. Antimicrobial photodynamic therapy for the treatment of teeth with apical periodontitis: a histopathological evaluation. J Endod 2012;38:360-6.
26. ANVISA Agência Nacional de Vigilância Sanitária. Consolidado de Normas COFID, versão IV, p. 178, Brasília, abril 2013. Disponível em: http://portal.anvisa.gov.br/wps/wcm/connect/6805ba804f5ea576920df79a71dcc661/ConsolidadoVersaoIVpublicar.pdf?MOD=AJPERES. Acesso 15 de julho de 2019.
27. Tardivo JP, Del Giglio A, de Oliveira CS, Gabrielli DS, Junqueira HC, Tada DB, Severino D, de Fátima Turchiello R, Baptista MS. Methylene blue in photodynamic therapy: From basic mechanisms to clinical applications. Photodiagnosis Photodyn Ther 2005;2:175-91.

28. Sivieri-Araujo G, Santos LMS, Queiroz IOA, Wayama MT, Yamanari GH, Martins CM, Dezan-Júnior E, Cintra LTA, Gomes-Filho JE. Photodynamic therapy in Endodontics: Use of a supporting strategy to deal with endodontic infection. Dental Press Endod. 2013;3:52-8.

29. Erickson RL, Barkmeier WW, Latta MA. The role of etching in bonding to enamel: A comparison of self-etching and etch-and-rinse adhesive systems. Dent Mater. 2009;11;1469-67.

30. Liu Y, Tjäderhane L, Breschi L, Mazzoni A, Li N, Mao J, Pashley DH, Tay FR. Limitations in bonding to dentin and experimental strategies to prevent bond degradation. Journal of Dental Research. 2011;90;953-68.

31. Souza MA, Lana DD, Gabrielli E, Ribeiro MR, Miyagaki DC, Cecchin D. Effectiveness of final decontamination protocols against Enterococcus faecalis and its influence on bond strength of filling material to root canal dentin. Photodiagnosis Photodyn Ther 2017;17;92-7.

32. Strazzi Sahyon HBS, Silva PP, Oliveira MS, Cintra LTA, Gomes-Filho JE, Santos PH, Sivieri-Araujo G. Effect of photodynamic therapy on the mechanical properties and bond strength of glass-fiber posts to endodontically treated intraradicular dentin. J Prosthet Dent 2018;120:317.

33. Ramos ATPR, Belizário LG, Venção AC, Jordão-Basso KCF, Rastelli ANS, Andrade MF, Kuga MC. Effects of Photodynamic Therapy on the Adhesive Interface of Fiber Posts Cementation Protocols. J Endod 2018;44:173-8.

34. Yavari H, Ghasemi N, Divband B, Rezaei Y, Jabbari G, Payahoo S. The effect of photodynamic therapy and polymer solution containing nano-particles of Ag /ZnO on push-out bond strength of the sealers AH-Plus and MTA Fillapex. J Clin Exp Dent 2017;9:1109–14.

35. Ok E, Ertas H, Saygili G, Gok T. Effect of Photoactivated Disinfection on Bond Strength of Root Canal Filling. J Endod 2013;39:1428-30.

36. Wainwright M, Phoenix DA, Rice L, Burrow SM, Waring J. Increased cytotoxicity and phototoxicity in the methylene blue series via chromophore methylation. J Photochem Photobiol B 1997;40;233-9.

37. Di Hipólito V, Rodrigues FP, Piveta FB, Azevedo Lda C, Bruschi Alonso RC, Silikas N, Carvalho RM, De Goes MF, D'Alpino PHP. Effectiveness of self-adhesive luting cements in bonding to chlorhexidine-treated dentin. Dent Mater 2012;28:495-501.

38. Santos PH, Karol S, Bedran-Russo AK. Long-term nano-mechanical properties of biomodified dentin-resin interface components. J Biomech 2011;44:1691-4.

39. Santos PH, Karol S, Bedran-Russo AK. Nanomechanical properties of biochemically modified dentin bonded interfaces. J Oral Rehabil 2011;38:541-6.

40. Berger SB, Pavan S, Vidal CM Santos PH, Giannini M, Bedran-Russo AK. Changes in the stiffness of demineralized dentin following application of tooth whitening agents. Acta Odontol Scand 2012;70:56-60.

41. Shahdad SA, McCabe JF, Bull S, Rusby S, Wassell RW. Hardness measured with traditional Vickers and Martens hardness method. Dent Mater 2007;23:1079-85.

42. Ilie N, Hilton TJ, Heintze SD, Hickel R, Watts DC, Silikas N, Stansbury JW, Cadenaro M, Ferracane JL. Academy of Dental Materials guidance-Resin composites: Part I-Mechanical properties. Dent Mater. 2017;33:880-94.

43. Suzuki TY, Gomes-Filho JE, Gallego J, Suzuki TY, Gomes-Filho JE, Gallego J, Pavan S, Dos Santos PH, Fraga Briso AL. Mechanical properties of components of the bonding interface in different regions of radicular dentin surfaces. J Prosthet Dent 2015;113:54-61.

44. Oliveira MS. Influência da terapia fotodinâmica com azul de metileno na dentina radicular: estudo das propriedades mecânicas (dureza e módulo de elasticidade). Iniciação Científica, 2015/2016-PROPe-UNESP.

45. Lezaja M, Veljovic D, Manojlovic D, Milosevic M, Mitrovic N, Janackovic D, Miletic V. Bond strength of restorative materials to hydroxyapatite inserts and dimensional changes of insert-containing restorations during polymerization. Dent Mater. 2015;31:171-81.

46. Araoka D, Hosaka K, Nakajima M, Foxton R, Thanatvarakorn O, Prasansuttiporn T, Chiba A, Sato K, Takahashi M, Otsuki M, Tagami J. The strategies used for curing universal adhesives affect the micro-bond strength of resin cement used to lute indirect resin composites to human dentin. Dent Mater J. 2018;37:506-14.

47. Suzuki TY, Godas AG, Guedes AP, Catelan A, Pavan S, Briso AL, Santos PH. Microtensile bond strength of resin cements to caries-affected dentin. J Prosthet Dent 2013;110:47-55.

48. Dimitrouli M, Geurtsen W, Lührs AK. Comparison of the push-out strength of two fiber post systems dependent on different types of resin cements. Clin Oral Investig 2012;16:899-908.

49. Strazzi Sahyon HB, Silva PPD, Oliveira MS, Cintra LTA, Dezan-Júnior E, Gomes-Filho JE, Jacinto RC, Dos Santos PH, Sivieri-Araujo G. Influence of curcumin photosensitizer in photodynamic therapy on the mechanical properties and push-out bond strength of glass-fiber posts to intraradicular dentin. Photodiagnosis Photodyn Ther. 2019 Mar;25:376-381.

50. Akbulut MB, Terlemez A. Does the Photon-Induced Photoacoustic Streaming Activation of Irrigation Solutions Alter the Dentin Microhardness? Photobiomodul Photomed Laser Surg. 2019 Jan;37(1):38-44.

51. Fagundes TC, Toledano M, Navarro MF, Osorio R. Resistance to degradation of resin-modified glass-ionomer cements dentine bonds.J Dent. 2009 May;37(5):342- 7.

52. Marigo L, Lajolo C, Castagnola R, Angerame D, Somma F. Morphological confocal laser scanning microscope evaluation of four different "etch and rinse" adhesives in post endodontic restoration. Dent Mater J. 2012;31(6):988-94.

53. Fagundes TC, Somensi DS, Dos Santos PH, Navarro MF. Confocal laser scanning microscopy investigation of Bond interfaces involved in fiber glass post cementation . Braz Dent Sci 2014 Apr/Jun;17(2).

54. Piai GG, Duarte MAH, Nascimento ALD, Rosa RAD, Só MVR, Vivan RR. Penetrability of a new endodontic sealer: A confocal laser scanning microscopy evaluation. Microsc Res Tech. 2018 Nov;81(11):1246-1249.

55. Rhodes JS, Ford TR, Lynch JA, Liepins PJ, Curtis RV. Micro-computed tomography: a new tool for experimental endodontology. Int Endod J. 1999 May;32(3):165-70.

56. Peters OA, Laib A, Rüegsegger P, Barbakow F. Three-dimensional analysis of root canal geometry by high-resolution computed tomography. J Dent Res. 2000 Jun;79(6):1405-9.

57. Versiani MA, Ordinola-Zapata R, Keleş A, Alcin H, Bramante CM, Pécora JD et al. Middle mesial canals in mandibular first molars: A micro-CT study in different populations. Arch Oral Biol. 2016 Jan;61:130-7.

58. Crozeta BM, Silva-Sousa YT, Leoni GB, Mazzi-Chaves JF, Fantinato T, Baratto-FilhoF et al. Micro computed tomography study of filling material removal from oval-shaped canals by using rotary, reciprocating and adaptive motion systems. J Endod. 2016 May;42(5):793-7.

59. Rivera-Peña ME, Duarte MAH, Alcalde MP, DE Andrade FB, Vivan RR. A novel ultrasonic tip for removal of filling material in flattened/oval-shaped root canals: a microCT study. Braz Oral Res. 2018 Aug 13;32:e88.

60. Oliveira MS. Efeito da terapia fotodinâmica com azul de metileno na resistência de união de pinos de fibra de vidro à dentina radicular. Iniciação Científica - PIBIC FOA-UNESP, 2015-2016.

61. Silva PP. Influência da terapia fotodinâmica na resistência de união de pinos de fibra de vidro à dentina radicular. Iniciação Científica - FOA-UNESP, 2015-2016. Processo FAPESP Nº: 2015/06056-3.

62. Silva PP. Resistência de união de pinos de fibra de vidro à dentina radicular submetido à duas sessões de terapia fotodinâmica. Iniciação Científica-FOA-UNESP, 2016-2017. Processo FAPESP Nº: 2016/24718-6.

63. Cintra LTA, Batistella AR, Marson FC, Archangelo CM, Gomes-Filho JE. Effect of different surface treatments on the push-out bond strength of fiber posts into the root canal. Dental Press Endod. 2015;5:33-9.

64. Sivieri-Araujo G. Influência de diferentes soluções irrigadoras associadas à terapia fotodinâmica: estudo in vitro e in vivo. Pós-Doutorado 2012-2014, Processo FAPESP Nº: 2011/23287-8.

65. D'Alpino PH, Silva MS, Vismara MV, Di Hipólito V, Miranda González AH, de Graeff CFO. The effect of polymerization mode on monomer conversion, free radical entrapment, and interaction with hydroxyapatite of commercial self-adhesive cements. J Mech Behav Biomed Mater 2015;46:83-92.

66. Kuguimiya RN, Rode KM, Carneiro PM, Aranha AC, Turbino ML. Influence of Curing Units and Indirect Restorative Materials on the Hardness of Two Dual-curing Resin Cements Evaluated by the Nanoindentation Test. J Adhes Dent 2015;17:243-8.

67. Komori PC, de Paula AB, Martin AA, Tango RN, Sinhoreti MA, Correr-Sobrinho L. Effect of light energy density on conversion degree and hardness of dual-cured resin cement. Oper Dent 2010; 35: 120-4.

68. Rubira RJG, Aoki PHB, Constantino CJL, Alessio P. Supramolecular architectures of iron phthalocyanine Langmuir-Blodgett films: The role played by the solution solvents. Appl Surf Sci 2017; 416: 482-91.

69. Frese C, Decker C, Rebholz J, Stucke K, Staehle HJ, Wolff D Original and repair bond strength of fiber-reinforced composites in vitro. Dent Mater 2014;30:456-62.

70. Pianelli C, Devaux J, Bebelman S, Leloup G. The micro-Raman spectroscopy, a useful tool to determine the degree of conversion of light-activated composite resins. J Biomed Mater Res 1999;48:675-81.

71. Vinagre A, Ramos J, Messias A, Marques F, Caramelo F, Mata A. Microtensile bond strength and micromorphology of bur-cut enamel using five adhesive systems. J Adhes Dent 2015;17:10-16.

72. Lee JH, Kang MS, Mahapatra C, Kim HW. Effect of Aminated Mesoporous Bioactive Glass Nanoparticles on the Differentiation of Dental Pulp Stem Cells. PLoS One 2016;14;11:e0150727.

73. Kim DA, Lee JH, Jun SK, Kim HW, Eltohamy M, Lee HH. Sol-gel-derived bioactive glass nanoparticle-incorporated glass ionomer cement with or without chitosan for enhanced mechanical and biomineralization properties. Dent Mater 2017;33:805-817.

74. D'Alpino PHP. Influência da fonte de luz fotoativadora na resistência de união e na micromorfologia da interface adesiva de restaurações de resina composta. Um estudo in vitro com microscopia de fluorescência. Tese de Doutorado. Faculdade de Odontologia de Bauru Universidade de São Paulo. 2005.

75. Moda MD, Fagundes TC, Briso ALF, Dos Santos PH. Analysis of the bond interface between self-adhesive resin cement to eroded dentin in vitro. *PLoS One*. 2018;26;13-11.

76. Fagundes TC, Somensi DS, Dos Santos PH, Navarro MF. Confocal laser scanning microscopy investigation of Bond interfaces involved in fiber glass post cementation. Braz Dent Sci 2014;17(2).

77. Bitter K, Paris S, Pfuertner C, Neumann K, Kielbassa AM. Morphological and bond strength evaluation of different resin cements to root dentin. Eur J Oral Sci. 2009;117(3):326-33.

78. Hoshino IAE. Análise da performance mecânico-estrutural e resistência de união de diferentes técnicas de utilização de pinos de fibra de vidro. Dissertação de Mestrado. Universidade Estadual Paulista UNESP, Brasil. 2019.

79. Banci HA, Strazzi-Sayhon HB, Duarte MAH, Cintra LTA, Gomes-Filho JE, Chalub LO, Berton SA, de Oliveira VHD, dos Santos PH, Sivieri-Araujo G. Influence of photodynamic

therapy on bond strength and adhesive interface morphology of MTA based root canal sealer to different thirds of intraradicular dentin. Photodiagn Photodyn Ther 2020;32:102031.

11) ANEXO 1 - COMITÊ DE ETICA NO USO DE ANIMAIS

unesp UNIVERSIDADE ESTADUAL PAULISTA "JÚLIO DE MESQUITA FILHO"

CAMPUS ARAÇATUBA
FACULDADE DE ODONTOLOGIA
FACULDADE DE MEDICINA VETERINÁRIA

CEUA - Comissão de Ética no Uso de Animais
CEUA - Ethics Committee on the Use of Animals

CERTIFICADO

Certificamos que o Projeto de Pesquisa intitulado **"Avaliação da terapia fotodinâmica e medicação intracanal de hidróxido de cálcio na interface adesiva entre o cimento resinoso e dentina intrarradicular"**, Processo FOA nº 01003-2018, sob responsabilidade de Gustavo Sivieri de Araújo apresenta um protocolo experimental de acordo com os Princípios Éticos da Experimentação Animal e sua execução foi aprovada pela CEUA em 15 de Fevereiro de 2019.

VALIDADE DESTE CERTIFICADO: 31 de Março de 2021.
DATA DA SUBMISSÃO DO RELATÓRIO FINAL: até 30 de Abril de 2021.

CERTIFICATE

We certify that the study entitled **"Evaluation of photodynamic therapy and intracanal medication of calcium hydroxide in the adhesive interface between the resin cement and the intraradadicular dentin"**, Protocol FOA nº 01003-2018, under the supervision of Gustavo Sivieri de Araújo presents an experimental protocol in accordance with the Ethical Principles of Animal Experimentation and its implementation was approved by CEUA on February 15, 2019.

VALIDITY OF THIS CERTIFICATE: March 31, 2021.
DATE OF SUBMISSION OF THE FINAL REPORT: April 30, 2021.

Prof. Ass. Dr. Leonardo Perez Faverani
Coordenador da CEUA
CEUA Coordinator

CEUA - Comissão de Ética no Uso de Animais
Faculdade de Odontologia de Araçatuba
Faculdade de Medicina Veterinária de Araçatuba
Rua José Bonifácio, 1193 – Vila Mendonça CEP: 16015-050 – ARAÇATUBA – SP
Fone (18) 3636-3234 Email CEUA: ceua@fo.unesp.br

12) ANEXO 2 - JOURNAL OF THE MECHANICAL BEHAVIOR OF BIOMEDICAL MATERIALS GUIDELINES

JOURNAL OF THE MECHANICAL BEHAVIOR OF BIOMEDICAL MATERIALS

AUTHOR INFORMATION PACK

TABLE OF CONTENTS

- **Description** **p.1**
- **Impact Factor** **p.2**
- **Abstracting and Indexing** **p.2**
- **Editorial Board** **p.2**
- **Guide for Authors** **p.4**



ISSN: 1751-6161

DESCRIPTION

The *Journal of the Mechanical Behavior of Biomedical Materials* is concerned with the **mechanical deformation**, **damage** and **failure** under applied forces, of **biological material** (at the tissue, cellular and molecular levels) and of **biomaterials**, i.e. those materials which are designed to mimic or replace biological materials.

The primary focus of the journal is the synthesis of materials science, biology, and medical and dental science. Reports of fundamental scientific investigations are welcome, as are articles concerned with the practical application of materials in medical devices. Both experimental and theoretical work is of interest; theoretical papers will normally include comparison of predictions with experimental data, though we recognize that this may not always be appropriate. The journal also publishes technical notes concerned with emerging experimental or theoretical techniques, letters to the editor and, by invitation, review articles and papers describing existing techniques for the benefit of an interdisciplinary readership.

The journal offers online submission, a short time to publication, the opportunity for ample space to develop an argument in full, and the services of referees with expertise in mechanical behaviour and an understanding of the special nature of biomedical materials.

Examples of relevant subjects include: Stress/strain/time relationships for biological materials (natural and engineered ones)Fracture mechanics of hard tissues (such as bone, teeth, and other mineralized tissues, ceramics and metals and various biomedically relevant alloys)Tribological properties of joint materials and their replacements, including coatings and surface modifications Mechanical characterisation of tissue engineering materials and scaffolds, and the investigation of mechanical cues in the context of biological processesThe mechanical behaviour of cells, including adhesion and failureMechanical properties of biological molecules such as proteins, DNA, and other biomoleculesLong-term fatigue, creep and wear properties of biomaterials used in implants and similar biomedical materials The behaviour of the human tissues under impact loading and other extreme conditionsAdditive manufacturing methods of all kinds, for metals, ceramics, polymers, composites, and other biomaterials (in medical, dental, bio-inspired and related fields)Mechanical performance of materials in plants and animals in all natural and engineered ecosystemsNew techniques for the measurement of mechanical properties in biomedical materials, in both laboratory and clinical practiceComputer simulations of material behavior at all time- and length-scales (from molecular to tissue scales), as well as the introduction of new computing techniques (such as machine learning and artificial intelligence) in the modeling and analysis of the mechanical properties of biomedical

GUIDE FOR AUTHORS

Your Paper Your Way

We now differentiate between the requirements for new and revised submissions. You may choose to submit your manuscript as a single Word or PDF file to be used in the refereeing process. Only when your paper is at the revision stage, will you be requested to put your paper in to a 'correct format' for acceptance and provide the items required for the publication of your article.
To find out more, please visit the Preparation section below.

INTRODUCTION

Authors are requested to submit a cover letter that clearly states the novelty of the work presented in their manuscript.

Types of Contributions

Research Paper: A full-length article describing original research. There is no limit on the number of words, figures etc but authors should be as succinct as possible.

Review Article: An article which reviews previous work in a given field. Reviews are written by invitation only but the editor would welcome suggestions.

Technical Note: A short article describing a new experimental technique or analytical approach.

Short Communication: An article presenting new work in reduced form, which for some reason is not suitable for a full research paper. For example a case study.

Opinion Piece: A short article presenting the author's opinion on a particular question. Normally shorter and less comprehensive than a review article, making use of published and/or unpublished results.

Tutorial: An article of an educational nature, explaining how to use a particular experimental technique or analytical method. Normally written by invitation only but the editor welcomes suggestions.

Please ensure that you select the appropriate article type from the list of options when making your submission. Authors contributing to **special issues** should ensure that they select the special issue article type from this list.

The journal also accepts **letters**, which should be sent directly to the editor in chief for consideration.

Submission checklist

You can use this list to carry out a final check of your submission before you send it to the journal for review. Please check the relevant section in this Guide for Authors for more details.

Ensure that the following items are present:

One author has been designated as the corresponding author with contact details:
• E-mail address
• Full postal address

All necessary files have been uploaded:
Manuscript:
• Include keywords
• All figures (include relevant captions)
• All tables (including titles, description, footnotes)
• Ensure all figure and table citations in the text match the files provided
• Indicate clearly if color should be used for any figures in print
Graphical Abstracts / Highlights files (where applicable)
Supplemental files (where applicable)

Further considerations
• Manuscript has been 'spell checked' and 'grammar checked'

materials Clinical case histories related to material performanceMechanobiology, focusing especially on the response of cells and tissues to biophysical stimuli at varied length- and time-scales

The journal publishes papers from the proceedings of the International Conference on the Mechanics of Biomaterials and Tissues; special issues devoted to particular subjects or events will also be considered.

IMPACT FACTOR

2021: 4.042 © Clarivate Analytics Journal Citation Reports 2022

ABSTRACTING AND INDEXING

PubMed/Medline
Scopus
Science Citation Index Expanded
INSPEC

EDITORIAL BOARD

Editor in Chief

Markus Buehler, Massachusetts Institute of Technology, Cambridge, Massachusetts, United States of America

Associate Editors

P. Vallittu, University of Turku, TURKU, Finland

Editor Emeritus

D. Taylor, University of Dublin Trinity College, Department of Mechanical & Manufacturing Engineering, Dublin, Ireland

Editorial Board

Adachi, Kyoto University, Kyoto, Japan
O. Akkus, Case Western Reserve University, Cleveland, Ohio, United States of America
M. Amabili, Université McGill, Montréal, Quebec, Canada
F. Barthelat, Université McGill, Montréal, Quebec, Canada
P. Y. Chen, National Tsing Hua University, Hsinchu, Taiwan
E. Dall'Ara, The University of Sheffield, Department of Oncology and Metabolism, Sheffield, United Kingdom
S. L. Evans, Cardiff University, Cardiff, United Kingdom
Gerbrand T Geesink, Maastricht University, Maastricht, Netherlands
A. Gefen, Tel Aviv University Iby and Aladar Fleischman, Faculty of Engineering, Tel Aviv, Israel
A. Geitmann, McGill University, Faculty of Agriculture and Environment, Sainte-Anne-de-Bellevue, Quebec, Canada
L. Johnson, University of Delaware, Newark, Delaware, United States of America
D. J. Kelly, The University of Dublin Trinity College, Dublin, Ireland
J. Kruzic, University of New South Wales, Sydney, New South Wales, Australia
U. Lohbauer, University of Erlangen-Nuremberg, Erlangen and Nuremberg, Germany
R. L. Mauck, University of Pennsylvania Perelman School of Medicine, Philadelphia, Pennsylvania, United States of America
R. M. McMeeking, University of California Santa Barbara, Santa Barbara, California, United States of America
M. A. Myers, University of California San Diego, Department of Mechanical and Aerospace Engineering, La Jolla, California, United States of America
T. V. Nguyen, Johns Hopkins University, Department of Mechanical Engineering, Baltimore, Maryland, United States of America
M. Niinomi, Tohoku University Institute for Materials Research, Sendai, Japan
C.W.J. Oomens, Eindhoven University of Technology, Eindhoven, Netherlands
M. L. Oyen, East Carolina University, Greenville, North Carolina, United States of America
P. Prendergast, University of Dublin Trinity College, Department of Mechanical & Manufacturing Engineering, Dublin, Ireland
R. O. Ritchie, University of California Berkeley, Department of Materials Science and Engineering, Berkeley, California, United States of America
R.K. Roeder, University of Notre Dame, Notre Dame, Indiana, United States of America
H. Screen, Queen Mary University of London, London, United Kingdom

C. Simms, University of Dublin Trinity College, Department of Mechanical & Manufacturing Engineering, Dublin, Ireland
S. Suresh, Carnegie Mellon University, Pittsburgh, Pennsylvania, United States of America
M. Swain, The University of Sydney, Sydney, New South Wales, Australia
S.H. Teoh, Nanyang Technological University, Singapore, Singapore
D. Vashishth, Rensselaer Polytechnic Institute, Troy, New York, United States of America
S. Vesentini, Polytechnic of Milan, Milano, Italy
U. Wegst, Dartmouth College, Hanover, New Hampshire, United States of America
S. Weiss, The University of Sydney, Sydney, New South Wales, Australia
J. A. Weiss, The University Of Utah, Department of Biomedical Engineering, Salt Lake City, Utah, United States of America
A. Wennerberg, Malmo University, Malmö, Sweden
L. N. Williams, University of Florida J Crayton Pruitt Family, Department of Biomedical Engineering, Gainesville, Florida, United States of America
W. Yang, ETH Zurich, Zurich, Switzerland
A. A. Zadpoor, Delft University of Technology, Delft, Netherlands
P. Zioupos, Cranfield University - Shrivenham Campus, Swindon, United Kingdom

• All references mentioned in the Reference List are cited in the text, and vice versa
• Permission has been obtained for use of copyrighted material from other sources (including the Internet)
• A competing interests statement is provided, even if the authors have no competing interests to declare
• Journal policies detailed in this guide have been reviewed
• Referee suggestions and contact details provided, based on journal requirements

For further information, visit our Support Center.

BEFORE YOU BEGIN

Ethics in publishing

Please see our information on Ethics in publishing.

Declaration of competing interest

All authors must disclose any financial and personal relationships with other people or organizations that could inappropriately influence (bias) their work. Examples of potential conflicts of interest include employment, consultancies, stock ownership, honoraria, paid expert testimony, patent applications/registrations, and grants or other funding. Authors should complete the declaration of competing interest statement using this template and upload to the submission system at the Attach/Upload Files step. **Note: Please do not convert the .docx template to another file type. Author signatures are not required.** If there are no interests to declare, please choose the first option in the template. More information.

Submission declaration and verification

Submission of an article implies that the work described has not been published previously (except in the form of an abstract, a published lecture or academic thesis, see 'Multiple, redundant or concurrent publication' for more information), that it is not under consideration for publication elsewhere, that its publication is approved by all authors and tacitly or explicitly by the responsible authorities where the work was carried out, and that, if accepted, it will not be published elsewhere in the same form, in English or in any other language, including electronically without the written consent of the copyright-holder. To verify compliance, your article may be checked by Crossref Similarity Check and other originality or duplicate checking software.

Preprints

Please note that preprints can be shared anywhere at any time, in line with Elsevier's sharing policy. Sharing your preprints e.g. on a preprint server will not count as prior publication (see 'Multiple, redundant or concurrent publication' for more information).

Preprint posting on SSRN

In support of Open Science, this journal offers its authors a free preprint posting service. Preprints provide early registration and dissemination of your research, which facilitates early citations and collaboration.

During submission to Editorial Manager, you can choose to release your manuscript publicly as a preprint on the preprint server SSRN once it enters peer-review with the journal. Your choice will have no effect on the editorial process or outcome with the journal. Please note that the corresponding author is expected to seek approval from all co-authors before agreeing to release the manuscript publicly on SSRN.

You will be notified via email when your preprint is posted online and a Digital Object Identifier (DOI) is assigned. Your preprint will remain globally available free to read whether the journal accepts or rejects your manuscript.

For more information about posting to SSRN, please consult the SSRN Terms of Use and FAQs.

Use of inclusive language

Inclusive language acknowledges diversity, conveys respect to all people, is sensitive to differences, and promotes equal opportunities. Content should make no assumptions about the beliefs or commitments of any reader; contain nothing which might imply that one individual is superior to another on the grounds of age, gender, race, ethnicity, culture, sexual orientation, disability or health condition; and use inclusive language throughout. Authors should ensure that writing is free from bias,

stereotypes, slang, reference to dominant culture and/or cultural assumptions. We advise to seek gender neutrality by using plural nouns ("clinicians, patients/clients") as default/wherever possible to avoid using "he, she," or "he/she." We recommend avoiding the use of descriptors that refer to personal attributes such as age, gender, race, ethnicity, culture, sexual orientation, disability or health condition unless they are relevant and valid. When coding terminology is used, we recommend to avoid offensive or exclusionary terms such as "master", "slave", "blacklist" and "whitelist". We suggest using alternatives that are more appropriate and (self-) explanatory such as "primary", "secondary", "blocklist" and "allowlist". These guidelines are meant as a point of reference to help identify appropriate language but are by no means exhaustive or definitive.

Reporting sex- and gender-based analyses

Reporting guidance

For research involving or pertaining to humans, animals or eukaryotic cells, investigators should integrate sex and gender-based analyses (SGBA) into their research design according to funder/sponsor requirements and best practices within a field. Authors should address the sex and/or gender dimensions of their research in their article. In cases where they cannot, they should discuss this as a limitation to their research's generalizability. Importantly, authors should explicitly state what definitions of sex and/or gender they are applying to enhance the precision, rigor and reproducibility of their research and to avoid ambiguity or conflation of terms and the constructs to which they refer (see Definitions section below). Authors can refer to the Sex and Gender Equity in Research (SAGER) guidelines and the SAGER guidelines checklist. These offer systematic approaches to the use and editorial review of sex and gender information in study design, data analysis, outcome reporting and research interpretation - however, please note there is no single, universally agreed-upon set of guidelines for defining sex and gender.

Definitions

Sex generally refers to a set of biological attributes that are associated with physical and physiological features (e.g., chromosomal genotype, hormonal levels, internal and external anatomy). A binary sex categorization (male/female) is usually designated at birth ("sex assigned at birth"), most often based solely on the visible external anatomy of a newborn. Gender generally refers to socially constructed roles, behaviors, and identities of women, men and gender-diverse people that occur in a historical and cultural context and may vary across societies and over time. Gender influences how people view themselves and each other, how they behave and interact and how power is distributed in society. Sex and gender are often incorrectly portrayed as binary (female/male or woman/man) and unchanging whereas these constructs actually exist along a spectrum and include additional sex categorizations and gender identities such as people who are intersex/have differences of sex development (DSD) or identify as non-binary. Moreover, the terms "sex" and "gender" can be ambiguous—thus it is important for authors to define the manner in which they are used. In addition to this definition guidance and the SAGER guidelines, the resources on this page offer further insight around sex and gender in research studies.

Author contributions

For transparency, we encourage authors to submit an author statement file outlining their individual contributions to the paper using the relevant CRediT roles: Conceptualization; Data curation; Formal analysis; Funding acquisition; Investigation; Methodology; Project administration; Resources; Software; Supervision; Validation; Visualization; Roles/Writing - original draft; Writing - review & editing. Authorship statements should be formatted with the names of authors first and CRediT role(s) following. More details and an example.

Changes to authorship

Authors are expected to consider carefully the list and order of authors **before** submitting their manuscript and provide the definitive list of authors at the time of the original submission. Any addition, deletion or rearrangement of author names in the authorship list should be made only **before** the manuscript has been accepted and only if approved by the journal Editor. To request such a change, the Editor must receive the following from the **corresponding author**: (a) the reason for the change in author list and (b) written confirmation (e-mail, letter) from all authors that they agree with the addition, removal or rearrangement. In the case of addition or removal of authors, this includes confirmation from the author being added or removed.

Only in exceptional circumstances will the Editor consider the addition, deletion or rearrangement of authors **after** the manuscript has been accepted. While the Editor considers the request, publication of the manuscript will be suspended. If the manuscript has already been published in an online issue, any requests approved by the Editor will result in a corrigendum.

Article transfer service
This journal uses the Elsevier Article Transfer Service to find the best home for your manuscript. This means that if an editor feels your manuscript is more suitable for an alternative journal, you might be asked to consider transferring the manuscript to such a journal. The recommendation might be provided by a Journal Editor, a dedicated Scientific Managing Editor, a tool assisted recommendation, or a combination. If you agree, your manuscript will be transferred, though you will have the opportunity to make changes to the manuscript before the submission is complete. Please note that your manuscript will be independently reviewed by the new journal. More information.

Copyright

Upon acceptance of an article, authors will be asked to complete a 'Journal Publishing Agreement' (see more information on this). An e-mail will be sent to the corresponding author confirming receipt of the manuscript together with a 'Journal Publishing Agreement' form or a link to the online version of this agreement.

Subscribers may reproduce tables of contents or prepare lists of articles including abstracts for internal circulation within their institutions. Permission of the Publisher is required for resale or distribution outside the institution and for all other derivative works, including compilations and translations. If excerpts from other copyrighted works are included, the author(s) must obtain written permission from the copyright owners and credit the source(s) in the article. Elsevier has preprinted forms for use by authors in these cases.

For gold open access articles: Upon acceptance of an article, authors will be asked to complete a 'License Agreement' (more information). Permitted third party reuse of gold open access articles is determined by the author's choice of user license.

Author rights
As an author you (or your employer or institution) have certain rights to reuse your work. More information.

Elsevier supports responsible sharing
Find out how you can share your research published in Elsevier journals.

Role of the funding source

You are requested to identify who provided financial support for the conduct of the research and/or preparation of the article and to briefly describe the role of the sponsor(s), if any, in study design; in the collection, analysis and interpretation of data; in the writing of the report; and in the decision to submit the article for publication. If the funding source(s) had no such involvement, it is recommended to state this.

Open access

Please visit our Open Access page for more information.

Elsevier Researcher Academy
Researcher Academy is a free e-learning platform designed to support early and mid-career researchers throughout their research journey. The "Learn" environment at Researcher Academy offers several interactive modules, webinars, downloadable guides and resources to guide you through the process of writing for research and going through peer review. Feel free to use these free resources to improve your submission and navigate the publication process with ease.

Language (usage and editing services)
Please write your text in good English (American or British usage is accepted, but not a mixture of these). Authors who feel their English language manuscript may require editing to eliminate possible grammatical or spelling errors and to conform to correct scientific English may wish to use the English Language Editing service available from Elsevier's Author Services.

Submission

Our online submission system guides you stepwise through the process of entering your article details and uploading your files. The system converts your article files to a single PDF file used in the peer-review process. Editable files (e.g., Word, LaTeX) are required to typeset your article for final publication. All correspondence, including notification of the Editor's decision and requests for revision, is sent by e-mail.

PREPARATION

Queries

For questions about the editorial process (including the status of manuscripts under review) or for technical support on submissions, please visit our Support Center.

NEW SUBMISSIONS

Submission to this journal proceeds totally online and you will be guided stepwise through the creation and uploading of your files. The system automatically converts your files to a single PDF file, which is used in the peer-review process.
As part of the Your Paper Your Way service, you may choose to submit your manuscript as a single file to be used in the refereeing process. This can be a PDF file or a Word document, in any format or lay-out that can be used by referees to evaluate your manuscript. It should contain high enough quality figures for refereeing. If you prefer to do so, you may still provide all or some of the source files at the initial submission. Please note that individual figure files larger than 10 MB must be uploaded separately.

References
There are no strict requirements on reference formatting at submission. References can be in any style or format as long as the style is consistent. Where applicable, author(s) name(s), journal title/book title, chapter title/article title, year of publication, volume number/book chapter and the article number or pagination must be present. Use of DOI is highly encouraged. The reference style used by the journal will be applied to the accepted article by Elsevier at the proof stage. Note that missing data will be highlighted at proof stage for the author to correct.

Formatting requirements
There are no strict formatting requirements but all manuscripts must contain the essential elements needed to convey your manuscript, for example Abstract, Keywords, Introduction, Materials and Methods, Results, Conclusions, Artwork and Tables with Captions.
If your article includes any Videos and/or other Supplementary material, this should be included in your initial submission for peer review purposes.
Divide the article into clearly defined sections.

Figures and tables embedded in text
Please ensure the figures and the tables included in the single file are placed next to the relevant text in the manuscript, rather than at the bottom or the top of the file. The corresponding caption should be placed directly below the figure or table.

Peer review

This journal operates a single anonymized review process. All contributions will be initially assessed by the editor for suitability for the journal. Papers deemed suitable are then typically sent to a minimum of two independent expert reviewers to assess the scientific quality of the paper. The Editor is responsible for the final decision regarding acceptance or rejection of articles. The Editor's decision is final. Editors are not involved in decisions about papers which they have written themselves or have been written by family members or colleagues or which relate to products or services in which the editor has an interest. Any such submission is subject to all of the journal's usual procedures, with peer review handled independently of the relevant editor and their research groups. More information on types of peer review.

REVISED SUBMISSIONS

Use of word processing software
Regardless of the file format of the original submission, at revision you must provide us with an editable file of the entire article. Keep the layout of the text as simple as possible. Most formatting codes will be removed and replaced on processing the article. The electronic text should be prepared in a way very similar to that of conventional manuscripts (see also the Guide to Publishing with Elsevier). See also the section on Electronic artwork.

To avoid unnecessary errors you are strongly advised to use the 'spell-check' and 'grammar-check' functions of your word processor.

LaTeX
You are recommended to use the Elsevier article class elsarticle.cls to prepare your manuscript and BibTeX to generate your bibliography.
Our LaTeX site has detailed submission instructions, templates and other information.

Article structure

Subdivision - numbered sections
Divide your article into clearly defined and numbered sections. Subsections should be numbered 1.1 (then 1.1.1, 1.1.2, ...), 1.2, etc. (the abstract is not included in section numbering). Use this numbering also for internal cross-referencing: do not just refer to 'the text'. Any subsection may be given a brief heading. Each heading should appear on its own separate line.

Introduction
State the objectives of the work and provide an adequate background, avoiding a detailed literature survey or a summary of the results.

Material and methods
Provide sufficient details to allow the work to be reproduced by an independent researcher. Methods that are already published should be summarized, and indicated by a reference. If quoting directly from a previously published method, use quotation marks and also cite the source. Any modifications to existing methods should also be described.

Theory/calculation
A Theory section should extend, not repeat, the background to the article already dealt with in the Introduction and lay the foundation for further work. In contrast, a Calculation section represents a practical development from a theoretical basis.

Results
Results should be clear and concise.

Discussion
This should explore the significance of the results of the work, not repeat them. A combined Results and Discussion section is often appropriate. Avoid extensive citations and discussion of published literature.

Conclusions
The main conclusions of the study may be presented in a short Conclusions section, which may stand alone or form a subsection of a Discussion or Results and Discussion section.

Appendices
If there is more than one appendix, they should be identified as A, B, etc. Formulae and equations in appendices should be given separate numbering: Eq. (A.1), Eq. (A.2), etc.; in a subsequent appendix, Eq. (B.1) and so on. Similarly for tables and figures: Table A.1; Fig. A.1, etc.

Essential title page information

• ***Title.*** Concise and informative. Titles are often used in information-retrieval systems. Avoid abbreviations and formulae where possible.
• ***Author names and affiliations.*** Please clearly indicate the given name(s) and family name(s) of each author and check that all names are accurately spelled. You can add your name between parentheses in your own script behind the English transliteration. Present the authors' affiliation addresses (where the actual work was done) below the names. Indicate all affiliations with a lower-case superscript letter immediately after the author's name and in front of the appropriate address. Provide the full postal address of each affiliation, including the country name and, if available, the e-mail address of each author.
• ***Corresponding author.*** Clearly indicate who will handle correspondence at all stages of refereeing and publication, also post-publication. This responsibility includes answering any future queries about Methodology and Materials. **Ensure that the e-mail address is given and that contact details are kept up to date by the corresponding author.**
• ***Present/permanent address.*** If an author has moved since the work described in the article was done, or was visiting at the time, a 'Present address' (or 'Permanent address') may be indicated as a footnote to that author's name. The address at which the author actually did the work must be retained as the main, affiliation address. Superscript Arabic numerals are used for such footnotes.

Highlights

Highlights are mandatory for this journal as they help increase the discoverability of your article via search engines. They consist of a short collection of bullet points that capture the novel results of your research as well as new methods that were used during the study (if any). Please have a look at the examples here: example Highlights.

Highlights should be submitted in a separate editable file in the online submission system. Please use 'Highlights' in the file name and include 3 to 5 bullet points (maximum 85 characters, including spaces, per bullet point).

Abstract

A concise and factual abstract is required. The abstract should state briefly the purpose of the research, the principal results and major conclusions. An abstract is often presented separately from the article, so it must be able to stand alone. For this reason, References should be avoided, but if essential, then cite the author(s) and year(s). Also, non-standard or uncommon abbreviations should be avoided, but if essential they must be defined at their first mention in the abstract itself.

Graphical abstract

A graphical abstract is mandatory for this journal. It should summarize the contents of the article in a concise, pictorial form designed to capture the attention of a wide readership online. Authors must provide images that clearly represent the work described in the article. Graphical abstracts should be submitted as a separate file in the online submission system. Image size: please provide an image with a minimum of 531 × 1328 pixels (h × w) or proportionally more. The image should be readable at a size of 5 × 13 cm using a regular screen resolution of 96 dpi. Preferred file types: TIFF, EPS, PDF or MS Office files. You can view Example Graphical Abstracts on our information site.

Abbreviations

Define abbreviations that are not standard in this field in a footnote to be placed on the first page of the article. Such abbreviations that are unavoidable in the abstract must be defined at their first mention there, as well as in the footnote. Ensure consistency of abbreviations throughout the article.

Acknowledgements

Collate acknowledgements in a separate section at the end of the article before the references and do not, therefore, include them on the title page, as a footnote to the title or otherwise. List here those individuals who provided help during the research (e.g., providing language help, writing assistance or proof reading the article, etc.).

Formatting of funding sources

List funding sources in this standard way to facilitate compliance to funder's requirements:

Funding: This work was supported by the National Institutes of Health [grant numbers xxxx, yyyy]; the Bill & Melinda Gates Foundation, Seattle, WA [grant number zzzz]; and the United States Institutes of Peace [grant number aaaa].

It is not necessary to include detailed descriptions on the program or type of grants and awards. When funding is from a block grant or other resources available to a university, college, or other research institution, submit the name of the institute or organization that provided the funding.

If no funding has been provided for the research, it is recommended to include the following sentence:

This research did not receive any specific grant from funding agencies in the public, commercial, or not-for-profit sectors.

Units

Follow internationally accepted rules and conventions: use the international system of units (SI). If other quantities are mentioned, give their equivalent in SI. Authors wishing to present a table of nomenclature should do so on the second page of their manuscript.

Math formulae

Please submit math equations as editable text and not as images. Present simple formulae in line with normal text where possible and use the solidus (/) instead of a horizontal line for small fractional terms, e.g., X/Y. In principle, variables are to be presented in italics. Powers of e are often more conveniently denoted by exp. Number consecutively any equations that have to be displayed separately from the text (if referred to explicitly in the text).

Footnotes
Footnotes should be used sparingly. Number them consecutively throughout the article. Many word processors build footnotes into the text, and this feature may be used. Should this not be the case, indicate the position of footnotes in the text and present the footnotes themselves separately at the end of the article.

Artwork

Electronic artwork
General points
• Make sure you use uniform lettering and sizing of your original artwork.
• Preferred fonts: Arial (or Helvetica), Times New Roman (or Times), Symbol, Courier.
• Number the illustrations according to their sequence in the text.
• Use a logical naming convention for your artwork files.
• Indicate per figure if it is a single, 1.5 or 2-column fitting image.
• For Word submissions only, you may still provide figures and their captions, and tables within a single file at the revision stage.
• Please note that individual figure files larger than 10 MB must be provided in separate source files.

A detailed guide on electronic artwork is available.
You are urged to visit this site; some excerpts from the detailed information are given here.
Formats
Regardless of the application used, when your electronic artwork is finalized, please 'save as' or convert the images to one of the following formats (note the resolution requirements for line drawings, halftones, and line/halftone combinations given below):
EPS (or PDF): Vector drawings. Embed the font or save the text as 'graphics'.
TIFF (or JPG): Color or grayscale photographs (halftones): always use a minimum of 300 dpi.
TIFF (or JPG): Bitmapped line drawings: use a minimum of 1000 dpi.
TIFF (or JPG): Combinations bitmapped line/half-tone (color or grayscale): a minimum of 500 dpi is required.
Please do not:
• Supply files that are optimized for screen use (e.g., GIF, BMP, PICT, WPG); the resolution is too low.
• Supply files that are too low in resolution.
• Submit graphics that are disproportionately large for the content.

Color artwork
Please make sure that artwork files are in an acceptable format (TIFF (or JPEG), EPS (or PDF) or MS Office files) and with the correct resolution. If, together with your accepted article, you submit usable color figures then Elsevier will ensure, at no additional charge, that these figures will appear in color online (e.g., ScienceDirect and other sites) in addition to color reproduction in print. Further information on the preparation of electronic artwork.

Figure captions
Ensure that each illustration has a caption. A caption should comprise a brief title (**not** on the figure itself) and a description of the illustration. Keep text in the illustrations themselves to a minimum but explain all symbols and abbreviations used.

Tables

Please submit tables as editable text and not as images. Tables can be placed either next to the relevant text in the article, or on separate page(s) at the end. Number tables consecutively in accordance with their appearance in the text and place any table notes below the table body. Be sparing in the use of tables and ensure that the data presented in them do not duplicate results described elsewhere in the article. Please avoid using vertical rules and shading in table cells.

References

Citation in text
Please ensure that every reference cited in the text is also present in the reference list (and vice versa). Any references cited in the abstract must be given in full. Unpublished results and personal communications are not recommended in the reference list, but may be mentioned in the text. If these references are included in the reference list they should follow the standard reference style of the journal and should include a substitution of the publication date with either 'Unpublished results' or 'Personal communication'. Citation of a reference as 'in press' implies that the item has been accepted for publication.

Citations may be made directly (or parenthetically). Groups of references can be listed either first alphabetically, then chronologically, or vice versa.
Examples: 'as demonstrated (Allan, 2000a, 2000b, 1999; Allan and Jones, 1999)…. Or, as demonstrated (Jones, 1999; Allan, 2000)… Kramer et al. (2010) have recently shown …'
List: References should be arranged first alphabetically and then further sorted chronologically if necessary. More than one reference from the same author(s) in the same year must be identified by the letters 'a', 'b', 'c', etc., placed after the year of publication.
Examples:
Reference to a journal publication:
Van der Geer, J., Hanraads, J.A.J., Lupton, R.A., 2010. The art of writing a scientific article. J. Sci. Commun. 163, 51–59. https://doi.org/10.1016/j.Sc.2010.00372.
Reference to a journal publication with an article number:
Van der Geer, J., Hanraads, J.A.J., Lupton, R.A., 2018. The art of writing a scientific article. Heliyon. 19, e00205. https://doi.org/10.1016/j.heliyon.2018.e00205.
Reference to a book:
Strunk Jr., W., White, E.B., 2000. The Elements of Style, fourth ed. Longman, New York.
Reference to a chapter in an edited book:
Mettam, G.R., Adams, L.B., 2009. How to prepare an electronic version of your article, in: Jones, B.S., Smith , R.Z. (Eds.), Introduction to the Electronic Age. E-Publishing Inc., New York, pp. 281–304.
Reference to a website:
Cancer Research UK, 1975. Cancer statistics reports for the UK. http://www.cancerresearchuk.org/aboutcancer/statistics/cancerstatsreport/ (accessed 13 March 2003).
Reference to a dataset:
[dataset] Oguro, M., Imahiro, S., Saito, S., Nakashizuka, T., 2015. Mortality data for Japanese oak wilt disease and surrounding forest compositions. Mendeley Data, v1. https://doi.org/10.17632/xwj98nb39r.1.
Reference to software:
Coon, E., Berndt, M., Jan, A., Svyatsky, D., Atchley, A., Kikinzon, E., Harp, D., Manzini, G., Shelef, E., Lipnikov, K., Garimella, R., Xu, C., Moulton, D., Karra, S., Painter, S., Jafarov, E., & Molins, S., 2020. Advanced Terrestrial Simulator (ATS) v0.88 (Version 0.88). Zenodo. https://doi.org/10.5281/zenodo.3727209.

Journal abbreviations source
Journal names should be abbreviated according to the List of Title Word Abbreviations.

Video
Elsevier accepts video material and animation sequences to support and enhance your scientific research. Authors who have video or animation files that they wish to submit with their article are strongly encouraged to include links to these within the body of the article. This can be done in the same way as a figure or table by referring to the video or animation content and noting in the body text where it should be placed. All submitted files should be properly labeled so that they directly relate to the video file's content. In order to ensure that your video or animation material is directly usable, please provide the file in one of our recommended file formats with a preferred maximum size of 150 MB per file, 1 GB in total. Video and animation files supplied will be published online in the electronic version of your article in Elsevier Web products, including ScienceDirect. Please supply 'stills' with your files: you can choose any frame from the video or animation or make a separate image. These will be used instead of standard icons and will personalize the link to your video data. For more detailed instructions please visit our video instruction pages. Note: since video and animation cannot be embedded in the print version of the journal, please provide text for both the electronic and the print version for the portions of the article that refer to this content.

Data visualization
Include interactive data visualizations in your publication and let your readers interact and engage more closely with your research. Follow the instructions here to find out about available data visualization options and how to include them with your article.

Supplementary material
Supplementary material such as applications, images and sound clips, can be published with your article to enhance it. Submitted supplementary items are published exactly as they are received (Excel or PowerPoint files will appear as such online). Please submit your material together with the article and supply a concise, descriptive caption for each supplementary file. If you wish to make changes to

Reference links
Increased discoverability of research and high quality peer review are ensured by online links to the sources cited. In order to allow us to create links to abstracting and indexing services, such as Scopus, Crossref and PubMed, please ensure that data provided in the references are correct. Please note that incorrect surnames, journal/book titles, publication year and pagination may prevent link creation. When copying references, please be careful as they may already contain errors. Use of the DOI is highly encouraged.

A DOI is guaranteed never to change, so you can use it as a permanent link to any electronic article. An example of a citation using DOI for an article not yet in an issue is: VanDecar J.C., Russo R.M., James D.E., Ambeh W.B., Franke M. (2003). Aseismic continuation of the Lesser Antilles slab beneath northeastern Venezuela. Journal of Geophysical Research, https://doi.org/10.1029/2001JB000884. Please note the format of such citations should be in the same style as all other references in the paper.

Web references
As a minimum, the full URL should be given and the date when the reference was last accessed. Any further information, if known (DOI, author names, dates, reference to a source publication, etc.), should also be given. Web references can be listed separately (e.g., after the reference list) under a different heading if desired, or can be included in the reference list.

Data references
This journal encourages you to cite underlying or relevant datasets in your manuscript by citing them in your text and including a data reference in your Reference List. Data references should include the following elements: author name(s), dataset title, data repository, version (where available), year, and global persistent identifier. Add [dataset] immediately before the reference so we can properly identify it as a data reference. The [dataset] identifier will not appear in your published article.

Preprint references
Where a preprint has subsequently become available as a peer-reviewed publication, the formal publication should be used as the reference. If there are preprints that are central to your work or that cover crucial developments in the topic, but are not yet formally published, these may be referenced. Preprints should be clearly marked as such, for example by including the word preprint, or the name of the preprint server, as part of the reference. The preprint DOI should also be provided.

References in a special issue
Please ensure that the words 'this issue' are added to any references in the list (and any citations in the text) to other articles in the same Special Issue.

Reference management software
Most Elsevier journals have their reference template available in many of the most popular reference management software products. These include all products that support Citation Style Language styles, such as Mendeley. Using citation plug-ins from these products, authors only need to select the appropriate journal template when preparing their article, after which citations and bibliographies will be automatically formatted in the journal's style. If no template is yet available for this journal, please follow the format of the sample references and citations as shown in this Guide. If you use reference management software, please ensure that you remove all field codes before submitting the electronic manuscript. More information on how to remove field codes from different reference management software.

Reference formatting
There are no strict requirements on reference formatting at submission. References can be in any style or format as long as the style is consistent. Where applicable, author(s) name(s), journal title/ book title, chapter title/article title, year of publication, volume number/book chapter and the article number or pagination must be present. Use of DOI is highly encouraged. The reference style used by the journal will be applied to the accepted article by Elsevier at the proof stage. Note that missing data will be highlighted at proof stage for the author to correct. If you do wish to format the references yourself they should be arranged according to the following examples:

Reference style
Text: All citations in the text should refer to:
1. *Single author:* the author's name (without initials, unless there is ambiguity) and the year of publication;
2. *Two authors:* both authors' names and the year of publication;
3. *Three or more authors:* first author's name followed by 'et al.' and the year of publication.

supplementary material during any stage of the process, please make sure to provide an updated file. Do not annotate any corrections on a previous version. Please switch off the 'Track Changes' option in Microsoft Office files as these will appear in the published version.

Research data

This journal requires and enables you to share data that supports your research publication where appropriate, and enables you to interlink the data with your published articles. Research data refers to the results of observations or experimentation that validate research findings. To facilitate reproducibility and data reuse, this journal also encourages you to share your software, code, models, algorithms, protocols, methods and other useful materials related to the project.

Below are a number of ways in which you can associate data with your article or make a statement about the availability of your data when submitting your manuscript. When sharing data in one of these ways, you are expected to cite the data in your manuscript and reference list. Please refer to the "References" section for more information about data citation. For more information on depositing, sharing and using research data and other relevant research materials, visit the research data page.

Data linking

If you have made your research data available in a data repository, you can link your article directly to the dataset. Elsevier collaborates with a number of repositories to link articles on ScienceDirect with relevant repositories, giving readers access to underlying data that gives them a better understanding of the research described.

There are different ways to link your datasets to your article. When available, you can directly link your dataset to your article by providing the relevant information in the submission system. For more information, visit the database linking page.

For supported data repositories a repository banner will automatically appear next to your published article on ScienceDirect.

In addition, you can link to relevant data or entities through identifiers within the text of your manuscript, using the following format: Database: xxxx (e.g., TAIR: AT1G01020; CCDC: 734053; PDB: 1XFN).

Research Elements

This journal enables you to publish research objects related to your original research – such as data, methods, protocols, software and hardware – as an additional paper in Research Elements.

Research Elements is a suite of peer-reviewed, open access journals which make your research objects findable, accessible and reusable. Articles place research objects into context by providing detailed descriptions of objects and their application, and linking to the associated original research articles. Research Elements articles can be prepared by you, or by one of your collaborators.

During submission, you will be alerted to the opportunity to prepare and submit a Research Elements article.

More information can be found on the Research Elements page.

Data statement

To foster transparency, we require you to state the availability of your data in your submission if your data is unavailable to access or unsuitable to post. This may also be a requirement of your funding body or institution. You will have the opportunity to provide a data statement during the submission process. The statement will appear with your published article on ScienceDirect. For more information, visit the Data Statement page..

AFTER ACCEPTANCE

Online proof correction

To ensure a fast publication process of the article, we kindly ask authors to provide us with their proof corrections within two days. Corresponding authors will receive an e-mail with a link to our online proofing system, allowing annotation and correction of proofs online. The environment is similar to

MS Word: in addition to editing text, you can also comment on figures/tables and answer questions from the Copy Editor. Web-based proofing provides a faster and less error-prone process by allowing you to directly type your corrections, eliminating the potential introduction of errors.
If preferred, you can still choose to annotate and upload your edits on the PDF version. All instructions for proofing will be given in the e-mail we send to authors, including alternative methods to the online version and PDF.
We will do everything possible to get your article published quickly and accurately. Please use this proof only for checking the typesetting, editing, completeness and correctness of the text, tables and figures. Significant changes to the article as accepted for publication will only be considered at this stage with permission from the Editor. It is important to ensure that all corrections are sent back to us in one communication. Please check carefully before replying, as inclusion of any subsequent corrections cannot be guaranteed. Proofreading is solely your responsibility.

Offprints

The corresponding author will, at no cost, receive a customized Share Link providing 50 days free access to the final published version of the article on ScienceDirect. The Share Link can be used for sharing the article via any communication channel, including email and social media. For an extra charge, paper offprints can be ordered via the offprint order form which is sent once the article is accepted for publication. Corresponding authors who have published their article gold open access do not receive a Share Link as their final published version of the article is available open access on ScienceDirect and can be shared through the article DOI link.

AUTHOR INQUIRIES

Visit the Elsevier Support Center to find the answers you need. Here you will find everything from Frequently Asked Questions to ways to get in touch.
You can also check the status of your submitted article or find out when your accepted article will be published.

© Copyright 2018 Elsevier | https://www.elsevier.com

13) ANEXO 3 - PHOTODIAGNOSIS AND PHOTODYNAMIC THERAPY GUIDELINES

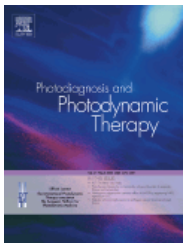


PHOTODIAGNOSIS AND PHOTODYNAMIC THERAPY

AUTHOR INFORMATION PACK

TABLE OF CONTENTS

- **Description** **p.1**
- **Audience** **p.1**
- **Impact Factor** **p.1**
- **Abstracting and Indexing** **p.1**
- **Editorial Board** **p.2**
- **Guide for Authors** **p.4**



ISSN: 1572-1000

DESCRIPTION

Official Journal of the European Platform for Photodynamic Medicine
Affiliated with the International Photodynamic Association
Also affiliated with the British Medical Laser Association and the Polish Society for Photodynamic Medicine

INDEXED in MEDLINE/PubMed, SciSearch/Science Citation Index Expanded, Current Contents/Clinical Medicine.

Aims and Scope:
Photodiagnosis and Photodynamic Therapy is an international journal for the dissemination of scientific knowledge and clinical developments of **Photodiagnosis** and **Photodynamic Therapy** in all medical specialties. The journal publishes original articles, review articles, case presentations, "how-to-do-it" articles, Letters to the Editor, short communications and relevant images with short descriptions. All submitted material is subject to a strict peer-review process.

AUDIENCE

Professionals in all medical disciplines with an interest in medical and biological applications of lasers and light sources, and photodiagnosis/photodynamic therapy in the treatment of human disease.

IMPACT FACTOR

2020: 3.631 © Clarivate Analytics Journal Citation Reports 2021

ABSTRACTING AND INDEXING

Current Contents - Clinical Medicine
Journal Citation Reports - Science Edition
Science Citation Index Expanded
Scopus
ScienceDirect
PubMed/Medline
PubMed/Medline

EDITORIAL BOARD

Editor-in-Chief

Ron Allison, 21st Century Oncology Greenville, Greenville, North Carolina, United States of America

Emeritus Editor

Keyvan Moghissi, Yorkshire Laser Centre, Goole, United Kingdom

Associate Editors

Barr, Gloucester, United Kingdom
Boyle, Hull, United Kingdom
Kate Dixon, Goole, United Kingdom
Eljamel, Lanark, United Kingdom
Freitag, Hemer, Germany
Furukawa, Tokyo, Japan
Michael Hamblin, Boston, Massachusetts, United States of America
Photodynamic therapy, photobiomodulation, low level laser therapy, photosensitizes, photochemical mechanisms, Anti-tumor/tumour immune response, cancer, Wound healing and infectious disease, Atherosclerotic vulnerable plaque
Hopper, Bromley, United Kingdom
Zheng Huang, Lakewood, Colorado, United States of America
Kato, Tokyo, Japan
Thomas S. Mang, Orchard Park, New York, United States of America
Moseley, Dundee, United Kingdom
Turnbull, Hull, United Kingdom
Walt, Zurich, Switzerland
Wolfson, Jacksonville, Florida, United States of America

Editorial Board

Adamek, Katowice, Poland
Andrey Akopov, St. Petersburg, Russian Federation
Thoracic surgery, Thoracic oncology
Donald Allan, Manchester, United Kingdom
Ernest Allan, Knutsford, United Kingdom
Barber, Dundee, United Kingdom
Alcira Batlle, Buenos Aires, Argentina
Berg, Oslo, Norway
Downie, Mount Pleasant, Texas, United States of America
Reza Fekrazad, Tehran, Iran
Gasparyan, Helsinki, Finland
Gilles Gasser, Zurich, Switzerland
Hillemanns, Hannover, Germany
Horvath, Brno, Czechia
Sally Ibbotson, Dundee, United Kingdom
PDT in clinical dermatology
Jichlinski, Lausanne, Switzerland
Asta Juzeniene, Oslo, Norway
Chronic Lymphocytic Leukemia CLL, tumor microenvironment, exosomes, extracellular vesicles, anti-tumor immunity, hematological malignancies
Nasim Kashef, Tehran, Iran
Herwig Kostron, Innsbruck, Austria
Lecleire, Rouen, France
Leroy, Suresnes, France
Li, Guangzhou, Guangdong, China
Makela, Helsinki, Finland
Nakamura, Shimotsuga-gun, Japan
Dominic Robinson, Rotterdam, Netherlands
Patrick Ross, Columbus, Ohio, United States of America
Sieron, Bytom, Poland
Stummer, Münster, Germany
Tan, Amsterdam, Netherlands
Thorpe, Leeds, United Kingdom
Waidelich, Munich, Germany
Mark Wainwright, Liverpool, United Kingdom
Dyes in medicine, photoantimicrobials, photodynamic therapy, medicinal chemistry
Wang, Shanghai, China

Woong-Shick, Seocho-gu, South Korea
Piotr Ziolkowski, Wroclaw, Poland

GUIDE FOR AUTHORS

INTRODUCTION

Scope

Photodiagnosis and Photodynamic Therapy is an international journal for the dissemination of scientific knowledge and clinical developments of Photodiagnosis and Photodynamic Therapy in all medical specialities. The journal publishes original articles, review articles, case presentations, "how-to-do-it" articles, Letters to the Editor, short communications and relevant images with short descriptions. All submitted material is subject to a strict peer review process.

Types of manuscript

Research Papers should report original clinical studies or research not previously published or being considered for publication elsewhere. Work in Progress may also be submitted. See below for the standard layout. Submission of a manuscript to this journal gives the publisher the right to publish that paper if it is accepted. Manuscripts may be edited to improve clarity and expression.

Review articles, including institutional reviews of recent developments are welcome, and will undergo peer review. Reviews should have an abstract of up to 250 words.

Editorials
Although most Editorials in the journal are commissioned, authors may contact the Editor-in-Chief to request submission of their own Editorial.

Correspondence. Readers are encouraged to write about any topic that relates to photodiagnosis or photodynamic therapy, clinical, scientific, educational, social or economic. Letters should be no longer than 500 words and may include discussions on material previously printed in the Journal.

Case report will be considered if formatted as a research letter with 2 figures maximum. Maximum length is up to 1000 words with no headings and up to 6 references and 2 tables or figures. An abstract of 150-200 words should also be provided.

Short Communications should not exceed 1000 words and should consist of a background section (not to exceed 100 words), aims (not to exceed 50 words), methods (not to exceed 250 words), results (not to exceed 250 words) and conclusion (not to exceed 250 words). An abstract of 150-200 words should also be provided. The editorial team reserves the right to decide which tables/figures submitted are necessary.

Submission checklist

You can use this list to carry out a final check of your submission before you send it to the journal for review. Please check the relevant section in this Guide for Authors for more details.

Ensure that the following items are present:

One author has been designated as the corresponding author with contact details:
• E-mail address
• Full postal address

All necessary files have been uploaded:
Manuscript:
• Include keywords
• All figures (include relevant captions)
• All tables (including titles, description, footnotes)
• Ensure all figure and table citations in the text match the files provided
• Indicate clearly if color should be used for any figures in print
Graphical Abstracts / Highlights files (where applicable)
Supplemental files (where applicable)

Further considerations
• Manuscript has been 'spell checked' and 'grammar checked'
• All references mentioned in the Reference List are cited in the text, and vice versa

• Permission has been obtained for use of copyrighted material from other sources (including the Internet)
• A competing interests statement is provided, even if the authors have no competing interests to declare
• Journal policies detailed in this guide have been reviewed
• Referee suggestions and contact details provided, based on journal requirements

For further information, visit our Support Center.

BEFORE YOU BEGIN

Ethics in publishing

Please see our information on Ethics in publishing.

Declaration of interest

All authors must disclose any financial and personal relationships with other people or organizations that could inappropriately influence (bias) their work. Examples of potential competing interests include employment, consultancies, stock ownership, honoraria, paid expert testimony, patent applications/registrations, and grants or other funding. Authors must disclose any interests in two places: 1. A summary declaration of interest statement in the title page file (if double anonymized) or the manuscript file (if single anonymized). If there are no interests to declare then please state this: 'Declarations of interest: none'. 2. Detailed disclosures as part of a separate Declaration of Interest form, which forms part of the journal's official records. It is important for potential interests to be declared in both places and that the information matches. More information.

Submission declaration and verification

Submission of an article implies that the work described has not been published previously (except in the form of an abstract, a published lecture or academic thesis, see 'Multiple, redundant or concurrent publication' for more information), that it is not under consideration for publication elsewhere, that its publication is approved by all authors and tacitly or explicitly by the responsible authorities where the work was carried out, and that, if accepted, it will not be published elsewhere in the same form, in English or in any other language, including electronically without the written consent of the copyright-holder. To verify originality, your article may be checked by the originality detection service Crossref Similarity Check.

Preprints

Please note that preprints can be shared anywhere at any time, in line with Elsevier's sharing policy. Sharing your preprints e.g. on a preprint server will not count as prior publication (see 'Multiple, redundant or concurrent publication' for more information).

Preprint posting on SSRN

In support of Open Science, this journal offers its authors a free preprint posting service. Preprints provide early registration and dissemination of your research, which facilitates early citations and collaboration.

During submission to Editorial Manager, you can choose to release your manuscript publicly as a preprint on the preprint server SSRN once it enters peer-review with the journal. Your choice will have no effect on the editorial process or outcome with the journal. Please note that the corresponding author is expected to seek approval from all co-authors before agreeing to release the manuscript publicly on SSRN.

You will be notified via email when your preprint is posted online and a Digital Object Identifier (DOI) is assigned. Your preprint will remain globally available free to read whether the journal accepts or rejects your manuscript.

For more information about posting to SSRN, please consult the SSRN Terms of Use and FAQs.

Use of inclusive language

Inclusive language acknowledges diversity, conveys respect to all people, is sensitive to differences, and promotes equal opportunities. Content should make no assumptions about the beliefs or commitments of any reader; contain nothing which might imply that one individual is superior to another on the grounds of age, gender, race, ethnicity, culture, sexual orientation, disability or health condition; and use inclusive language throughout. Authors should ensure that writing is free from bias,

stereotypes, slang, reference to dominant culture and/or cultural assumptions. We advise to seek gender neutrality by using plural nouns ("clinicians, patients/clients") as default/wherever possible to avoid using "he, she," or "he/she." We recommend avoiding the use of descriptors that refer to personal attributes such as age, gender, race, ethnicity, culture, sexual orientation, disability or health condition unless they are relevant and valid. When coding terminology is used, we recommend to avoid offensive or exclusionary terms such as "master", "slave", "blacklist" and "whitelist". We suggest using alternatives that are more appropriate and (self-) explanatory such as "primary", "secondary", "blocklist" and "allowlist". These guidelines are meant as a point of reference to help identify appropriate language but are by no means exhaustive or definitive.

Author contributions

For transparency, we encourage authors to submit an author statement file outlining their individual contributions to the paper using the relevant CRediT roles: Conceptualization; Data curation; Formal analysis; Funding acquisition; Investigation; Methodology; Project administration; Resources; Software; Supervision; Validation; Visualization; Roles/Writing - original draft; Writing - review & editing. Authorship statements should be formatted with the names of authors first and CRediT role(s) following. More details and an example.

Changes to authorship

Authors are expected to consider carefully the list and order of authors **before** submitting their manuscript and provide the definitive list of authors at the time of the original submission. Any addition, deletion or rearrangement of author names in the authorship list should be made only **before** the manuscript has been accepted and only if approved by the journal Editor. To request such a change, the Editor must receive the following from the **corresponding author**: (a) the reason for the change in author list and (b) written confirmation (e-mail, letter) from all authors that they agree with the addition, removal or rearrangement. In the case of addition or removal of authors, this includes confirmation from the author being added or removed.
Only in exceptional circumstances will the Editor consider the addition, deletion or rearrangement of authors **after** the manuscript has been accepted. While the Editor considers the request, publication of the manuscript will be suspended. If the manuscript has already been published in an online issue, any requests approved by the Editor will result in a corrigendum.

Copyright

Upon acceptance of an article, authors will be asked to complete a 'Journal Publishing Agreement' (see more information on this). An e-mail will be sent to the corresponding author confirming receipt of the manuscript together with a 'Journal Publishing Agreement' form or a link to the online version of this agreement.

Subscribers may reproduce tables of contents or prepare lists of articles including abstracts for internal circulation within their institutions. Permission of the Publisher is required for resale or distribution outside the institution and for all other derivative works, including compilations and translations. If excerpts from other copyrighted works are included, the author(s) must obtain written permission from the copyright owners and credit the source(s) in the article. Elsevier has preprinted forms for use by authors in these cases.

For gold open access articles: Upon acceptance of an article, authors will be asked to complete a 'License Agreement' (more information). Permitted third party reuse of gold open access articles is determined by the author's choice of user license.

Author rights

As an author you (or your employer or institution) have certain rights to reuse your work. More information.

Elsevier supports responsible sharing
Find out how you can share your research published in Elsevier journals.

Role of the funding source

You are requested to identify who provided financial support for the conduct of the research and/or preparation of the article and to briefly describe the role of the sponsor(s), if any, in study design; in the collection, analysis and interpretation of data; in the writing of the report; and in the decision to submit the article for publication. If the funding source(s) had no such involvement, it is recommended to state this.

Open access
Please visit our Open Access page for more information.

Elsevier Researcher Academy
Researcher Academy is a free e-learning platform designed to support early and mid-career researchers throughout their research journey. The "Learn" environment at Researcher Academy offers several interactive modules, webinars, downloadable guides and resources to guide you through the process of writing for research and going through peer review. Feel free to use these free resources to improve your submission and navigate the publication process with ease.

Language (usage and editing services)
Please write your text in good English (American or British usage is accepted, but not a mixture of these). Authors who feel their English language manuscript may require editing to eliminate possible grammatical or spelling errors and to conform to correct scientific English may wish to use the English Language Editing service available from Elsevier's Author Services.

Submission
Our online submission system guides you stepwise through the process of entering your article details and uploading your files. The system converts your article files to a single PDF file used in the peer-review process. Editable files (e.g., Word, LaTeX) are required to typeset your article for final publication. All correspondence, including notification of the Editor's decision and requests for revision, is sent by e-mail.

Referees
Referees

Please submit, with the manuscript, the names, addresses and e-mail addresses of three potential referees who are willing to review the article (please obtain confirmation from the referees before submitting your manuscript). Note that the editor retains the sole right to decide whether or not the suggested reviewers are used.

Revised version of the manuscript
On the basis of the comments of the referees and editors, Authors may be asked to revise their manuscript. In order to facilitate the evaluation of the revisions by the referees and editors, upon revision, Authors are asked:
• to indicate all changes to the original manuscript by means of 'track changes'
• to add a letter for the referees, explaining how they dealt with all of the recommendations and questions from the referees. Authors should submit their revised version no later than 9 months after they were informed about the decision that the manuscript needs revision. If no revised manuscript is received 9 months after the decision, the manuscript will be considered as rejected.

PREPARATION
Style
Please use **no abbreviations**. Headlines and Subheadlines should be liberally employed in the Methods, Results, and Discussion sections. Use short paragraphs whenever possible. Clarity of expression, good syntax and the avoidance of medical jargon will be appreciated by the editors, reviewers and readers.

Queries
For questions about the editorial process (including the status of manuscripts under review) or for technical support on submissions, please visit our Support Center.

References
There are no strict requirements on reference formatting at submission. References can be in any style or format as long as the style is consistent. Where applicable, author(s) name(s), journal title/ book title, chapter title/article title, year of publication, volume number/book chapter and the article number or pagination must be present. Use of DOI is highly encouraged. The reference style used by the journal will be applied to the accepted article by Elsevier at the proof stage. Note that missing data will be highlighted at proof stage for the author to correct.

Peer review
This journal operates a single anonymized review process. All contributions will be initially assessed by the editor for suitability for the journal. Papers deemed suitable are then typically sent to a minimum of one independent expert reviewer to assess the scientific quality of the paper. The Editor is responsible

for the final decision regarding acceptance or rejection of articles. The Editor's decision is final. Editors are not involved in decisions about papers which they have written themselves or have been written by family members or colleagues or which relate to products or services in which the editor has an interest. Any such submission is subject to all of the journal's usual procedures, with peer review handled independently of the relevant editor and their research groups. More information on types of peer review.

Open access

This journal offers authors two choices to publish their research;
1. *Open Access*
o Articles are freely available to both subscribers and the wider public with permitted reuse
o An open access publication fee is payable by authors or their research funder
2. *Subscription*
o Articles are made available to subscribers as well as developing countries and patient groups through our access programs
o No open access publication fee

All articles published open access will be immediately and permanently free for everyone to read and download. Permitted reuse is defined by your choice of one of the following Creative Commons user licenses:

Creative Commons Attribution-NonCommercial-NoDerivs (CC-BY-NC-ND): for non-commercial purposes, lets others distribute and copy the article, and to include in a collective work (such as an anthology), as long as they credit the author(s) and provided they do not alter or modify the article.

Elsevier has established agreements with funding bodies. This ensures authors can comply with funding body open access requirements, including specific user licenses, such as CC-BY. Some authors may also be reimbursed for associated publication fees. https://www.elsevier.com/fundingbodies

If you need to comply with your funding body policy you can apply for the CC-BY license after your manuscript is accepted for publication.

To provide open access, this journal has a publication fee which needs to be met by the authors or their research funders for each article published open access. Your publication choice will have no effect on the peer review process or acceptance of submitted articles.

The open access publication fee for this journal is **$USD 2,500** excluding taxes.

Learn more about Elsevier's pricing policy https://www.elsevier.com/openaccesspricing

Layout of manuscript

Divide the manuscript into the following sections: Title page, Structured Abstract, Key words (3-6), Introduction, Materials and Methods, Results, Discussion, Acknowledgments, References. The editors will consider the use of other sections if more suitable for certain manuscripts.

Essential title page information

• ***Title.*** Concise and informative. Titles are often used in information-retrieval systems. Avoid abbreviations and formulae where possible.
• ***Author names and affiliations.*** Please clearly indicate the given name(s) and family name(s) of each author and check that all names are accurately spelled. You can add your name between parentheses in your own script behind the English transliteration. Present the authors' affiliation addresses (where the actual work was done) below the names. Indicate all affiliations with a lower-case superscript letter immediately after the author's name and in front of the appropriate address. Provide the full postal address of each affiliation, including the country name and, if available, the e-mail address of each author.
• ***Corresponding author.*** Clearly indicate who will handle correspondence at all stages of refereeing and publication, also post-publication. This responsibility includes answering any future queries about Methodology and Materials. **Ensure that the e-mail address is given and that contact details are kept up to date by the corresponding author.**

• ***Present/permanent address.*** If an author has moved since the work described in the article was done, or was visiting at the time, a 'Present address' (or 'Permanent address') may be indicated as a footnote to that author's name. The address at which the author actually did the work must be retained as the main, affiliation address. Superscript Arabic numerals are used for such footnotes.

The **Structured Abstract,** of no more than 250 words, should be written with particular care since this will be the only part of the article studied by some readers. The preferred subheadings are: Background, Methods, Results and Conclusions.

The **Introduction** should be brief and set out the purposes for which the study has been performed along with relevant previous studies only where essential.

The **Materials and Methods** should be sufficiently detailed so that readers and reviewers can understand precisely what has been done without studying the references directly. The description may be abbreviated when well accepted techniques are used.

The **Results** should be presented precisely. Keep discussion of their importance to a minimum in this section of the manuscript.

The **Discussion** should directly relate to the study being reported. Do not include a general review of the topic.

Tables should be typed with double spacing and each should be on a separate sheet. They should be numbered consecutively with Arabic numerals, and contain only horizontal lines. Provide a short descriptive heading above each table with footnotes and/or explanations underneath.

Figures should ideally be submitted in high-resolution TIF format, or alternatively in GIF, JPEG/JPG, or EPS format. The figures should be placed in separate files, named purely with the figure numbers (e.g. "Figure1.tif".) The cost of colour figures will be paid by the author.

Legends for Figures should be typed with double-spacing on a separate sheet.

Gene Accession Numbers
For each and every gene accession number cited in an article, authors should type the accession number in bold, underlined text. Letters in the accession number should always be capitalised. Example: (GenBank accession nos. AI631510 , AI631511 , AI632198, and BF223228), a B-cell tumor from a chronic lymphatic leukemia (GenBank accession no. BE675048), and a T-cell lymphoma (GenBank accession no. AA361117).

Supplementary data
The journal accepts electronic supplementary material to support and enhance your scientific research. Supplementary files offer the author additional possibilities to publish supporting applications, movies, animation sequences, high-resolution images, background datasets, sound clips and more. Supplementary files supplied will be published online alongside the electronic version of your article in Elsevier web products, including ScienceDirect: http://www.sciencedirect.com

Highlights
Highlights are mandatory for this journal as they help increase the discoverability of your article via search engines. They consist of a short collection of bullet points that capture the novel results of your research as well as new methods that were used during the study (if any). Please have a look at the examples here: example Highlights.

Highlights should be submitted in a separate editable file in the online submission system. Please use 'Highlights' in the file name and include 3 to 5 bullet points (maximum 85 characters, including spaces, per bullet point).

Graphical abstract
Although a graphical abstract is optional, its use is encouraged as it draws more attention to the online article. The graphical abstract should summarize the contents of the article in a concise, pictorial form designed to capture the attention of a wide readership. Graphical abstracts should be submitted as a separate file in the online submission system. Image size: Please provide an image with a minimum

of 531 × 1328 pixels (h × w) or proportionally more. The image should be readable at a size of 5 × 13 cm using a regular screen resolution of 96 dpi. Preferred file types: TIFF, EPS, PDF or MS Office files. You can view Example Graphical Abstracts on our information site.
Authors can make use of Elsevier's Illustration Services to ensure the best presentation of their images and in accordance with all technical requirements.

Formatting of funding sources
List funding sources in this standard way to facilitate compliance to funder's requirements:

Funding: This work was supported by the National Institutes of Health [grant numbers xxxx, yyyy]; the Bill & Melinda Gates Foundation, Seattle, WA [grant number zzzz]; and the United States Institutes of Peace [grant number aaaa].

It is not necessary to include detailed descriptions on the program or type of grants and awards. When funding is from a block grant or other resources available to a university, college, or other research institution, submit the name of the institute or organization that provided the funding.

If no funding has been provided for the research, it is recommended to include the following sentence:

This research did not receive any specific grant from funding agencies in the public, commercial, or not-for-profit sectors.

Electronic artwork
General points
• Make sure you use uniform lettering and sizing of your original artwork.
• Embed the used fonts if the application provides that option.
• Aim to use the following fonts in your illustrations: Arial, Courier, Times New Roman, Symbol, or use fonts that look similar.
• Number the illustrations according to their sequence in the text.
• Use a logical naming convention for your artwork files.
• Provide captions to illustrations separately.
• Size the illustrations close to the desired dimensions of the published version.
• Submit each illustration as a separate file.
• Ensure that color images are accessible to all, including those with impaired color vision.

A detailed guide on electronic artwork is available.
You are urged to visit this site; some excerpts from the detailed information are given here.
Formats
If your electronic artwork is created in a Microsoft Office application (Word, PowerPoint, Excel) then please supply 'as is' in the native document format.
Regardless of the application used other than Microsoft Office, when your electronic artwork is finalized, please 'Save as' or convert the images to one of the following formats (note the resolution requirements for line drawings, halftones, and line/halftone combinations given below):
EPS (or PDF): Vector drawings, embed all used fonts.
TIFF (or JPEG): Color or grayscale photographs (halftones), keep to a minimum of 300 dpi.
TIFF (or JPEG): Bitmapped (pure black & white pixels) line drawings, keep to a minimum of 1000 dpi.
TIFF (or JPEG): Combinations bitmapped line/half-tone (color or grayscale), keep to a minimum of 500 dpi.
Please do not:
• Supply files that are optimized for screen use (e.g., GIF, BMP, PICT, WPG); these typically have a low number of pixels and limited set of colors;
• Supply files that are too low in resolution;
• Submit graphics that are disproportionately large for the content.

Color artwork
Please make sure that artwork files are in an acceptable format (TIFF (or JPEG), EPS (or PDF) or MS Office files) and with the correct resolution. If, together with your accepted article, you submit usable color figures then Elsevier will ensure, at no additional charge, that these figures will appear in color online (e.g., ScienceDirect and other sites) in addition to color reproduction in print. Further information on the preparation of electronic artwork.

Reference links
Increased discoverability of research and high quality peer review are ensured by online links to the sources cited. In order to allow us to create links to abstracting and indexing services, such as Scopus, CrossRef and PubMed, please ensure that data provided in the references are correct. Please note that incorrect surnames, journal/book titles, publication year and pagination may prevent link creation. When copying references, please be careful as they may already contain errors. Use of the DOI is highly encouraged.

A DOI is guaranteed never to change, so you can use it as a permanent link to any electronic article. An example of a citation using DOI for an article not yet in an issue is: VanDecar J.C., Russo R.M., James D.E., Ambeh W.B., Franke M. (2003). Aseismic continuation of the Lesser Antilles slab beneath northeastern Venezuela. Journal of Geophysical Research, https://doi.org/10.1029/2001JB000884. Please note the format of such citations should be in the same style as all other references in the paper.

Data references
This journal encourages you to cite underlying or relevant datasets in your manuscript by citing them in your text and including a data reference in your Reference List. Data references should include the following elements: author name(s), dataset title, data repository, version (where available), year, and global persistent identifier. Add [dataset] immediately before the reference so we can properly identify it as a data reference. The [dataset] identifier will not appear in your published article.

Reference management software
Most Elsevier journals have their reference template available in many of the most popular reference management software products. These include all products that support Citation Style Language styles, such as Mendeley. Using citation plug-ins from these products, authors only need to select the appropriate journal template when preparing their article, after which citations and bibliographies will be automatically formatted in the journal's style. If no template is yet available for this journal, please follow the format of the sample references and citations as shown in this Guide. If you use reference management software, please ensure that you remove all field codes before submitting the electronic manuscript. More information on how to remove field codes from different reference management software.

Reference formatting
There are no strict requirements on reference formatting at submission. References can be in any style or format as long as the style is consistent. Where applicable, author(s) name(s), journal title/book title, chapter title/article title, year of publication, volume number/book chapter and the article number or pagination must be present. Use of DOI is highly encouraged. The reference style used by the journal will be applied to the accepted article by Elsevier at the proof stage. Note that missing data will be highlighted at proof stage for the author to correct. If you do wish to format the references yourself they should be arranged according to the following examples:

Reference style
Text: Indicate references by number(s) in square brackets in line with the text. The actual authors can be referred to, but the reference number(s) must always be given.
Example: '..... as demonstrated [3,6]. Barnaby and Jones [8] obtained a different result ....'
List: Number the references (numbers in square brackets) in the list in the order in which they appear in the text.
Examples:
Reference to a journal publication:
[1] J. van der Geer, J.A.J. Hanraads, R.A. Lupton, The art of writing a scientific article, J. Sci. Commun. 163 (2010) 51–59. https://doi.org/10.1016/j.Sc.2010.00372.
Reference to a journal publication with an article number:
[2] J. van der Geer, J.A.J. Hanraads, R.A. Lupton, 2018. The art of writing a scientific article. Heliyon. 19, e00205. https://doi.org/10.1016/j.heliyon.2018.e00205.
Reference to a book:
[3] W. Strunk Jr., E.B. White, The Elements of Style, fourth ed., Longman, New York, 2000.
Reference to a chapter in an edited book:
[4] G.R. Mettam, L.B. Adams, How to prepare an electronic version of your article, in: B.S. Jones, R.Z. Smith (Eds.), Introduction to the Electronic Age, E-Publishing Inc., New York, 2009, pp. 281–304.
Reference to a website:
[5] Cancer Research UK, Cancer statistics reports for the UK. http://www.cancerresearchuk.org/aboutcancer/statistics/cancerstatsreport/, 2003 (accessed 13 March 2003).

Reference to a dataset:
[dataset] [6] M. Oguro, S. Imahiro, S. Saito, T. Nakashizuka, Mortality data for Japanese oak wilt disease and surrounding forest compositions, Mendeley Data, v1, 2015. https://doi.org/10.17632/xwj98nb39r.1.
Reference to software:
[7] E. Coon, M. Berndt, A. Jan, D. Svyatsky, A. Atchley, E. Kikinzon, D. Harp, G. Manzini, E. Shelef, K. Lipnikov, R. Garimella, C. Xu, D. Moulton, S. Karra, S. Painter, E. Jafarov, S. Molins, Advanced Terrestrial Simulator (ATS) v0.88 (Version 0.88), Zenodo, March 25, 2020. https://doi.org/10.5281/zenodo.3727209.

Data visualization

Include interactive data visualizations in your publication and let your readers interact and engage more closely with your research. Follow the instructions here to find out about available data visualization options and how to include them with your article.

Research data

This journal encourages and enables you to share data that supports your research publication where appropriate, and enables you to interlink the data with your published articles. Research data refers to the results of observations or experimentation that validate research findings. To facilitate reproducibility and data reuse, this journal also encourages you to share your software, code, models, algorithms, protocols, methods and other useful materials related to the project.

Below are a number of ways in which you can associate data with your article or make a statement about the availability of your data when submitting your manuscript. If you are sharing data in one of these ways, you are encouraged to cite the data in your manuscript and reference list. Please refer to the "References" section for more information about data citation. For more information on depositing, sharing and using research data and other relevant research materials, visit the research data page.

Data linking
If you have made your research data available in a data repository, you can link your article directly to the dataset. Elsevier collaborates with a number of repositories to link articles on ScienceDirect with relevant repositories, giving readers access to underlying data that gives them a better understanding of the research described.

There are different ways to link your datasets to your article. When available, you can directly link your dataset to your article by providing the relevant information in the submission system. For more information, visit the database linking page.

For supported data repositories a repository banner will automatically appear next to your published article on ScienceDirect.

In addition, you can link to relevant data or entities through identifiers within the text of your manuscript, using the following format: Database: xxxx (e.g., TAIR: AT1G01020; CCDC: 734053; PDB: 1XFN).

Mendeley Data
This journal supports Mendeley Data, enabling you to deposit any research data (including raw and processed data, video, code, software, algorithms, protocols, and methods) associated with your manuscript in a free-to-use, open access repository. During the submission process, after uploading your manuscript, you will have the opportunity to upload your relevant datasets directly to *Mendeley Data*. The datasets will be listed and directly accessible to readers next to your published article online.

For more information, visit the Mendeley Data for journals page.

Data statement
To foster transparency, we encourage you to state the availability of your data in your submission. This may be a requirement of your funding body or institution. If your data is unavailable to access or unsuitable to post, you will have the opportunity to indicate why during the submission process, for example by stating that the research data is confidential. The statement will appear with your published article on ScienceDirect. For more information, visit the Data Statement page.

Process of submission
Online submission

Photodiagnosis and Photodynamic Therapy uses an online submission and review system. Authors can upload their article via the Elsevier Editorial System at https://www.editorialmanager.com/PDPDT. By accessing the website Authors will be guided stepwise through the uploading of the various files. Editable file formats are necessary. We accept most wordprocessing formats, but Word, WordPerfect or LaTeX is preferred. Figure files (TIFF, EPS, JPEG) should be uploaded separately. Always keep a backup copy of the electronic file for reference and safety. Save your files using the default extension of the program used. The system generates an Adobe Acrobat PDF version of the article which is used for the reviewing process. Authors, Reviewers and Editors send and receive all correspondence by e-mail and no paper correspondence is necessary. For assistance please visit our Support Center.

AFTER ACCEPTANCE

Online proof correction

To ensure a fast publication process of the article, we kindly ask authors to provide us with their proof corrections within two days. Corresponding authors will receive an e-mail with a link to our online proofing system, allowing annotation and correction of proofs online. The environment is similar to MS Word: in addition to editing text, you can also comment on figures/tables and answer questions from the Copy Editor. Web-based proofing provides a faster and less error-prone process by allowing you to directly type your corrections, eliminating the potential introduction of errors.
If preferred, you can still choose to annotate and upload your edits on the PDF version. All instructions for proofing will be given in the e-mail we send to authors, including alternative methods to the online version and PDF.
We will do everything possible to get your article published quickly and accurately. Please use this proof only for checking the typesetting, editing, completeness and correctness of the text, tables and figures. Significant changes to the article as accepted for publication will only be considered at this stage with permission from the Editor. It is important to ensure that all corrections are sent back to us in one communication. Please check carefully before replying, as inclusion of any subsequent corrections cannot be guaranteed. Proofreading is solely your responsibility.

Offprints

The corresponding author will, at no cost, receive a customized Share Link providing 50 days free access to the final published version of the article on ScienceDirect. The Share Link can be used for sharing the article via any communication channel, including email and social media. For an extra charge, paper offprints can be ordered via the offprint order form which is sent once the article is accepted for publication. Both corresponding and co-authors may order offprints at any time via Elsevier's Author Services. Corresponding authors who have published their article gold open access do not receive a Share Link as their final published version of the article is available open access on ScienceDirect and can be shared through the article DOI link.

AUTHOR INQUIRIES

Visit the Elsevier Support Center to find the answers you need. Here you will find everything from Frequently Asked Questions to ways to get in touch.
You can also check the status of your submitted article or find out when your accepted article will be published.

© Copyright 2018 Elsevier | https://www.elsevier.com

14) Anexo 4 - Publicação do Artigo - In vitro study on how photodynamic therapy and calcium hydroxide medication influence adhesive interface properties of glass-fiber posts to intraradicular dentin

journal of the mechanical behavior of biomedical materials 141 (2023) 105757

Contents lists available at ScienceDirect

Journal of the Mechanical Behavior of Biomedical Materials

journal homepage: www.elsevier.com/locate/jmbbm

In vitro study on how photodynamic therapy and calcium hydroxide medication influence adhesive interface properties of glass-fiber posts to intraradicular dentin

Henrico Badaoui Strazzi-Sahyon [a,b,1], Henrique Augusto Banci [c,1], Fernanda Santos de Melo [c], Lucas Silva Soares [d], Rubens Spin-Neto [e], Marco Antonio Hungaro Duarte [f], Luciano Tavares Angelo Cintra [c], Paulo Henrique dos Santos [a,h], Gustavo Sivieri-Araujo [c,*]

[a] Department of Dental Materials and Prosthodontics, Araçatuba School of Dentistry, São Paulo State University, UNESP, Araçatuba, SP, Brazil
[b] Department of Prosthodontics and Periodontology, Bauru School of Dentistry, University of Sao Paulo, USP, Bauru, SP, Brazil
[c] Department of Preventive and Restorative Dentistry, Discipline of Endodontics, Araçatuba School of Dentistry, São Paulo State University, UNESP, Araçatuba, SP, Brazil
[d] Etec Araçatuba -Public School, Centro Paula Souza Araçatuba, SP, Brazil
[e] Section of Oral Radiology, Department of Dentistry and Oral Health, Aarhus University, Aarhus, Denmark
[f] Department of Restorative Dentistry, Endodontics and Dental Materials, Bauru School of Dentistry, São Paulo University, USP, Bauru, SP, Brazil
[h] Dental Research Institute, University of Toronto, Faculty of Dentistry, Toronto, ON, Canada

ARTICLE INFO

Keywords:
Bond strength
Dentin
Calcium hydroxide
Methylene blue
Photodynamic therapy
Resin cements

ABSTRACT

Purpose: This *in vitro* study evaluated the influence of antimicrobial photodynamic therapy (aPDT), using methylene blue (MB) as photosensitizer (PS) and calcium hydroxide (CH) as intracanal medication on adhesive bond strength, sealing, and integrity of the luting interface of glass-fiber posts to different thirds of endodontically treated root canal dentin.

Material and methods: 102 incisors were sorted into 6 groups: a negative control irrigated with deionized water; a positive control irrigated with deionized water and filled with CH; CH + MB 50 mg/L without laser radiation; CH + MB 100 mg/L without laser radiation; CH + MB 50 mg/L radiated by red laser; and CH + MB 100 mg/L radiated by red laser. Push-out bond strength (n = 8), adhesive interface sealing (n = 3), and volume and quantification of voids (n = 6) were assessed using a universal testing machine, confocal laser scanning microscope, and computerized microtomography, respectively. Scanning electron micrographs were obtained from representative samples to qualify the fracture patterns. Push-out bond strength and adhesive interface integrity data were subjected to 2-way ANOVA for repeated measures followed by Tukey's test ($\alpha = 0.05$). Adhesive interface sealing was evaluated by the inter-examiner Kappa test and submitted to Kruskal-Wallis and Dunns tests ($\alpha = 0.05$).

Results: Assessing the apical region, the positive control and $MB_{100WA} + Ca(OH)_2$ groups showed lower adhesive bond strength compared to the $MB_{100A} + Ca(OH)_2$ group ($P < 0.05$). The cervical third showed higher bond strength than the apical third for the positive control, $MB_{50WA} + Ca(OH)_2$, $MB_{100WA} + Ca(OH)_2$, and $MB_{50A} + Ca(OH)_2$ groups ($P < 0.05$). A prevalence of mixed failure was observed in all experimental groups. There were no statistically significant differences in adhesive interface sealing for any of the parameters assessed ($P > 0.05$). $MB_{100WA} + Ca(OH)_2$ and $MB_{100A} + Ca(OH)_2$ groups promoted a higher volume and quantification of voids compared to the negative control group evaluating the cervical third ($P < 0.05$). In general, there were no differences in the quantification of voids comparing the intraradicular thirds ($P > 0.05$), differently to the volume of voids in which, in general, the cervical third promoted higher values compared to the middle and apical thirds ($P < 0.05$).

* Corresponding author. Department of Preventive and Restorative Dentistry, Discipline of Endodontics, São Paulo State University (UNESP), Araçatuba School of Dentistry, Rua José Bonifácio, 1193, 16015-050, Araçatuba, SP, Brazil.
E-mail addresses: ico_strazzi@usp.br (H.B. Strazzi-Sahyon), henrique.banci@unesp.br (H.A. Banci), fernanda2953@hotmail.com (F.S. Melo), lucas.ssoares249@gmail.com (L.S. Soares), rsn@dent.au.dk (R. Spin-Neto), mhungaro@fob.usp.br (M.A.H. Duarte), luciano.cintra@unesp.br (L.T.A. Cintra), pauloh.dossantos@utoronto.ca (P.H. dos Santos), gustavo.sivieri@unesp.br, gustavosivieri@uol.com.br (G. Sivieri-Araujo).
[1] H.B.S.S., H.A.B: Both authors contributed equally to this manuscript.

https://doi.org/10.1016/j.jmbbm.2023.105757
Received 5 January 2023; Received in revised form 28 February 2023; Accepted 3 March 2023
Available online 5 March 2023
1751-6161/© 2023 Elsevier Ltd. All rights reserved.

Conclusion: aPDT with methylene blue PS at 50 mg/L associated with calcium hydroxide as intracanal medication demonstrated satisfactory bond strength, sealing, and integrity of the adhesive interface at any intraradicular depth.

Clinical relevance

Antimicrobial photodynamic therapy with methylene blue photosensitizer at 50 mg/L, associated with calcium hydroxide as an intracanal medication, is a suitable endodontic therapy that can be used before luting of glass-fiber posts to intraradicular dentin as it does not alter the adhesive interface properties.

1. Introduction

The success and longevity of endodontic treatment and the reconstruction of teeth with excessive coronal structure loss using glass-fiber posts or endocrowns are directly related to factors such as the mechanical properties of intraradicular dentin, adhesion effectiveness, and satisfactory bacterial microbiota eradication (StrazziSahyon et al., 2018). Several clinicians still use post retained restoration and a crown, as this technique increases the assembly restoration into the root canal (Govare and Contrepois, 2020; Lin et al., 2010). According to Lin et al., endocrown and post retained restorations present similar performance under normal occlusion, showing similarity of failure probability (Govare and Contrepois, 2020). Studies demonstrate unsatisfactory results of conventional methods on the reduction in microorganisms and inflammatory processes, such as biomechanical instrumentation and irrigating agents (Josic et al., 2022; Martinho et al., 2023). Due to the anatomical complexity of root canal systems, endodontic instruments and chemical solutions are unable to completely reach deeper intraradicular regions, such as apical thirds, favoring the occurrence of persistent infections (Chalub et al., 2022).

Enterococcus faecalis is one of the main causes of persistent infections in endodontic treatment (Rodrigues et al., 2018; Balto et al., 2020). Calcium hydroxide ($Ca[OH]_2$) is a strongly alkaline compound, with a pH ≅ 12.5, presenting antimicrobial and biological effects, such as the dissolution of tissues and biofilms, inhibition of tooth resorption, and induction of hard tissue repair, being the gold standard of intracanal medication for persistent infections (Corazza et al., 2020; Best et al., 2021). However, *Enterococcus faecalis* presents a proton pump that promotes the acidulation of its cytoplasm, and due to its ability to penetrate deep into complex anatomical regions, such as apical deltas, lateral canals, and dentinal tubule constrictions, this pathogen hinders the efficacy of calcium hydroxide medication (Chalub et al., 2022; Evans et al., 2002). Several adjunctive therapy modalities have been introduced in oral health to improve the disinfection effectiveness of root canal systems, such as antimicrobial photodynamic therapy (aPDT) (Keskin and Çiloğlu, 2021; Nunes et al., 2022).

Previous studies claim that aPDT alone is unable to completely eradicate the presence of biofilm (Singh et al., 2014; Garcez et al., 2007). Biofilm is composed of a community of microorganisms, and its maturation can be 10–1000 times more resistant to treatment using antimicrobial medication, contributing to the development of tolerance in microorganisms (Ferrisse et al., 2022; Davies, 2003). This scenario suggests that aPDT application associated with calcium hydroxide intracanal medication potentializes the microbial load reduction (Meire et al., 2012; Hidalgo et al., 2016). Thus, the literature establishes that aPDT is not intended to substitute conventional endodontic therapies, but operates concomitantly with them, aiming at the eradication of persistent infections (Garcez et al., 2007). Several studies have assessed the influence of different photosensitizers (PSs) at distinct concentrations, irradiated or not by laser, on the mechanical properties and bond strength of glass-fiber posts luted to intraradicular dentin (Strazzi-Sahyon et al., 2018, 2019; Strazzi-Sahyon et al., 2020, 2021a). However, studies investigating the influence of methylene blue and other PSs at distinct concentrations, activated or not by red laser, concomitantly with calcium hydroxide action as intracanal medication along the intraradicular dentin are scarce in the literature (Strazzi-Sahyon et al., 2021b).

Methylene blue is a hydrophilic compound, presenting a low molecular weight and positive charge, which allow it to easily pass through the membrane of gram-positive and negative bacteria, being a satisfactory choice to be used as PS in PDT (Strazzi-Sahyon et al., 2020). Strazzi-Sahyon et al. assessed the influence of calcium hydroxide intracanal medication and two sessions of methylene blue PS application, radiated or not by red laser, on intraradicular dentin mechanical properties (Strazzi-Sahyon et al., 2021b). However, because of the lack of in-depth information regarding the influence of aPDT and calcium hydroxide as intracanal medication on the adhesion process, there is no consensus on how the association of these therapies could affect the sealing and integrity of the luting interface of glass-fiber posts to intraradicular dentin. Thus, the purpose of this *in vitro* study was to determine the influence of methylene blue PS, radiated or not by red laser, with aPDT and calcium hydroxide administered as intracanal medication on the adhesion effectiveness of glass-fiber posts. The push-out bond strength, sealing, and integrity of the luting interface were evaluated of intraradicular restorations to different thirds of endodontically treated root canal dentin. Two null hypotheses were tested, as follows: 1) The performance of methylene blue, activated or not, and calcium hydroxide intracanal medication would not result in differences on push-out bond strength, sealing, and integrity of the luting interface of glass-fiber posts to intraradicular dentin; and 2) different depths of intraradicular dentin treated with methylene blue PS, activated or not, and calcium hydroxide intracanal medication would not promote differences on glass-fiber post adhesion effectiveness.

2. Material and methods

2.1. Experimental design

The information regarding the materials used in the present study is listed in Table 1. This *in vitro* study was analyzed and approved by the local ECUA (Ethics Committee on the Use of Animals; Protocol: #18–01003).

A total of one hundred and two bovine incisors, from cattle aged from 28 to 34 months, were used (Silva et al., 2019; Schilke et al., 2000; Camargo et al., 2006). Teeth were discarded and substituted if they exhibited any curved roots, fractures, or cracks. Using a low-speed diamond disc under water cooling, the anatomical crowns were divided from the root portion 1.0 mm above the cementum-enamel junction (Fig. 1–A). The canal length and diameter were standardized at 20 mm and 4 mm, respectively (Fig. 1-B). Prior to mechanical instrumentation, the measurement of 1.0 mm less than the original tooth length was established for the working length of the root canals (Fig. 1–B). The root canal instrumentation was performed using endodontic files until reaching the #80 K-file (Maillefer Instruments, Tulsa, OK, USA) (Fig. 1–B), and for each file change the root canals were irrigated with 10 ml of 1% sodium hypochlorite for 15 s. The canals were then filled with 10 ml of 17% ethylenediaminetetraacetic acid (EDTA) (Biodinâmica Química e Farmacêutica LTDA, Ibiporã, PR, Brazil) for smear layer removal, which remained in contact with the root dentin substrate for 3 min, before being removed using irrigation with 10 ml of distilled water for 15 s and dried with sterile absorbent paper tips (Dentsply Sirona, York, PA, USA) and air jets. To avoid any PS escape,

Table 1
Materials, classification, composition, and batch numbers of the materials used.

Material	Classification	Composition [a]	Batch
Adper Single Bond 2 (3M ESPE)	Adhesive System	BisGMA, HEMA, glycerol 1,3-dimethacrylate, diurethane dimethacrylate, water, ethanol, photoinitiators, 5 nm silanized silica, polyacrylic and itaconic acid copolymer.	N820206
Filtek Z350XT (3M ESPE)	Resin Composite	Bis-EMA, Bis-GMA, TEGDMA, UDMA, silica and zirconia nanofillers, and, agglomerated zirconia silica nanoclusters.	HB004209993
Calcium Hydroxide (Biodinamica)	Intracanal Medication	38% of calcium hydroxide and, 62% of barium oxide.	36870
Iodoform (Biodinamica)	Intracanal Medication	Iodoform (99–100%)	005–22
Propylene Glycol (Farma Formula)	Intracanal Medication	100% propylene glycol	530080
MTA Fillapex (Angelus)	Endodontic Sealer	Salicylate resin, natural resin, diluting resin, bismuth oxide, nanoparticulated silica, MTA (mineral trioxide aggregate) and pigments.	102564
RelyX Ceramic Primer (3M ESPE)	Ceramic Primer	Ethyl alcohol, water, and 3-MPS.	2106800707
RelyX U200 (3M ESPE)	Resin Cement	Base: methacrylate phosphoric acid esters, glass fiber, triethylene glycol dimethacrylate, sodium persulfate, silane-treated silica. Catalyst: substitute dimethacrylate, glass fiber, sodiump-toluenesulfonate, silane-treated silica, calcium.	2115100124

Abbreviations: Bis-EMA, ethoxylated bisphenol A glycol dimethacrylate; HEMA, hydroxyethyl methacrylate; UDMA, urethane dimethacrylate; Bis-GMA, bisphenol-A diglycidyl ether dimethacry-late; TEGDMA, triethylene glycol dimethacrylate; MTA, mineral trioxide aggregate; 3-MPS, 3-methacrylox-ypropyl-trimethoxy silane.
[a] According to manufacturer's information.

the apical foramens were restored and sealed with dental adhesive (Adper Single Bond 2; 3 M ESPE) and resin composite (Filtek Z350 XT; 3 M ESPE) according to the manufacturer's recommendations (Fig. 1– C). (StrazziSahyon et al., 2018, 2019; Strazzi-Sahyon et al., 2020, 2021a; Banci et al., 2020)

2.2. Experimental groups and aPDT

The endodontically-treated root specimens were randomly sorted into six experimental groups (n = 17), as described in Table 2. In the experimental groups, the methylene blue PS was submitted to a 3 min pre-irradiation period (Banci et al., 2020), and agitated for 1 min using ultrasonic equipment (Nac Plus, Adiel LTDA, São Paulo, SP, Brazil) coupled to an ultrasonic tip (Irrisonic E1; Helse Dental Technology, Santa Rosa de Viterbo, SP, Brazil) (StrazziSahyon et al., 2018, 2019; Strazzi-Sahyon et al., 2020, 2021a; Banci et al., 2020). During the PS agitation, the ultrasonic tip was carefully handled to avoid contact with the root canal walls (StrazziSahyon et al., 2018, 2019; Strazzi-Sahyon et al., 2020, 2021a, 2021b).

The methylene blue PS from the MB_{50A} and MB_{100A} groups was radiated with the red laser (Laser Duo - 660 nm wavelength; MMO, São Carlos, SP, Brazil) for 1 min using a 300-μm flexible optical fiber, resulting in a final energy of 72 J/cm^2 (Fig. 1–Da). (StrazziSahyon et al., 2018; Strazzi-Sahyon et al., 2020, 2021a; Banci et al., 2020; Jurič et al., 2014) The radiation was performed by applying helicoidal movements of the optical fiber in the cervical-apical direction (10 times/minute) at a depth of 2 mm less than the root canal working length (Banci et al., 2020). In the MB_{50WA} and MB_{100WA} groups, the methylene blue PS was not radiated (without activation) (Fig. 1–Db). After the treatment, the methylene blue dye was removed from the root canals by irrigation with 10 mL of deionized water, then the canals were dried with air jets and sterile paper (Strazzi-Sahyon et al., 2021b).

2.3. Calcium hydroxide medication

All the experimental groups, except the negative control group, were filled with calcium hydroxide (Biodinâmica Química e Farmacêutica) mixed with propylene glycol (Farma Formula) and iodoform (Biodinâmica Química e Farmacêutica) using a #4 Lentulo instrument (Maillefer Instruments) for a period of 14 days (Fig. 1–E). (Strazzi--Sahyon et al., 2021b) Interim cement (Cimpat Branco; Septodont Ltda, Barueri, SP, Brazil) was used to seal the coronal region of the root canal samples. To certify the complete filling of the root canal extension with intracanal medication, radiographic analysis as performed on the tooth specimens (Digital X-Ray – 1.0.9.1; Micro Image, Indaiatuba, SP, Brazil). All sealed root canal specimens were stored at 100% relative humidity at 37 °C. After 14 days, coronal sealing and calcium hydroxide intracanal medication were removed, and the root canals were cleaned under irrigation with 10 ml of 1% sodium hypochlorite solution and a K #80 file (Strazzi-Sahyon et al., 2021b).

2.4. Push-out bond strength analysis

Forty-eight teeth were used for the push-out bond strength analysis (n = 8). MTA Fillapex endodontic cement (Angelus, Londrina, PR, Brazil) and #80 gutta-percha cones and fine (F) and medium-fine (MF) auxiliary cones (Tanari, Manacapuru, AM, Brazil) were inserted into the root canals. The obturation method used was Tagger's technique, with a McSpadden compactor #70 (Maillefer Instruments) (Fig. 1-F). (Banci et al., 2020) Provisional cement (Cimpat Branco; Septodont Ltda) was used to seal the coronal portion of the specimens, then the samples were kept at 37 °C in 100% humidity for 7 days (Strazzi-Sahyon et al., 2021b).

Nine millimeters of gutta-percha was removed using #1 and #2 White Post DCE system drills (White Post DCE #2; FGM, Joinville, SC, Brazil). The #2 double-tapered glass-fiber post (18 mm length, 2.2 mm top diameter, and 1.05 mm bottom diameter) was inserted into the post space to verify the adaptation. The post space was then irrigated with 10 ml of physiological saline solution (0.9%) to remove any debris or residual gutta-percha. The root canals were dried with sterile paper and an air jet (StrazziSahyon et al., 2018, 2019; Strazzi-Sahyon et al., 2020, 2021a).

The surface of the glass-fiber posts was conditioned with 35% phosphoric acid (3M ESPE) during 60 s, washed, and dried with an air jet. The conditioned surfaces were then silanized (RelyX Ceramic Primer; 3 M ESPE) for 60 s, and intraradicular posts that would not be further manipulated were gently dried with an air jet, preventing surface contamination. Dual-cured self-adhesive resin cement (RelyX U200; 3M ESPE) coupled to a mixing root canal tip was used. The tip was introduced into the root canal and the cement was injected into the post space and on the post surface, before the glass-fiber post was settled into the intraradicular canal. The assembly was polymerized for 40 s from the top root canal surface using a single wave LED light curing unit (Radii-Cal; SDI, Bayswater, Australia) at 1200 mW/cm^2. After being stored in 100% relative humidity at 37 °C for seven days, the specimens were cut into 1.3-thick slices for each intraradicular third (cervical, middle, and apical), obtaining one slice per specimen for each intraradicular region

(Fig. 1– G). The intraradicular slice thicknesses were confirmed using a digital caliper (Mitutoyo, Aurora, IL, USA) (StrazziSahyon et al., 2018, 2019; Strazzi-Sahyon et al., 2020, 2021a).

Three distinct diameters of active tips were used according to the intraradicular thirds to perform the extrusion testing (push-out bond strength). The tips were coupled to a universal testing machine (DL3000, EMIC, Sao José dos Pinhais, PR, Brazil). The active tip diameter used for the cervical third was 1.90 mm, for the middle third was 1.40 mm, and for the apical third was 1.20 mm (Fig. 1– G). A compressive load was applied onto the center of the glass-fiber post to each root third in a top (coronal) to bottom (apical) direction, not touching the intraradicular dentin substrate, using the tips at a crosshead speed of 0.5 mm/min (StrazziSahyon et al., 2018, 2019; Strazzi-Sahyon et al., 2020, 2021a). The push-out bond strength of the glass-fiber posts to the intraradicular dentin was determined according to the following formula (Strazzi-Sahyon et al., 2018, 2019; Strazzi-Sahyon et al., 2020, 2021a; Banci et al., 2020):

$$POBS = F/A$$

where *POBD* is the push-out bond strength, expressed in MPa; F is the maximum force, expressed in N; and A is the adhesive interface area, expressed in mm^2, calculated using the following equation: (Strazzi-Sahyon et al., 2018, 2019; Strazzi-Sahyon et al., 2020, 2021a; Banci et al., 2020)

$$A = \pi\,(R_C + R_A)\,\sqrt{(R_C - R_A)^2 + h^2}$$

where π is 3.14; R_C and R_A are the largest (coronal) and smallest (apical) post radii, respectively; and h is the height of the third slice, measured with a digital caliper (Mitutoyo). (StrazziSahyon et al., 2018, 2019; Strazzi-Sahyon et al., 2020, 2021a; Banci et al., 2020)

Table 2
Distribution of the experimental groups.

Group Abbreviation	Group Treatment Details
Negative Control	Root canals non-treated with photosensitizer and photodynamic therapy. Root canals were irrigated with deionized water.
Positive Control	Root canals non-treated with photosensitizer and photodynamic therapy. Root canals were irrigated with deionized water and filled with intracanal calcium hydroxide medication.
MB_{50WA} + Ca $(OH)_2$	Root canals were filled with 50 mg/L of methylene blue photosensitizer without red laser activation and filled with intracanal calcium hydroxide medication.
MB_{100WA} + Ca $(OH)_2$	Root canals were filled with 100 mg/L of methylene blue photosensitizer without red laser activation and filled with intracanal calcium hydroxide medication.
MB_{50A} + $Ca(OH)_2$	Root canals were filled with 50 mg/L of methylene blue photosensitizer activated by red laser (λ 660 nm) and filled with intracanal calcium hydroxide medication.
MB_{100A} + Ca $(OH)_2$	Root canals were filled with 100 mg/L of methylene blue photosensitizer activated by red laser (λ 660 nm) and filled with intracanal calcium hydroxide medication.

2.5. Scanning electron microscopy (SEM)

After the bond strength test, root canal dentin samples were cleaved into two pieces to expose the bonding interface and analyzed by a stereomicroscope (Stemi SV11, Zeiss, NY, USA) at × 6 and × 66 magnification to analyze the fracture pattern (Strazzi-Sahyon et al., 2021b). The fracture patterns were divided and classified into 1) cohesive failure in dentin; 2) adhesive failure on dentin substrate; and 3) mixed failure. The most representative specimens of each group were sputter-coated with

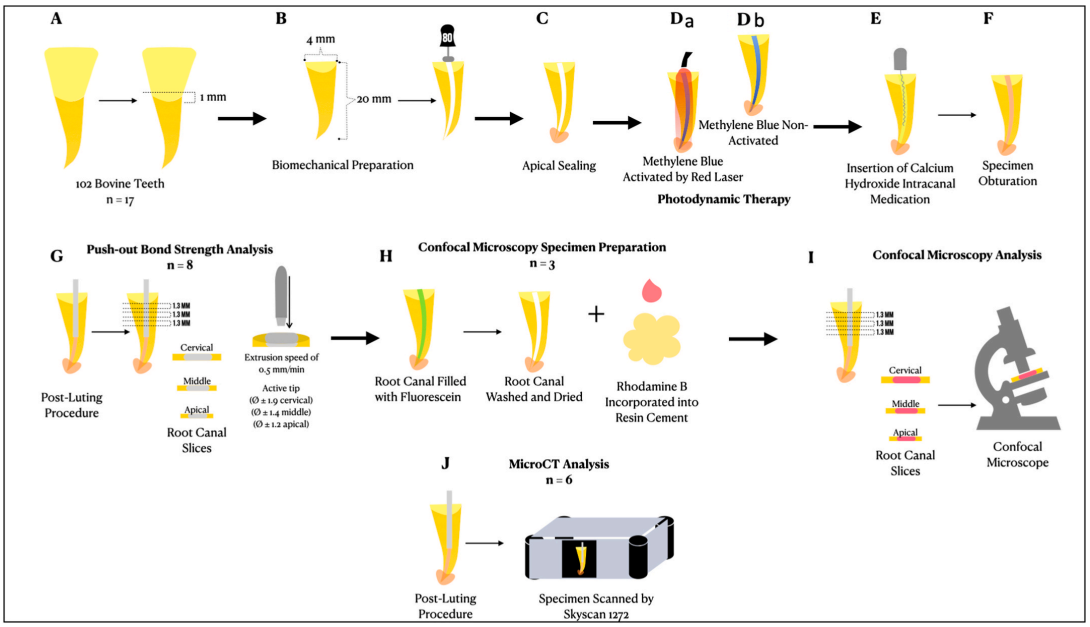


Fig. 1. - Preparation of the specimens. A, Removal of anatomical crowns of the bovine incisors. B, Length and diameter standardization of root canals. C, Sealing of the apical region of the root canals. D, Photodynamic therapy session with methylene blue photosensitizer with red Laser (λ = 660 nm). E, Insertion of calcium hydroxide medication into root canals. F, Obturation process of the specimens. G, Obtainment of 1.3-mm thick intraradicular slices for push-out bond strength test. H, Specimen preparation for the confocal microscopy analysis with fluorescein and rhodamine B dyes. I, Obtainment of 1.3-mm thick intraradicular slices for the confocal microscopy analysis. J, Adhesive interface integrity analysis (volume and quantification of voids) using microtomography equipment.

gold using a vacuum metalizing machine (Balzers SCD-050 Sputter Coater, Germany), and submitted to scanning electron microscopy (JSM5600LV, JEOL, Tokyo, Japan) to illustrate the fracture patterns. The micrographs were obtained and recorded under × 30 and × 300 magnification.

2.6. Adhesive interface sealing analysis

Eighteen root canals were arranged into six experimental groups (n = 3) as described above and filled with distilled water and fluorescein dye (0.1%) (FDA, Sigma Chemical Co, St. Louis, MO, USA) for 4 h for the dye to infiltrate into the dentinal tubules (Fig. 1-H).(Strazzi-Sahyon et al., 2022a) Then, to remove the fluorescein, 10 mL of deionized water was inserted into the intraradicular canals, and the root canals were dried with an air jet and sterile paper points. For adhesive interface sealing analysis, Rhodamine B (FDA, Sigma Chemical Co, St. Louis, MO, USA) was incorporated into the resin cement (16 μg/g) (Fig. 1-H), (Strazzi-Sahyon et al., 2022a) and the luting procedure was performed as described above for push-out bond strength analysis. Specimens were stored at 100% relative humidity and at 37 °C for 7 days and then sectioned using a diamond saw under water-cooling to obtain different thirds of the intraradicular dentin, as described above (Fig. 1-I). Slices were assessed from coronal to apex surfaces with a confocal laser scanning microscope (Leica TCS SP2; Leica Microsystems, Heidelberg, Germany), excited with an argon laser at 488 nm and an He–Ne laser at 453 nm (Fig. 1-I). Confocal micrographs were obtained and recorded in the fluorescent mode with oil-immersion objective lenses (× 40, numerical aperture 1.25) (Strazzi-Sahyon et al., 2022a). The confocal micrographs were evaluated using two previously calibrated examiners. The evaluation was performed using the double-blind method. In cases where there was disagreement between the two evaluators, the confocal micrographs were re-evaluated until a final consensus was reached.

The following criteria were evaluated.

a) Quality of the dentin/cement adhesive interface(Moda et al., 2018):

Score 0 - no cracks, clear, continuous adhesive interface;
Score 1 - partial presence of cracks, partially continuous adhesive interface, present in less than 50% of the interface;
Score 2 - presence of cracks with discontinuous interface, present in more than approximately 50% of the interface.

b) Formation of tags in intraradicular dentin(Moda et al., 2018):

Score 0 - not detectable;
Score 1- few tags visible;
Score 2- uniform formation of tags with few lateral branches;
Score 3- formation of long tags with many side branches.

c) Tag penetration depth(Moda et al., 2018):

Score 0 - no tags;
Score 1 - tags ≤ 3 μm on average;
Score 2 - tags = 3–8.9 μm on average;
Score 3 - tags ≥9 μm on average.

2.7. Adhesive interface integrity analysis

Adhesive interface integrity was evaluated in relation to the volume and quantification of voids on the adhesive interface. Six specimens from each experimental group (n = 6) were analyzed in high resolution microtomography (SkyScan 1272; Bruker, Kontich, Belgium) (Hoshino et al., 2022; Rivera-Peña et al., 2018). The microtomography was calibrated using the standard "phantom" function and operated under power conditions of 80 kilovolts and 125 milli-amps. The images were generated at medium resolution (13 μm/slice) and at 180°, the specimens were rotated at 0.4° angular steps, with an exposure time of 3000 ms; a 16.5 mm tube and a 1 mm thick aluminum filter were also used (Hoshino et al., 2022; Rivera-Peña et al., 2018).

The specimens were scanned following the restorative procedures. The data obtained in the scan were converted into DICOM files and later rendered into 3D models (SolidWorks Corp., MA, USA). Initially, the images were reconstructed in 3D in NRecon software (SkyScan, Kontich, Belgium) from the coronal to the apical portion of the roots. Then, using DataViewer software (SkyScan, Kontich, Belgium), the images were visualized and linearly analyzed in the coronal, sagittal, and transaxial axes, as well as the determination of a standard position for the measurement of volume and quantification of voids (Hoshino et al., 2022; Rivera-Peña et al., 2018).

Quantification of voids in the cement layer was performed using CTAnalyser software (SkyScan, Kontich, Belgium) in the transaxial position of the images (Hoshino et al., 2022). Initially, the area to be analyzed was established by selecting an average of 1013–1200 slices, followed by image segmentation to separate the desired object from other objects present in the image. Then, a freehand template (area of interest) was designed, delimiting only the cement layer. Subsequently, the images were binarized, and the quantification and volume of voids present in the root canal were calculated (Hoshino et al., 2022). Finally, CTVOX software (SkyScan, Kontich, Belgium) was used to reconstruct these images into three-dimensional models to assess the integrity of the interface by observing areas of the cement that were in discontinuity with the walls of the root canal (Hoshino et al., 2022).

2.8. Statistical analysis

Push-out bond strength, sealing, and integrity of adhesive interface data were submitted to normality (Shapiro-Wilk; Bioestat 2.0 Program) and homogeneity tests (Bartlett; Bioestat 2.0 Program). Push-out bond strength and adhesive interface integrity data were analyzed using two-way repeated measures Analysis of Variance (ANOVA; 5.0 Statview Program; Version 5.0.1). The Tukey protected least significant difference test ($\alpha = 0.05$) was also performed. Adhesive interface sealing was evaluated by the inter-examiner Kappa test and submitted to Kruskal-Wallis and Dunns tests ($\alpha = 0.05$) (SigmaPlot; Version 12.0).

3. Results

3.1. Push-out bond strength

The push-out bond strength values are listed in Table 3. There were no significant differences among the experimental groups for cervical and middle thirds ($P > 0.05$), however, for the apical third, the positive control and MB_{100WA} + $Ca(OH)_2$ groups presented lower values compared to the MB_{100A} + $Ca(OH)_2$ group ($P < 0.05$) (Table 3).

There were no significant differences among distinct intraradicular thirds for the negative control and MB_{100A} + $Ca(OH)_2$ groups ($P > 0.05$) (Table 3). However, for the positive control and MB_{100WA} + $Ca(OH)_2$ groups, the cervical and middle thirds promoted higher bond strength values compared to the apical third ($P < 0.05$). For the MB_{50WA} + $Ca(OH)_2$ and MB_{50A} + $Ca(OH)_2$ groups, only the cervical region promoted higher bond strength values compared to the apical region ($P < 0.05$) (Table 3).

When analyzing the intraradicular thirds for each group, a higher incidence of mixed-type failure was observed in all experimental groups (Fig. 2). Fig. 3 (A–L) presents the representative scanning electron micrographs of this fracture pattern, showing the presence of resin cement particles bonded to the intraradicular dentin surface.

3.2. Adhesive interface sealing

The adhesive interface sealing scores and representative confocal scanning laser micrographs are illustrated in Table 4 and Fig. 4,

Table 3
– Mean ± standard deviation values of push-out bond strength (MPa) of the intraradicular dentin as a function of the experimental groups and intraradicular thirds.

Groups / Thirds	Negative Control	Positive Control	$MB_{50WA} + Ca(OH)_2$	$MB_{100WA} + Ca(OH)_2$	$MB_{50A} + Ca(OH)_2$	$MB_{100A} + Ca(OH)_2$
Cervical	7.12 ± 2.85 Aa	5.21 ± 1.10 Aa	8.13 ± 3.04 Aa	5.33 ± 2.74 Aa	7.50 ± 3.21 Aa	6.74 ± 3.11 Aa
Middle	5.55 ± 2.54 Aa	4.52 ± 0.80 Aa	6.37 ± 3.07 ABa	5.04 ± 1.76 Aa	4.95 ± 2.14 ABa	5.92 ± 2.78 Aa
Apical	4.74 ± 2.36 Aab	2.81 ± 1.51 Bbc	4.40 ± 1.94 Babc	2.21 ± 0.88 Bc	3.65 ± 0.60 Babc	5.62 ± 2.00 Aa

Different letters, uppercase in column and lowercase in row, indicate statistically significant differences ($P < 0.05$).

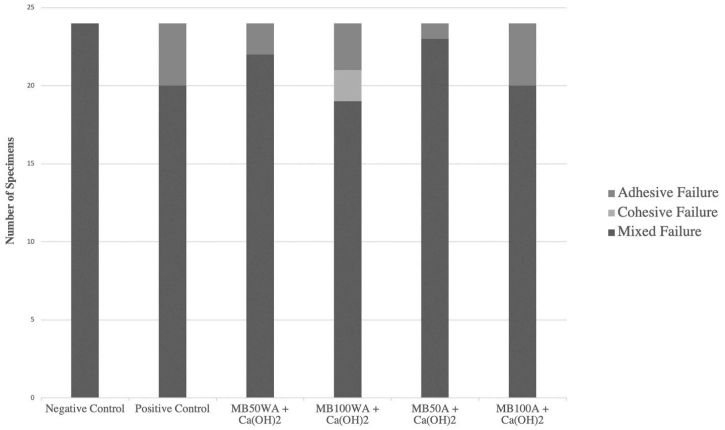


Fig. 2. - Fracture pattern incidence (samples thirds numbers) according to type of specimen failure.

respectively. A kappa inter-examiner test was carried out and values of 0.77, 0.81, and 0.78 were obtained for adhesive interface quality, tag formation in dentin, and tag penetration depth parameters, respectively. Regarding the adhesive interface quality, there were no significant differences among the groups ($P > 0.05$) (Table 4), with the score 0 being prevalent, as integrity and a well-organized adhesive interface were noted (Fig. 4). In relation to the tag formation in dentin parameter, there were no significant differences between the groups ($P > 0.05$), with a score of 1 prevailing for the negative control, $MB_{50WA} + Ca(OH)_2$, and $MB_{100WA} + Ca(OH)_2$ groups, and a score of 2 prevailing for the positive control, $MB_{50A} + Ca(OH)_2$, and $MB_{100A} + Ca(OH)_2$ experimental groups (Table 4). Regarding the tag penetration depth parameter, there were no significant differences among the experimental groups ($P > 0.05$) (Table 4), with a score of 1 prevailing for the negative control, positive control, $MB_{50A} + Ca(OH)_2$, and $MB_{100A} + Ca(OH)_2$ groups, and a score of 2 prevailing for the $MB_{50WA} + Ca(OH)_2$ and $MB_{100WA} + Ca(OH)_2$ groups (Table 4).

3.3. Adhesive interface integrity

The volume and quantification of voids on the adhesive interface, and representative microcomputed tomography images are illustrated in Table 5 and Fig. 5, respectively. Comparing the groups for the cervical third, the negative control group showed a lower volume of void values compared to the $MB_{100WA} + Ca(OH)_2$, $MB_{50A} + Ca(OH)_2$, and $MB_{100A} + Ca(OH)_2$ groups ($P < 0.05$) (Table 5). However, there were no significant differences in volume of void values among the experimental groups for middle and apical thirds ($P > 0.05$). Comparing the thirds, there were no differences in volume of void values for the negative control group ($P > 0.05$) (Table 5). However, for positive control, $MB_{50WA} + Ca(OH)_2$, $MB_{100WA} + Ca(OH)_2$, and $MB_{50A} + Ca(OH)_2$ groups, the cervical third promoted a higher volume of voids compared to the middle and apical regions ($P < 0.05$). For the $MB_{100A} + Ca(OH)_2$ group, there were significant differences among the thirds, as the cervical region promoted a higher volume of voids compared to the middle and apical thirds ($P < 0.05$), and the apical region showed higher values compared to the middle slice ($P < 0.05$) (Table 5).

Comparing the groups for the cervical third, the negative control, positive control, $MB_{50WA} + Ca(OH)_2$, and $MB_{50A} + Ca(OH)_2$ promoted lower void quantification values compared to the $MB_{100WA} + Ca(OH)_2$ group ($P < 0.05$) (Table 5). For the middle region, the negative control, positive control, and $MB_{50WA} + Ca(OH)_2$ groups promoted lower void quantification values compared to the $MB_{100WA} + Ca(OH)_2$ and $MB_{100A} + Ca(OH)_2$ groups ($P < 0.05$). For the apical intraradicular thirds, only the negative control and positive control groups showed lower void quantification values compared to the $MB_{100WA} + Ca(OH)_2$ and $MB_{100A} + Ca(OH)_2$ groups ($P < 0.05$). There were no statistical differences in void quantification values among distinct thirds for any experimental groups ($P > 0.05$), except for the negative control group in which the cervical and middle thirds promoted higher void quantification values compared to the apical region ($P < 0.05$) (Table 5).

4. Discussion

The administration of aPDT with methylene blue PS at different concentrations, activated or not by red laser, and associated with calcium hydroxide intracanal medication influenced the push-out bond strength and adhesive interface integrity analyses, thus rejecting the first null hypothesis of the study (Tables 3 and 5). Additionally, significant differences were observed among distinct depths of intraradicular dentin treated with aPDT associated with calcium hydroxide intracanal medication on adhesive resistance and volume of voids of the bonding interface, leading to rejection of the second null hypothesis (Tables 3 and 5).

According to Strazzi-Sahyon et at., aPDT is characterized by photon absorption by a specific PS from a precise wavelength irradiation,

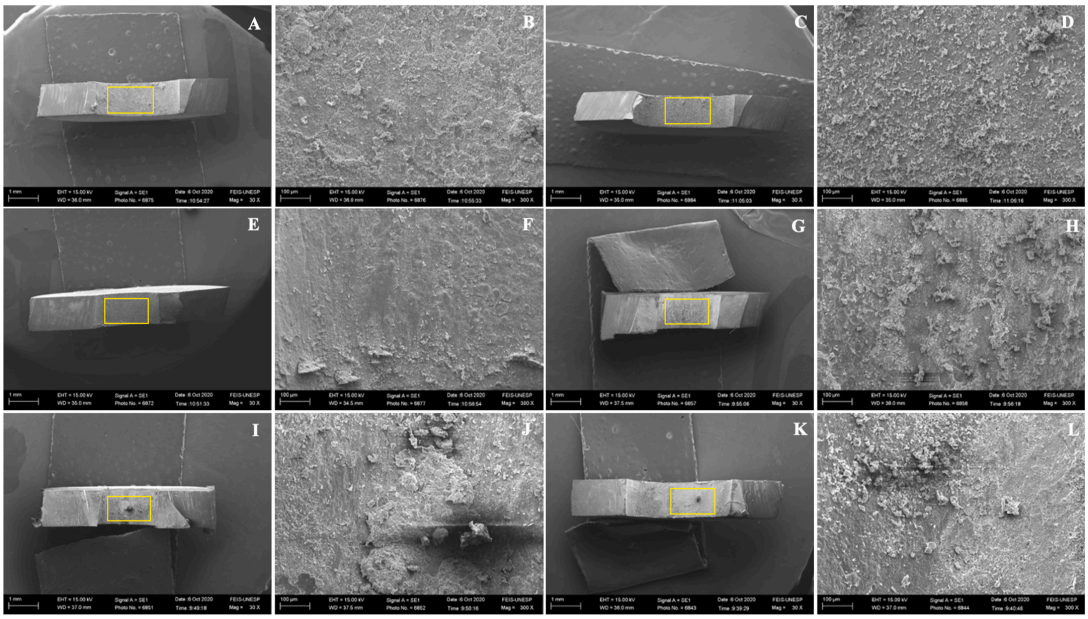


Fig. 3. - Scanning electron micrographs of representative failure types of the experimental groups under original magnification of × 30 and × 300. AB – mixed-type failure of root canals non-treated with methylene blue photosensitizer, photodynamic therapy, and calcium hydroxide medication (negative control group); CD – mixed-type failure of root canals filled with calcium hydroxide medication and non-treated with methylene blue photosensitizer and photodynamic therapy (positive control group); EF – mixed-type failure of root canals filled with calcium hydroxide medication and 50 mg/L of methylene blue photosensitizer and non-treated with photodynamic therapy ($MB_{50WA} + Ca(OH)_2$ group); GH – mixed-type failure of root canals filled with calcium hydroxide medication and 100 mg/L of methylene blue photosensitizer and non-treated with photodynamic therapy ($MB_{100WA} + Ca(OH)_2$ group); IJ – mixed-type failure of root canals filled with calcium hydroxide medication and 50 mg/L of methylene blue photosensitizer and treated with photodynamic therapy ($MB_{50A} + Ca(OH)_2$ group); KL – mixed-type failure of root canals filled with calcium hydroxide medication and 100 mg/L of methylene blue photosensitizer and treated with photodynamic therapy ($MB_{100A} + Ca(OH)_2$ group).

promoting electron stimulation. This energy is transmitted to the dental substrate, and in the presence of oxygen promotes free radical generation and highly reactive oxygen species, denominated singlet oxygen (Strazzi-Sahyon et al., 2022b). This photophysical-chemical reaction is characterized by an irreversible oxidation process, damaging the target cells and microorganism, and thus promoting microbial load reduction (Banci et al., 2022). However, there is a lack of in-depth information regarding the possible effects of this reactive oxygen on the adhesive interface properties, such as bonding resistance, and adhesive interface sealing and integrity, when assessing different concentrations of methylene blue PS, irradiated or not by red laser, associated with calcium hydroxide as intracanal medication along the intraradicular dentin.

Debonding of the resin cement/intraradicular dentin interface is one of the most common factors of intracanal restoration failure, due to the inefficient root canal substrate hybridization (Strazzi-Sahyon et al., 2021b). From this perspective, the push-out test is a satisfactory method to investigate the bond strength performance of materials determinate to the intraradicular dentin substrate by applying a specific force compatible with a clinical situation, promoting the restorative assembly displacement (Strazzi-Sahyon et al., 2021b). In the present study, despite the non-statistical difference, the administration of methylene blue PS at the higher concentration tended to present glass-fiber posts with lower bond strength values compared to the PS at the lower concentration, regardless of the irradiation by red laser or not (Table 2). Methylene blue PS is characterized as a hydrophilic compound, allowing water sorption, and thus jeopardizing the bond strength of the resin cement to the dentin substrate (Strazzi-Sahyon et al., 2020). According to a study by Wainwright et al., the water sorption intensity is directly proportional to the PS concentration (Wainwright et al., 1997), corroborating the push-out bond strength results and the failure patterns assessed, which demonstrated a higher incidence of mixed failures in the groups submitted to the lowest PS concentration, activated or not by red laser (Figs. 2 and 3).

The adhesive interface was also assessed by micromechanical interactions between the resin cement and intraradicular dentin substrate using confocal laser scanning microscopy. This methodology consists of the micropermeability evaluation and sealing capacity of the resin monomer infiltration into dentin substrate, qualitatively representing the adhesive interface, containing less artifact interference compared to scanning electron microscopy (Strazzi-Sahyon et al., 2022a). As shown by the scores of the confocal analysis and confocal micrographs, there were no differences in the adhesive interface parameters evaluated (Table 4) (Fig. 4). A study carried out by de Oliveira et al. compared different techniques of removing calcium hydroxide intracanal medication from the dentin walls of radicular canals, such as conventional irrigation, passive ultrasonic irrigation, and Easy Clean tools, and observed that none of these alternatives were able to satisfactorily remove all calcium hydroxide medication (de Oliveira et al., 2019). Thus, it can be speculated that the presence of remaining calcium hydroxide on intraradicular dentin walls may have influenced the adhesive interface parameters, hampering satisfactory resinous monomer infiltration in the dentinal tubules, and this could explain the lack of differences found in these parameters in the current study (Table 4). Furthermore, the adhesive interface data obtained may be influenced by the penetration depth measurement method adopted in the present investigation, as Eğemen and Belli claim that tubule penetration depth

Table 4
Scores of the adhesive interface sealing as a function of the experimental groups and intraradicular thirds. Different letters, uppercase in column and lowercase in row, indicate statistically significant differences for each adhesive interface parameter ($P < 0.05$).

Adhesive Interface Quality																														
Groups	Negative Control				Positive Control				$MB_{50WA} + Ca(OH)_2$				$MB_{100WA} + Ca(OH)_2$				$MB_{50A} + Ca(OH)_2$				$MB_{100A} + Ca(OH)_2$									
Scores	0	1	2	3	0	1	2	3	0	1	2	3	0	1	2	3	0	1	2	3	0	1	2	3						
Thirds																														
Cervical	2	1	–	–	Aa	2	1	–	–	Aa	3	–	–	–	Aa	3	–	–	–	Aa	3	–	–	–	Aa	–	2	1	–	Aa
Middle	2	1	–	–	Aa	1	2	–	–	Aa	3	–	–	–	Aa	3	–	–	–	Aa	3	–	–	–	Aa	–	2	1	–	Aa
Apical	3	–	–	–	Aa	2	1	–	–	Aa	1	2	–	–	Aa	2	1	–	–	Aa	3	–	–	–	Aa	2	1	–	–	Aa
Tags Formation in Dentin																														
Groups	**Negative Control**				**Positive Control**				**$MB_{50WA} + Ca(OH)_2$**				**$MB_{100WA} + Ca(OH)_2$**				**$MB_{50A} + Ca(OH)_2$**				**$MB_{100A} + Ca(OH)_2$**									
Scores	**0**	**1**	**2**	**3**	**0**	**1**	**2**	**3**	**0**	**1**	**2**	**3**	**0**	**1**	**2**	**3**	**0**	**1**	**2**	**3**	**0**	**1**	**2**	**3**						
Thirds																														
Cervical	–	1	2	–	Aa	–	2	1	–	Aa	–	1	2	–	Aa	–	1	2	–	Aa	–	1	2	–	Aa	–	1	2	–	Aa
Middle	–	2	1	–	Aa	–	–	3	–	Aa	–	1	2	–	Aa	–	2	1	–	Aa	–	1	2	–	Aa	–	1	2	–	Aa
Apical	–	3	–	–	Aa	–	1	2	–	Aa	–	3	–	–	Aa	–	2	1	–	Aa	–	2	1	–	Aa	–	1	2	–	Aa
Tags Penetration Depth																														
Groups	**Negative Control**				**Positive Control**				**$MB_{50WA} + Ca(OH)_2$**				**$MB_{100WA} + Ca(OH)_2$**				**$MB_{50A} + Ca(OH)_2$**				**$MB_{100A} + Ca(OH)_2$**									
Scores	**0**	**1**	**2**	**3**	**0**	**1**	**2**	**3**	**0**	**1**	**2**	**3**	**0**	**1**	**2**	**3**	**0**	**1**	**2**	**3**	**0**	**1**	**2**	**3**						
Thirds																														
Cervical	–	2	–	1	Aa	–	1	2	–	Aa	–	2	1	–	Aa	–	1	2	–	Aa	–	3	–	–	Aa	–	3	–	–	Aa
Middle	–	1	2	–	Aa	–	3	–	–	Aa	–	1	2	–	Aa	–	1	2	–	Aa	–	3	–	–	Aa	–	3	–	–	Aa
Apical	–	2	1	–	Aa	–	1	1	1	Aa	–	1	2	–	Aa	–	1	2	–	Aa	–	3	–	–	Aa	–	3	–	–	Aa

measurement techniques may present varying performances for the intraradicular thirds (Eğemen and Belli, 2022). Therefore, tubule penetration depth data measured by distinct methods must be interpreted carefully.

However, despite the non-statistical difference, the experimental group of methylene blue PS at the higher concentration, activated by red laser promoted a higher incidence of cracks present on the dentin/cement adhesive interface (Table 4) (Fig. 4). The singlet oxygen formation resulting from an irreversible oxidation process may have interfered in the sealing capacity and quality of the dentin/cement adhesive interface (Table 4) (Fig. 4). This performance corroborates the tendency of the PS to present lower bond strength values at a higher concentration (Table 3).

Common methodologies applied to evaluate void formation at the glass-fiber post/resin cement/dental interface are characterized by destructive and 2D tests, which are vulnerable to false-positive data, without a volumetric scale precision (Hoshino et al., 2022). 3D scanning of luted root canals with intraradicular retainers by microcomputed tomography technology promotes a non-destructive analysis of the external and internal structures of the specimens, allowing their visualization and reconstruction in 3D to detect and measure the presence of gaps and voids in the bonding interface (Hoshino et al., 2022). Furthermore, evaluation of the adhesive interface integrity can be related to push-out analysis(Hoshino et al., 2022), which increases understanding about the influence of aPDT on the adhesion process along the intraradicular dentin.

It can be noted by the microcomputed tomography images that the adhesive interface integrity showed a higher volume and quantification of voids for the experimental groups submitted to methylene blue PS at the higher concentration, activated or not by red laser (Table 5) (Fig. 5). The quantity of singlet oxygen formation is directly equivalent to the PS concentration used(Strazzi-Sahyon et al., 2021b), and its presence may affect the adhesive interface of resin-based materials due to the competition of free radicals necessary for the methacrylate polymerization process (Ramos et al., 2018). Furthermore, it can be speculated that the released oxygen trapped inside the dentinal tubules from the aPDT process may act as a mechanical barrier, hampering the more intimate contact between the resin cement and the intraradicular dentine wall (Ramos et al., 2018). This fact could corroborate the incidence of a higher adhesive-type failure for the experimental group of methylene blue PS at the higher concentration activated by red laser (Fig. 2), in addition to the greater volume and quantification of voids at the luting interface (Table 5) (Fig. 5).

Comparing distinct regions of intraradicular dentin, there was a tendency for the apical third to exhibit lower bond strength, and volume and quantification of voids than the cervical region (Tables 3 and 5) (Fig. 5). These results can be explained by some factors, such as the anatomical configurations of the root canals, presence of apical sclerosis, difficulty accessing and cleaning the apical third, and reduction in light diffusion capacity at this depth, promoting a lower degree of conversion of the resin cement (StrazziSahyon et al., 2019; Strazzi-Sahyon et al., 2020, 2021a, 2021b). All these conditions can result in inhomogeneous distribution of the luting agent on the apical third, resulting in lower bond strength values (Table 3).

Furthermore, methylene blue is characterized as a cationic compost that allows binding to anionic compounds, such as the phosphate ions incorporated into hydroxyapatite crystals, thereby reacting with, and influencing the phosphate/calcium ratio (StrazziSahyon et al., 2018; Strazzi-Sahyon et al., 2020, 2021a, 2021b). This reaction forms precipitates, accumulating in higher concentrations in the apical third due to gravity, acting as a physical barrier and satisfactorily avoiding the resin cement/dentin surface interaction (Strazzi-Sahyon et al., 2020). This photosensitizer/phosphate interaction could also justify the lower bond strength values in the apical region (Table 3).

The cervical third exhibits the biggest diameter when compared with the middle and apical intraradicular regions, presenting a higher volume

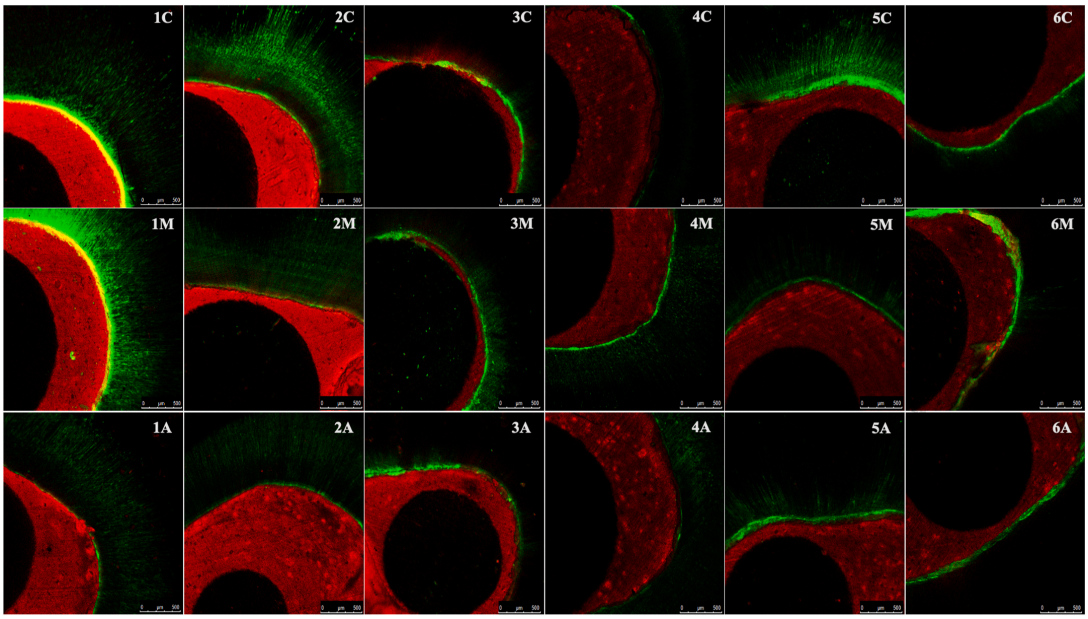


Fig. 4. - Confocal laser scanning micrographs of adhesive interface sealing according to the experimental groups and intraradicular thirds under original magnification of × 5.1C, 1M, 1A - Cervical, middle, and apical slices of intraradicular dentin irrigated with deionized water solution (negative control group). 2C, 2M, 2A - Cervical, middle, and apical slices of intraradicular dentin after irrigated with deionized water and filled with calcium hydroxide intracanal medication (positive control group). 3C, 3M, 3A - Cervical, middle, and apical slices of intraradicular dentin after treatment with calcium hydroxide intracanal medication +50 mg/L of methylene blue without activation (MB_{50WA} + $Ca[OH]_2$). 4C, 4M, 4A - Cervical, middle, and apical slices of intraradicular dentin after treatment with calcium hydroxide intracanal medication +100 mg/L of methylene blue without activation (MB_{100WA} + $Ca[OH]_2$). 5C, 5M, 5A - Cervical, middle, and apical slices of intraradicular dentin after treatment with calcium hydroxide intracanal medication +50 mg/L of methylene blue activated by red laser (λ 660 nm) (MB_{50A} + $Ca[OH]_2$). 6C, 6M, 6A - Cervical, middle, and apical slices of intraradicular dentin after treatment with calcium hydroxide intracanal medication +100 mg/L of methylene blue activated by red laser (λ 660 nm) (MB_{100A} + $Ca[OH]_2$).

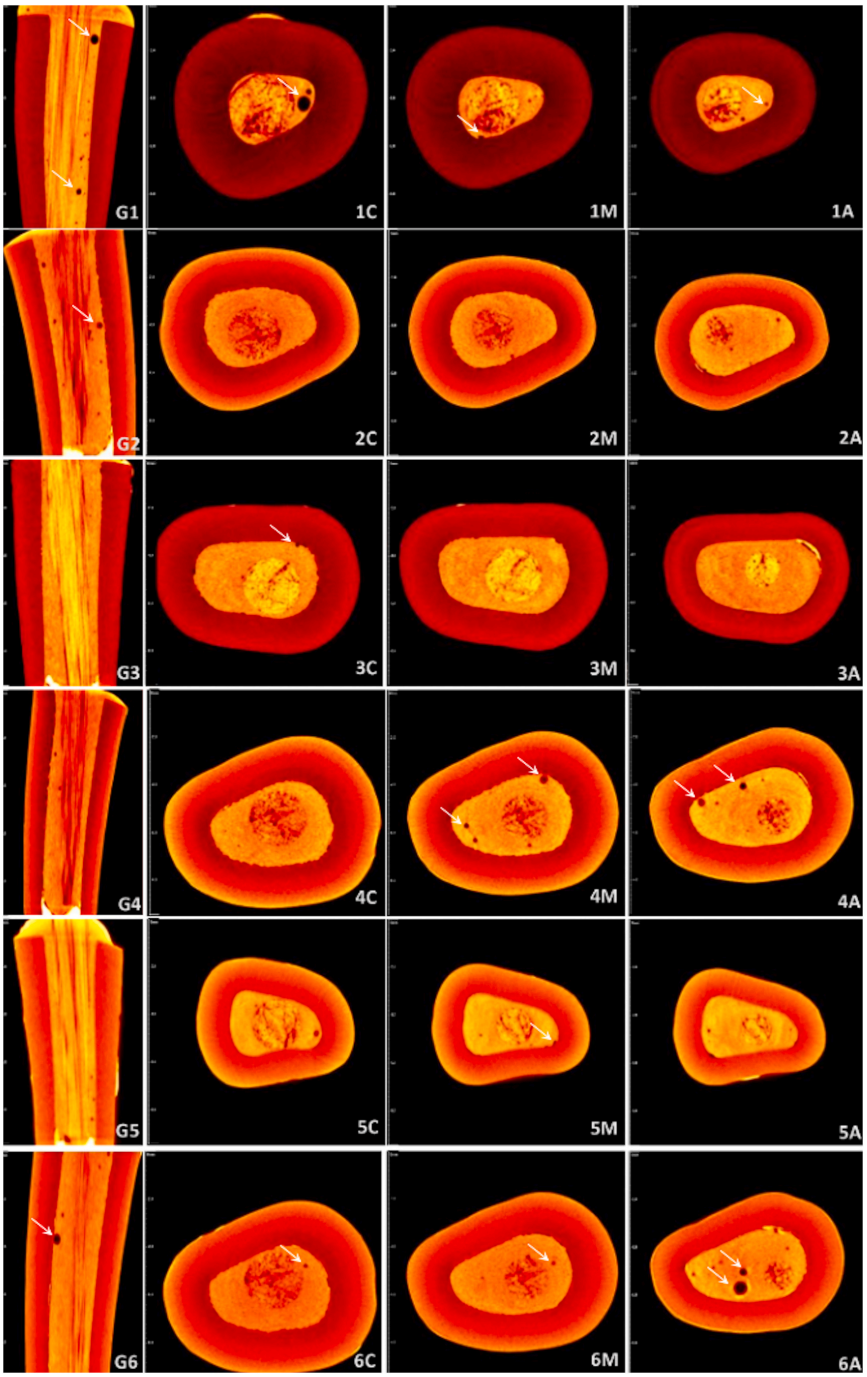
Table 5
– Mean ± standard deviation values of volume (mm^3) and quantification of void formation on resin cement as a function of the experimental groups and intraradicular thirds.

Groups / Thirds	Negative Control	Positive Control	MB_{50WA} + $Ca(OH)_2$	MB_{100WA} + $Ca(OH)_2$	MB_{50A} + $Ca(OH)_2$	MB_{100A} + $Ca(OH)_2$
Volume						
Cervical	2.04 ± 0.95 Ab	4.01 ± 2.40 Aab	4.01 ± 1.26 Aab	4.80 ± 0.86 Aa	4.86 ± 0.93 Aa	6.08 ± 1.02 Aa
Middle	1.50 ± 0.35 Aa	1.50 ± 0.90 Ba	1.38 ± 0.37 Ba	1.68 ± 0.37 Ba	2.26 ± 0.98 Ba	2.02 ± 0.34 Ca
Apical	2.04 ± 0.95 Aa	1.94 ± 1.24 Ba	1.91 ± 1.43 Ba	2.12 ± 0.44 Ba	2.43 ± 0.47 Ba	3.04 ± 0.51 Ba
Quantification						
Cervical	9.56 ± 0.76 Ac	9.85 ± 0.72 Ac	12.55 ± 1.24 Abc	15.99 ± 2.76 Aa	12.50 ± 0.79 Abc	15.28 ± 2.99 Aab
Middle	9.40 ± 0.36 Ac	9.74 ± 0.50 Ac	12.21 ± 0.36 Abc	15.21 ± 2.96 Aa	12.68 ± 1.27 Aab	15.26 ± 2.29 Aa
Apical	7.67 ± 0.39 Bc	10.04 ± 0.68 Abc	12.44 ± 0.52 Aab	15.50 ± 3.36 Aa	12.40 ± 1.20 Aab	14.40 ± 2.59 Aa

Different letters, uppercase in column and lowercase in row, indicate statistically significant differences for each parameter evaluated ($P < 0.05$).

of resin cement, which makes it more susceptible to void formation, proven by the adhesive interface integrity analysis and microcomputed tomography images in the present study (Table 5) (Fig. 5). The highest volume and quantification of voids in the cervical region can be justified by the amount of resin cement and the shrinkage stress performed by the photoactivation process (D'Arcangelo et al., 2007). According to D'Arcangelo et al., polymerization stress is a crucial factor for the longevity of restorations, and a thicker cement layer would generate higher microporosity and polymerization shrinkage (D'Arcangelo et al., 2007). Another reason that can be mentioned is that the cervical region was subjected to a higher volume of methylene blue compound, increasing its susceptibility to the PS effects and action. All these factors may result in higher void formation, affecting the adhesive interface integrity, as proven by the microcomputed tomography images (Table 5) (Fig. 5).

Strazzi-Sahyon et al., in previous studies, investigated the influence of one and two sessions of aPDT combined with 50 mg/L and 100 mg/L of methylene blue PS, associated or not with laser radiation, on the push-out bond strength of the glass-fiber post to the intraradicular dentin, demonstrating substantially lower bond strength values than those found in the present study (Table 3). (StrazziSahyon et al., 2018; Strazzi-Sahyon et al., 2020, 2021a) Despite methodological similarities, this difference may be related by the fact that these previous



(caption on next page)

Fig. 5. - Microcomputed tomography images of adhesive interface integrity according to the experimental groups and intraradicular thirds. G1, 1C, 1M, 1A – Transaxial, cervical, middle, and apical slices of intraradicular dentin irrigated with deionized water solution (negative control group). G2, 2C, 2M, 2A – Transaxial, cervical, middle, and apical slices of intraradicular dentin after irrigated with deionized water and filled with calcium hydroxide intracanal medication (positive control group). G3, 3C, 3M, 3A – Transaxial, cervical, middle, and apical slices of intraradicular dentin after treatment with calcium hydroxide intracanal medication +50 mg/L of methylene blue without activation (MB_{50WA} + $Ca[OH]_2$). G4, 4C, 4M, 4A – Transaxial, cervical, middle and apical slices of intraradicular dentin after treatment with calcium hydroxide intracanal medication +100 mg/L of methylene blue without activation (MB_{100WA} + $Ca[OH]_2$). G5, 5C, 5M, 5A - Transaxial, cervical, middle, and apical slices of intraradicular dentin after treatment with calcium hydroxide intracanal medication +50 mg/L of methylene blue activated by red laser (λ 660 nm) (MB_{50A} + $Ca[OH]_2$). G6, 6C, 6M, 6A – Transaxial, cervical, middle, and apical slices of intraradicular dentin after treatment with calcium hydroxide intracanal medication +100 mg/L of methylene blue activated by red laser (λ 660 nm) (MB_{100A} + $Ca[OH]_2$). White arrows indicate the presence of voids on the luting interface.

investigations did not evaluate the association of calcium hydroxide as an intracanal medication (StrazziSahyon et al., 2018; Strazzi-Sahyon et al., 2020, 2021a). According to Singh et al., calcium hydroxide-based medication leads to an increase in pH in the environment that may favor the photoreaction process, since highly reactive oxygen formation is intensified in an alkaline medium, which could justify the bond strength values of the present study (Singh et al., 2014).

As mentioned previously, investigations regarding the influence of methylene blue PS at distinct concentrations, activated or not by red laser, concomitantly with the action of calcium hydroxide as intracanal medication along the intraradicular dentin are scarce in the literature, which makes it difficult to correlate the present results with previously published data. Only one study conducted by Strazzi-Sahyon et al. presented similarities in the methodology and factors evaluated, enabling this correlation (Strazzi-Sahyon et al., 2021b). It can be noted that the mentioned study showed slightly higher push-out bond strength values than the present study (Table 3). (Strazzi-Sahyon et al., 2021b) A possible explanation for this slight difference is that the aforementioned study evaluated two sessions of aPDT, after biomechanical preparation and before the glass-fiber post luting procedure, while the present study assessed only one session (Strazzi-Sahyon et al., 2021b). A second therapy session could have potentialized the PS action on the Ca–P ratio, influencing the mineral content of dentin substrate, inducing higher microporosity generation, and promoting higher interaction between the root canal substrate and resin cement, thus favoring the micromechanical retentions (Strazzi-Sahyon et al., 2021a).

On the other hand, distinct concentrations of methylene blue PS, associated or not with aPDT, may not always promote satisfactory results in all analyses. In general, the use of laser-irradiated 50 mg/L methylene blue PS associated with calcium hydroxide as intracanal medication resulted in closer values to the negative control group regarding the adhesive interface properties than laser-irradiated PS at 100 mg/L (Tables 3–5) (Figs. 2–5).This enables us to assume that using aPDT with methylene blue sensitizer at 50 mg/L associated with calcium hydroxide as intracanal medication is a viable choice as it does not alter the adhesive interface properties of glass-fiber posts to intraradicular dentin.

The use of bovine root canals in this *in vitro* study is an appropriate and acceptable substitute to human teeth for push-out bond strength analysis (Soares et al., 2016). Silva et al. state that bovine teeth exert no influence on the bond strength of intracanal restorations (Silva et al., 2019). The authors claim that in this experimental model, the load is applied only to the intracanal retainer and resin cement that completely filled the root canals, providing better control over the type of failure (Silva et al., 2019). Furthermore, the choice of employing this experimental model is based on a study previously evaluated by Camargo et al. that investigated the diffusion rate of $Ca(OH)_2$ medication in both human and bovine substrate and found no significant differences between them (Camargo et al., 2006).

The present *in vitro* study presents some limitations that should be pointed out, such as the non-homogeneity of dental substrate in relation to the quantity and size of dentinal tubules, non-standardization of the mineral concentrations, difficulty in performing procedures in regions of limited access and visibility, and the use of only one type of $Ca(OH)_2$ paste. The applicability of laboratory results to clinical circumstances must be correlated carefully, as this *in vitro* research precludes accurately simulating oral cavity conditions, such as the interference of saliva, enzymes, temperature, and microorganisms. Thus, further in-depth longitudinal and clinical investigations should be performed to enrich discussions regarding the influence of aPDT on collagen fibers, permeability, and other physical-mechanical properties under aging conditions, aimed at increasing the use of this therapy in Dentistry.

5. Conclusion

Based on the methodology and findings of this *in vitro* study, it is possible to conclude that.

1. Antimicrobial photodynamic therapy with methylene blue photosensitizer, associated with calcium hydroxide as intracanal medication influenced the bond strength and adhesive interface integrity of glass-fiber posts to intraradicular dentin.
2. Intraradicular depth also had an influence on push-out bond strength and adhesive interface integrity.
3. Methylene blue at 50 mg/L associated with calcium hydroxide as intracanal medication is a suitable photosensitizer and concentration to be applied for intracanal disinfection subsequent to the biomechanical procedure, as, in general, it yields satisfactory bond strength, sealing, and integrity of the adhesive interface at any intraradicular depth.

CRediT authorship contribution statement

Henrico Badaoui Strazzi-Sahyon: Writing – review & editing, Writing – original draft, Visualization, Validation, Supervision, Software, Resources, Methodology, Investigation, Formal analysis, Data curation, Conceptualization. **Henrique Augusto Banci:** Writing – review & editing, Writing – original draft, Visualization, Validation, Software, Resources, Methodology, Investigation, Funding acquisition, Formal analysis, Data curation, Conceptualization. **Fernanda Santos de Melo:** Methodology, Investigation, Funding acquisition. **Lucas Silva Soares:** Methodology, Investigation, Funding acquisition. **Rubens Spin-Neto:** Writing – review & editing, Validation, Methodology, Conceptualization. **Marco Antonio Hungaro Duarte:** Writing – review & editing, Validation, Methodology, Conceptualization. **Luciano Tavares Angelo Cintra:** Writing – review & editing, Validation, Methodology, Conceptualization. **Paulo Henrique dos Santos:** Writing – review & editing, Validation, Methodology, Formal analysis, Conceptualization. **Gustavo Sivieri-Araujo:** Writing – review & editing, Validation, Project administration, Methodology, Funding acquisition, Conceptualization.

Declaration of competing interest

The authors declare that they have no known competing financial interests or personal relationships that could have appeared to influence the work reported in this paper.

Data availability

Data will be made available on request.

Acknowledgments

This study was supported by grants #19/24328-1 and #19/16171-5, São Paulo Research Foundation (FAPESP), Brazil; Coordenação de Aperfeiçoamento de Pessoal de Nível Superior – Brazil (CAPES) – Finance Code 001; and grant #019/6028 Institutional Scientific Initiation Scholarship Program (PIBIC/Prope), Brazil. The authors thank Elton José de Souza from the Physics and Chemistry Department, São Paulo State University (UNESP), School of Engineering, Ilha Solteira, SP, Brazil, for contributing to the SEM analyses, and Marcia Sirlene Zardin Graeff from University of São Paulo (USP), Bauru School of Dentistry, Bauru, SP, Brazil, for contributing to the confocal laser scanning microscopy analysis.

References

Balto, H., Bukhary, S., Al-Omran, O., BaHammam, A., Al-Mutairi, B., 2020. Combined effect of a mixture of silver nanoparticles and calcium hydroxide against enterococcus faecalis biofilm. J. Endod. 46 (11), 1689–1694.

Banci, H.A., Strazzi-Sahyon, H.B., Duarte, M., Cintra, L., Gomes-Filho, J.E., Chalub, L.O., Berton, S.A., de Oliveira, V., Dos Santos, P.H., Sivieri-Araujo, G., 2020. Influence of photodynamic therapy on bond strength and adhesive interface morphology of MTA based root canal sealer to different thirds of intraradicular dentin. Photodiagnosis Photodyn. Ther. 32, 102031.

Banci, H.A., Strazzi-Sahyon, H.B., Bento, V.A.A., Sayeg, J.M.C., Bachega, M.O., Pellizzer, E.P., Sivieri-Araujo, G., 2022. Influence of antimicrobial photodynamic therapy on the bond strength of endodontic sealers to intraradicular dentin: a systematic review and meta-analysis. Photodiagnosis Photodyn. Ther. 31, 103270.

Best, S., Ammons, C.L., Karunanayake, G.A., Saemundsson, S.R., Tawil, P.Z., 2021. Outcome assessment of teeth with necrotic pulps and apical periodontitis treated with long-term calcium hydroxide. J. Endod. 47 (1), 11–18.

Camargo, C.H.R., Bernardineli, N., Valera, M.C., de Carvalho, C.A.T., de Oliveira, L.D., Menezes, M.M., Afonso, S.E., Mancini, M.N., 2006. Vehicle influence on calcium hydroxide pastes diffusion in human and bovine teeth. Dent. Traumatol. 22 (6), 302–306.

Chalub, L.O., Nunes, G.P., Ferrisse, T.M., Strazzi-Sahyon, H.B., Dos Santos, P.H., Gomes-Filho, J.E., Cintra, L.T.A., Sivieri-Araujo, G., 2022. Postoperative pain in root canal treatment with ultrasonic versus conventional irrigation: a systematic review and meta-analysis of randomized controlled trials. Clin. Oral Invest. 26 (4), 3343–3356.

Corazza, B.J., Martinho, F.C., Khoury, R.D., Toia, C.C., Orozco, E.I., Prado, R.F., Machado, F.P., Valera, M.C., 2020. Clinical influence of calcium hydroxide and n-acetylcysteine on the levels of resolvins E1 and D2 in apical periodontitis. Int. Endod. J. 54 (1), 61–73.

Davies, D., 2003. Understanding biofilm resistance to antibacterial agents. Nat. Rev. Drug Discov. 2 (2), 114–122.

de Oliveira, R.L., Guerisoli, D.M.Z., Duque, J.A., Alcalde, M.P., Onoda, H.K., Domingues, F.H.F., Vivan, R.R., Duarte, M.A.H., 2019. Computed microtomography evaluation of calcium hydroxide-based root canal dressing removal from oval root canals by different methods of irrigation. Microsc. Res. Tech. 82 (3), 232–237.

D'Arcangelo, C., Cinelli, M., De Angelis, F., D'Amario, M., 2007. The effect of resin cement film thickness on the pullout strength of a fiber-reinforced post system. J. Prosthet. Dent 98 (3), 193–198.

Eğemen, A., Belli, S., 2022. The effect of primary root canal treatment on dentinal tubule penetration of calcium silicate-based sealers during endodontic retreatment. J. Endod. 48 (9), 1169–1177.

Evans, M., Davies, J.K., Sundqvist, G., Figdor, D., 2002. Mechanisms involved in the resistance of enterococcus faecalis to calcium hydroxide. Int. Endod. J. 35 (3), 221–228.

Ferrisse, T.M., Dias, L.M., de Oliveira, A.B., Jordão, C.C., Mima, EG. de O., Pavarina, A. C., 2022. Efficacy of curcumin-mediated antibacterial photodynamic therapy for oral antisepsis: a systematic review and network meta-analysis of randomized clinical trials. Photodiagnosis Photodyn. Ther. 39, 102876.

Garcez, A.S., Ribeiro, M.S., Tegos, G.P., Núñez, S.C., Jorge, A.O.C., Hamblin, M.R., 2007. Antimicrobial photodynamic therapy combined with conventional endodontic treatment to eliminate root canal biofilm infection. Laser Surg. Med. 39 (1), 59–66.

Govare, N., Contrepois, M., 2020. Endocrowns: a systematic review. J. Prosthet. Dent 123 (3), 411–418.

Hidalgo, L.R., da Silva, L.A.B., Nelson-Filho, P., da Silva, R.A.B., de Carvalho, F.K., Lucisano, M.P., Novaes Jr., A.B., 2016. Comparison between one-session root canal treatment with aPDT and two-session treatment with calcium hydroxide-based antibacterial dressing, in dog's teeth with apical periodontitis. Laser Med. Sci. 31 (7), 1481–1491.

Hoshino, I.A.E., dos Santos, P.H., Briso, A.L.F., Sundfeld, R.H., Yamaguchi, S., Rocha, E. P., Anchieta, R.B., 2022. Biomechanical performance of three fiberglass post cementation techniques: imaging, in vitro, and in silico analysis. J. Prosthodontic Res.

Josic, U., Mazzitelli, C., Maravic, T., Fidler, A., Breschi, L., Mazzoni, A., 2022. Biofilm in endodontics: in vitro cultivation possibilities, sonic-, ultrasonic- and laser-assisted removal techniques and evaluation of the cleaning efficacy. Polymers 14 (7), 1334.

Jurić, I.B., Plečko, V., Panduric, D.G., Anić, I., 2014. The antimicrobial effectiveness of photodynamic therapy used as an addition to the conventional endodontic re-treatment: a clinical study. Photodiagnosis Photodyn. Ther. 11 (4), 549–555.

Keskin, G., Çiloğlu, M., 2021. Efficacy of antimicrobial photodynamic therapy and ER, CR:YSGG laser-activated irrigation on dentinal tubule penetration of MTA-based root canal sealer: a confocal microscopy study. Photodiagnosis Photodyn. Ther. 36, 102584.

Lin, C.L., Chang, Y.H., Chang, C.Y., Pai, C.A., Huang, S.F., 2010. Finite element and Weibull analyses to estimate failure risks in the ceramic endocrown and classical crown for endodontically treated maxillary premolar. Eur. J. Oral Sci. 118 (1), 87–93.

Martinho, F.C., Corazza, B.J.M., Khoury, R.D., Orozco, E.I.F., Toia, C.C., Machado, F.P., Valera, M.C., 2023. Impact of N-acetylcysteine (NAC) and calcium hydroxide intracanal medications in primary endodontic infection: a randomized clinical trial. Clin. Oral Invest. 27 (2), 817–826.

Meire, M.A., Coenye, T., Nelis, H.J., De Moor, R.J.G., 2012. Evaluation of Nd:YAG and Er:YAG irradiation, antibacterial photodynamic therapy and sodium hypochlorite treatment on Enterococcus faecalis biofilms. Int. Endod. J. 45 (5), 482–491.

Moda, M.D., Fagundes, T.C., Briso, A.L.F., dos Santos, P.H., 2018. Analysis of the bond interface between self-adhesive resin cement to eroded dentin in vitro. PLoS One 13 (11), 0208024.

Nunes, L.P., Nunes, G.P., Ferrisse, T.M., Strazzi-Sahyon, H.B., Cintra, L.T.Â., dos Santos, P.H., Sivieri-Araujo, G., 2022. Antimicrobial Photodynamic Therapy in Endodontic Reintervention: A Systematic Review and Meta-Analysis *Photodiagnosis and Photodynamic Therapy*, 39, 103014.

Ramos, A.T.P.R., Belizário, L.G., Jordão-Basso, K.C.F., Shinohara, A.L., Kuga, M.C., 2018. Effects of photodynamic therapy on the adhesive interface using two fiber posts cementation systems. Photodiagnosis Photodyn. Ther. 24, 136–141.

Rivera-Peña, M.E., Duarte, M.A.H., Alcalde, M.P., DE Andrade, F.B., Vivan, R.R., 2018. A novel ultrasonic tip for removal of filling material in flattened/oval-shaped root canals: a microCT study. Braz. Oral Res. 13 (32), 88.

Rodrigues, C.T., de Andrade, F.B., de Vasconcelos, L.R., Midena, R.Z., Pereira, T.C., Kuga, M.C., Duarte, M.A.H., Bernardineli, N., 2018. Antibacterial properties of silver nanoparticles as a root canal irrigant against enterococcus faecalis biofilm and infected dentinal tubules. Int. Endod. J. 51 (8), 901–911.

Schilke, R., Lisson, J.A., Bauß, O., Geurtsen, W., 2000. Comparison of the number and diameter of dentinal tubules in human and bovine dentine by scanning electron microscopic investigation. Arch. Oral Biol. 45 (5), 355–361.

Silva, E.J.N.L., Carvalho, N.K., Prado, M.C., Senna, P.M., Souza, E.M., De-Deus, G., 2019. Bovine teeth can reliably substitute human dentine in an intra-tooth push-out bond strength model? Int. Endod. J. 52 (7), 1063–1069.

Singh, S., Nagpal, R., Manuja, N., Tyagi, S.P., 2014. Photodynamic therapy: an adjunct to conventional root canal disinfection strategies. Aust. Endod. J. 41 (2), 54–71.

Soares, F.Z.M., Follak, A., da Rosa, L.S., Montagner, A.F., Lenzi, T.L., Rocha, R.O., 2016. Bovine tooth is a substitute for human tooth on bond strength studies: a systematic review and meta-analysis of in vitro studies. Dent. Mater. 32 (11), 1385–1393.

Strazzi-Sahyon, H.B., de Oliveira, M.S., da Silva, P.P., Banci, H.A., de Melo, F.S., Martinez, C.M.T., Cintra, L.T.A., Gomes-Filho, J.E., Dezan-Júnior, E., Dos Santos, P. H., Sivieri-Araujo, G., 2020. Does photodynamic therapy with methylene blue affect the mechanical properties and bond strength of glass-fiber posts in different thirds of intraradicular dentin? Photodiagnosis Photodyn. Ther. 30, 101673.

Strazzi-Sahyon, H.B., da Silva, P.P., Nakao, J.M., da Silva, P.Z., Nunes, L.P., Seron, M.A., Cintra, L.T.A., Dos Santos, P.H., Sivieri-Araujo, G., 2021a. Influence of two photodynamic therapy sessions and different photosensitizers on the bond strength of glass-fiber posts in different regions of intraradicular dentin. Photodiagnosis Photodyn. Ther. 33, 102193.

Strazzi-Sahyon, H.B., Oliveira, A.K.L., Carvalho, A.P., Figueiredo, R.B., Cintra, L.T.A., Gomes-Filho, J.E., Dos Santos, P.H., Sivieri-Araujo, G., 2021b. Influence of photodynamic therapy and intracanal medication on Martens hardness, elastic modulus and bond strength of glass-fiber posts to endodontically treated root dentin. Photodiagnosis Photodyn. Ther. 36, 102571.

Strazzi-Sahyon, H.B., da Silva, L.M.A.V., Briso, A.L.F., dos Santos, P.H., 2022a. In vitro study on how antioxidant solutions affect enamel surface characteristics and bonding interface of ceramic laminate veneers luting after dental bleaching. J. Mech. Behav. Biomed. Mater. 133, 105322.

Strazzi-Sahyon, H.B., Cintra, L.T.A., Nakao, J.M., Takamiya, A.S., Queiroz, I.O.A., Dos Santos, P.H., Oliveira, S.H.P., Sivieri-Araujo, G., 2022b. Cytotoxicity of root canal irrigating solutions and photodynamic therapy using curcumin photosensitizer. Photodiagnosis Photodyn. Ther. 38, 102795.

Strazzi Sahyon, H.B., Pereira da Silva, P., Silva de Oliveira, M., Angelo Cintra, L.T., Gomes-Filho, J.E., Henrique dos Santos, P., Sivieri-Araujo, G., 2018. Effect of photodynamic therapy on the mechanical properties and bond strength of glass-fiber posts to endodontically treated intraradicular dentin. J. Prosthet. Dent 120 (2), 317.

Strazzi Sahyon, H.B., Silva, P.P., Oliveira, MS de, Cintra, L.T.A., Dezan-Júnior, E., Gomes-Filho, J.E., Jacinto, R.C., Dos Santos, P.H., Sivieri-Araujo, G., 2019. Influence of curcumin photosensitizer in photodynamic therapy on the mechanical properties and push-out bond strength of glass-fiber posts to intraradicular dentin. Photodiagnosis Photodyn. Ther. 25, 376–381.

Wainwright, M., Phoenix, D.A., Rice, L., Burrow, S.M., Waring, J., 1997. Increased cytotoxicity and phototoxicity in the methylene blue series via chromophore methylation. J. Photochem. Photobiol. B Biol. 40 (3), 233–239.